

1996

Research and Technology
NASA Ames Research

Research and Technology

1996

Ames Research Center

National Aeronautics
and Space Administration

Ames Research Center
Moffett Field, California

NASA TM-112195

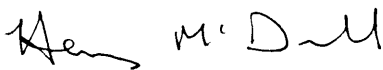
Foreword

The mission of NASA Ames Research Center is to research, develop, verify, and transfer advanced aeronautics, space, and related technologies; to advance and communicate scientific knowledge and understanding of the universe, the solar system, and the Earth; and to enable the development of space for human enterprise. Emphasis is placed on information systems technologies for aeronautics and space applications; on aviation operations systems; and on the discipline of astrobiology, the study of life in the universe encompassing the Earth, space, and life sciences.

This report highlights the challenging work accomplished during fiscal year 1996 by Ames research scientists, engineers, and technologists. It discusses research and technologies that enable the Information Age, that expand the frontiers of knowledge for aeronautics and space, and that help to maintain U. S. leadership in aeronautics and space research and technology development. The accomplishments span the range of goals of NASA's four Strategic Enterprises: Aeronautics and Space Transportation Technology, Space Science, Human Exploration and Development of Space, and Mission to Planet Earth.

The primary purpose of this report is to communicate information—to inform our stakeholders, customers, and partners, and the people of the United States about the scope and diversity of Ames' mission, the nature of Ames' research and technology activities, and the stimulating challenges ahead. The accomplishments cited illustrate the contributions that Ames is making to improve the quality of life for our citizens and the economic position of the United States in the world marketplace.

For further information on Ames research and technology projects, please contact the person designated as the point of contact at the end of each article. An electronic version of this report is available at URL <http://jit.arc.nasa.gov/atrs/index.html>.



Henry McDonald
Director

Aeronautics Enterprise

Overview	1
Global Civil Aviation/Safety	
Aviation Performance Measuring System	3
<i>Irving C. Statler</i>	
Aviation Safety Reporting System	4
<i>Linda J. Connell</i>	
Crew Activity Tracking System	5
<i>Todd J. Callantine</i>	
Study of Line Oriented Flight Training	6
<i>Key R. Dismukes</i>	
Measuring Air Traffic Complexity	7
<i>Irene V. Laudeman, Connie Brasil, Robert Branstrom</i>	
Operational Interventions to Human Error in Aircraft Maintenance	8
<i>Barbara G. Kanki, Vicki Dulchinos</i>	
Aircraft Separation Risk Model	9
<i>Mary M. Connors</i>	
The Final Approach Spacing Tool	11
<i>Tom Davis</i>	
Air/Ground Integration	11
<i>R. Slattery</i>	
The Traffic Management Advisor	12
<i>Harry N. Swenson</i>	
Surface Movement Advisor	13
<i>Brian J. Glass</i>	
Simplified Vision Models for Display Quality Assessment	14
<i>Al Ahumada</i>	
Perceptually Tuned Visual Simulation	15
<i>Mary K. Kaiser</i>	
Entropy Masking in Visual Displays	17
<i>Andrew B. Watson</i>	
Vertical Motion Simulator Advanced Simulator Network	18
<i>William B. Cleveland</i>	
Intelligent Aircraft Control System	19
<i>Charles C. Jorgensen</i>	

Aeronautics Enterprise (continued)

Global Civil Aviation/Affordability

Facilitating User Route Preferences in En Route Airspace	20
<i>Bob Vivona, Mark Ballin, Steve Green, Ralph Bach, Dave McNally</i>	
Conflict Probability Estimation for Free Flight	21
<i>Russell A. Paielli, Heinz Erzberger</i>	
Conflict Prediction Algorithms: Initial Field Test	23
<i>Dave McNally, Bob Vivona, Karl Bilimoria, Gerd Kanning, Steve Green, Ralph Bach, Allan McCrary, Ed Lewis</i>	
Assessing Controller Performance Under Simulated Free-Flight Conditions	24
<i>Roger Remington, James Johnston, Eric Ruthruff, Maria Romera</i>	
Evaluating Cockpit Display of Traffic Information Displays and Route Assessment Tools for a Free Flight Environment	25
<i>Vernol Battiste, Walter W. Johnson</i>	
Cockpit Displays for Low-Visibility Taxiing	27
<i>David Foyle, Elizabeth M. Wenzel, Durand R. Begault</i>	
Multi-Sensor Image Registration	29
<i>Misha Pavel, Al Ahumada, Barbara Sweet</i>	
Flow Visualization of a Full-Scale Rotor in Hover	29
<i>Benton H. Lau, Alan J. Wadcock, Gloria K. Yamauchi</i>	
Skin-Friction Measurements on a Hovering Rotor	30
<i>Alan J. Wadcock, Gloria K. Yamauchi</i>	
Rotor Data Correlation	31
<i>Randall Peterson</i>	
Canard Rotor/Wing Hover Test	32
<i>Stephen Swanson, John Madden</i>	
In-flight Dynamic Stall Research	34
<i>Robert Kufeld, William Bousman</i>	
Stall Control of Helicopter Rotors	34
<i>Khanh Q. Nguyen</i>	
Apache AH-64D Flight Test Predictions	35
<i>Earl P. N. Duque</i>	
Rotor-Wake/Fuselage Interaction	36
<i>Paul M. Stremel</i>	
Navier-Stokes Simulation of High-Lift Aerodynamics	37
<i>Karlin Roth, Stuart Rogers</i>	
Lift-Jet Effects on Powered-Lift STOVL Model	38
<i>Karlin Roth</i>	
Vortex Core Detection for Computational Grid Refinement.....	38
<i>David Kenwright</i>	

Aeronautics Enterprise (continued)

Global Civil Aviation/Affordability (continued)

Wingtip Vortex Flows	39
<i>Jennifer Dacles-Mariani, Dochan Kwak</i>	
Transonic Overset Potential Solver	40
<i>Terry Holst</i>	
Real-Time Particle Tracing in Time-Varying Flows	41
<i>David Kenwright, David Kao</i>	
NASA Metacenter	42
<i>Mary Hultquist</i>	
Portable Batch System	43
<i>David Tweten</i>	
Developing a Cluster Computer from Workstations	43
<i>Reese L. Sorenson</i>	
Planar Doppler Velocimetry Using Pulsed Lasers	44
<i>Robert L. McKenzie</i>	
Pressure-Sensitive Paint and Photogrammetry for Aeroelastic Experiments	45
<i>Edward T. Schairer, Lawrence A. Hand</i>	
Visualizing Wind-Tunnel Experimental Data	47
<i>Samuel P. Uselton, Glenn Deardorff, Leslie Keely, Yinsyi Hung, Arsi Vaziri</i>	
Surface Tension Effects on Skin Friction Measurements	48
<i>G. Zilliac, A. Celic</i>	
Fullerene Gear Design, Simulation, and Visualization	49
<i>Albert Globus</i>	

Global Civil Aviation/Environmental Compatibility

Civil Tiltrotor Noise Abatement Approaches	51
<i>William A. Decker, Rickey C. Simmons</i>	
XV-15 Blade-Vortex Interaction Noise	52
<i>C. W. Acree, Megan S. McCluer, Cahit Kitaplioglu</i>	
Tiltrotor Aeroacoustic Model	53
<i>Larry Young</i>	
Predicting and Analyzing Rotorcraft Noise	54
<i>Roger C. Strawn, Rupak Biswas, Lenny Olikier</i>	
Airframe Noise Measurements: Atmospheric Pressure	55
<i>W. Clifton Horne, Julie A. Hayes, Michael E. Watts, Paul H. Bent</i>	
Airframe Noise Measurements: Pressures to 4.7 Atmospheres	56
<i>W. Clifton Horne, Stephen M. Jaeger, Mahendra Joshi, James R. Underbrink</i>	

Aeronautics Enterprise (continued)

Revolutionary Technology Leaps/Innovative Technology and Tools

X-36 Pioneers Advanced Aerodynamics and Flight Controls	57
<i>Rodney Bailey, Mark Sumich</i>	
Closed-Loop Neural Control of Rotorcraft Vibration	57
<i>Sesi Kottapalli</i>	
Coupled Navier–Stokes and Optimizer Analysis of a Transonic Wing	58
<i>Roxana M. Greenman, Samson Cheung, Eugene L. Tu</i>	
Parallel Unstructured Mesh Adaption	59
<i>Rupak Biswas, Leonid Olikier, Roger Strawn</i>	
Load Balancing Adaptive Unstructured Meshes	59
<i>Rupak Biswas, Leonid Olikier, Andrew Sohn</i>	
Initial Release of the Field Encapsulation Library	61
<i>Steve Bryson</i>	
RANS-MP: Portable Parallel Navier–Stokes Solver	61
<i>R. Van der Wijngaart, Maurice Yarrow</i>	
Parallel Tools for Parallel and Distributed Computer Systems	63
<i>D. DiNucci, M. Frumkin, R. Hood, H. Jin, L. Lopez, R. Papasin, C. Schulbach, J. Yan</i>	
Numerical Aerodynamic Simulation Parallel Benchmarks 2.2	65
<i>William Saphir, R. Van der Wijngaart, Alex Woo, Maurice Yarrow</i>	
Large-Scale Parallel Semiconductor Simulation	65
<i>Subhash Saini</i>	

Revolutionary Technology Leaps/Supersonic Technology

Nonlinear Aerodynamic Shape Optimization of High-Speed Research Configurations	66
<i>Susan Cliff, James Reuther, Ray Hicks</i>	
Surface Operations Behavioral Evaluation Interim Testbed for High-Speed Research	68
<i>Mary K. Kaiser</i>	

Revolutionary Technology Leaps/Access to Space

Propulsion Checkout and Control System	69
<i>Ann Patterson-Hine</i>	

Space Science Enterprise

Overview	71
----------------	----

Progress in Exobiology

Remote Analysis of Martian Surface Materials	74
<i>D. Blake, P. Sarrazin, D. Bish, D. Vaniman, S. Chipera, S. A. Collins, T. Elliott</i>	
Stable Isotope Biogeochemistry of Hydrothermal Systems	76
<i>David J. Des Marais</i>	
Fossilization Processes in Thermal Springs	77
<i>Jack Farmer, Sherry Cady, David J. Des Marais</i>	
Molecular Biomarkers for Stromatolite-Building Cyanobacteria	78
<i>Linda L. Jahnke, Roger E. Summons, Harold P. Klein</i>	
Earth-Threatening Comets Leave Tell-Tale Dust Trails	80
<i>Peter Jenniskens, David Morrison</i>	
Capturing Cosmic Dust on Mir	81
<i>Kenji Nishioka, Ted Bunch, Mark Fonda, Glenn Carle, Sherwood Chang, James Ryder, Janet Borg</i>	
Simple Peptides at Water-Membrane Interfaces	82
<i>Andrew Pohorille, Christophe Chipot</i>	
Silicon-Micromachined Gas Chromatography System	84
<i>Thomas Shen, James Suminto, Frank Yang, Daniel Kojiro, Glenn Carle</i>	
Nitrogen Sources and Sinks on Early Earth	85
<i>David P. Summers</i>	

Progress in Planetary Systems

Planetary Rings	86
<i>Jeff Cuzzi</i>	
Planetesimal Formation in the Protoplanetary Nebula	87
<i>Jeff Cuzzi</i>	
PASCAL: A Mars Climate Network Mission	87
<i>Robert M. Haberle, David C. Catling, Steven C. Merrihew</i>	
The Center for Star Formation	88
<i>D. Hollenbach, P. Cassen</i>	
Energetic Trapped Particles near Jupiter	89
<i>John D. Mihalov</i>	
Wavelet Software	90
<i>Jeff Scargle</i>	
Time-Dependent Structures in Galaxies	90
<i>Bruce F. Smith, Richard A. Gerber, Richard H. Miller, Thomas Y. Steiman-Cameron</i>	
Galileo Encounters Jupiter: Results from the Probe	91
<i>Richard E. Young</i>	

Space Science Enterprise (continued)

Progress in Planetary Systems (continued)

Regolith Effects on Mars' Climate	92
<i>Aaron Zent</i>	
The Nature of the Martian Oxidants	92
<i>Aaron Zent</i>	
A Thermo-Acoustic Oxidant Sensor	93
<i>Aaron Zent</i>	

Progress in Astrophysics

Astrobiology in the Astrochemistry Laboratory	93
<i>Louis J. Allamandola, Scott Sandford, Max Bernstein, Robert Walker, Dave Deamer</i>	
Spectrum Synthesis of Hot Water in Sunspots and Selected Cool Stars	94
<i>Duane F. Carbon, David Goorvitch</i>	
A High-Altitude Site Survey for SOFIA	95
<i>Michael R. Haas, Leonhard Pfister</i>	
Kepler Mission Educational and Public Outreach Software	96
<i>David Koch</i>	
Mid-Infrared Studies of Diffuse Interstellar Material	97
<i>Thomas L. Roellig</i>	
Infrared Observations of G0.18-0.04	98
<i>Janet P. Simpson, Sean W. J. Colgan, Angela S. Cotera, Edwin F. Erickson, Michael R. Haas, Mark Morris, Robert H. Rubin</i>	
New 3.405-Micron Interstellar Emission from Organic Hydrocarbons	99
<i>Gregory C. Sloan, Jesse D. Bregman</i>	

Progress in Space Technologies

Assessment of the Cassini Command and Data Subsystem	101
<i>Edward A. Addy</i>	
Automatic Telescope Project	101
<i>John Bresina</i>	
Guide Star Tracker for Gravity Probe B Relativity Mission	103
<i>John H. Goebel</i>	
Pulse-Tube Cryocooler Development	103
<i>Peter Kittel</i>	
Automated Space System Experimental Testbed Project	105
<i>Christopher Kitts</i>	
Amphion and Meta-Amphion	105
<i>Michael Lowry</i>	

Space Science Enterprise (continued)

Progress in Space Technologies (continued)

Focal-Plane Sensor Array Development for Astronomy in Space	106
<i>Mark E. McKelvey, Robert E. McMurray, Jr., Craig R. McCreight</i>	
Intelligent Execution for Autonomous Spacecraft.....	108
<i>Barney Pell</i>	
New Millennium Program Deep Space 1 Flight Software Program Management	108
<i>Scott Sawyer</i>	

Human Exploration and Development of Space Enterprise

Overview	111
----------------	-----

Astronaut Health/Science

Biochemical Markers of Bone Metabolism in a Rat Spaceflight Model	114
<i>Meena Navidi, Jeanne Wren, Sara Arnaud</i>	
Cerebrovascular Responses Prior to Fainting	115
<i>Kana Kuriyama, Toshiaki Ueno, Richard E. Ballard, Donald E. Watenpaugh, Suzanne M. Fortney, Alan R. Hargens</i>	
Chronic Exposure to Hyper-G Suppresses Otolith-Spinal Reflex in the Rat	116
<i>Nancy G. Daunton, Merylee Corcoran, Robert A. Fox, Li-Chun Wu</i>	
“Dual Adaptation” to Space-Related Sensory Rearrangements.....	118
<i>Robert B. Welch</i>	

Technology Applications to Human Health

Virtual Environment Surgery Workbench	119
<i>Muriel D. Ross</i>	
Noninvasive Estimation of Pulsatile Intracranial Pressure Using Ultrasound	120
<i>Toshiaki Ueno, Richard E. Ballard, John H. Cantrell, William T. Yost, Alan R. Hargens</i>	
MRI-Compatible Spinal Compression Harness	122
<i>Richard E. Ballard, Donald E. Watenpaugh, Iwane Mitsui, Klaus P. Fechner, Douglas S. Schwandt, Alan R. Hargens</i>	
Near-Infrared Spectroscopy to Monitor Forearm Muscle Oxygenation	123
<i>Gita Murthy, Alan R. Hargens</i>	
BIONA 1—Blood Flow Ion Analyzer.....	125
<i>John W. Hines, Christopher J. Soms</i>	
Intelligent Controller for Neurosurgery	126
<i>Robert Mah</i>	

Human Exploration and Development of Space Enterprise (continued)

Technology Applications to Human Health (continued)

Center for Health Applications of Aerospace Related Technologies (CHAART)	128
<i>Byron Wood, Louisa Beck, Sheri Dister, Brad Lobitz</i>	
Telemedicine Spacebridge to Russia	128
<i>Steve N. Kyramarios</i>	

Progress in Improving Space Travel

Advanced Life Support/Human Exploration and Development of Space Enterprise Activities	129
<i>Dick Lamparter, Mark Kliss</i>	
Mir Hardware—Stepping Stone to Station	130
<i>Bonnie P. Dalton, James Connolly, Gary Jahns, Paul Savage</i>	
Wireless Network Experiment for Space Shuttle/Mir	131
<i>Richard Alena</i>	
Engine Diagnostic Filter System	132
<i>Tarang Patel</i>	
Formal Lightweight Approaches to Validation of Requirements Specifications	133
<i>Steve Easterbrook</i>	

Astronaut Health/Countermeasures

Autogenic-Feedback Training as a Potential Treatment for Postflight Orthostatic Intolerance	135
<i>Patricia S. Cowings, William B. Toscano</i>	
Exercise for Long-Duration Spaceflight	138
<i>Donald E. Watenpaugh, Richard E. Ballard, Karen J. Hutchinson, Jaqueline M. William, Andrew C. Ertl, Suzanne M. Fortney, Lakshi Putcha, Wanda L. Boda, Stuart M. C. Lee, Alan R. Hargens</i>	
Keiser SX-1 Variable Resistance Exercise Device	139
<i>Jennifer Pedley, Anthony Artino, Richard Ballard, Alan R. Hargens</i>	
Dehydration at Airline Cabin Altitude	141
<i>John E. Greenleaf, Peter A. Farrell, Helmut Hinghofer-Szalkay</i>	

Mission to Planet Earth Enterprise

Overview	145
----------------	-----

Ecosystem Science and Technology

AIRDAS—Use of Remote Sensing for Disaster Assessment and Management	147
<i>James Brass, Vincent Ambrosia, Robert Slye</i>	
Bay Area Digital Georesource	147
<i>Edwin Sheffner, Sheri Dister, Don Sullivan</i>	
Brazil/United States Environmental Monitoring and Global Change Program	148
<i>James Brass, Vincent Ambrosia</i>	
Carnegie/Ames/Stanford Approach Model	149
<i>Christopher Potter</i>	
Digital Array Scanning Interferometer	149
<i>Steve Dunagan, Philip Hammer</i>	
Effect of Landuse on Regional Estimates of Coniferous Forest Water and Carbon Budgets	151
<i>Joseph Coughlan, Jennifer Dungan</i>	
Landsat Program	152
<i>Edwin Sheffner</i>	
Leaf Modeling	152
<i>Lee F. Johnson, Chris Hlavka, Philip D. Hammer, David L. Peterson</i>	
Mapping Northern Ecosystems: Applications for Circumpolar Methane Exchange	153
<i>Vern Vanderbilt, Guillaume Perry, Joel Stearn</i>	
Modern Ecosystems Research: Effects of Increased UV-B Radiation	153
<i>Hector L. D'Antoni, J. W. Skiles</i>	
Optimizing an Ecosystem Model for Use on Parallel/Distributed Processors	154
<i>J. W. Skiles, Cathy Schulbach</i>	
Paleoenvironmental Research	155
<i>Hector L. D'Antoni</i>	
Scientists' Intelligent Graphical Modeling Assistant	155
<i>Jennifer Dungan</i>	

Atmospheric Chemistry

Airborne Natural Radionuclide Measurements in the Development and Validation of Global Three-Dimensional Models	156
<i>Mark Kritz, Stefan Rosner, Robert Chatfield, Leonard Pfister</i>	
Reactive Nitrogen Data from the Upper Troposphere and Lower Stratosphere	156
<i>Hanwant B. Singh, Alakh Thakur, Peter Mariani</i>	
Airborne Autotracking Sunphotometry	157
<i>Philip B. Russell, John M. Livingston, James Hanratty, Damon Ried, Jill Bauman</i>	

Mission to Planet Earth Enterprise (continued)

Atmospheric Chemistry (continued)

Analysis of Stratosphere/Troposphere Exchange	157
<i>Leonhard Pfister, Henry Selkirk</i>	
Use of Argus in Atmospheric Studies	158
<i>Max Loewenstein</i>	
Airborne Tunable Laser Absorption Spectrometer	158
<i>Max Loewenstein, James R. Podolske</i>	
Convectively Generated Gravity Waves	159
<i>Leonhard Pfister</i>	
The ER-2 and DC-8 Meteorological Measurement Systems	159
<i>K. Roland Chan, T. Paul Bui, Antonio A. Trias, Stuart W. Bowen, Jonathan Dean-Day</i>	
Environmental Research Aircraft and Sensor Technology	160
<i>Steve Wegener</i>	
Global Emissions Inventories for Radon and the Cosmogenic Radionuclides.....	161
<i>Mark Krutz</i>	
The Great African Plume: Tropical Carbon Monoxide and Ozone Simulation	162
<i>Robert B. Chatfield</i>	
Instrument for Tropospheric Nitrogen Studies	163
<i>James R. Podolske</i>	
Reactive Nitrogen and Oxygenated Hydrocarbon Measurements during the Pacific Exploratory Mission	163
<i>Hanwant B. Singh, W. Viezee, R. Chatfield, Y. Chen, D. Herlth, R. Kolye</i>	
Subsonic Aircraft: Contrail and Cloud Effects Special Study	163
<i>Owen B. Toon, Steve Hipskind, Duane Allen, Paul Bui, Roland Chan, Mike Craig, Guy Ferry, Steve Gaines, Warren Gore, Eric Jensen, Joe Jordan, Stefan Kinne, Bill McKie, Peter Pilewskie, Rudi Pueschel, Tony Strawa, Annette Walker</i>	
Stratospheric Tracers of Atmospheric Transport	164
<i>Stephen Hipskind, Michael Craig</i>	
Tropospheric Aerosol Radiative Forcing Observational Experiment	165
<i>Philip B. Russell, John M. Livingston, Wendy Whiting</i>	

Atmospheric Physics

Fine Particle Emissions by Aircraft	166
<i>Rudolf F. Pueschel, Guy V. Ferry, Anthony W. Strawa, Duane Allen</i>	
FIRE Phase III	166
<i>Peter Pilewskie, Warren Gore</i>	
Laboratory Spectroscopy of Carbon Dioxide in Support of Planetary Atmospheres Research	167
<i>Lawrence P. Giver, Charles Chackerian, Jr.</i>	

Mission to Planet Earth Enterprise (continued)

Atmospheric Physics (continued)

Near-Infrared Remote Sensing of Cloud Liquid Water	167
<i>Peter Pilewski, Warren Gore</i>	
Quantitative Infrared Spectroscopy of Minor Constituents of the Earth's Atmosphere	168
<i>Charles Chackerian, Jr., Lawrence P. Giver</i>	
Stratospheric Transport.....	169
<i>Rudolf F. Pueschel, Guy V. Ferry, Anthony W. Strawa, Duane Allen</i>	
SUCCESS Irradiance Measurements	170
<i>Peter Pilewski, Warren Gore</i>	

Appendix

Color Plates (1–22)	172
---------------------------	-----

Aeronautics and Space Transportation Technology Enterprise



Overview

NASA's mission for the Aeronautics and Space Transportation Technology (ASTT) Enterprise is to pioneer the identification, verification, transfer, application, and commercialization of high-payoff aeronautics and space transportation technologies. Ames' researchers and technologists support this mission by seeking enabling revolutionary technological advances that will provide air and space travel for anyone, anytime, anywhere more safely and more affordably, and with less effect on the environment and with improved business opportunities and global security.

This pursuit of revolutionary technologies addresses bold, mid-term and long-term goals of the ASTT Enterprise to enable dramatic improvements in aviation and space transportation. This reflects national priorities as outlined by the National Science and Technology Council. These goals are grouped into three areas, or as they are called, three pillars: "Global Civil Aviation," "Revolutionary Technology Leaps," and "Access to Space." The following sections outline these goals and Ames' FY96 accomplishments toward achieving them.

Pillar 1: Global Civil Aviation

Today, with over 11,000 airplanes in commercial service worldwide, the United States faces strong international competition in this vital area whose products are the largest positive industrial contributor to the U.S. balance of trade. Projects linked to world economic growth suggest that air travel demand will triple over the next 20 years. Therefore, to preserve our Nation's economic health and the welfare of the traveling public, NASA must provide high-risk technology advances that will contribute to safer, more affordable, more environmentally compatible air travel.

The highlighted FY96 accomplishments address the following goals of the Global Civil Aviation pillar:

1. Safety goal: Reduce the aircraft accident rate by a factor of 5 within 10 years, and by a factor of 10 within 20 years.
2. Affordability goals: (a) While maintaining safety, triple the aviation system throughput, in all weather conditions, within 10 years and (b) reduce the cost of air travel by 25% within 10 years, and by 50% within 20 years.
3. Environmental compatibility goal: Reduce the perceived noise levels of future aircraft by a factor of 2 (from those of today's subsonic aircraft) within 10 years, and by a factor of 4 within 20 years.

Research and development conducted by the ASTT Enterprise has been structured to be led by specified NASA research centers according to the primary roles and missions that have been assigned to each center. Ames is the lead center for the High Performance Computing and Communications (HPCC) Program and for the research and technology (R&T) base programs in aviation operations systems, information technology, and rotorcraft. In addition, Ames leads the Enterprise core competencies in the areas of human factors, air-traffic management, information system technologies, and rotorcraft R&T.

Ames' significant involvement in the safety goal includes human factors, information technology, and condition-based maintenance. Ames made significant contributions toward addressing this goal, contributions that led to advances in aviation performance measuring, aviation safety reporting, crew activity tracking, air-traffic complexity, aircraft-separation risk modeling, air and ground integration, and human error in aircraft maintenance.

Airlines and businesses lose billions of dollars annually as a result

of delays and lost productivity owing to weather and congestion in the airspace system. Under affordability goal (a) (above), Ames' major effort in research and development of air-traffic management automation constitutes virtually all of NASA's work in that area. Accomplishments include articles on controller performance under simulated free-flight conditions, techniques for low-visibility taxi and ground-collision avoidance, and conflict-prediction algorithms.

Reducing the costs of aircraft operation and maintenance is a major challenge. NASA's test facilities and core expertise in materials, structures, aerodynamics, propulsion, analytical methods, and computational tools are key elements in helping to revolutionize aircraft design and manufacturing. NASA's research efforts are focused on innovative design techniques and structural concepts. Ames' contributions to affordability goal (b) come from rotorcraft, national tasking facilities, and research and development of computational tools. Several Ames projects contributed to rotorcraft research and technology activities, which include rotor aerodynamics, testing of new concepts, stall control, in-flight dynamic stall research, and vortex flows. Examples of accomplishments that enhance computational tools are vortex-core detection and tracking of particles in time-varying flows. Improvements in the use of facilities are highlighted in the following pages by articles on planar Doppler velocimetry, pressure-sensitive paint and photogrammetry, and visualization of experimental data. A high-risk, long-term research effort directed to the manufacture of fullerene nanotechnology gears is also described.

For research related to the environmental compatibility goal, Ames has significant aeroacoustic research and testing capabilities, the most recent advance in those capabilities being the Aeroacoustic

Modification Project at Ames' National Full-Scale Aerodynamics Complex (NFAC), which is currently being completed. In this report, accomplishments related to helicopter noise and airframe noise are presented.

Pillar 2: Revolutionary Technology Leaps

NASA's charter is to explore high-risk technology areas that can revolutionize air travel and create new markets for U.S. industry. The technology challenges for NASA include accelerating the application of technology advances, eliminating the barriers to affordable supersonic travel, and expanding general aviation,

The highlighted FY96 accomplishments address the following two goals of the Revolutionary Technology Leaps pillar:

1. Provide next-generation design tools and experimental aircraft to increase design confidence, and cut the aircraft development cycle time in half.
2. Reduce the travel time to the Far East and Europe by 50% within 20 years, and do so at today's subsonic ticket prices.

The next-generation design tools and experimental aircraft goal will dramatically affect the way in which business is conducted. Its effect will be felt across the three pillars, contributing to every technology goal. Ames has significant work in integrated design systems and the X-36 aircraft. Research is done at Ames in information technology to elevate the power of computing tools through fuzzy logic, neural networks, and artificial intelligence. These tools will integrate multidisciplinary product development activities to dramatically cut design cycle times. Examples of accomplishments include neural control of rotorcraft vibration, coupling of flow-field computation tools with design optimization tools, and parallel computational tools and

computations. Experimental aircraft are also invaluable tools for exploring new ideas. An example is provided with the use of advanced aerodynamics and flight controls on the X-36 aircraft.

Under the high-speed transport goal, Ames has diverse activities in wind-tunnel testing and simulation, external visibility, sonic boom minimization, and wing aerodynamic optimization. Articles are presented in this report to highlight these activities.

Pillar 3: Access to Space

In coming decades, NASA envisions the space frontier as a busy crossroads of U.S.-led international science, research, commerce, and exploration. Experience with this vast resource has already yielded new treasures of scientific knowledge, life-enhancing applications for use on Earth, and fantastic celestial discoveries. The potential for the future seems almost limitless.

Ames addresses the following goal of the third pillar, Access to Space:

1. Reduce the payload cost to low-Earth orbit by an order of magnitude, from \$10,000 to \$1,000 per pound, within 10 years.

As NASA's lead center for thermal protection systems (TPS) technology, Ames is charged with developing new thermal protection systems that will enable vehicles of the future to be built more economically and that will enable existing ones to be upgraded at reduced cost. Ames maintains one of the world's premier arc-jet complexes for providing realistic simulations of entry environments. These simulations are essential for technology development, system validation, and system qualifications. Ames supports the U.S. aerospace community in developing TPSs that will be necessary for the nation's future space vehicles.

GLOBAL CIVIL AVIATION/SAFETY

Aviation Performance Measuring System

Irving C. Statler

Flight Operations Quality Assurance (FOQA) programs using flight-recorded data have been providing critical safety information to non-U.S. airlines for over two decades. Although the benefits of these programs have been demonstrated, the U.S. air carriers have found them impractical to implement because of the extensive labor required to process the great amounts of data that would typically be generated. A collaborative effort was initiated in August 1993 between the Federal Aviation Administration (FAA) and NASA to establish and demonstrate the feasibility of developing a set of tools that would allow very large quantities of flight data to be pro-

cessed automatically in order to address questions relating to operational performance and safety.

The Aviation Performance Measuring System (APMS) is providing technical tools to facilitate the large-scale implementation of flight-data analyses at both the air-carrier and the national-air-space levels. APMS enhances the existing Commercial Off The Shelf (COTS) capabilities of FOQA, including the capability of analyzing all the data collected, in addition to merely identifying "exceedances" or "special events" (the figure shows the APMS functions).

Phase 1 of the APMS effort ended in December 1995. Phase 2 focuses on three tasks: (1) selection and implementation of an APMS client-server database architecture; (2) development of a knowledge-based system for verifying and diagnosing "special events" flagged by COTS packages; and (3) construction of a friendly user-interface in

Visual Basic. The client-server database architecture and method for the initial build have been selected. Teledyne Control's FLIDRAS software has been acquired to read Flight Data Recorder raw data parameters, to convert the data into engineering units, and to perform data dumps into the database management system. As the flight database is built, the baselines of various routine operations will be established. Knowledge-based tools, currently under development by the APMS team, will, in later iterations when an adequate database is available, provide statistical trending and predictive capabilities. The first prototype system was delivered in July 1996 to the first airline partner. The prototype system is now operational and currently being used to process airline flight data.

With the industry becoming aware of the capabilities of the APMS suite of tools, the team is being approached by other airlines that had not been solicited to participate in the research project. So far, one additional major airline and one major cargo airline have asked to participate in the program. User-needs studies have been completed with four U.S. airlines and a fifth has been started. Agreements have been signed with two of these to cooperatively develop customized suites of APMS tools. The APMS effort continues to work with collaborators to improve system design.

Point of Contact: I. Statler
(650) 604-6655
istatler@mail.arc.nasa.gov

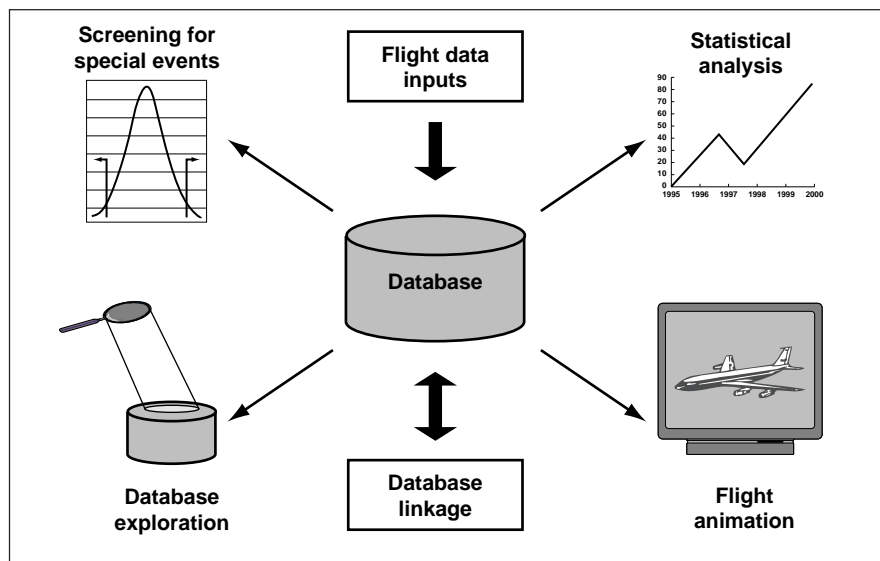


Fig. 1. APMS functions.

Aviation Safety Reporting System

Linda J. Connell

The Aviation Safety Reporting System (ASRS) solicits, processes, and analyzes aviation safety incident reports from pilots, air-traffic controllers and others and uses the data it collects to further aviation safety. The ASRS (1) codifies the reports it receives (31,096 in FY96) and inserts them into a computer database; (2) issues alerting messages on pressing safety problems described by incoming reports; (3) provides data retrieval services (search requests) for aviation safety researchers and others; (4) publishes a monthly safety bulletin, *CALLBACK*, and a periodic safety journal, *DIRECTLINE*; (5) performs Quick Response analytic efforts for the Federal Aviation Administration (FAA), the National Transportation Safety Board (NTSB), and other governmental entities; and (6) does applied research on aviation operational problems, especially those involving human performance (see the figure). The ASRS is heavily reliant on information technology, and a portion of program resources is devoted to maintaining and upgrading that technology.

The following list is a summary of some of ASRS's FY96 activities. In FY96, the ASRS program:

- Initiated an ASRS Internet site in November 1995. Through its Web site, ASRS offers its publications, program information, and downloadable (using an Adobe Acrobat reader) versions of the NASA Incident Reporting Forms.

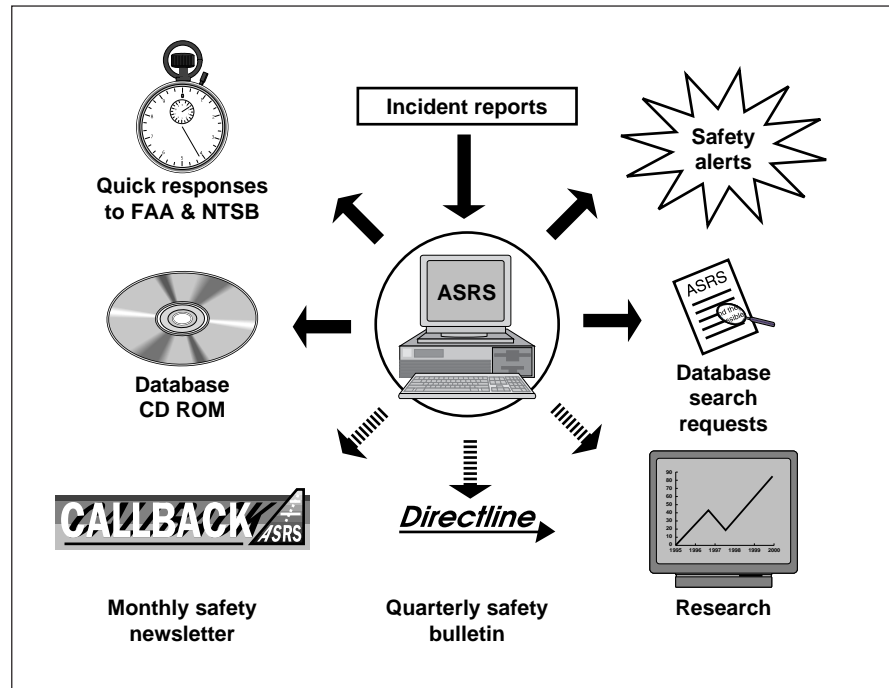


Fig. 1. ASRS products.

- Accomplished a Multi-Engine Turbojet Uncommanded Upsets Structured Callback Analysis for the NTSB. The analysis was subsequently adopted into the USAir B-737 accident investigation report.
- Completed a GPS Safety Impact Analysis for the FAA Associate Administrator of Research and Acquisitions.
- Accomplished a Quick Response analysis of Runway Transgression Data for the FAA Office of System Safety. These data were subsequently presented to the FAA deputy administrator.
- Completed Quick Response No. 289 entitled "Near Mid-Air Collision Data Analysis" for the FAA Office of System Safety.
- Accomplished the second installment of the Wake Turbulence Structured Callback Project Reports; it included the analysis of 51 wake turbulence incidents and was submitted to the FAA.
- Produced search requests for the NTSB and the FAA on DC-9 cabin/cockpit smoke and aircraft equipment problems in support of the investigation of the DC-9 accident near Miami, Florida, on May 11, 1996.
- Produced a Quick Response analysis of Part 135 Aircraft Incidents for the Australian Bureau of Air Safety Investigation. The data are being used to develop a proactive aviation safety hazard monitoring system.

- Transmitted 30 runway-incursion reports at Cleveland-Hopkins Airport, Ohio, to the FAA Office of System Safety and the Air Line Pilots Association. As a result of ALPA and FAA follow-up actions, revised ground-control procedures were implemented for departures using runways 23L/23R.
- Transmitted 24 reports to FAA and ALPA involving altitude deviations at FUELR Intersection on the CIVET ONE ARRIVAL to Los Angeles International Airport. Subsequent investigation by the FAA determined that the recent installation of a new ILS had changed the glidepath angle at FUELR.
- Published one issue of DIRECTLINE in FY96. Its research articles addressed aircraft call-sign confusion and ramp safety.
- Developed a trial version of the ASRS Intranet communications system. It runs on an NT Server and is available to the ASRS staff. The decision was made in January 1996 to develop this internal Intranet communications system based on existing Internet applications in order to lower costs and increase efficiency internally at the ASRS.
- Commenced a collaborative research project between NASA and its French counterpart, ONERA, to evaluate an ONERA human factors coding scheme and taxonomy for possible application to ASRS incident data.

- Completed a conceptual and editorial review for a second NASA project, a study on the use of modes in human-machine interactions. This study, which was completed, made use of ASRS data.

Point of Contact: L. Connell
(650) 604-6654
lconnell@mail.arc.nasa.gov

Crew Activity Tracking System

Todd J. Callantine

Human operators supervising advanced automation systems can have difficulties that have the potential to compromise safety. For example, a recent study found that over 44% of flight deck problems cited in a large body of incident and accident reports were related to automation. Autoflight system modes, in particular, are often implicated because they can cause

unexpected behavior. One remedy is to develop technology that can detect potential operator errors and provide the operator with context-sensitive advice and reminders. To be effective, such technology must incorporate knowledge about operator-automation interaction in context; for flight deck application, this includes knowledge about mode management.

This research addresses an enabling technology called activity tracking, a way of inferring intent. As the name implies, the Crew Activity Tracking System (CATS) is an architecture that implements a method for activity tracking (see the first figure). CATS represents knowledge about the operator's tasks using an explicit, task-analytic model based on the goal-based decomposition of tasks into subgoals and primitive tasks. CATS uses the model to predict operator intentions and to interpret subsequent operator actions. The predictions and interpretations are designed to supply the knowledge required for intelligent aiding and training systems.

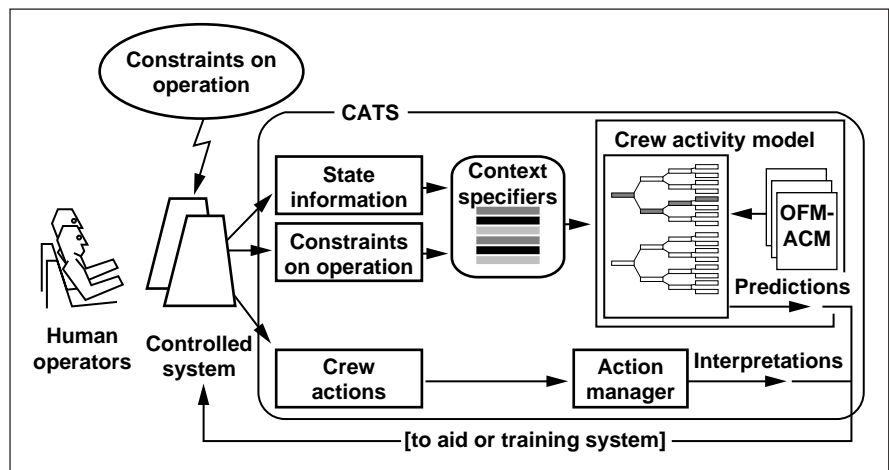


Fig. 1. The Crew Activity Tracking System in context.

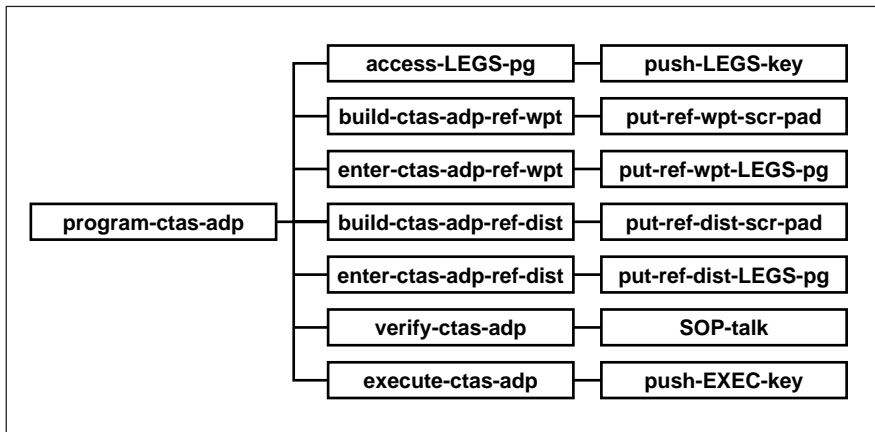


Fig. 2. A simplified task decomposition from the enhanced CATS model.

CATS was implemented to track the activities of Boeing 757 pilots using autopilot flight modes under normal operating conditions. An experimental evaluation was conducted to assess the effectiveness of the CATS method. Ten type-rated line pilots from a major airline participated in the study. Each flew five experimental scenarios on a real-time part-task simulation of the Boeing 757. Of the 2,089 pilot actions detected in the study, CATS correctly interpreted 81%. A subsequent analysis identified adjustments to the CATS model and processing scheme that would allow CATS to correctly interpret 94% of pilot actions.

Current research seeks to extend the capabilities of CATS and to explore new applications. Specifically, the objective is to enable CATS to predict and interpret the actions of two-person crews by using complex functions of the Flight Management Computer Control and Display Unit (FMC CDU), and data-link communications. These activities are critical for procedures that

are being developed for use with new air-traffic control automation.

The second figure shows a simplified task decomposition from the enhanced CATS model, from which most cognitive, verbal, and perceptual activities are omitted. The task shown supports a new descent procedure that uses an assigned descent point (“adp”), in addition to the top-of-descent point computed by the FMC. When the crew has been cleared for the procedure, CATS uses this portion of the model to predict and interpret the CDU programming activities required to perform the task. For example, CATS first predicts which pilot is responsible for programming the assigned descent point to go to the CDU LEGS page. CATS next predicts that a reference way point will be built in the CDU scratchpad, then line-selected to the appropriate place on the LEGS page, and so on. As these actions are performed, CATS checks the entered values for accuracy and then either interprets the actions to support the task of entering the

assigned descent point or signals a potential error.

A Boeing 747-400 simulator study to investigate pilot performance on a new descent procedure was conducted at Ames Research Center. The data show that although pilots performed the new procedure effectively in most cases, there were still a number of compliance violations. These data are used to investigate a new application of CATS: tracking crew activities to automatically identify departures from the procedure and capture the context in which these departures occurred. With this information, the procedure may be refined to address problems, and thereby improve compliance.

Point of Contact: T. Callantine
(650) 604-2631
tcallantine@mail.arc.nasa.gov

Study of Line Oriented Flight Training

Key R. Dismukes

Airlines train pilots to work together as safe, efficient crews by using a realistic full-mission flight simulation approach called Line Oriented Flight Training (LOFT). In this annual recurrent training, crews encounter challenging situations that they must manage by coordinating their efforts, exercising good judgment and decision-making, and drawing upon all available resources. After the LOFT, the instructor leads the crew in a debriefing in which they are expected to analyze what happened, evaluate their own performance,

and identify ways to improve performance. Because the LOFT is a very busy, intense experience, how much the crews learn from the LOFT and take back to line operations hinges on the effectiveness of the debriefing.

Both the airlines and the FAA espouse the idea that LOFT instructors should refrain from lecturing the crews in the traditional “teacher-tell” manner. Instead, instructors are encouraged to “facilitate” self-analysis by the crew so that they will learn more deeply. However, there has been little study of how to facilitate this self-analysis; as a consequence, the airlines have not had good data-based techniques for training their instructors in debriefing procedures.

Human factors scientists at Ames recently completed a study, in collaboration with major U.S. airlines, to evaluate LOFT debriefings and to provide guidelines for training instructors. The study evaluated the effectiveness of LOFT debriefings at a cross section of airlines, analyzed facilitation techniques, and identified common errors. The study demonstrated that instructors who are effective in facilitating self-analysis substantially increase the depth of crew participation and self-analysis; however, individual instructors differed greatly in their effectiveness as facilitators.

In conjunction with the technical report of the study, the research team prepared a detailed manual for use in training instructors to facilitate debriefings. This manual explains the concepts of facilitation, describes effective techniques, explains how

and when to use these techniques, and shows how to engage crews that do not initially respond. Immediately after receiving the study materials, several major airlines reprinted the manual for the use of their instructors. Other airlines have overhauled their training of instructors to incorporate the findings from the study; they later reported significant benefits to their crew training programs.

Point of Contact: K. Dismukes
(650) 604-0150
kdismukes@mail.arc.nasa.gov

Measuring Air Traffic Complexity

Irene V. Laudeman, Connie Brasil, Robert Branstrom

An important goal in advanced air-traffic operations is that of providing more system flexibility to the user. The idea of sharing the responsibility for aircraft separation, in which pilots and air-traffic controllers work together to ensure separation, is designed to provide such flexibility. Currently, under instrument flight rules the air-traffic controller is tasked with ensuring the proper separation of aircraft. Under shared separation-responsibility procedures, pilots in appropriately equipped aircraft would assume some responsibility for the management of aircraft separation. The proportion of responsibility assigned to pilots and air-traffic controllers

would be a function of the complexity of the airspace.

Shifts in operational procedures will be specified as a function of airspace complexity, making the development of separation procedures dependent on the development of a complexity metric. The complexity of air-traffic patterns, and hence the workload related to the management of air traffic, is known to include more than a simple count of aircraft contained in a volume of airspace. However, the traffic complexity factors beyond that of aircraft number have not been clearly identified, nor has any relationship among the factors been established.

A human-in-the-loop simulation study was conducted to evaluate three modes of separation responsibility and to provide data for use in developing a complexity metric. Ten groups of four currently qualified air-traffic controllers participated in nine simulation scenarios. In each group one participant acted as the controller in a sector of airspace and three participants acted as pilots.

Aircraft data in the form of latitude, longitude, heading, altitude, and speed were collected for all of the aircraft in each of the nine 30-minute scenarios. The complexity of the simulated airspace was computed from the aircraft data at every 2 minutes of the 30-minute scenarios. Complexity functions were computed as a sum of traffic factors that included aircraft count, aircraft converging at the same altitude, and aircraft changing heading, speed, or altitude.

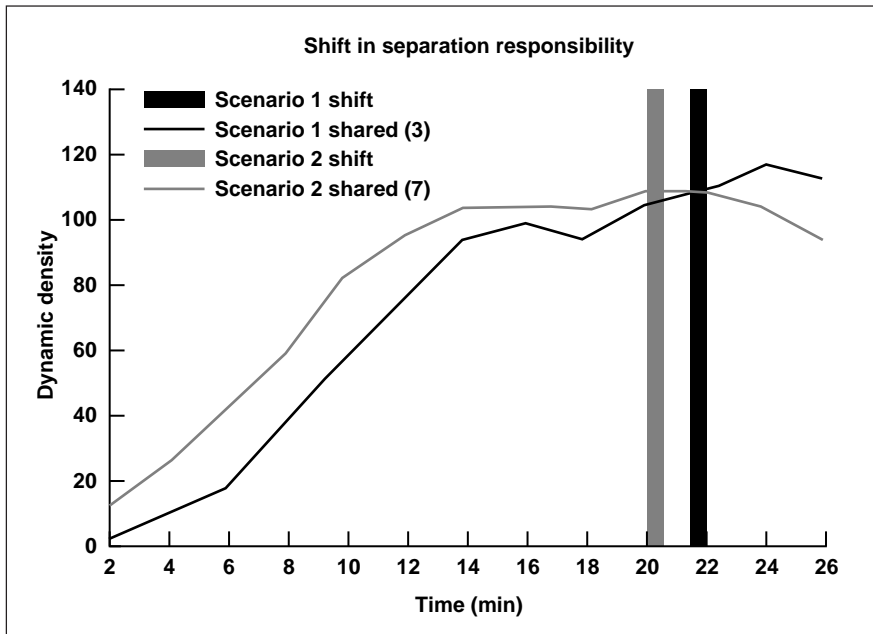


Fig. 1. Air-traffic complexity functions and points at which separation responsibility was shifted for two types of traffic scenarios.

The complexity functions predicted an operational shift related to the sharing of separation responsibility (see the figure) indicating that such functions might be useful in specifying shared separation responsibility procedures.

Point of Contact: I. Laudeman
(650) 604-0018
laudeman@eos.arc.nasa.gov

Operational Interventions to Human Error in Aircraft Maintenance

Barbara G. Kanki, Vicki Dulchinos

A significant proportion of aviation accidents and incidents are known to be tied to human error. However, research of flight operational errors has shown that so-called “pilot error” often involves a variety of human factors issues and not a simple lack of individual technical skills. In aircraft maintenance operations, there is similar concern that maintenance errors which may lead to incidents and accidents are related to a large variety of human factors problems.

Although industry initiatives involving human factors training in maintenance have become increasingly accepted as one type of maintenance error intervention, there remains a dual challenge: (1) to develop human factors interventions that are directly supported by reliable human error data, and (2) to integrate human factors concepts into the procedures and practices of everyday technical tasks.

These challenges are being addressed at Ames Research Center. First, industry-wide incidents reported to the Aviation Safety Reporting System are being analyzed in order to identify and characterize high priority problem areas. When analyzed for contributing factors, at least 50% of the incidents involved more than one technician—other maintenance personnel, flight crew members, and airport personnel.

Consistent with these findings, research is being conducted that focuses on human factors interventions related to practices and procedures; namely, structured on-the-job training and procedure re-design. In both areas, particular attention is being centered on areas in which maintenance tasks require coordination both within and between maintenance teams.

In the area of structured on-the-job training, field applications of the Task Analytic Training System—a performance-based system that involves full workforce participation in its design, development, and implementation—have been conducted.

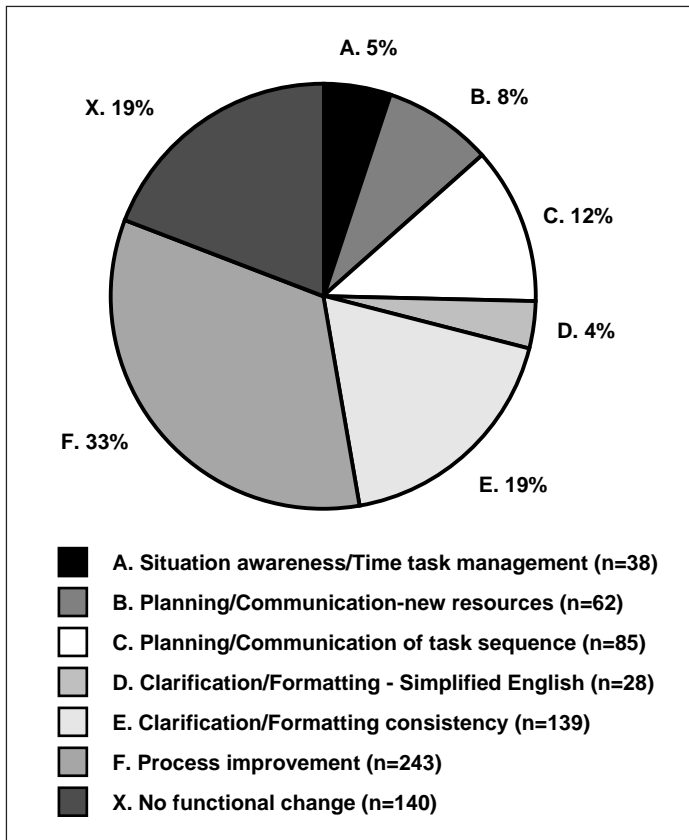


Fig. 1. Distribution of reason codes in the revised procedure (N = 735 procedural steps).

Human factors principles may also be incorporated into the maintenance procedures themselves. When Boeing modified its B-737 CFM56-7 engine-change procedure, the efficiency of the engine-change process was significantly improved. A 14% increase in efficiency, attributed to changes in the maintenance manual alone, presented an opportunity to conduct a systematic comparison between original and revised procedures. The goal was to analyze the specific modifications that led to the improvement in efficiency and to identify the contribution of human factors. Some

results of this item-by-item comparison are found in the summary of functional changes shown in the figure.

Finally, a collaborative relationship has been established with the human factors team at Kennedy Space Center; a series of workshops for discussing human factors issues in aviation and space vehicle maintenance is being conducted. The first workshop was held at Ames Research Center in September 1966; it focused on error analysis (incidents, accidents, mishaps, and close-calls). This workshop facilitated the

free exchange of human factors information between aircraft and shuttle maintenance operations.

Point of Contact: B. Kanki
(650) 604-5785
bkanki@mail.arc.nasa.gov

Aircraft Separation Risk Model

Mary M. Connors

Increased demand for air travel translates into a need to accommodate more aircraft in the terminal airspace. Separations between aircraft pairs must be small enough to be efficient while remaining sufficiently large to be safe. Present separation standards are considered safe for the equipment and conditions that presently prevail. It is possible that new technologies could result in maintaining the present safety level while permitting the distances between aircraft pairs to be reduced. What is needed is a quantitative method of evaluating safety. The objective of this research is to develop a computer model that will provide this link between aircraft separation and a quantitative method of assessing safety risk.

The model, called the Reduced Aircraft Separation Risk Assessment Model (RASRAM), evaluates safety risks for a variety of flight scenarios relating to final approach, landing, and rollout for parallel and single runways. The basic approach of RASRAM is to quantify the risk associated with current separation standards and to then compare it with that for reduced separation

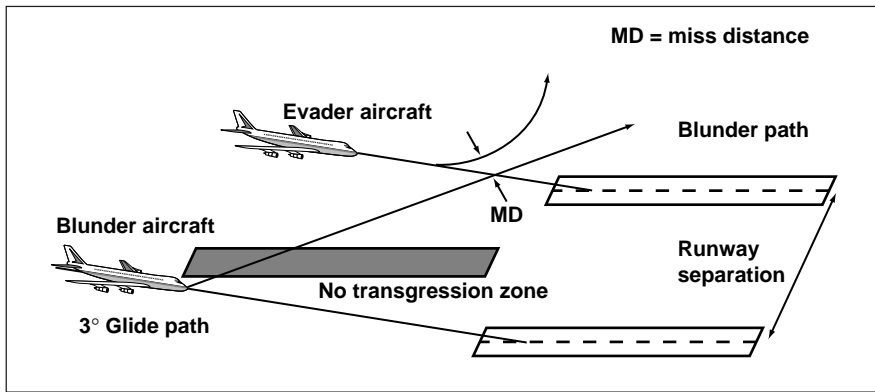


Fig. 1. Parallel approach lateral separation geometry.

operations during instrument meteorological conditions, considering procedural and technological changes. The research is being performed for Ames Research Center as an integral part of NASA's Terminal Area Productivity (TAP) program, and in coordination with the Federal Aviation Administration.

RASRAM includes the following two scenarios that measure the effect of separation on safety: lateral separation for parallel approaches; and in-trail separation during single runway operations, accounting for runway occupancy and wake vortex effects. The figure illustrates the parallel approach scenario, for which independent approaches to parallel runways constitute the operational context. The primary separation criterion is the distance between the runway centerlines for the two approach paths. The defining characteristic of the scenario in the model is a blundering aircraft that strays from its own final approach, crossing the path of the other approach stream. The safety of the scenario (for current operations)

is determined (1) by the performance of the controller in detecting the blunder and issuing breakout instructions to the evader aircraft, and (2) by the performance of the pilot and aircraft in completing the evasive maneuver. RASRAM models all of these effects and quantifies the safety of the operation. The standard risk measure is the probability that the blundering aircraft will approach within 500 feet of an aircraft in the other approach stream.

NASA's TAP Program anticipates procedural changes for terminal-area operations along with the introduction of new technologies. These new technologies include Differential GPS (DGPS), Automatic Dependent Surveillance (ADS-B), and several technologies under development by the NASA TAP program: the Center-TRACON Automation System (CTAS), the Aircraft Vortex Spacing System (AVOSS), the Dynamic Runway Occupancy Measurement (DROM), and the Airborne Information for Lateral Spacing (AILS). RASRAM begins the process of

quantifying the safety risk associated with the effects of these technologies on separation standards. The model can also be used to provide a relative comparison of the safety of proposed new procedures with the safety of current operations and technologies. Using RASRAM, the safety of further separation reductions for parallel approaches that rely on new technologies can be analyzed and compared with current procedures. Similarly, the safety of reductions of in-trail separation can be compared with current procedures. Although it is being developed for initial application to final approach and landing, the basic approach to modeling separation risk has direct application to all phases of flight. The potential application of these models to en route and approach airspace is being undertaken in the Advanced Air Transportation Technology program at Ames.

Point of Contact: M. Connors
(650) 604-6114
mconnors@mail.arc.nasa.gov

The Final Approach Spacing Tool

Tom Davis

The Center/TRACON Automation System (CTAS) is an air-traffic control automation system under development at Ames Research Center. The system is designed to support increasing demands for capacity and efficiency in the National Airspace System. The terminal-area component of the system, the Final Approach Spacing Tool (FAST), is designed to assist terminal air-traffic controllers in efficiently managing and controlling arrival air traffic for the last 40 miles of flight down to the runway. The FAST system issues the controllers a series of sequencing, runway, heading, and speed advisories to achieve an efficient flow of traffic that increases airport capacity, reduces delays, and reduces controller workloads.

The objective of the research and development effort is to test the FAST system operationally in a series of phased functionality enhancements at the Dallas/Fort Worth TRACON (Terminal Radar Approach Control) (see figure (see Color Plate 1 in the Appendix)). The operational field testing of the FAST system allows researchers to further develop and assess the system with the end-users, that is, with the air-traffic controllers. The assessments include a series of observations with the FAST system operating in a shadow mode on live traffic data, real-time simulation evaluations of

the FAST system at Ames and at the FAA Technical Center, and a limited operational assessment of the FAST system functionalities at Dallas/Fort Worth.

Development and field testing of the FAST system achieved a significant milestone during FY96; the "Passive" FAST functionality, which includes the sequence and runway advisories, underwent operational testing at the Dallas/Fort Worth TRACON. The tests, which were conducted in cooperation with the FAA, the National Air Traffic Controllers Association, and the Airline Transport Association, began in January 1996 and continued through July 1996. The objectives of the test were: (1) to confirm the technical performance of the Passive FAST functionalities, (2) to assess the airport delay and capacity benefits of Passive FAST, and (3) to assess the controller workload benefits of Passive FAST. The testing demonstrated an arrival rate improvement at Dallas/Fort Worth of 13%, a departure queue backlog reduction of 9%, and an overall increase in total airport operations (arrivals and departures) of 13%, all with no increase in taxi times and with little or no increase in controller workload. The system has received overwhelmingly positive support from all participants.

The Active FAST system functionalities, including speed and heading advisories, remain to be developed and operationally evaluated. The Active FAST system will undergo operational testing similar

to that of the Passive FAST before a national deployment system is specified.

Point of Contact: T. Davis
(650) 604-5438
tdavis@mail.arc.nasa.gov

Air/Ground Integration

R. Slattery

The Center/TRACON Automation System (CTAS) was developed for use in the air traffic-control environment. As part of the Terminal Area Productivity Air Traffic Management program, research has begun to expand CTAS to coordinate with aircraft that are equipped with Flight Management Systems (FMSs) using data-link. A large portion of the commercial aircraft fleet is so equipped and many older aircraft are being retrofitted with an FMS. However, busy air-traffic controllers do not often allow pilots to fully utilize the FMS. An FMS calculates the most efficient trajectory, thus saving fuel, and then follows the trajectory very accurately, increasing trajectory prediction accuracy. Thus, if the CTAS helps the controllers take advantage of the FMS trajectory, the performance of the airspace system should be improved.

The objectives of the research and development effort are to quantify the actual benefits of the air/ground system with both controllers and pilots in the loop. Theoretical benefits have been studied, under the assumption that the trajectories are followed with the

maximum accuracy possible for the FMS. These benefits may be diminished, however, by the extra workload imposed on the controllers and pilots; also, they may not be realizable because of operator error.

A piloted simulation was performed using the CVSRF 747-400 simulator. Since the simulator was not equipped with data-link at the time, the routes were defined as stored arrivals in the FMS (an example is shown in the figure). The pilots were issued FMS route changes, while still performing the rest of their normal duties. For a baseline comparison, equivalent routes were flown using current controller clearances. The aircraft was flown in the Dallas/Fort Worth terminal area, starting at the two

eastern arrival gates into the TRACON (Terminal Radar Approach Control) and finishing at the runway. The accuracy of the horizontal route increased for the FMS cases, but the vertical predictability was lower.

This was because the vertical portion of the FMS route is entered as crossing altitudes at way points. As long as the pilots meet the required altitude, the point at which they begin their descent and the way in which they make the descent are open. Offsetting the achievable accuracy, the pilots felt that the FMS route changes produced far more workload with current generation FMS systems than did current procedures. They also expressed concerns about the amount of heads-down time spent loading the

trajectory while in the busy terminal area. There were also more errors in loading and in following the FMS route, though these should be reduced by data-link and by interface changes to the FMS.

Point of Contact: R. Slattery
(650) 604-5435
rslattery@mail.arc.nasa.gov

The Traffic Management Advisor

Harry N. Swenson

The growth of commercial air travel within the United States has put a severe strain on the nation's air traffic capacity. This, coupled with the "hub-and-spoke" procedures used by the major air carriers and the marketing requirements for aircraft to take off and land at optimum times, has required an improvement in the Air Traffic Control System. The Center-TRACON Automation System (CTAS) is a decision-support concept being developed to improve airport capacity and to reduce delays while maintaining controller workload at a reasonable level. The extended terminal-area component of the system is the Traffic Management Advisor (TMA). The TMA is a time-based strategic planning tool that provides traffic management coordinators and en route air traffic controllers the ability to efficiently optimize the capacity of a demand-impacted airport. The TMA consists of trajectory prediction, constraint-based runway scheduling, traffic

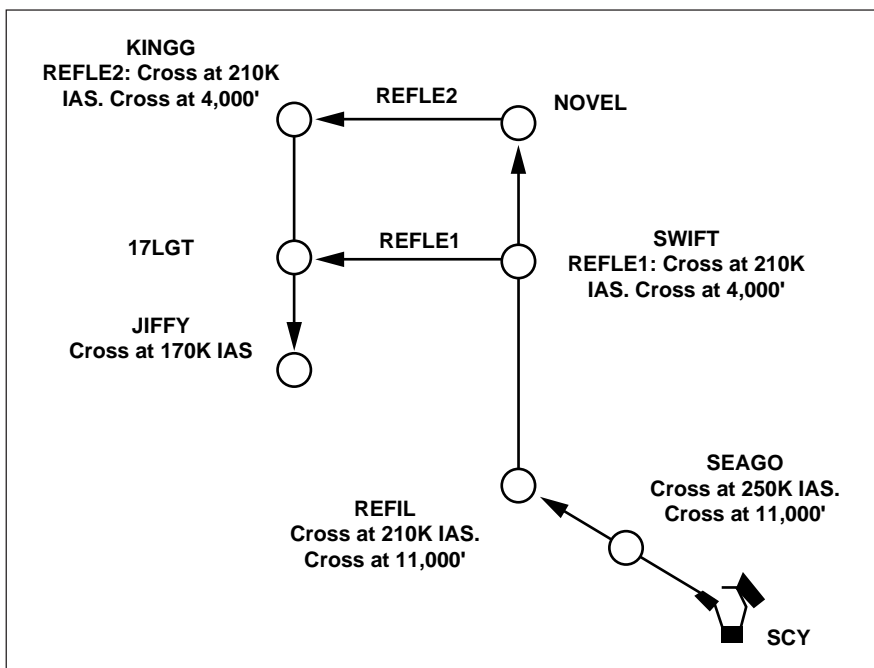


Fig. 1. Scurry FMS arrivals, REFLE1 and REFLE2.

flow visualization, and controller arrival sequence, time, and delay advisories.

The TMA and all other CTAS tools are being developed to demonstrate user benefits both to air-traffic controllers and commercial air carriers. Air-traffic control is a very complex multivariable problem requiring teams of highly skilled individuals to safely and efficiently move traffic from terminal departure point to terminal arrival. This extended complexity requires that automation aids designed to assist these teams be proven and validated in actual operations. The objective of the TMA 1996 research and development effort was focused toward an operational evaluation at the Ft. Worth Air Route Traffic Control Center, Ft. Worth, Texas. The evaluations also focus research into areas and concepts that provide user benefits.

The TMA achieved several major milestones in this focused effort toward operational evaluations. The first was controller and operational hardware in-the-loop simulations at the William J. Hughes FAA Technical Center with the National Air Traffic Controllers Association (NATCA) Ft. Worth Center System Design Team. This was followed by the installation and checkout of the TMA hardware/software components at the Ft. Worth Center, the nation's fifth busiest Center, which manages and controls traffic into the second busiest airport in the world (Dallas/Ft. Worth). Upon completion of the system installations, on-site shadow evaluations and nighttime simula-

tions were conducted. Subsequently, the formal operational evaluations were conducted. The TMA demonstrated delay reductions of 1–2 minutes per aircraft, as well as a significant reduction in controller workload. The original plan was to remove the TMA upon completion of the formal evaluation, but, based on the benefits achieved, the FAA, the Air Transport Association, and NATCA requested that NASA operationally support the TMA on a continuous basis. NASA has complied with that request, and the TMA has been used operationally since the completion of the formal evaluations. Since the evaluations, a 10% capacity increase has been attributed to TMA operations.

Point of Contact: H. Swenson
(650) 604-5469
hswenson@mail.arc.nasa.gov

Surface Movement Advisor

Brian J. Glass

Recurrent delays during departure taxiing at large airports have become commonplace with the prevalence of “hub-and-spoke” airline operations, as large numbers of aircraft attempt to land, taxi, be serviced, taxi, and depart, all within 60–90 minute “banks.” Airfield tower controllers strive to avoid imbalances and bottlenecks by integrating data from visual cues and from a variety of other sources. However, lengthy, imbalanced taxi

queues are evidence that although sufficient and safe, the controller's mental planning process (given current data sources) is not necessarily optimal. By providing data fusion and automated optimal taxi plan advisories to the ground controller, the controller can operate with improved data-gathering and planning capabilities. Improved dynamic taxi routing, and hence smoother airport operations with less surface taxi delay should result. Eventual national implementation of the Surface Movement Advisor systems (SMA) at the 13 largest U.S. airports is projected to save users at least 5% of the \$1.6 billion annual ground-delay costs incurred as a result of inefficient taxi and runway queuing—based on recent FAA simulations and Air Transport Association cost figures.

The SMA is a series of successive airfield data systems that is being developed as a joint effort between Ames Research Center and the Federal Aviation Administration (FAA). The first proof-of-concept SMA (Build-1) electronically connects the air-traffic control, airline, and airport operations users at Atlanta-Hartsfield airport (ATL) to facilitate information-sharing and data fusion. SMA Build-1 has been in use on a daily basis at ATL by airlines and airport ramp towers since June 1996 and was brought online in the FAA control tower in September 1996. The figure shows an overview of the SMA system that was deployed to Atlanta in 1996.

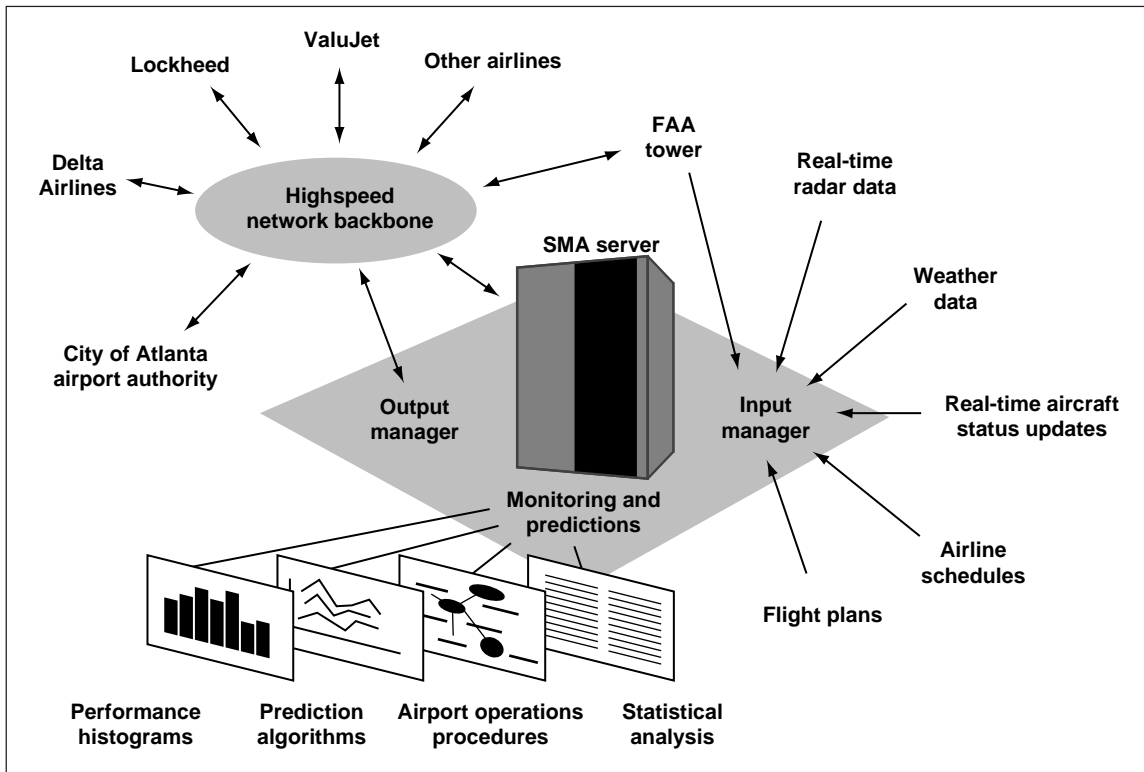


Fig. 1. Overview of the SMA system deployed to Atlanta in 1996.

Running in a commercial transaction-processing database on an off-the-shelf UNIX server, the SMA software currently contains its own tracking, time estimation, data fusion, monitoring and prediction software modules. SMA furnishes data as an ASCII text stream to airline servers, or as separate X/Motif-based touchscreen-capable graphical-user interfaces for the FAA, airline, and airport operations personnel.

Point of Contact: B. Glass
 (650) 604-3512
 bglass@mail.arc.nasa.gov

Simplified Vision Models for Display Quality Assessment

Al Ahumada

Detection and recognition of obstacles (aircraft, trucks, etc.) is crucial for safe aviation operation in the terminal area. Vision models can make an important contribution to display design by allowing computational predictions of the visual adequacy of potential designs for obstacle detection and recognition. The first figure shows a pair of simulated display images, one (panel b) with an obstacle on the runway and one without. Investigators have been measuring the ability

of human observers to make such discriminations and have been constructing and testing computational models to predict their abilities.

Image discrimination models that have been used as image-quality metrics range in complexity from single filter models to multiple-channel models with channels that are selective in spatial frequency and orientation. The simple filter models can be thought of as representing the visual information at precortical levels of the visual system. These models can predict the variations in the visibility of targets that occur as the target spatial frequency changes. The multiple-channel models

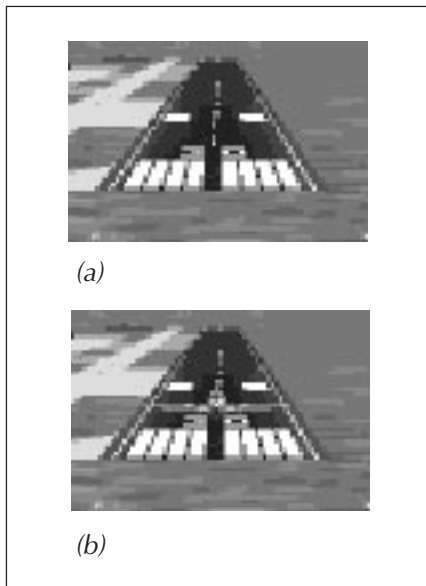


Fig. 1. Panel (a) is a 128 x 128 pixel gray-scale digital image of a simulated airport runway scene. Panel (b) shows the runway scene with an aircraft obstacle.

simulate the orientation and spatial frequency selectivity of cortical cells. Because the channel outputs are nonlinear, the channel models predict masking of targets in high-contrast image regions. For example, the channel models outperform contrast-sensitivity filter models in predicting the detectability of targets in a natural background.

Some recent vision models include between-channel interactions that allow the models to predict masking from image components exciting different channels from those responding to the target. These models have even greater computational complexity. Assuming homogeneity of these interactions leads to a simple contrast masking correction. The second figure diagrams the image discrimination model that results from

applying this correction to a contrast-sensitivity filter model. In comparing the predictions of this model with those of the complex models, it is found that the simple model predicts human visual detection performance just as well.

Point of Contact: A. Ahumada
(650) 604-6257
aahumada@mail.arc.nasa.gov

Perceptually Tuned Visual Simulation

Mary K. Kaiser

Human factors engineering is required to improve the quality of visual displays in aerospace systems. Advanced computer-generated imagery (CGI) systems are used to create compelling visual displays for navigation/control systems, vehicle/system simulation, telerobotics, and scientific visualization applications. The quality of these displays can affect the safety and productivity of flight and ground-based operations. Inevitably, the realism of these displays is constrained by limitations in CGI hardware and software, especially if images need to be generated in real-time. Despite rapid advances in image-generation technology, human operators desire more realistic, higher-fidelity displays; it is likely that this demand for improved fidelity will continue for the foreseeable future.

Research is being conducted to examine techniques aimed at reducing the computational cost required to achieve a desired level of image quality and frame rate. These

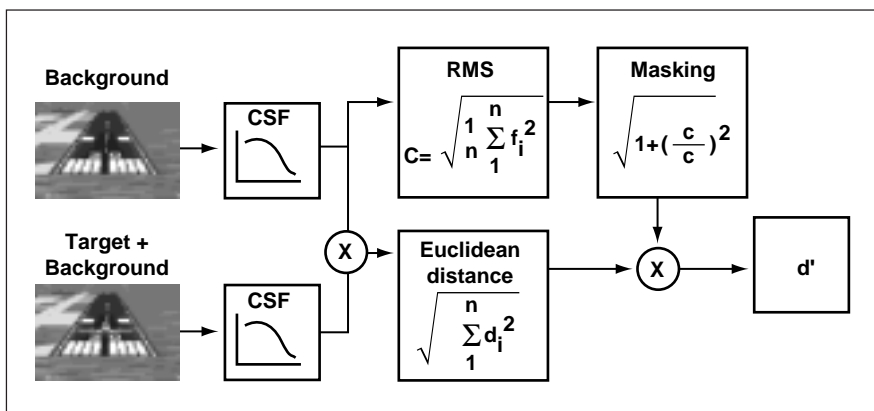


Fig. 2. Schematic of the simple image discrimination model. At the left, the upper image is the background image and the lower image is the target-plus-background image. After the luminance images are converted to contrast images (a step not illustrated), the contrast images are filtered by a contrast sensitivity function (CSF). On the top path, the masking parameter c is the rms value of the background-filtered contrast values f_i . On the bottom path, the corresponding filtered values from the image are differenced and the vector length of these d_i values is divided by the contrast factor to get the predicted number of just-noticeable-differences between the two images.

techniques exploit principles of visual processing to reduce the computational load. This multi-disciplinary research involves a collaboration among research scientists at the Ames Research Center; professors in computer science at Carnegie Mellon University and in psychology/biomedical engineering at the University of Virginia; and designers and engineers at various industry sites.

A set of techniques has been developed for rendering images with enhanced apparent resolution. NASA has applied for a patent for this process (NASA Case: ARC 12080-1). In using this process to create stereo displays, images with different resolutions are shown to the two eyes; examples of this technique are shown in the figures below. The first figure demonstrates varying texture complexity; the second

demonstrates varying polygonal complexity. The resulting fused image appears to possess the higher-resolution detail. User studies conducted with these “hi-lo” stereo displays indicate that people are able to extract stereo-specified depth with these displays about as well as they do with traditional (“hi-hi”) displays. Further, no interference with normal stereo vision results from exposure to the hi-lo displays.

Present efforts focus on further evaluation of the algorithms, the extension of techniques to larger object classes, and the development of generalizable tools suitable for inclusion in a graphics modeling toolbox. Coordination with hardware and software developers seeks to maximize the utility of these techniques and to ensure compatibility with hardware architecture.

The development of a number of rendering techniques that significantly enhance the performance of graphics systems is expected. The goal is to both extend the upper range of graphical rendering performance and to enable lower-end systems to produce visual imagery that currently can be produced only with high-end systems.

Point of Contact: M. Kaiser
(650) 604-4448
mkaiser@mail.arc.nasa.gov

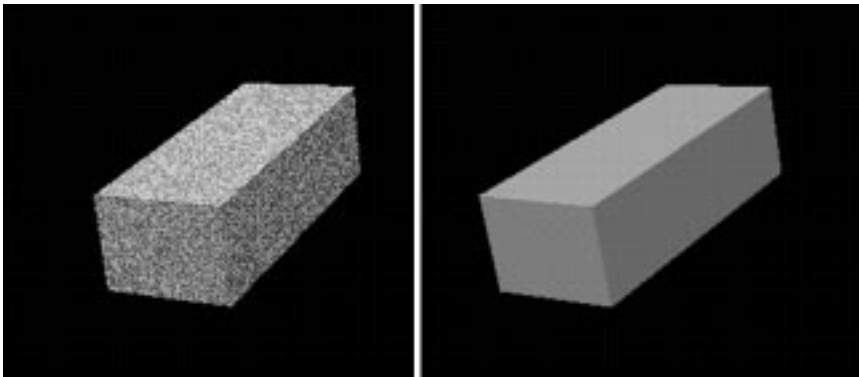


Fig. 1. Only the image presented to the left eye in this stereo pair has texture mapping. Nonetheless, the resulting stereo percept appears textured.

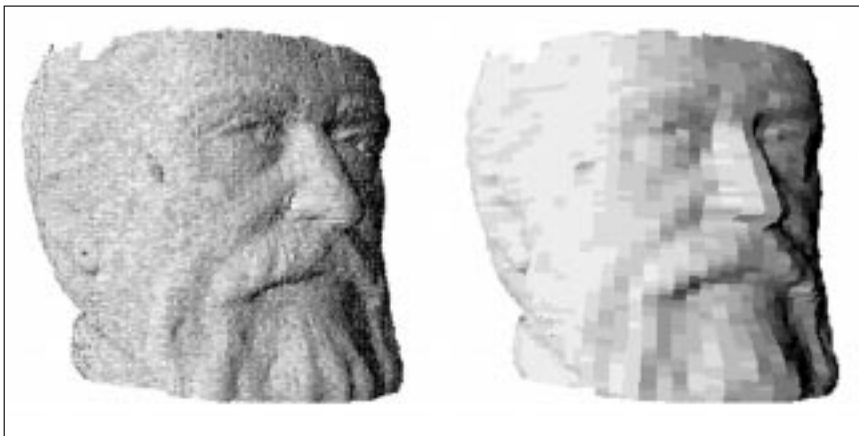


Fig. 2. Another example of “hi-lo” stereo images. Here the left image is created with far more detail (that is, a larger number of polygons is used to model the object) than the one on the right. The resulting stereo perception appears high resolution.

Entropy Masking in Visual Displays

Andrew B. Watson

As part of NASA's Human Exploration and Development of Space Enterprise and Aeronautics and Space Transportation Technology Enterprise, the Vision Science and Technology Group at Ames Research Center is doing research on the human factors of visual displays and visual communication systems. A primary thrust of this effort is to develop computational models of human visual performance that can be used in the engineering design of imaging and display devices. A first goal of human vision models is to predict visibility of arbitrary targets, especially against noisy or cluttered backgrounds that are typical of real imaging environments. This problem is central to applications such as image compression, flat-panel display design, sensor fusion, and design of helmet-mounted and other head-up displays. To meet this challenge, a program has been initiated involving experiments on visual masking: the interference of the background with the detection of visual targets.

As a result of this research, a new category of visual masking has been identified; it is called entropy masking. Previous research over many decades had identified two principal varieties of visual masking: *contrast* masking and *noise* masking. The former refers to a reduction in visual sensitivity resulting from a passive adaptive process. In effect, the gain of visual neurons is turned down when there is a large amount of pattern stimulation, in order to

prevent saturation of the limited dynamic range of the neural response. Noise masking refers to an inevitable reduction in visibility when a random component is added to the visual stimulus. Entropy masking depends on neither gain control nor randomness. Instead, it is due to the observers lack of knowledge about the obscuring background, and it may be ameliorated by increasing that knowledge through learning.

The following experiments illustrate the essentials of entropy masking. The observer attempted to detect the Gabor-function target pictured in part (a) of the first figure; the target was obscured by the addition of one of the masks shown in parts (b) and (c). The mask shown in part (b) is a cosine luminance grating with the same spatial frequency as the target, and that shown in part (c) is a sample of one-octave, bandpass noise with a center spatial frequency equal to that of the Gabor-function target. The two masks were equated in contrast energy so that they would have equal effects on the contrast gain-control system, that is, equivalent contrast masking.

On each trial, the observer received two brief presentations on a cathode-ray-tube monitor. One contained a background only, the other contained a background plus the target. The observer tried to identify the presentation containing the target. The contrast of the target was varied from trial to trial in order to estimate the contrast required for 82% correct performance. To manipulate the degree of randomness, the bandpass mask was (1) new on each presentation

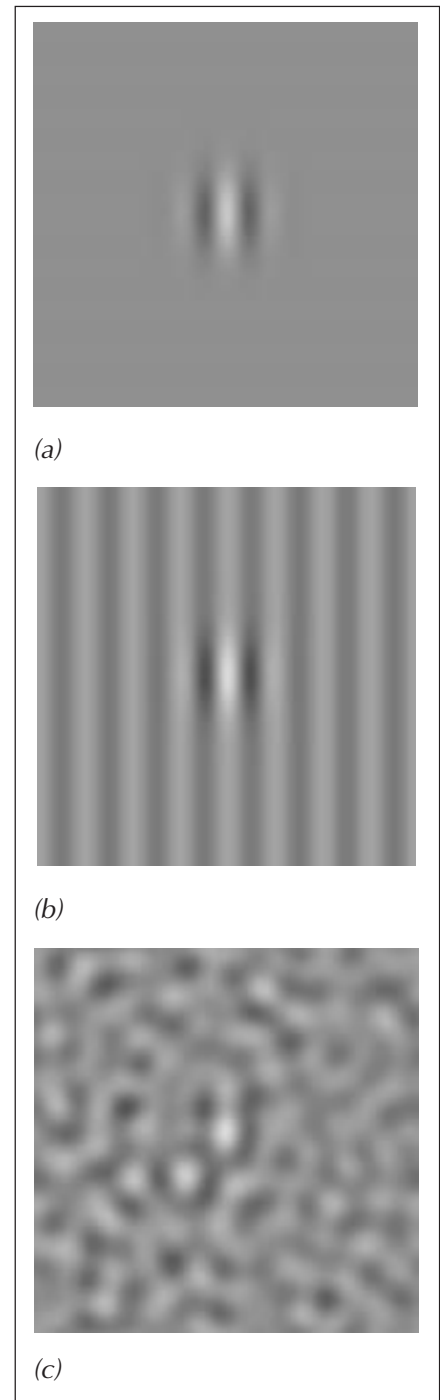


Fig. 1. Visual target (a) and two masks: cosine grating (b) and bandpass noise (c). Each mask is shown with the target added.

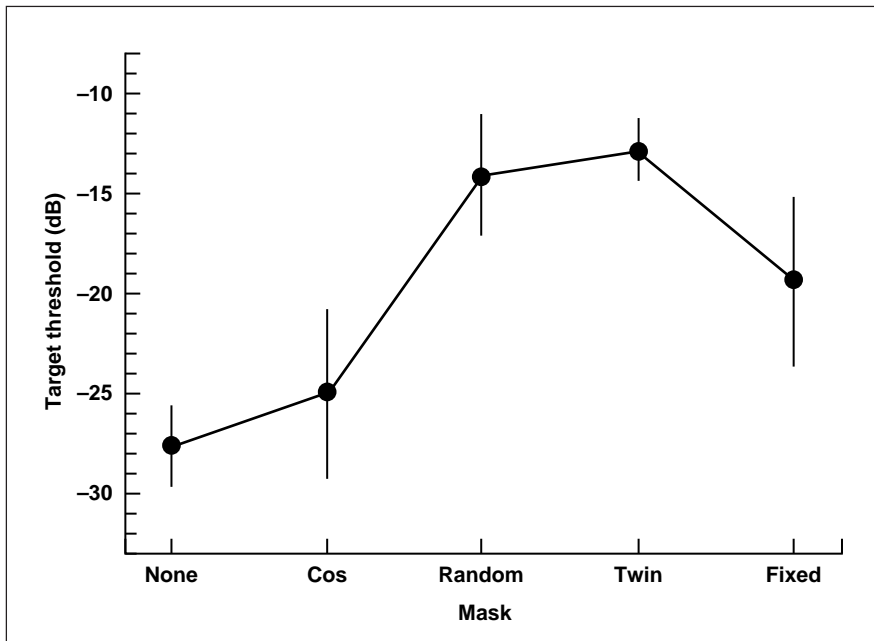


Fig. 2. Target thresholds as a function of mask condition.

(random condition), (2) the same for both presentations of a trial but new for each trial (twin condition), or (3) always the same (fixed condition).

The results are shown in the second figure. The cosine mask elevates the target threshold by a small amount (about 3 decibels), but the random condition produces much more masking. However, the twin condition shows that this masking is not due to randomness, since the masks are identical in the two presentations of each trial. The fixed condition shows that with learning (640, 2176, and 3584 trials were collected from the three observers), a significant reduction in masking is obtained. Indeed, at the end of learning, the threshold is similar to that for the cosine condition. It can be concluded that the

masking effect of the bandpass noise is due to the observer's ignorance about its structure (its entropy).

It is thought that entropy masking is the dominant form of masking in many applied situations. Consequently, it is important to verify its existence and properties in order to enable optimal design of visual communications systems. This work moves NASA closer to its goal of developing a set of general human factors engineering tools that will enhance the safety and effectiveness of its Space and Aeronautics missions.

Point of Contact: A. Watson
(650) 604-5419
abwatson@mail.arc.nasa.gov

Vertical Motion Simulator Advanced Simulator Network

William B. Cleveland

The Advanced Simulator Network (ASN) is an integration of newer and higher-performance host computers and real-time data acquisition networks into the Vertical Motion Simulator (VMS) complex at Ames Research Center. The system provides significantly better performance while retaining the powerful functionality of the previous system. As shown in the figure, the system consists of the data network, instrumentation input/output (I/O), and a host computer together with its interface to the network. In a simulation setting, the pilot's controls are input through the Cockpit CAMAC (Computer Automated Measurement and Control) I/O, passed via the Data Highway and VME interface to the host computer where the aircraft's response is computed and returned via the network highway elements to the motion, cockpit display, and laboratory display devices.

The performance increase of the operational systems is dramatic. By themselves the computers are twice as fast as the computers of just 4-5 years ago. Testing of the new CAMAC instrumentation shows a factor of 10 speed-up in performance over that of the old hardware. These improvements reduce time delays that cause a simulated aircraft to lose stability in comparison with the real aircraft. When there is no real aircraft for comparison, incorrect conclusions are often made

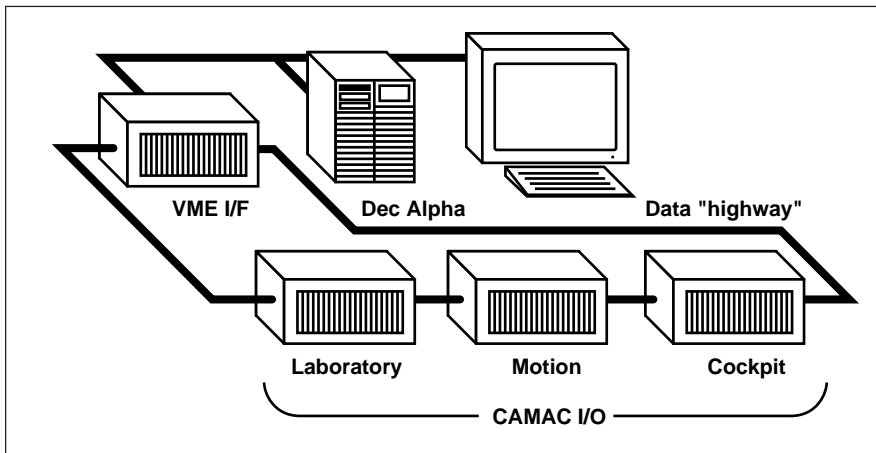


Fig. 1. Advanced Simulator Network.

when the simulator uses poor equipment or techniques. Although the VMS system can operate at 1000 hertz when only I/O is performed with the motion, laboratory, and cockpit subsystems, adding the typical aircraft model allows a 200-hertz operation. Most simulations are near the 60-hertz rate of the associated graphics generators, but the ASN system performance reserve will allow larger model options and I/O rates when needed.

Early in FY96, the first of the systems was installed into an Interchangeable Cab fixed-base simulation laboratory, where it was tested and perfected before it was installed into the VMS. Before the end of FY96, the VMS system had been used in five simulations including astronauts flying the space shuttle vehicle.

Point of Contact: W. Cleveland
(650) 604-5352
wcleveland@mail.arc.nasa.gov

Intelligent Aircraft Control System

Charles C. Jorgensen

The intelligent aircraft control system provides a safety-oriented flight control technology that can efficiently deal with off-nominal and unforeseen changes in aircraft systems or operating environments. The effort accomplishes reconfigurable flight control under damage scenarios by using a modified F-15 aircraft's (ACTIVE) differential canard and vectored thrust capabilities. This effort is a four-year cooperative research contract begun in 1995. It comprises three phases: Phase I, create neural nets (NNs) that model stability and control derivatives in the pitch, roll, yaw, lift, and side force axes of the F-15 ACTIVE aircraft in 1995–96 (see the figure (see Color Plate 2 in the Appendix)); Phase II, develop on-line NNs to process aircraft sensor data in real-time and update the stability and control derivatives in 1997; and

Phase III, flight demonstration of real-time NN control and accident reconfiguration (1997, 1998).

In 1996 major progress was made. Phase I NNs were generated that match the ACTIVE aerodynamics and were programmed into the F-15E computer. Three Phase I NNs were produced: (1) the Leavenburg-Marquardt network at Ames Research Center (ARC), (2) an active selection net at McDonnell Douglas Aircraft Corporation (MDAC), and (3) a neural fuzzy (ANFIS) at Tennessee State University.

Four second-generation on-line networks were developed for Phase II: Radial Basis Networks (MDAC), Recursive Higher Order Neural Network (Washington University), Feedback Linearization Neural Net (ARC), and Dynamic Cell Structures (ARC).

Two on-line aerodynamic derivative estimation methods were developed by MDAC: Kalman Filtering/Recursive Prediction and Locally Weighted Regression. Three Linear Quadratic Regulator Methods were designed by MDAC: (1) Robust Servo, (2) Setpoint Regulator, and (3) SOFFT, Langley Research Center. A full-scale parameter sensitivity analysis was begun for performance envelope, stability, and robustness using the new techniques. A real-time Ricatti equation solver was developed (MDAC), and a new Virtual Reality test environment was developed by ARC using a nonlinear F-15E model.

Point of Contact: C. Jorgensen
(650) 604-6725
cjorgensen@mail.arc.nasa.gov

Facilitating User Route Preferences in En Route Airspace

Bob Vivona, Mark Ballin,
Steve Green, Ralph Bach,
Dave McNally

Under the current air-traffic system, aircraft generally must fly on fixed routes. On the other hand, the Air Transport Association estimates that its member airlines could save \$1.2 billion per year if they were able to fly direct routes. However, relaxing existing routing restrictions will require new conflict-prediction and resolution automation to help controllers maintain required separation while minimizing their effect on their workload. Although some automation now exists (for example, Conflict Alert, which uses a 2-minute prediction based on previous radar hits), for the most part air-traffic controllers detect conflicts by visually monitoring radar tracks and, when necessary, issuing resolution advisories to aircraft to avoid loss of separation (5 nautical miles horizontal, 2000 feet vertical). Conflict-prediction and resolution tools for controllers are being developed under the Advanced Air Transportation Technology program at Ames Research Center. The objective of this work is to develop an operational concept and associated software for use of conflict-prediction information in order to generate minimum-cost resolution advisories to facilitate increased user route preference in en route airspace.

A wide range of traffic environments is found in the National Airspace System. At one extreme is en route airspace away from busy terminal areas consisting of aircraft generally not constrained by traffic or weather. If traffic density is low, very little ground-based air-traffic control intervention is required. At

the other extreme is the en route area near busy terminal areas where aircraft must be merged for spacing and sequencing. The system is supplied with real-time tracking radar and flight plan information from the air-traffic control facility's host computer. The Airspace Tool (AT) is designed to achieve user

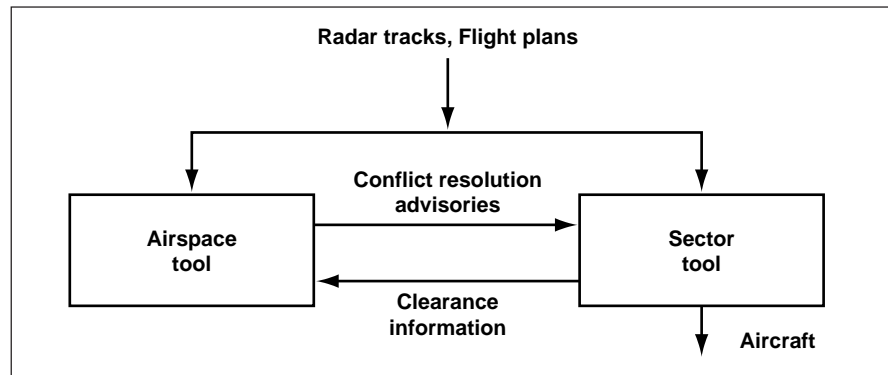


Fig. 1. Operational concept for user-preferred routing in en route airspace.

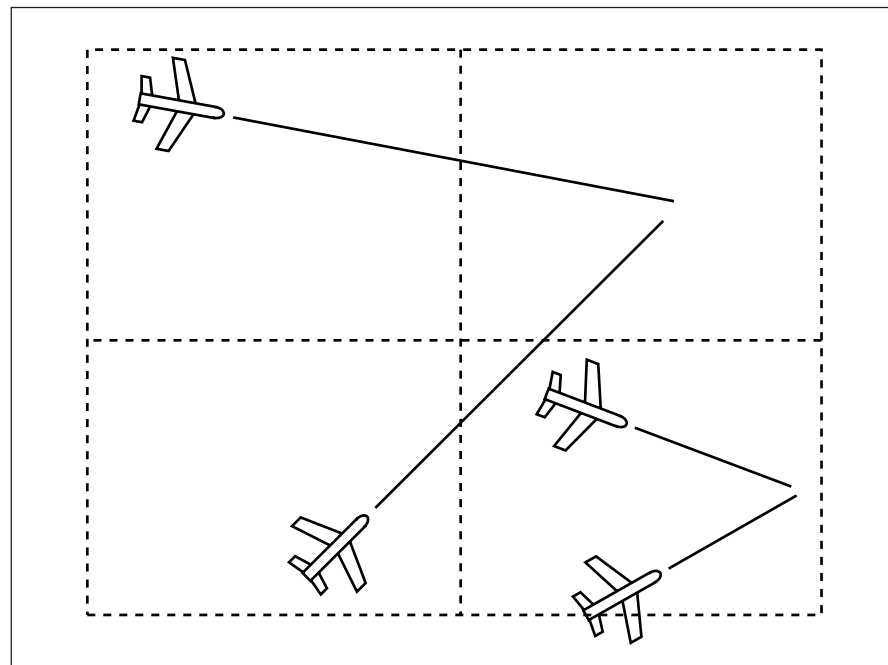


Fig. 2. Sample airspace with four sectors showing two typical conflict scenarios.

efficiency for long time-horizon (15–25 minutes), generally inter-sector conflict-predictions by generating resolution advisories based on minimum cost deviation from user-preferred routes. Reduced controller workload is also achieved through inter-sector conflict resolution. The Sector Tool (ST) facilitates controller planning within a sector for short time-horizon conflict-prediction, trial plan (“what if”) solutions, and transition to the terminal area (see first figure).

The second figure shows a simple example of en route airspace with four sectors and two sample conflict scenarios. In both cases a minimum-cost resolution advisory is computed by the AT. For the case in which the conflict is predicted across sector boundaries, the AT passes a suggested advisory to the appropriate sector. Each resolution is checked by the sector controller with the aid of the ST, and, if acceptable, is issued to the aircraft by the controller.

The Center-TRACON Automation System software is being used as a baseline for development, simulation, and field testing of the operational concept.

Point of Contact: D. McNally
(650) 604-5440
dmcnally@mail.arc.nasa.gov

Conflict Probability Estimation for Free Flight

Russell A. Paielli, Heinz Erzberger

The Air Transport Association estimates that the U.S. airline industry could save several billion

dollars annually in direct operating costs if the Federal Aviation Administration (FAA) would relax routing restrictions and adopt a policy of “free flight.” The safety and efficiency of free flight will benefit from automated conflict-prediction and resolution advisories to help air-traffic controllers maintain the required separation between aircraft while minimizing the effect on trajectories. Trajectory prediction is less certain the further in advance a prediction is made, however, so conflicts cannot be predicted exactly. A method is needed,

therefore, to estimate the probability that a conflict will occur between a given pair of aircraft. This conflict-probability estimate is important for determining both how and when to optimally resolve conflicts.

An error model and an algorithm have been developed to determine conflict probability. Based on analysis of actual air-traffic data, the trajectory-prediction errors are modeled as being normally distributed (Gaussian), with the along-track error growing with prediction time as a result of wind modeling error, as shown in the first figure. The two

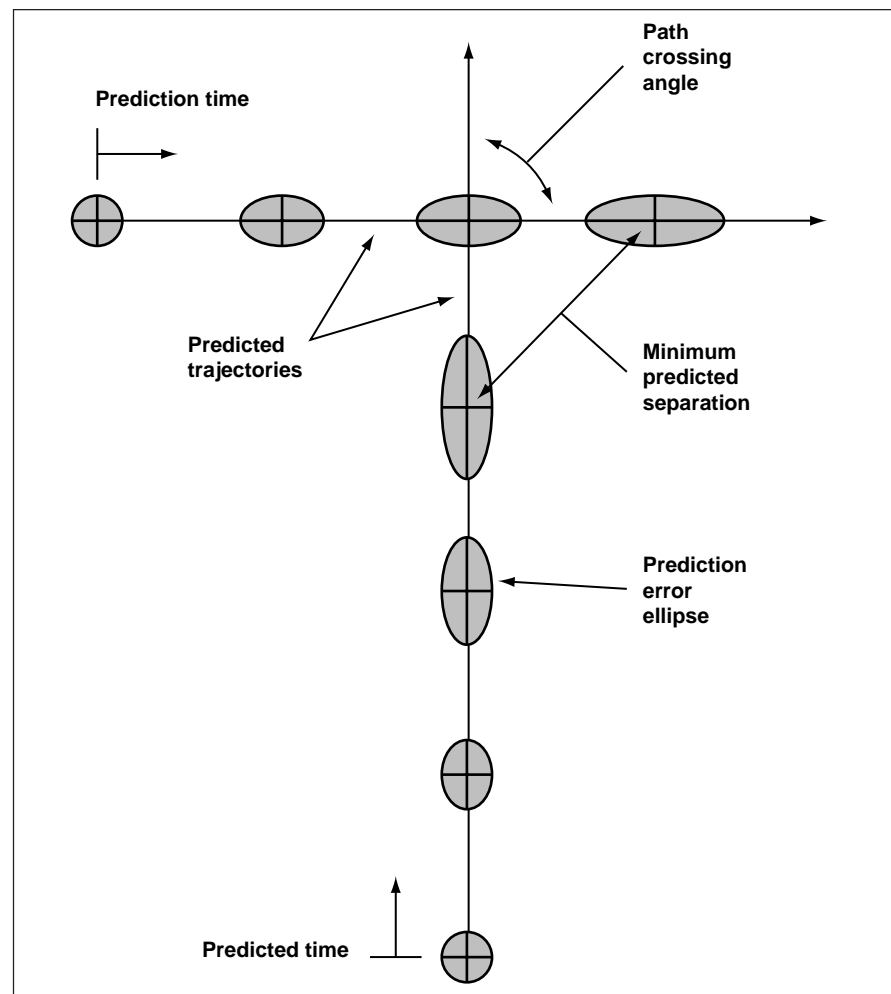


Fig. 1. Trajectory prediction error ellipses.

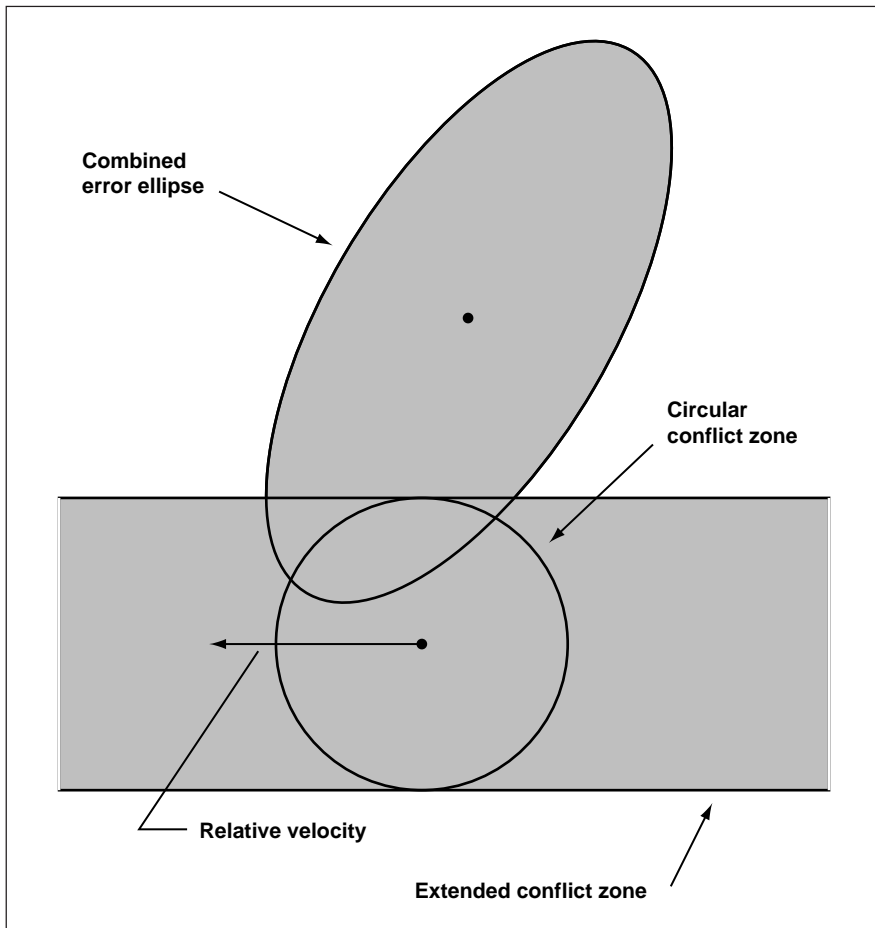


Fig. 2. Encounter geometry.

error covariances for an aircraft pair are combined into a single equivalent covariance of the relative position. The second figure shows the combined error ellipse (based on the combined covariance) centered on one aircraft and the circular conflict zone centered on the other. The extended conflict zone is the projection of the circular conflict zone in the direction of the relative velocity. In two dimensions the conflict probability is the volume under the probability-density function that is within that extended

conflict zone. In three dimensions the basic concept is similar but more difficult to illustrate.

A coordinate transformation based on the Cholesky decomposition (“square-root” factorization) of the combined covariance is used to derive an analytical solution for the conflict probability. If the Gaussian error model were exact, this solution would be exact for level flight and a good approximation for nonlevel flight. This analytical solution is computationally far more efficient than an alternative solution based on

numerical integration. Efficiency is important because the algorithm is intended to run in real time. The high efficiency also makes the algorithm a convenient tool for analyzing the effects of various parameters.

The algorithm was programmed in C++ and successfully tested by Monte Carlo simulation over a wide range of encounter geometries. It has also been integrated into the Center/TRACON Automation System (CTAS). CTAS is a large software system developed at Ames Research Center to help air-traffic controllers do their job more efficiently and with less stress. In this context, CTAS predicts the trajectories, determines the states of the aircraft at the predicted point of minimum separation, and sends that state information to the conflict-probability algorithm. The probability results are then used by CTAS to determine if a predicted conflict should be displayed to the controller. The system is currently being tested on both live and recorded air-traffic data that are sent to Ames on a dedicated line from Denver Center.

Point of Contact: R. Paielli
(650) 604-5454
rpaielli@etna.arc.nasa.gov

Conflict Prediction Algorithms: Initial Field Test

Dave McNally, Bob Vivona,
Karl Bilimoria, Gerd Kanning,
Steve Green, Ralph Bach,
Allan McCrary, Ed Lewis

The Federal Aviation Administration (FAA) is responding to the needs of the aviation community by exploring the concept of “free flight” for aircraft flying under instrument flight rules. In free flight, en route aircraft fly user-defined trajectories (defined by pilots or airlines) with only minimal air-traffic control (ATC) adjustments to avoid restricted airspace and loss of separation from other aircraft. To facilitate user-preferred routing in all en route environments, an extension of the ground-based Center-TRACON Automation System (CTAS) is being developed under the Advanced Air Transportation Technology program at Ames Research Center. The first step is to add en route conflict-prediction capability to the CTAS software baseline. When fully developed, en route conflict-prediction and resolution capability should achieve many free-flight benefits without significantly altering current ATC procedures or requiring modification of airborne equipment.

An initial field test was conducted from September 24 through October 8, 1996, at the Denver Air Route Traffic Control Center (ARTCC or “Center”). The purpose was to conduct an initial evaluation of an en route conflict-prediction software, to evaluate an advanced tracker developed by the BDM Corporation

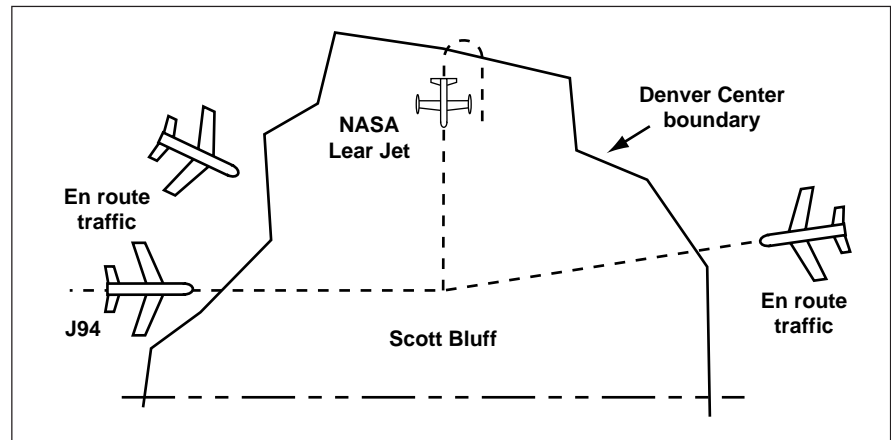


Fig. 1. Flight profiles for initial field test of en route conflict prediction.

and the FAA Host computer tracker, and to get an initial look at operational issues pertaining to en route conflict prediction. The Ames Lear Jet flew at angles of 0, 45, 90, 135, and 180 degrees with respect to jet route J94 near Scotts Bluff (see figure) to create (horizontal plane) conflicts with normal Center traffic, while maintaining normal safe altitude separation at all times. The NASA Jet recorded differential Global Positioning System (GPS) position and velocity data to evaluate the trackers. A version of CTAS software, modified for en route conflict prediction, processed live radar, flight plan, and wind data for all aircraft in the Denver Center. Predictions of minimum horizontal separation between the NASA aircraft and each selected aircraft were begun nominally 20 minutes

before the predicted time of minimum horizontal separation and continued just beyond minimum separation.

A preliminary analysis of the data shows that minimum horizontal separation was predicted with 1.5-mile accuracy during the 15–25 minute period before the time of actual minimum separation. This is well within the FAA separation criteria of 5 miles for en route airspace and 3 miles for the terminal area. These results are based on horizontal separation data related to the distances between the NASA Jet and each of 59 other aircraft of various types over 8 days of test flights.

Point of Contact: D. McNally
(650) 604-5440
dmcnally@mail.arc.nasa.gov

Assessing Controller Performance Under Simulated Free-Flight Conditions

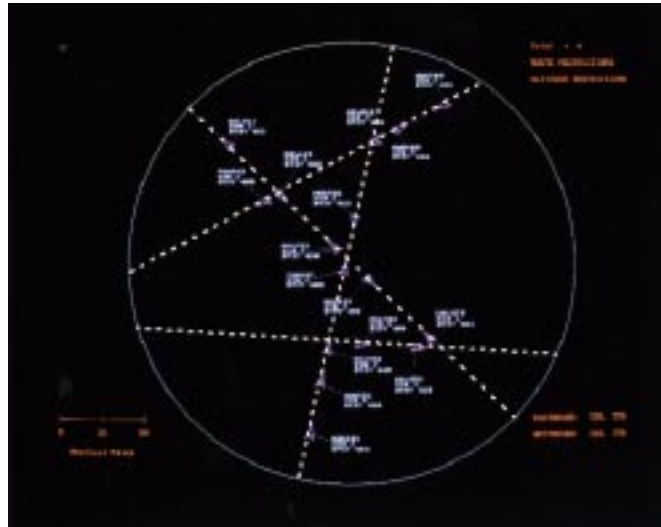
Roger Remington, James Johnston, Eric Ruthruff, Maria Romera

Traditional air-traffic control procedures restrict air traffic to designated routes and altitudes, analogous to highways in the sky. It is well understood that these regulations, although promoting safe air travel, impose a price on the airlines in increased flight time and increased fuel consumption. NASA is presently working with the Federal Aviation Administration (FAA) to develop plans to relax these constraints on air traffic so that airlines would be free to choose routes that minimized delays and fuel costs. Free-flight refers to a family of proposed concepts ranging from the relaxation of a few constraints to total freedom of choice of flightpath. The goal of this joint NASA-FAA activity, the Advanced Air Transportation Technology program, is to ensure that the relaxation of constraints on airspace operations do not compromise safety. The Cognition Laboratory at Ames Research Center has been investigating the effects that relaxing airspace constraints can have on controller performance.

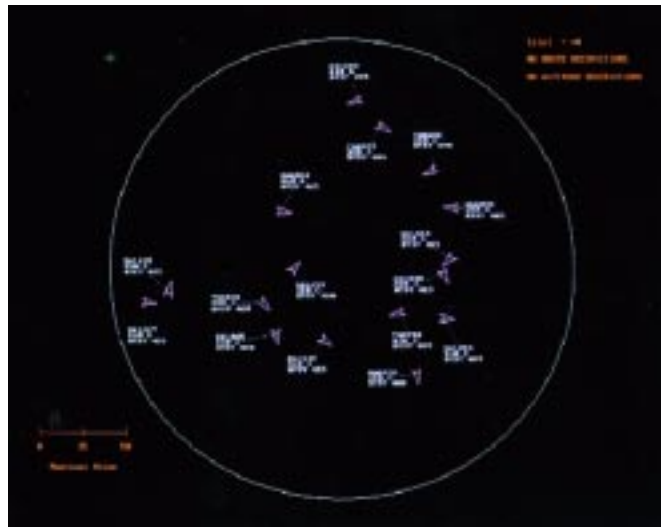
The extent to which constraints can be relaxed and free flight enhanced is assumed to depend, in part, on the workload of flightcrew and air-traffic control (ATC). Regardless of how future responsibility is

divided between pilots and controllers, the safety of the overall system will depend heavily on the ability of controllers to perform their jobs well. One of the tasks of controllers will be to look at situation displays and understand the traffic, including the position and paths of the aircraft

displayed. Under the present system this kind of “situation awareness” is facilitated by virtue of traffic patterns that are orderly and have a familiar structure. Research on human cognition suggests that reducing the structure present in traffic flows might make it more difficult for



(a)



(b)

Fig. 1. A traffic display. (a) With route restrictions. (b) Without route restrictions.

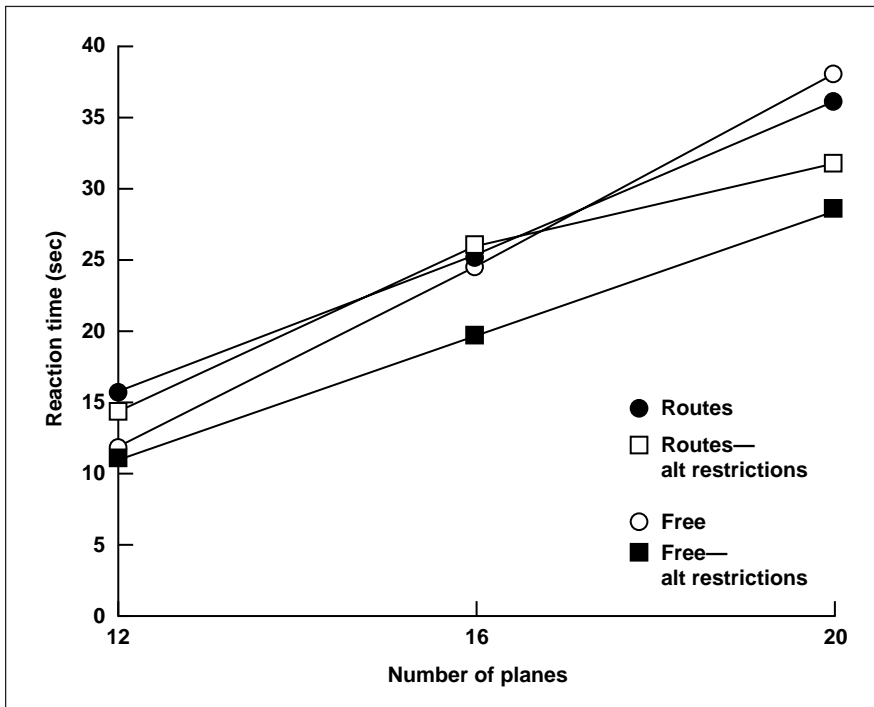


Fig. 2. Conflict detection time as a function of number of aircraft on screen for the four restriction conditions.

controllers to maintain situation awareness.

A series of experiments has been conducted to determine empirically whether controller situation awareness is hindered by the loss of traffic constraints under free flight. To measure situation awareness, the experiments tested the speed with which controllers could find conflicts in traffic displays. The experimental design contained four conditions: the status quo (both fixed routes and fixed altitude restrictions), free flight (neither fixed routes nor fixed altitude restrictions, fixed routes only, or fixed altitude restrictions only). Part (a) of the first figure shows a traffic display with route restrictions; part (b) of the first figure

shows a traffic display with the same number of aircraft in which route restrictions have been eliminated. In addition, the number of planes displayed was systematically varied. The second figure shows the results of one of the experiments in which experienced controllers detected the presence of conflicts with the aid of a computer conflict-assessment tool. The number of aircraft had strong effects on performance; detection times increased with increased number of planes in all conditions. Removing route restrictions did not negatively affect performance, but removing altitude restrictions did have a modest negative effect. Similar results have been obtained in conditions without computer-

assisted conflict detection. The overall results to date provide no reasons for pessimism about the feasibility of considerable progress toward the objective of free flight.

Point of Contact: R. Remington
(650) 604-6243
rremington@mail.arc.nasa.gov

Evaluating Cockpit Display of Traffic Information Displays and Route Assessment Tools for a Free Flight Environment

Vernol Battiste, Walter W. Johnson

The Radio Technical Commission for Aeronautics (RTCA) Task Force 3 report on free flight recommends the immediate initiation of “the development of standards for a cockpit situational awareness display of traffic information.” In response to these recommendations, the Advanced Air Transportation Technologies Program and the Flight Management and Human Factors Division at Ames Research Center have initiated research on display designs and formats to support flight deck self-separation during free-flight operations.

The primary goals of this effort are to (1) conduct research to support the development of display guidelines, and (2) evaluate and design cockpit display concepts and prototypes in support of cockpit-based separation during nominal and off-nominal operations from departure to arrival including the en route and transition phases of flight.

Three critical areas have been identified in the display design research: (1) alerting; (2) situational awareness; and (3) conflict resolution. These three areas are interrelated, and require an integrated approach to arrive at good Human Centered Design recommendations.

The research approach has been to identify attributes of displays that are critical to crew alerting and conflict resolution, and also to apply basic and advanced principles of good display design. Two critical attributes that have been identified are the surveillance data needed and the format of the display. The main principles guiding the Cockpit Display of Traffic Information (CDTI) design effort are to minimize head-down time and dwell time, to reduce scan frequency, and to improve information extraction. Another principle is minimizing the effect of alerts by providing enough advanced warning so pilots can have adequate time to plan for potential problems. Finally, the design considers that other cockpit duties prevent the crew from focusing their full attention on the task of self-separation.

Based on these principles and guidelines, an initial prototype Airborne Management of En route Separation (AMES) display was designed. To support the assessment of alternative route planning, a Route Assessment Tool (RAT) was designed and incorporated into the display design. The AMES display prototype was integrated with the B-747 Navigation display and the RAT controls were located on the top of the dash (see figure). The display was a two-dimensional track-up god's eye view of the traffic situation that provided pilots with an

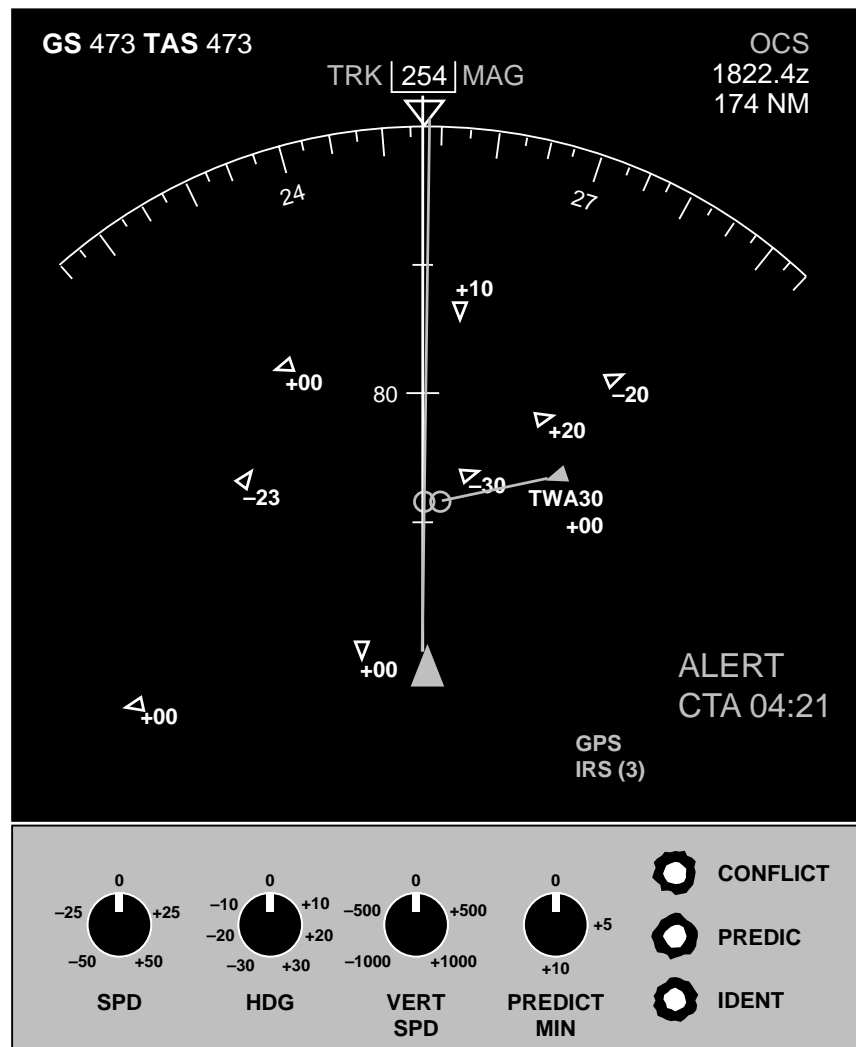


Fig. 1. Airborne Management of En Route Separation (AMES) display and Route Assessment Tool (RAT).

evolving four stage (threat-level) depiction of the traffic, based on the output of a collision alert system developed at the Massachusetts Institute of Technology. In addition, this display allowed pilots to depict the predicted location of traffic up to 10 minutes in the future, and to assess the safety of pilot-proposed route deviations.

The AMES display and RAT were evaluated by 10 Boeing 747

line pilots during a Crew Vehicle Systems Research Facility B-747 simulation of free-flight operations. During the simulation the AMES display was compared with a more basic display that had only one level of alerting and no RAT tool. This simulation examined performance during eight en route traffic scenarios incorporating multiple "traffic" aircraft, and one "intruder"

aircraft on a conflict course, and used flight procedures based, in part, on FAA rules guiding separation during VFR flight. The data from the simulation show that pilots using the AMES display were able to maintain a significantly wider margin of safety between own-ship and intruder, and a lower overall level of conflict probabilities between own-ship and intruder, and between own-ship and other context aircraft. The analysis also showed no increase in the amount of maneuvering with the AMES compared with the basic display, and in fact showed less maneuvering with the AMES display under some circumstances. Crew comments on the display design were all very favorable, and suggested that self-separation would be possible if these types of displays and tools were available on the flight deck.

**Point of Contact: V. Battiste/
W. Johnson**
(650) 604-3666/3667
vbattiste@mail.arc.nasa.gov
wjohnson@mail.arc.nasa.gov

Cockpit Displays for Low-Visibility Taxiing

David Foyle, Elizabeth M. Wenzel,
Durand R. Begault

These cockpit display projects (as part of NASA's Terminal Area Productivity (TAP) program) are aimed at developing candidate cockpit display and audio technology for the improvement of civil transport (airline) taxi performance for navigation and traffic avoidance,

when visibility is limited to 300 to 700 feet by fog or rain.

Two display technologies were investigated: a head-up display and an audio collision avoidance system. In the first, taxi guidance symbols are shown on a head-up display (HUD). A HUD is a clear, glass display mounted in the aircraft such that the pilot can see through it to view the out-the-window taxiway, and at the same time see information that is reflected on the display itself. This allows for display information viewing while still maintaining out-the-window viewing.

The taxi symbology for the HUD is a subsystem of the Taxiway Navigation and Situation Awareness (T-NASA) System. The other subsystems are a perspective moving-map display, showing the plane's position at the airport, and three-dimensional (3-D) audio which alerts to the direction of potential traffic incursions. For this project, superimposed HUD symbols showing current location and ground speed, as well as pictorial

augmentations to the scene, have been developed (see first figure). The superimposed text symbols, the "Inner, Alpha/Bravo" format, represents the current runway or taxiway segment ("Inner Taxiway"), the last intersection passed ("Alpha"), and the next intersection upcoming ("Bravo").

The pictorial scene augmentations include visual enhancements that aid the pilot in following the taxiway clearance and completing turns. Using satellite positioning, the symbology is projected virtually in 3-D such that the symbols move and change size in the same manner as if they actually existed in the out-the-window scene. We have termed this "scene-linked symbology." Vertical cones on the side of the commanded taxiway path depict the cleared route on the HUD in superimposed symbols. These are conformal and represent a virtual representation of the cleared taxi route on the HUD. The side cones and the centerline markings are shown repeated every

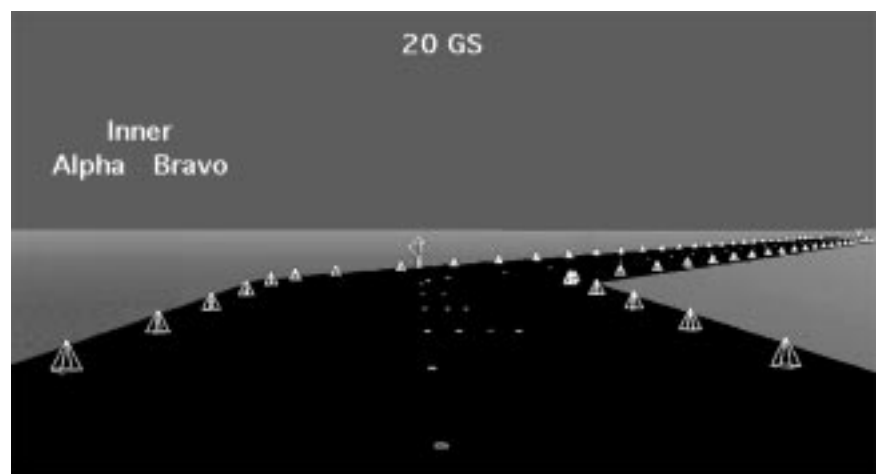


Fig. 1. Scene-linked symbols (in white) superimposed on runway scene.

50 feet down the taxiway. The vertical development and constant spacing should yield increased capability for estimating ground speed, drift, and look-ahead capability for turns. Turn “countdown” warnings are shown in which each turn has countdown (4, 3, and 2) centerline lights that are 300, 200, and 100 feet, respectively, before each turn. This gives added distance cues for the turn. Virtual turn signs (with the arrows) give an added cue that a turn is necessary. In addition, the angle of the arrow on the sign represents the true angle of the turn (that is, 30 degrees right for a 30-degree right turn). All of the HUD symbols are scene-linked (virtually projected as if they were real objects in the world), allowing the pilot to process the symbology in parallel with other traffic, including possible incursions.

Simulation results have shown that the taxi HUD symbology allows pilots to taxi faster in low-visibility conditions and essentially eliminates straying off of the cleared ground taxi route. These benefits have the added bonus of also being associated with decreased workload.

The second display technology investigated was a 3-D audio Ground Collision Avoidance System (GCAS) and navigation system—spatially localized auditory traffic and navigation alerts. Additionally, the Crew Roles and Procedures project is assessing the effect of these advanced technologies on the cockpit crew and controllers, as well as recommending procedure modifications as necessary.

Broadly stated, the TAP initiative utilizes differential global position

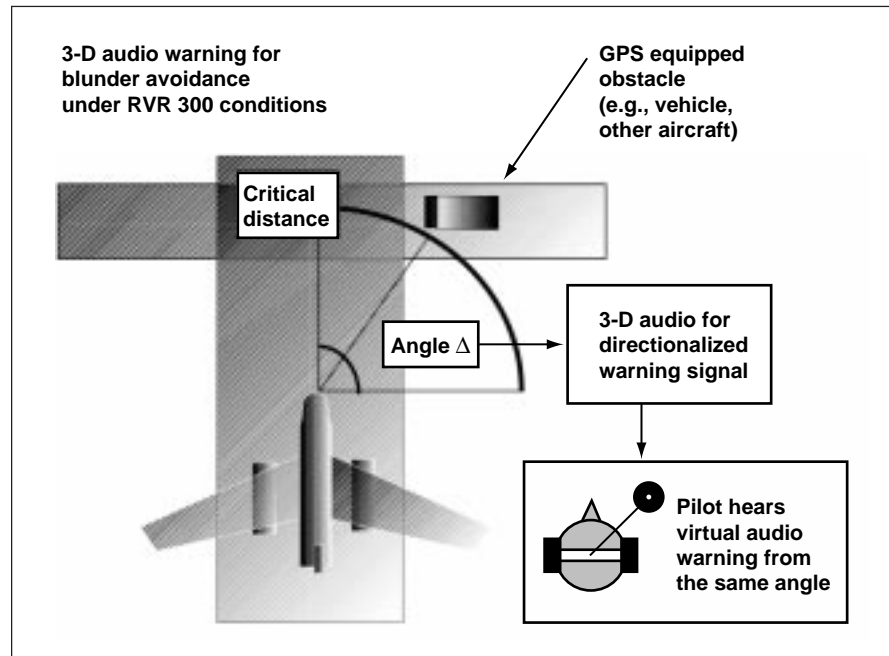


Fig. 2. Illustration of the 3-D audio GCAS display for the terminal-area productivity program.

sensing (DGPS) to track aircraft and other vehicles on the ground, and then uses this information to provide visual and auditory situational awareness by means of advanced guidance systems and displays. A 3-D auditory display is used as a ground collision avoidance system (audio GCAS; see second figure) to provide immediate situational awareness of crossing runways, of potential incursions, and of the aircraft being “off-track” (deviating from centerline).

A full-mission simulation study was run using 12 crews in a B-747-400 simulator. It was hypothesized that there would be a significant pilot preference for an audio GCAS system to be included on the flight deck. That preference for the audio GCAS system was found. The

main conclusions of the study were that an audio GCAS system would be useful for avoiding potential incursions under both normal and low-visibility conditions, and that an auditory system presenting incursion alerts would be a useful adjunct to a moving-map display. A positive preference was also found for the stereo headsets that were used to provide the 3-D audio cueing.

**Point of Contact: D. Foyle/
E. Wenzel
(650) 604-3053/6290
dfoyle@mail.arc.nasa.gov
bwenzel@mail.arc.nasa.gov**

Multi-Sensor Image Registration

Misha Pavel, Al Ahumada,
Barbara Sweet

The use of various imaging sensors that can penetrate obscuring visual phenomena (such as fog, snow and smoke) has been proposed to enable aircraft landings in low-visibility conditions. Images can be obtained from both active and passive sensors that are sensitive to electromagnetic energy in the visible, infrared, and millimeter wavelengths. Images can also be constructed from database information, by rendering an image of the database viewed from the estimated position of the aircraft. The focus of the current research effort is the development of image registration (superimposition) techniques in support of this application.

Two challenges specific to multisensor registration must be overcome. First, the features in two different sensor images can be quite different. For example, the contrasts can be reversed; the runway might be bright in a visible-light image and dark in an infrared image. Previously derived procedures for image registration rely on a high degree of common features between the two images. However, for this application, there is no guarantee that this exists; features apparent in one sensor might not be apparent in the other. Secondly, the two sensors are usually sited at different locations. This differential positioning can produce distortions of the images

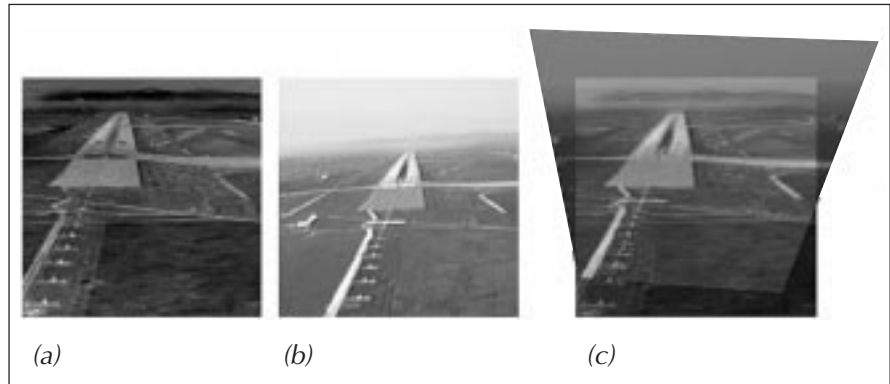


Fig. 1. Forward-looking infrared image (a), visible-light image (b), and the registered image pair (c).

relative to each other which make registration more challenging.

A standard method of registering two images is to find a spatial warping of one image that minimizes the sum of the squared differences between the two images. However, for images from different sensors, this does not work because the images are not the same when the warping is correct.

The figure shows results from NASA's new method. It estimates the image polarity relationship separately in local regions and drops regions from the difference measure that do not correlate well locally. The new method makes it possible to find the correct spatial transformation despite local differences in feature polarity and despite image features that are unique to a sensor.

**Point of Contact: A. Ahumada/
B. Sweet**
(650) 604-6257/0006
aahumada@mail.arc.nasa.gov
bsweet@mail.arc.nasa.gov

Flow Visualization of a Full-Scale Rotor in Hover

Benton H. Lau, Alan J. Wadcock,
Gloria K. Yamauchi

The rotorcraft industry has strongly recommended that wake geometry and vortex strength be measured in addition to airloads and acoustic measurements during rotorcraft wind-tunnel tests. The existing aeroacoustic analyses require all three kinds of data for validation purposes, especially when predicting blade-vortex interaction (BVI) noise. Accounting for blade deflection is also important in accurately predicting BVI noise and in validating aeroelastic analyses. In response to industry, Ames Research Center initiated a test program to evaluate several flow-visualization and blade-displacement measurement techniques for a full-scale rotor. Three techniques were evaluated on an XV-15 tiltrotor in hover in the Ames 80- by 120-Foot Wind Tunnel.

Flow patterns on a rotating blade can be visualized using fluorescent microtufts. Thousands of fluorescent microtufts were installed on the upper surface of a rotor blade. When illuminated by a powerful ultraviolet strobe, the blade motion was frozen and the microtufts displayed the flow pattern. The microtuft images were subsequently captured on film over a

range of thrust conditions including rotor stall.

Rotor-wake geometry can be measured using laser-sheet and flow visualization (see figure). A smoke dispenser was installed near the rotor tip, and an optics pod was placed below the rotor plane on the wind-tunnel floor. When fed with a laser beam via a fiber optic cable, the pod generated a thin laser sheet

and illuminated the entrained smoke in the rotor wake. Images of the rotor-wake geometry were recorded on video at several thrust conditions. In addition to testing the standard tiltrotor blades, a series of subwings were tested and their effects on wake geometry and tip-vortex roll-up were evaluated.

Blade displacement was measured using a stereo imaging technique. Retro-reflective targets were placed along the blade span on the upper surface. Two asynchronous video cameras and strobes mounted in the wind-tunnel ceiling were used to capture the frozen blade motion. The blade displacement or deformation can be deduced from the positions of these targets.

The success of these test techniques provides promising results for hover testing of a full-scale rotor. The test techniques can be applied to forward flight testing.

Point of Contact: B. Lau
(650) 604-6714
blau@mail.arc.nasa.gov

Skin-Friction Measurements on a Hovering Rotor

Alan J. Wadcock, Gloria K. Yamauchi

A technique for acquiring skin-friction measurements on a fixed wing using a fringe-imaging skin-friction (FISF) technique was developed at Ames Research Center in the early 1990s. As long as the flow conditions are steady, as they are in hover, this technique can also be applied to rotary wings. During a

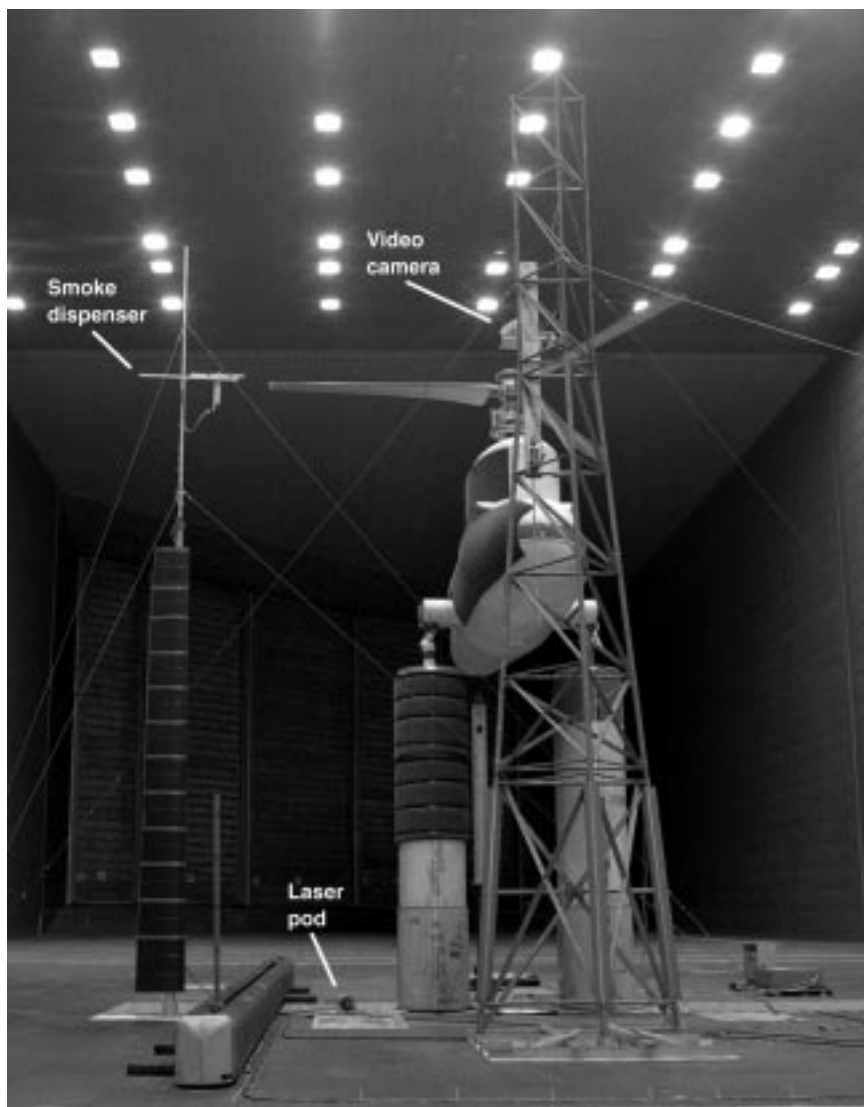


Fig. 1. XV-15 tiltrotor and laser sheet setup in the 80- by 120-Foot Wind Tunnel at Ames.

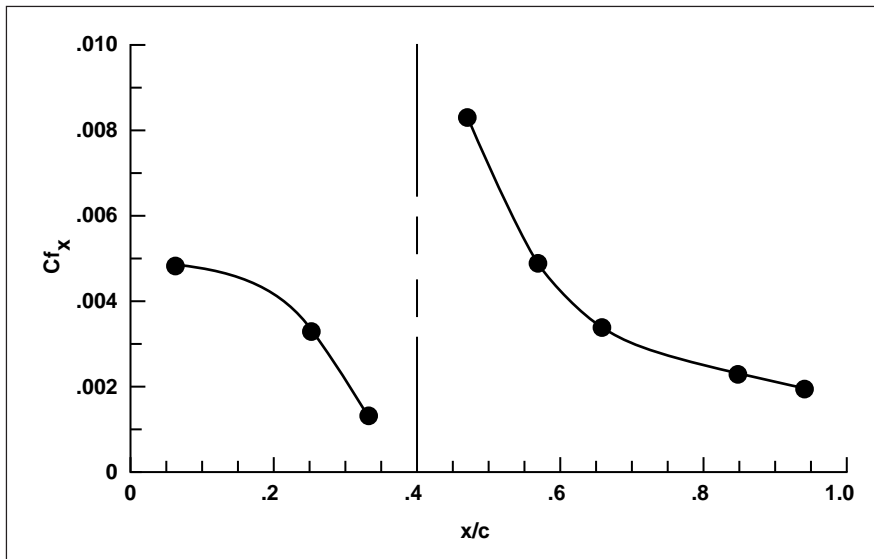


Fig. 1. Chordwise skin-friction coefficient.

hover test of a full-scale XV-15 tiltrotor in the 80- by 120-Foot Wind Tunnel at Ames, the FISF technique was demonstrated for the first time on a rotor.

The objective of this first demonstration was to determine the practicality of the FISF technique when applied to a full-scale rotor. Since the FISF technique had not been used previously in a rotating-flow environment, the effect of centrifugal force on the fringe patterns was a concern, as were the transient effects caused by starting and stopping the rotor. The effect of transients was minimized by remaining on the test condition for a suitable length of time. The effect of centrifugal force was shown to be negligible, once the oil-film thickness was reduced sufficiently. Chordwise skin-friction coefficient measurements were acquired at one low-thrust condition at three blade radial stations. Measurements on the XV-15 tiltrotor blade at a radial

station of $r/R = 0.24$ are shown in the accompanying figure for a tip Mach number of 0.59, a thrust coefficient of 0.0035, and a Reynolds number of 1.1 million. The measurements clearly indicate the location of the transition from laminar to turbulent flow.

Point of Contact: A. Wadcock
(650) 604-4573
awadcock@mail.arc.nasa.gov

Rotor Data Correlation

Randall Peterson

The use of wind-tunnel test measurements, flight-test measurements, and analytical predictions plays a key role in the development of new rotor systems. Such tests are typically performed by using a range of rotor-system sizes and wind-tunnel test facilities. To ensure the accuracy of wind-tunnel testing

methods, an experimental validation study was conducted using test results from model- and full-scale tests to compare with flight-test data.

Accurate measurements of rotorcraft performance as measured in a wind tunnel are strongly influenced by the test-section configuration, that is, whether it is a closed or open jet. The influence of wind-tunnel walls on the induced velocity of lifting bodies has been studied by many researchers over the years. Methods have been developed to adjust the angle of attack and dynamic pressure for fixed-wing aircraft in wind tunnels to approximate free-flight conditions. These methods have largely been adopted by the rotorcraft community with very little testing to verify their applicability to helicopter rotors and flight-test measurements.

Tests conducted by the Deutsche Forschungsanstalt für Luft- und Raumfahrt e.V. (DLR) in the Duits-Nederlandse Wind Tunnel (DNW), under the auspices of the U.S. Army/German Memorandum of Understanding on Cooperative Research in the Field of Helicopter Aeromechanics, have provided data suitable for evaluating these methods. A 40% scale-model BO-105 rotor was tested in five different wind-tunnel test sections: (1) 6- by 6-m closed, (2) 8- by 6-m closed, (3) 8- by 6-m open slots, (4) 9.5- by 9.5-m closed, and (5) the 8- by 6-m open jet. These data along with full-scale data from an Ames 40- by 80-Foot Wind Tunnel test and a DLR flight-test program provided a means to evaluate wind-tunnel wall-correction methods specifically for helicopter rotors. Good correlation

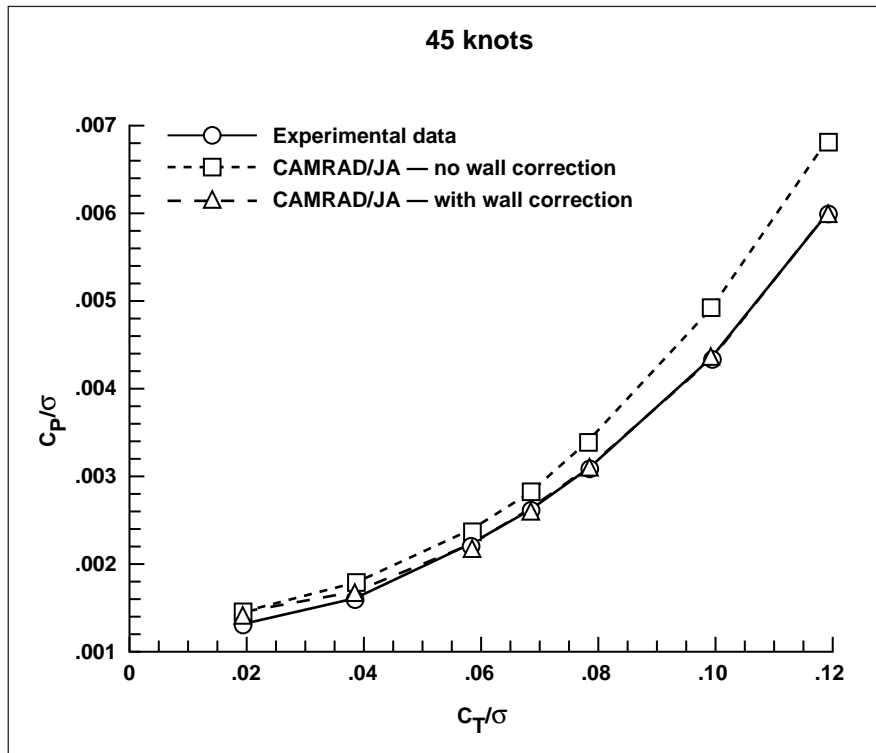


Fig. 1. Rotor power with and without angle-of-attack correction applied to the trim conditions of the rotor in the analysis.

of rotor power over a range of advance ratios for these three datasets was shown using wall-correction methods after accounting for trim differences between the datasets.

Recent rotor-data correlation work has focused on the ability of analytical prediction methods such as CAMRAD/JA (Comprehensive Analytical Model of Rotorcraft Aerodynamics and Dynamics, Johnson Aeronautics) to accurately predict rotorcraft performance. Full-scale BO-105 rotor-system data acquired in the Ames 40- by 80-Foot Wind Tunnel are being used in this analytical study. From previous experimental comparisons, it was shown that the rotor-performance measurements were strongly

influenced by the presence of the wind-tunnel walls. Using the wall-correction method of Glauert, the angle of attack of the rotor system in the tunnel was corrected and used in the trim conditions of the CAMRAD/JA analysis. As shown in the figure, the accuracy of predicted rotor power is significantly improved when the angle-of-attack correction of Glauert is applied to the trim conditions of the rotor in the analysis. The analytical predictions of rotor power as a function of rotor thrust using a free-wake analysis are shown.

Point of Contact: R. Peterson
(650) 604-5044
rpeterson@mail.arc.nasa.gov

Canard Rotor/Wing Hover Test

Stephen Swanson, John Madden

In a joint program between NASA and McDonnell Douglas Helicopter Systems, a one-half-scale rotor model of the McDonnell Douglas Canard Rotor/Wing (CRW) rotorcraft was tested in the 80- by 120-Foot Wind Tunnel at Ames Research Center. This test was conducted to evaluate the hover performance of the unique elliptical-airfoil rotor being planned for the CRW. The CRW is a stoppable-rotor design which can hover and fly at low-speeds like a conventional helicopter, whereas in its stopped-rotor mode it can fly at high speeds comparable to those of fixed-wing aircraft. Initial concepts include a land- or ship-based medium-range vertical takeoff and landing, remotely piloted vehicle.

A two-bladed teetering rotor is used to generate the required lift for hover and low-speed forward flight. Once the rotorcraft is at a sufficient forward velocity, the required lift generation is transferred from the rotor to a canard and horizontal tail. What is unique about this rotor is that it is driven by high-pressure air exhausted at the rotor tips as opposed to the conventional helicopter in which the rotor is shaft-driven. In the flight vehicle, conventional turbofan engines are used to supply the high-pressure air to the rotor. Because the CRW's rotor is stopped to allow high-speed forward flight, the rotor's airfoil cross section must be elliptical. This is a compromise between the optimum

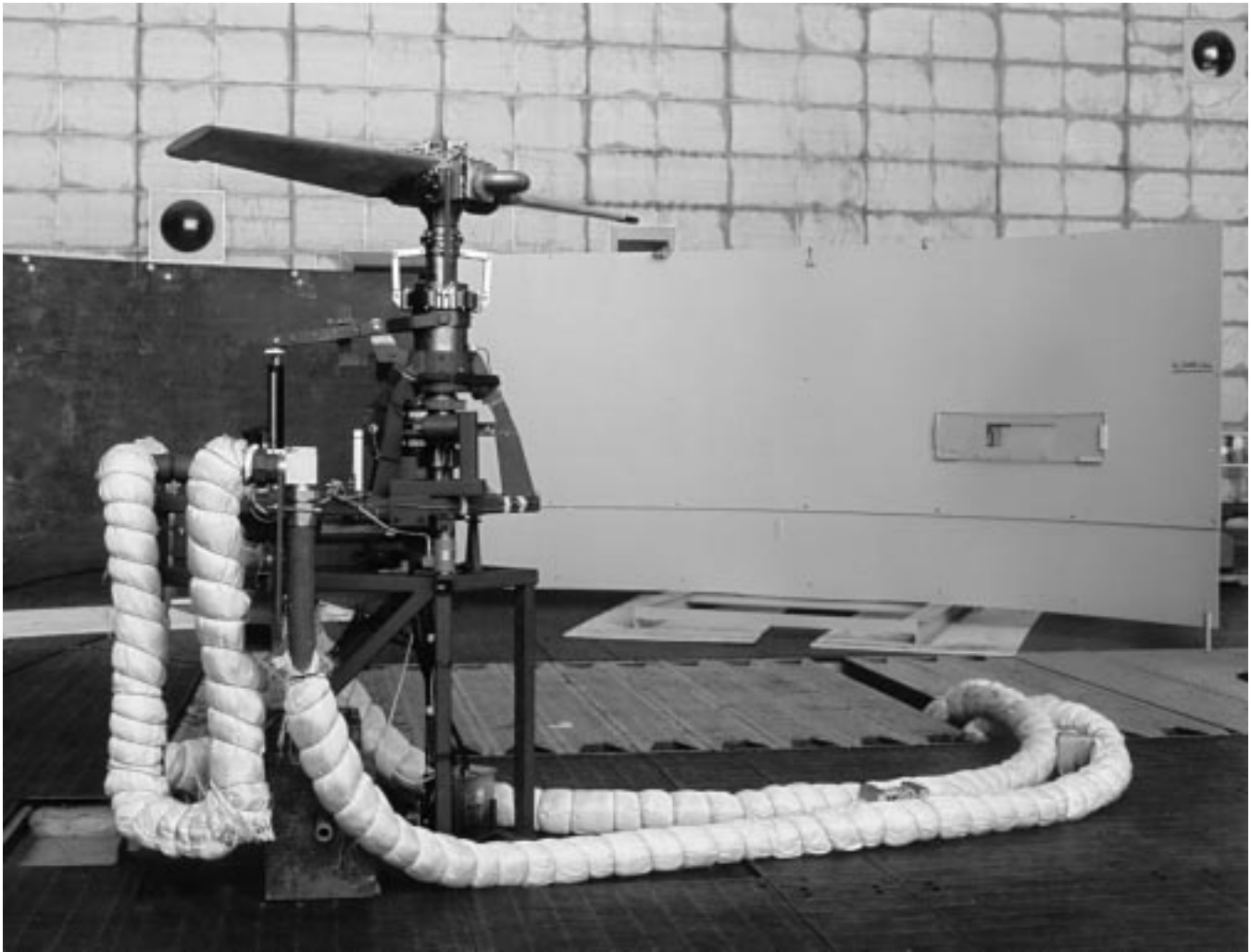


Fig. 1. Isolated rotor model installed in the Ames 80- by 120-Foot Wind Tunnel.

airfoil shape for conventional rotor flight and that for high-speed stopped-rotor flight.

The fixed-wing aerodynamic characteristics of the complete aircraft were evaluated in earlier tests. In this recent test, the isolated rotor was evaluated in hover in the Ames 80- by 120-Foot Wind Tunnel; that tunnel was used because it has the unique capability to provide heated, high-pressure air that could be used to simulate the exhaust

gases of the CRW's engine. The figure shows the isolated rotor installed in the test section and connected to the high-pressure air system. Preliminary results indicate that the rotor was capable of generating the required lift for takeoff and hovering flight. Comparisons with predicted aerodynamic performance showed that the actual thrust generated was greater than predicted for the same power input. On the other hand, comparisons of the

actual and predicted internal pressure measurements indicated higher than expected duct losses within the rotor internal piping.

**Point of Contact: S. Swanson
(650) 604-4565
sswanson@mail.arc.nasa.gov**

In-flight Dynamic Stall Research

Robert Kufeld, William Bousman

The objective of this work is to improve the complex dynamic-stall aerodynamic models of a helicopter rotor in high-speed, high-load conditions. The improvement of these models should serve to reduce the design and development cost of new helicopters, because the dynamic-stall condition is the driving force in determining the strength of the helicopter control system. Test conditions were identified and studied from the flight-maneuver data collected during the UH-60A Airloads Program, which provides information about the

dynamic-stall phenomena. UH-60A airloads data are available to NASA's customers for similar studies through an electronic database and search engine called "TRENDS," which is maintained at Ames Research Center.

The figure shows some of the complex loading a helicopter rotor is subjected to during a high-speed turn. The data show the measured pitching-moment calculation derived from pressure transducers located at radial station $r/R = 0.92$, at an advance ratio of 0.39 and a load factor of 1.5. The figure clearly shows the five rapid and large negative pitching-moment departures the blade experiences as it makes one revolution during this

test condition. The two pitching-moment departures near 280 and 355 degrees have been clearly identified as dynamic-stall events. The two pitching-moment departures near 95 and 135 degrees have been linked to passage of shock waves over the airfoil; the final pitching-moment departure near 50 degrees appears to be caused by a combination of two effects: supersonic aerodynamic and dynamic-stall vortex shedding. These data show the need for dynamic-stall model improvement at both the traditional low-speed range of the fourth quadrant and the unexpected high-speed range found in the first quadrant of the rotor.

Point of Contact: R. Kufeld
(650) 604-5664
rkufeld@mail.arc.nasa.gov

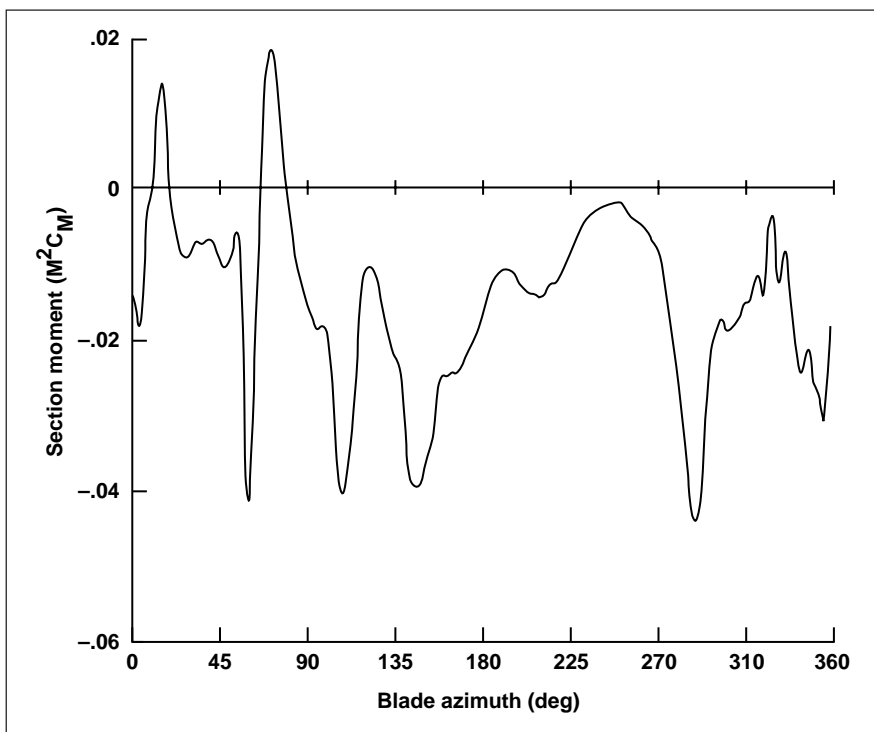


Fig. 1. Section moment versus rotor azimuth for $r/R = 0.920$ in a high-speed turn; advance ratio = 0.390 and load factor = 1.50.

Stall Control of Helicopter Rotors

Khanh Q. Nguyen

A control system based on blade-pitch actuation was developed to suppress stall on helicopter rotors. Stall suppression would allow the helicopter flight envelope to be expanded and would alleviate stall-induced loads and vibration. The control system was implemented in a comprehensive rotorcraft analysis, which was based on a finite-element method and which included unsteady aerodynamic effects (dynamic stall) and nonuniform inflow models. The stall-suppression system is based on a transfer-matrix approach; it employs

a stall index as a measure of stall. The results showed that stall could effectively be suppressed using higher harmonic control at both cruise and high-speed flight conditions. The effectiveness of the stall-suppression system is shown in the

figure in which the stall regions are shown without the system (part (a)) and with the system (part (b)) at a high-thrust, high-speed flight condition. The control amplitude was small, less than 1 degree.

In general, however, stall suppression did not guarantee performance improvements. The results also showed the distinction between stall suppression and performance improvement with active control. When the controller aimed to reduce the shaft torque, rotor-performance improvement could be achieved, but with a small degradation in stall behavior.

Point of Contact: K. Nguyen
(650) 604-5043
knguyen@mail.arc.nasa.gov

Apache AH-64D Flight Test Predictions

Earl P. N. Duque

Recent design changes to the AH-64D (Apache) helicopter have created unfavorable handling qualities that may be caused by changes in the aerodynamic flow field. Engineers at McDonnell Douglas Helicopter Systems needed to quickly understand the flow characteristics and to evaluate potential ways to alleviate the problem. Computational fluid dynamics (CFD) is an ideal tool for examining the effect of late-cycle design changes because it is much faster and cheaper than flight testing.

The objective of this project was to use CFD methods to study the flow field around the helicopter in its current configuration and then with several variations which designers proposed to improve the handling qualities. The simulation results had to be obtained quickly in order to

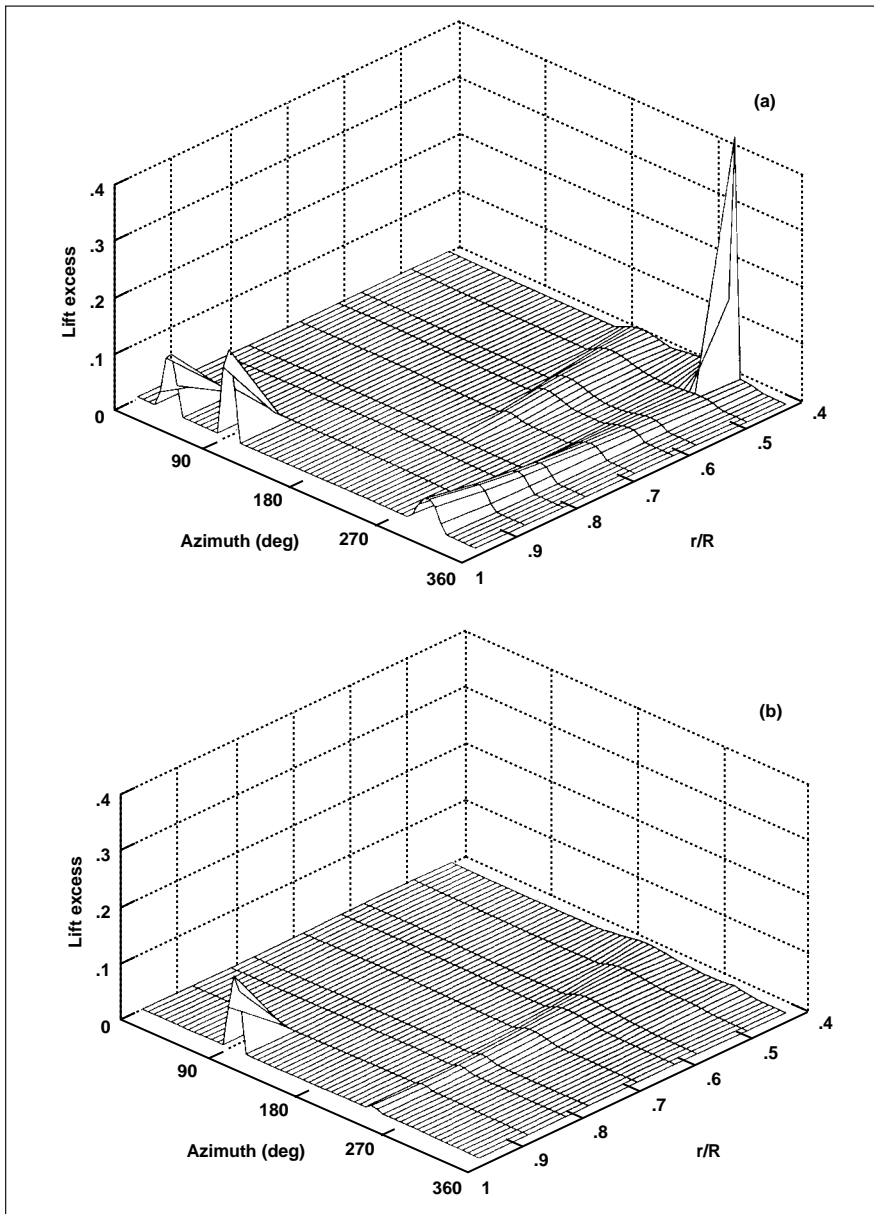


Fig. 1. Stall regions over rotor disk without the stall-suppression system (a) and with the system (b).

decide which designs would be built and tested in flight.

Inviscid simulations were done with the TIGER code by John Melton of Ames Research Center (ARC). Its unstructured Cartesian formulation largely bypasses the time-consuming and tedious task of grid generation, allowing for fast turnaround of very complicated models. Results from the initial geometry (see figure (see Color Plate 3 in the Appendix)) influenced two of the proposed design solutions. Subsequent study of five new designs showed that one did not warrant further investigation. Since the validity of an inviscid approximation is questionable in a complex, vortex-dominated flow, intensive study of a geometrically simplified model (the isolated fuselage without engine, wing, or tail surfaces) using the thin-layer Navier-Stokes equations was conducted using the OVERFLOW code by Pieter Buning of ARC. These simulations gave further credence to the baseline inviscid computations. The combination of complex-geometry/simplified-physics simulations with simplified-geometry/complex-physics simulations provided McDonnell Douglas's engineers with an overall understanding of the Apache flow field and with quick feedback on proposed design changes.

Point of Contact: E. Duque
(650) 604-4489
eduque@mail.arc.nasa.gov

Rotor-Wake/Fuselage Interaction

Paul M. Stremel

The interaction of the wake generated by a rotor with the fuselage of the vehicle has profound effects on the overall efficiency of the vehicle. These effects have been clearly demonstrated in flight as vehicle vibration and download. Although they are clearly demonstrable in flight, the quantitative aspects of the interactions are not clearly understood. Numerous numerical and experimental investigations have been conducted in efforts to better understand the rotor-wake/fuselage interaction. However, each of these investigations concentrated on a unique rotor/geometry combination for which conclusions can be drawn only for that particular configuration. A generalized method for optimizing rotor performance and minimizing fuselage interaction is not forthcoming. As a result, numerical methods must be applied to each configuration to better identify the aerodynamic effects of the rotor/fuselage interaction.

The present research was conducted to obtain baseline interaction results—aerodynamic and acoustics data—for the flow surrounding the Tilt Rotor Aeroacoustic Model (TRAM) isolated-rotor configuration. It is extremely important to minimize the interaction of the support hardware with the rotor to insure quality data. However, because of geometric limitations of the support hardware, tunnel installation, and test envelope, a perfectly isolated rotor cannot be tested. The numerical

method used to model the TRAM isolated-rotor configuration is a combination of the OVERFLOW computational fluid dynamics code and the PEGSUS domain connectivity program. The isolated-rotor configuration consists of a rotor and a motor/gearbox assembly. In the current investigation, the rotor is represented by an actuator-disk model. Results were computed for $C_T = 0.14$ at angles of incidence of 0 and 15 degrees. The results are shown in the first figure (see Color Plate 4 in the Appendix) for 0-degree incidence and in the second figure (see Color Plate 5 in the Appendix) for 15-degree incidence. Shown in each figure are the vertical velocity contours and the flow-field streamlines. The vertical velocity contours are shown at the rotor plane and at a station on the model support. In comparing the streamline results, the rotor wake for the 0-degree angle of incidence directly interacts with the motor assembly. However, at the 15-degree angle of incidence the rotor wake is completely clear of the motor assembly. In comparing the velocity contours at the rotor plane, the contours indicate an interaction over the motor assembly for the 0-degree angle of incidence but considerably less interaction at the 15-degree angle.

Point of Contact: P. Stremel
(650) 604-4563
pstremel@mail.arc.nasa.gov

Navier-Stokes Simulation of High-Lift Aerodynamics

Karlin Roth, Stuart Rogers

The use of the methods of computational fluid dynamics (CFD) in order to understand the flow over high-lift wings configured for takeoff and landing with leading-edge slats and slotted trailing-edge flaps will contribute to the design of simpler or more efficient high-lift systems for subsonic transport aircraft. The long-range objectives of this work are to develop an accurate and efficient Navier-Stokes analysis method for flow over the high-lift systems of subsonic transport aircraft and to examine critical physics affecting high-lift system design. The particu-

lar near-term objective is to predict the flow about a subsonic transport configured for high lift and to assess wind-tunnel interference effects on the flow about this test article.

The OVERFLOW code was used to investigate the flow about a subsonic transport configuration. The simulations are steady-state, employ the Spalart-Allmaras turbulence model, and utilize multigrid convergence improvement schemes. The structured, overset grid system which discretizes the fuselage, high-lift wing elements, and nacelles consists of 16 million points within 36 zones (see figure). During FY96, surface grids were generated from the computer-aided design definition; volume grid methods including

element edge grids, wake placement, and wake smoothing strategies were developed, verified, and applied. Importantly, the simulation team demonstrated first-of-a-kind computations in utilizing a viscous CFD analysis for a complex three-dimensional high-lift configuration. The solution matrix includes a total of 18 cases which document the flow for a range of angles of attack, with and without powered engines, and in free-air and within the 12-Foot Pressure Wind Tunnel at Ames Research Center.

Comparison of the free-air and wind-tunnel simulations shows significant wall-interference effects which vary with the model attitude. In general, simulations conducted in the wind tunnel exhibit earlier stall than do the free-air calculations. Further, in addition to an earlier stall angle, powered simulations in the wind tunnel attain lift values near stall which are about 8% higher than the free-air values. In order to test the Wall Interference Correction System developed for the 12-Foot Pressure Wind Tunnel on a powered, high-lift model, it was applied to the simulated data at selected conditions. The initial analysis indicates that this correction method may not be appropriate at conditions near maximum lift.

Point of Contact: K. Roth/S. Rogers
(650) 604-6678/4481
kroth@mail.arc.nasa.gov
srogers@mail.arc.nasa.gov

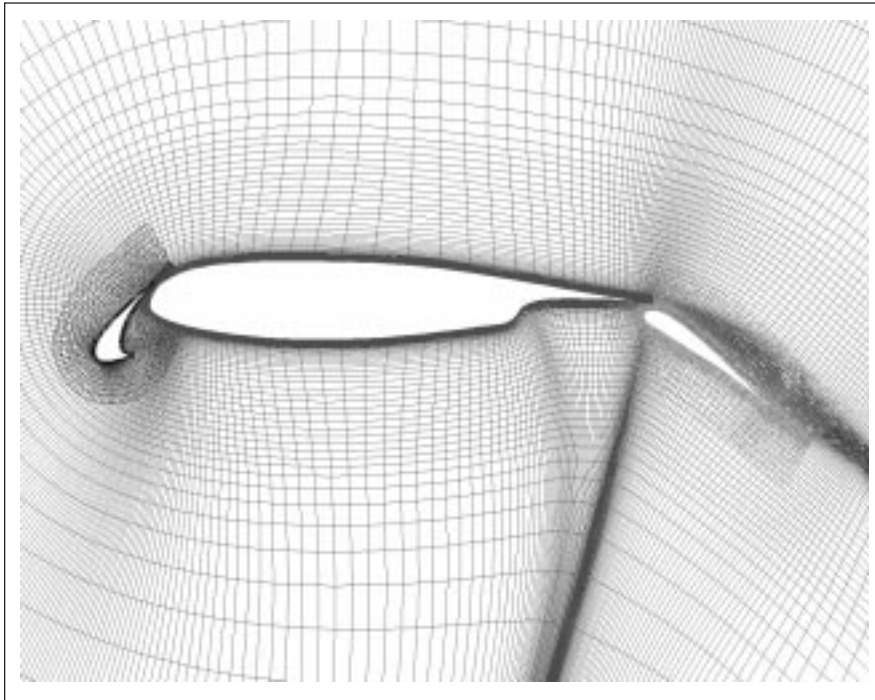


Fig. 1. Overset grid system within cross section of a multi-element high-lift wing.

Lift-Jet Effects on Powered-Lift STOVL Model

Karlin Roth

During the transition from hover to wingborne flight, short takeoff and vertical landing (STOVL) aircraft rely on the direct thrust of lift jets to supplement aerodynamic wing lift. The jets usually induce a loss of lift and a change in the nose-up pitching moment on the vehicle; both of these effects increase with increasing forward velocity. Thus, proper design of STOVL aircraft requires an understanding of the physics of the lift-jet/airframe interaction.

The ability of three-dimensional, laminar and turbulent Navier-Stokes computations to simulate the performance of a geometrically simplified STOVL model during transition flight was investigated. Simulations were made using the OVERFLOW code for the model which consists of a 60-degree cropped delta wing planform; a simple fuselage shape blended to the wing; and tandem, circular, high-pressure-air lift jets that exit perpendicularly to the flat lower surface. Predictions were compared with measurements at a free-stream Mach number of 0.146, a 10-degree angle of attack, and with sonic lift jets. Flow visualization shows the structure of the wing leading-edge vortices and the lift jets; the deflection of the lift jets is illustrated in the figure using Mach number contours in the model's symmetry plane.

Although grid refinements improve the computational results, none of the computations completely characterize the wing



Fig. 1. Mach number contours taken in the symmetry plane to illustrate the deflection of lift jets.

leading-edge flow field or the flow within 2 diameters of the jet exits. For laminar calculations, the pressure suction peaks at the wing leading edge tend to be initiated farther inboard, to cover more area on the wing, to have slightly less suction, and to agree better with the measurements than the turbulent predictions. Notably, the simulations predict a jet-induced lift loss for the model that is mostly due to decreased suction at the wing leading edge.

Point of Contact: K. Roth
(650) 604-6678
kroth@mail.arc.nasa.gov

Vortex Core Detection for Computational Grid Refinement

David Kenwright

Predicting rotor wake is one of the most challenging problems in rotorcraft computational fluid dynamics (CFD). The rotor wake is the disturbed flow that is left behind as the rotor blade cuts through the air. The wake rolls up into vortices near the blade tips, a result of the pressure differences caused by the moving rotor. These vortices, an unwanted side effect of lift, cause control buffeting, airframe vibration, and noise. The requirement for low noise is particularly important for

civilian helicopters and tiltrotors which operate in highly populated areas.

A major problem with the CFD simulation of rotorcraft is that the tip vortices diffuse too quickly because of inadequate grid resolution. Adaptive grid-refinement schemes developed at Ames Research Center have been partially successful in capturing these vortices, although inadequate grid resolution near the vortex core causes discrepancies between computed and wind-tunnel results.

A vortex-core detection technique was implemented in the Unsteady Flow Analysis Toolkit (UFAT) to permit scientists to locate and visualize the regions of swirling or rotating flow. This technique is based on an eigenvector method developed at the Massachusetts Institute of Technology with funding from Ames. The figure (see Color Plate 6 in the Appendix) shows vortex cores extracted from a simulation of a helicopter rotor in forward flight. The vortex cores (red lines) become disjointed where the computational grid is too coarse. In this simulation, the grid was refined based on the vorticity magnitude. From the visualization, it is apparent that the grid refinement process failed to capture the vortex core.

The vortex cores are extracted in a batch computation which can take from seconds to hours to complete depending on the size of the dataset and the complexity of the flow. For the rotorcraft simulation shown in the figure which consisted of 800,000 tetrahedral elements, the extraction process took less than 8 seconds on a Silicon Graphics

Power Onyx workstation. The same technique has also been applied to much larger, unsteady simulations of aircraft to reveal the time-evolution of vortex cores.

Point of Contact: D. Kenwright
(650) 604-1704
davidk@nas.nasa.gov

Wingtip Vortex Flows

Jennifer Dacles-Mariani,
Dochan Kwak

The wingtip vortex flow has been the subject of numerous studies. Its significance has been seen in practical problems such as landing separation distances for aircraft, blade-vortex interaction, and cavitation on ship propeller blades (see first figure). Despite these numerous studies, most of the wake-vortex flow behavior is still not clearly understood.

This work is part of an ongoing computational study of the tip-vortex flow through initial formation/roll-up, growth, and decay. In this particular study, the near- and intermediate-fields behind the wings are investigated to (1) explore a more physical modeling of the flow by including the viscous upstream effects; (2) provide an improved vortex flow field to be used as inflow for the intermediate-wake; and (3) investigate the validity and applicability of a simplified Navier-Stokes solver using the velocity/vorticity formulation in tip-vortex flow prediction.

The approach taken is to derive a wake model from the full Navier-Stokes equations using the velocity/vorticity formulation. It has the advantage of being able to retain some of the flow physics without a lot of empiricism. These equations allow physical diffusion in the streamwise direction, including viscous upstream effects and vortex

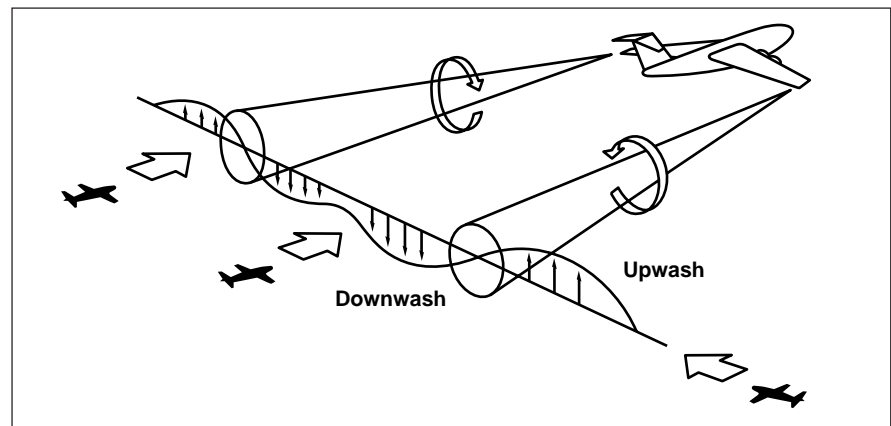


Fig. 1. Schematic of a downstream wake of an aircraft.

stretching. For vortex-dominated flows, vorticity is the natural choice of variable. The accuracy of the method may be better preserved since it is being calculated directly.

From this study, a detailed account of tip-vortex formation and of the roll-up process was accomplished. The roles of numerics and turbulence models in tip-vortex prediction was also studied in detail. The preliminary results indicated that the velocity/vorticity formulation using the preconditioned conjugate gradient method was successful in predicting wake-vortex flow. Comparison with measured data of a 0.03 scale model of the Boeing 747 aircraft, taken in the 80- by 120-Foot

Wind Tunnel at Ames Research Center showed a similar trend between the measured and the computed upwash and downwash velocities (see second figure). The slopes of the velocity across the vortex were predicted well by the computation. Most of the disagreement is in the region where the sampling period of the measured data was not long enough, which resulted in the irregularity of the data.

Point of Contact: J. Dacles-Mariani
 (650) 604-5369
 jdacles-mariani@mail.arc.nasa.gov

Transonic Overset Potential Solver

Terry Holst

The “full-potential+boundary-layer” approach for transonic cruise analysis and design can be up to 100 times faster than Navier-Stokes approaches and just as applicable over a wide range of cases involving weak shock waves with little or no boundary-layer separation. A fast full-potential capability using a zonal grid approach for general geometry modeling will be a valuable tool for near real-time assessment of aerodynamic shapes in the design or wind-tunnel environments.

The objective of the present work is to develop a full-potential analysis and design capability utilizing the Chimera zonal grid approach that will be compatible with the well-established OVERFLOW Euler/Navier-Stokes flow solver. Such an approach would be extremely cost effective, especially considering that all of these approaches would utilize the same problem setup and post-processing software, and to a large extent, the same grid-generation software.

A transonic three-zone wing-fuselage solver (for inviscid flow) has been developed and validated using experimental pressure measurements (see figure). This half-million-grid-point computation, which includes surface definition, surface-grid generation, volume-grid generation, Chimera hole-cutting, donor-cell search, flow-field generation, and PLOT3D file generation, required about 1 minute of computer

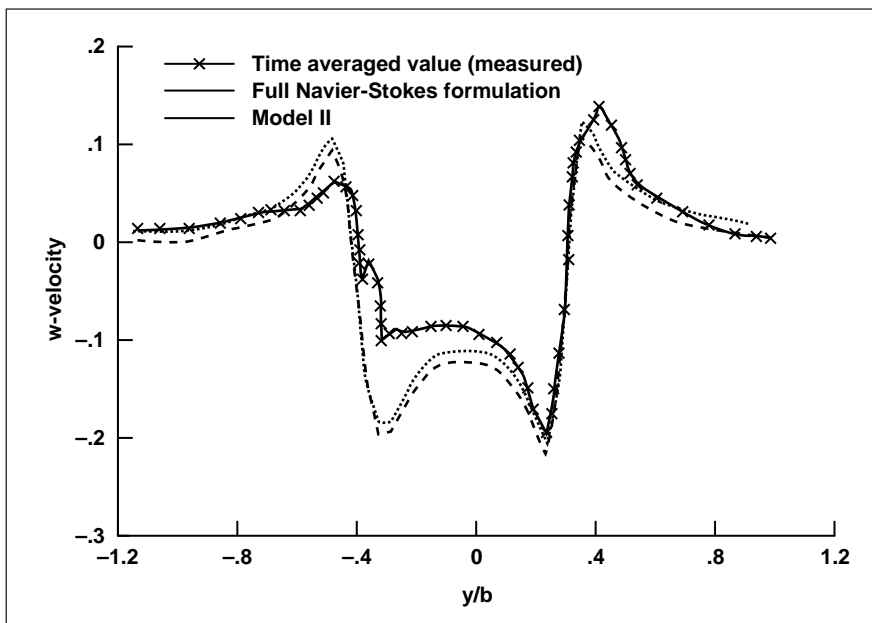


Fig. 2. Upwash and downwash velocity profile at $x/c = 162$ feet.

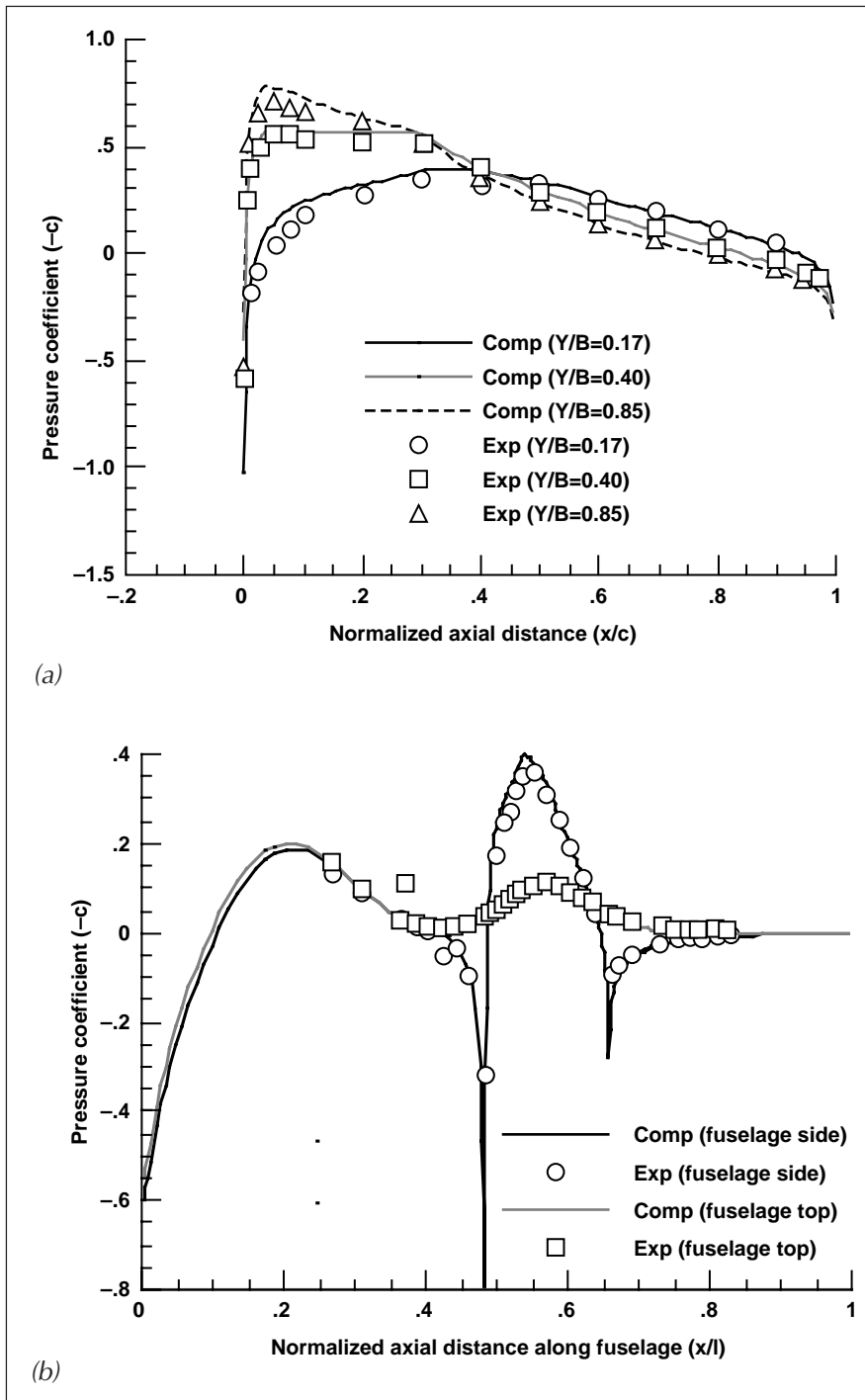


Fig. 1. Wing/fuselage surface-pressure comparisons RAE wing-fuselage, $M_\infty = 0.8$, $\alpha = 2^\circ$. (a) Upper wing; (b) upper fuselage.

time on a single processor Cray C90 computer.

In developing this solver, a new, approximate Chimera donor-cell search algorithm has been developed that is up to 100 times faster than previous techniques. For example, in two-zone cases, the new algorithm can find donor cells at a rate in excess of 60,000 cells per second on a single processor Cray C90 computer. This search algorithm has an approximate characteristic that will automatically utilize a nearest-neighbor cell when the actual donor cell cannot be found, thus reducing the chance for orphan points to exist.

Point of Contact: T. Holst
(650) 604-6032
tholst@mail.arc.nasa.gov

Real-Time Particle Tracing in Time-Varying Flows

David Kenwright, David Kao

Particle tracing is a scientific visualization technique that is widely used to study aeronautical simulations. In time-varying flows, particle tracing can be used to produce streaklines (a visualization technique commonly used in wind-tunnel experiments) by simulating the continuous injection of particles into a flow. To detect important flow features, several thousand particles must be injected and traced through a flow field by using numerical integration, which makes particle tracing computationally intensive. Consequently, streaklines are usually pre-computed in a batch process

by using programs, such as the Unsteady Flow Analysis Toolkit, and then playing them back later in animations or videos—a process which can take hours.

A real-time algorithm for computing and displaying streaklines known as the tetrahedra method, was developed by members of the visualization technologies group at Ames Research Center. The improved performance offered by the tetrahedra method now allows streaklines to be computed and visualized in real time on high-end Silicon Graphics, Inc. workstations. The benefit to scientists is immediate visualization of their data and the capability to interactively explore time-varying flows. Comparisons with conventional particle-tracing algorithms have verified that the tetrahedra method is accurate as well as fast.

The tetrahedra method has been installed in two visualization systems developed at Ames: the Virtual Windtunnel (see the figure (see Color Plate 7 in the Appendix)) and the Unsteady Flow Analysis Toolkit.

Point of Contact: D. Kenwright
 (650) 604-1704
 davidk@nas.nasa.gov

NASA Metacenter

Mary Hultquist

The NASA Metacenter is an exploratory project of the Parallel Systems Groups at Ames Research Center and Langley Research Center. The focus of the project is to achieve more effective use of NASA supercomputers by making the systems

more readily available to researchers, and by providing quicker turnaround for batch jobs, a larger range of available resources for computation, and better distribution of the computational workload across multiple supercomputers.

The current homogeneous configuration of the Metacenter links the IBM SP2 computers at Ames and those at Langley. With the systems similarly configured, each Center can rely on help from the other for troubleshooting difficult problems. Planning and problems are discussed at weekly teleconferences, and problems are resolved more quickly because the experience of personnel at both sites is utilized.

The implementation of the Metacenter includes a “peer scheduler” to interact with the Portable Batch System (PBS) queuing system used on each system. In this model, as long as all systems have work to do, they act as independent computers. But when the utilization of one system drops below a predefined utilization threshold, then peer scheduling begins. A system that is short of jobs, “asks” the other systems in the Metacenter (its “peers”) for a list of all the queued jobs on the remote systems. It then goes through a series of checks, verifying that it can indeed run a specific job. If all the tests are passed, the scheduler requests the

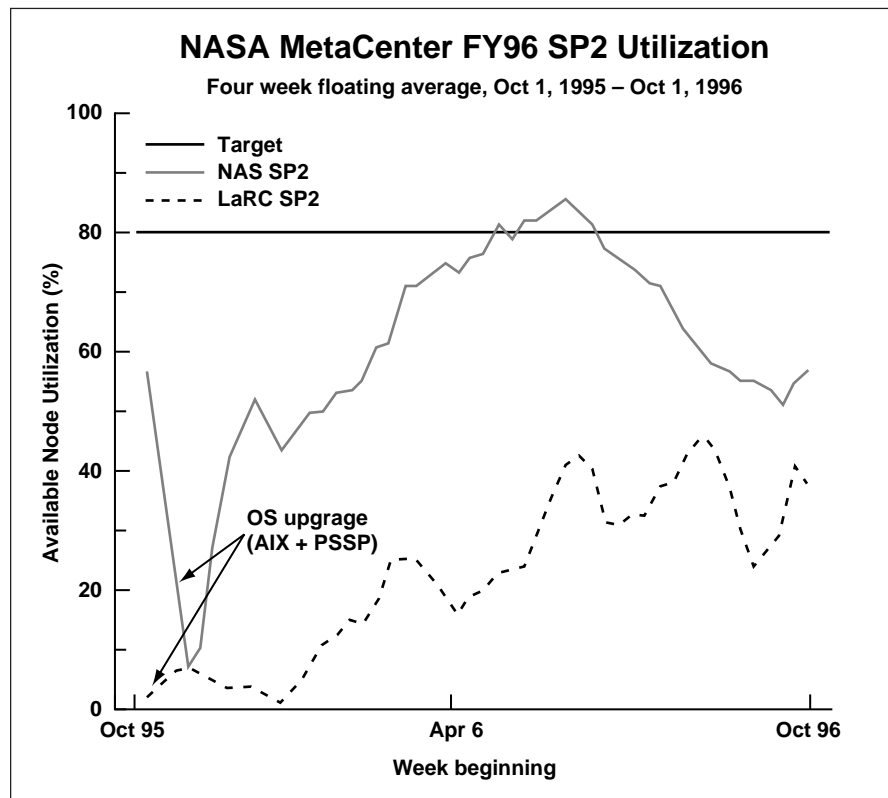


Fig. 1. FY96 utilization on the IBM SP2.

PBS to move the job to the local server. The job is then run locally, and the results sent back to the user.

This implementation has resulted in a more balanced utilization of the Metacenter systems, as shown in the figure. The users are thus able to get jobs returned more quickly, because a job does not wait in a queue at one system while another system sits idle. Moreover, system downtime is decreased because personnel at both sites can work together to get down systems back into production.

Point of Contact: M. Hultquist
(650) 604-0814
maryh@nas.nasa.gov

Portable Batch System

David Tweten

As of this year, all supercomputers at Ames Research Center, whether production or testbed, and regardless of manufacture, run the same batch and cluster control system, the Portable Batch System (PBS). Most recently, Ames's two Cray C-90s, called the vonNeumann and Eagle, as well as the Center's Cray J-90 cluster, called the Newton, were converted to use the PBS as their sole production batch system. The PBS is a research batch processing and cluster control software package written at the Center.

VonNeumann is NASA's largest supercomputer; it is used to perform cutting-edge research for NASA's aeronautics-focused programs and for base research and technology.

Eagle is the production supercomputer for general science and engineering research for the Office of Aeronautics and Space Transportation Technology. Newton is a testbed supercomputer cluster, intended to ease migration of computer codes between vector computing and distributed-computing paradigms. The PBS allows construction of custom schedulers using any of three different languages. It is a key component in NASA's plan to develop metacenters, virtual computer centers composed of machines potentially supplied from several vendors, and potentially sited in several locations.

The PBS beta program ended the fiscal year with 51 client sites, distributed among government, universities, and private industry.

Point of Contact: D. Tweten
(650) 604-4416
tweten@nas.nasa.gov

Developing a Cluster Computer from Workstations

Reese L. Sorenson

Finding adequate computational resources to meet the ever-expanding needs of aerodynamic simulation by computational fluid dynamics (CFD) has always been a challenge, one exacerbated by recent budgetary constraints and redirected priorities. Facing a possible decrease of available computer time in the face

of growing needs, it is important that a new source of computing power be found for researchers at Ames Research Center.

It was realized that in terms of raw computer power the Silicon Graphics, Inc. (SGI) workstations sitting on the researchers' desks, considered together, had power approximately equal to that of a four-processor CRAY C-90. Since this resource was sitting idle every night and most weekends, a project was undertaken to link these workstations, thus creating a cluster computer.

Two needs had to be met to make this a reality. One was for fast interprocessor communication. A Grand Junction fast Ethernet data switch was obtained, and the 24 most powerful of the approximately 60 workstations in use were installed on the data switch. It is expected that this switch will at least double the interprocessor communication speed for these workstations by eliminating "data collisions" at a local network router.

The second need was for scheduling software to queue jobs, oversee their execution, and generally make the workstations function together as a computer. The Portable Batch System (PBS) software, developed locally at Ames and already functioning as the operating system on a CRAY supercomputer and on a dedicated workstation cluster, was ported to these machines and customized for this implementation.

The cluster is scheduled to be available 12 hours per day throughout the year. Test cases have been run successfully on it. Recently

acquired workstations, even more powerful than those originally used, are being installed in the cluster. Documentation to be posted on the World Wide Web has been written.

The significance of this project is twofold: first, the critically important work of aerodynamic simulation at Ames will continue to have adequate computational resources; second, the software techniques and the experience of this project are available to others facing similar constraints.

Point of Contact: R. Sorenson
(650) 604-4471
rsorenson@mail.arc.nasa.gov

Planar Doppler Velocimetry Using Pulsed Lasers

Robert L. McKenzie

Recently, planar doppler velocimetry (PDV) has been shown by several laboratories to offer an attractive means for measuring three-dimensional velocity vectors everywhere in a light sheet placed in a flow. Unlike other optical means of measuring flow velocities, PDV is particularly attractive for use in large wind tunnels where distances to the sample region may be several meters, because it does not require the spatial resolution and tracking of individual scattering-particles or the alignment of crossed beams at large distances. To date, demonstrations of PDV (called "doppler global velocimetry" by some authors) have been made either in low-speed flows

without quantitative comparison with other measurements, or in supersonic flows where the Doppler shift is large and its measurement is relatively insensitive to instrumental errors. Moreover, most reported applications have relied on the use of continuous-wave lasers, which limit the measurement to time-averaged velocity fields.

The objective of this study has been to quantitatively determine the limits of PDV capabilities for applications in large-scale wind tunnels that are intended primarily for production testing of subsonic aircraft. For such applications, the adequate resolution of low-speed flow fields requires accurate measurements of small Doppler shifts that are obtained at distances of several meters from the sample region. In addition, the use of pulsed lasers provides the unique capability to obtain not only time-averaged fields, but also their statistical fluctuation amplitudes and the spatial excursions of unsteady flow regions such as wakes and separations.

To accomplish the objectives, the PDV measurement process was first modeled and its performance evaluated computationally. The noise sources considered included those related to the optical and electronic properties of charge-coupled device (CCD) arrays and to speckle effects associated with coherent illumination from pulsed lasers. The signal-noise estimates were incorporated into the PDV signal analysis process and combined with a spectroscopic model of the iodine vapor cell used to discriminate Doppler frequency

shifts and with computed scattering signals using a Mie scattering theory for polydisperse smoke particles. The relevant parameters incorporated a range of practical aerodynamic test conditions and facility sizes. The results (1) helped define the optimum values of the instrument parameters, (2) showed that the expected signal levels from a practical PDV system were sufficiently large to allow its useful application in large facilities, and (3) showed that the expected velocity measurement uncertainties were small relative to the mean velocities of interest for most subsonic, large-scale wind-tunnel testing.

PDV performance was then demonstrated by using several bench-top setups, including a rotating wheel where the exact velocity field was always known everywhere, a turbulent air jet with flow properties that were calibrated using pitot and hot-wire probes, and stationary solid and aerosol targets where only the PDV noise is observed. Images from these targets were used to validate the model description of noise magnitudes and to confirm the minimum velocities that could be resolved. The bench-top experiments also allowed the optical configuration and calibration procedures of the instrument to be developed into a robust and easily operated system that is applicable to the environment of large-scale wind tunnels. An example of some results is shown in the figure (see Color Plate 8 in the Appendix) where the average axial velocity field and its root-mean-square fluctuation amplitudes are displayed for the flow in a low-speed, turbulent, free jet.

The plane of the image is normal to the jet centerline. The velocity profiles are taken along the grid lines shown in each image. The velocity field, part (a) in the figure, shows the average velocity distribution of the core flow and the fluctuation field; part (b) of the figure shows the high relative fluctuation amplitudes in the turbulent shear layer at the edge of the jet. These measurements were made with a preliminary PDV optical system that was capable of determining only one velocity component. The combined use of two additional systems would allow the determination of all three velocity components simultaneously from each laser pulse.

The PDV measurement capabilities developed in this study demonstrate that PDV offers significant advantages when compared with other means of measuring velocity fields in large-scale, subsonic wind tunnels. Measurements obtained from each laser pulse allow the accurate resolution of complete velocity vector fields with resolutions of instantaneous speeds as low as 2 m/sec. Much smaller average speeds can also be resolved. From the pulse-to-pulse data, both mean velocities and their fluctuation amplitudes can be determined in any aerosol-seeded flow with adequate optical access, including complex, three-dimensional, turbulent flows. The method has no upper limit above which velocity can not be measured, other than in extreme hypersonic flow situations containing strong shock waves; in the latter case, the necessary scattering particles or aerosols in the flow do

not follow the sudden changes in flow speeds or directions. The method has further advantages: the measurement procedures are compatible with the production testing environment of large-scale wind tunnels, the experimental setup is relatively simple, and the system could be operated by trained wind-tunnel technicians as a production instrument.

Point of Contact: R. McKenzie
(650) 604-6158
rmckenzie@mail.arc.nasa.gov

Pressure-Sensitive Paint and Photogrammetry for Aeroelastic Experiments

Edward T. Schairer,
Lawrence A. Hand

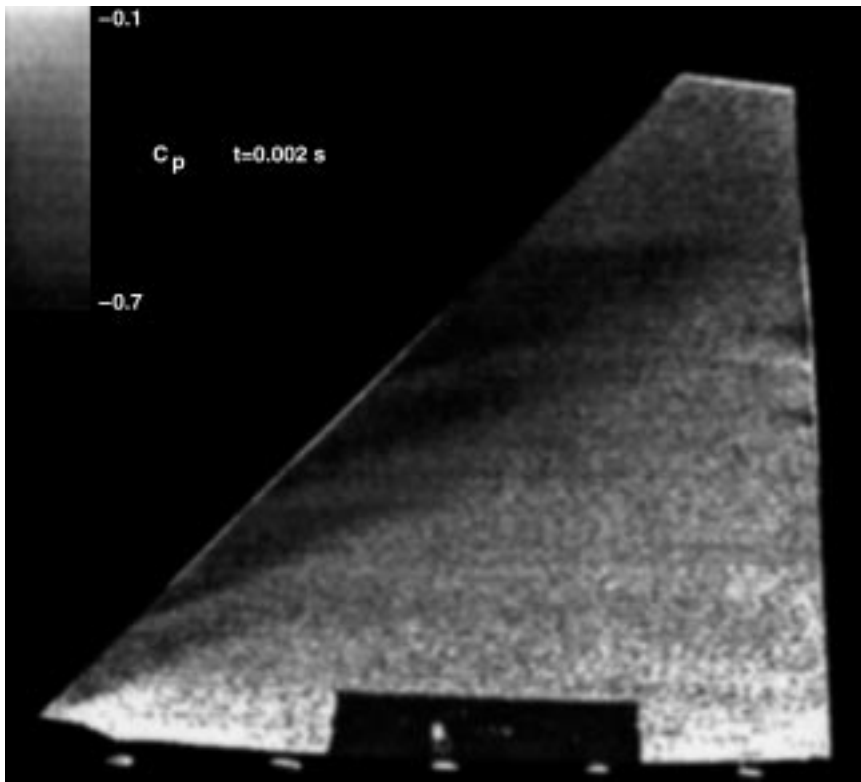
Methods for predicting the aeroelastic stability of aerospace structures are generally based on linearized aerodynamic theory. The accuracy of these methods suffers when nonlinear flow features (for example, shock waves, vortices, separated flow) interact with the aircraft structure. For example, at transonic speeds, where significant shock waves may be present, two- and three-dimensional wings tend to flutter at lower dynamic pressures than predicted by linear flutter analyses.

Since the late 1970s, considerable progress has been made in using computational fluid dynamics (CFD) to account for nonlinear aerodynamics in aeroelastic analy-

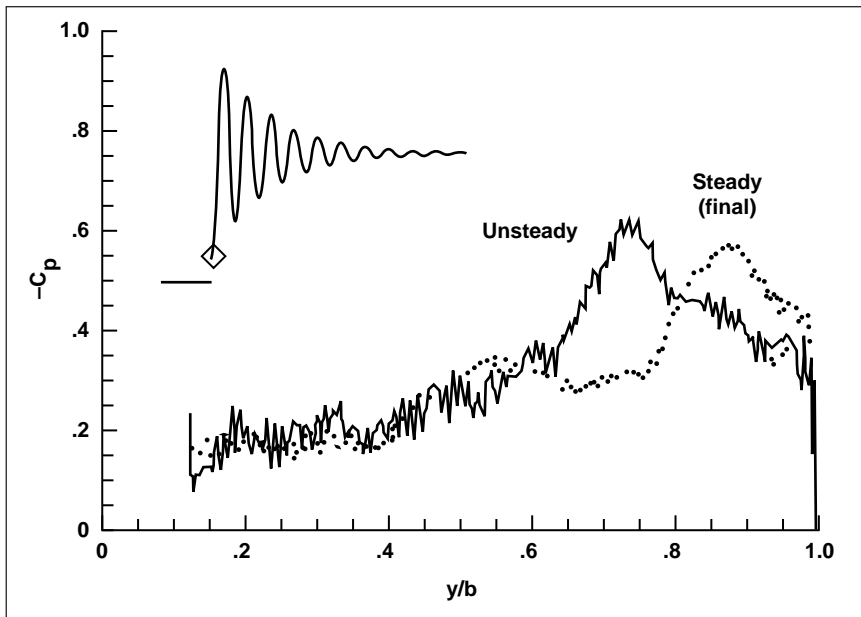
ses. Before these more powerful methods can be of practical value to aircraft designers, however, they must be tested by comparing their results with reliable experimental data. In particular, it is important to verify that unsteady, nonlinear aerodynamic features and their interactions with the structure are properly represented.

To help address this need, simple, small-scale, aeroelastic experiments were conducted in the High Reynolds Number Channel 2 (HRC-2) at Ames Research Center. The objective of the experiments was to (1) evaluate the use of pressure-sensitive paint (PSP) to measure unsteady pressure distributions on aeroelastic models and (2) stereophotogrammetry to measure unsteady model deformations. Semispan, clipped delta-wing models built from thin flat plates were tested at transonic speeds. The models were imaged by three synchronized black-and-white video cameras, and the data were recorded on videotape. Correlated images from two of these cameras were used to estimate the space coordinates of reference marks on the model at each instant, and the motion of each mark was estimated by fitting the deflection data with a damped sinusoid. The third camera was used for PSP.

All the procedures needed to measure unsteady pressure distributions using PSP were successfully demonstrated. The PSP measurements were seriously compromised, however, because the response time of the pressure paint was too slow, resulting in significant attenuation



(a)



(b)

Fig. 1. PSP image of flexible wing and corresponding pressure coefficient along $x/C = 0.75$.

of the unsteady component of the PSP signal. The first figure presents typical PSP data from a run (Mach = 0.85), where the wingtip was deflected and released. The gray levels in the image (part (a)) which was acquired just after the wingtip was released, are proportional to the pressure coefficient. Part (b) of the figure compares the pressure coefficient along a spanwise line from root to tip with steady data acquired after the unsteady transient had disappeared. Note that the suction peak associated with the leading-edge vortex has moved outboard in the steady condition.

The second figure presents photogrammetry data acquired during a run at Mach = 0.85, where the tip of the model was unrestrained as the pressure in the tunnel was slowly increased. Part (a) of the figure shows the time history of the deflection of the wingtip at three dynamic pressures just before the model became unstable; part (b) shows the phases and amplitudes of points on the wing compared with the trailing edge of the wingtip. The onset of instability was marked by a large increase in the amplitude of the motion, as well as an increase in the phase difference between the leading and trailing edges.

This work is a first step in using PSP and photogrammetry to document complex, unsteady aeroelastic responses. Once these techniques are further refined, they can be used to better understand these responses and to help validate higher-order aeroelasticity methods. A natural

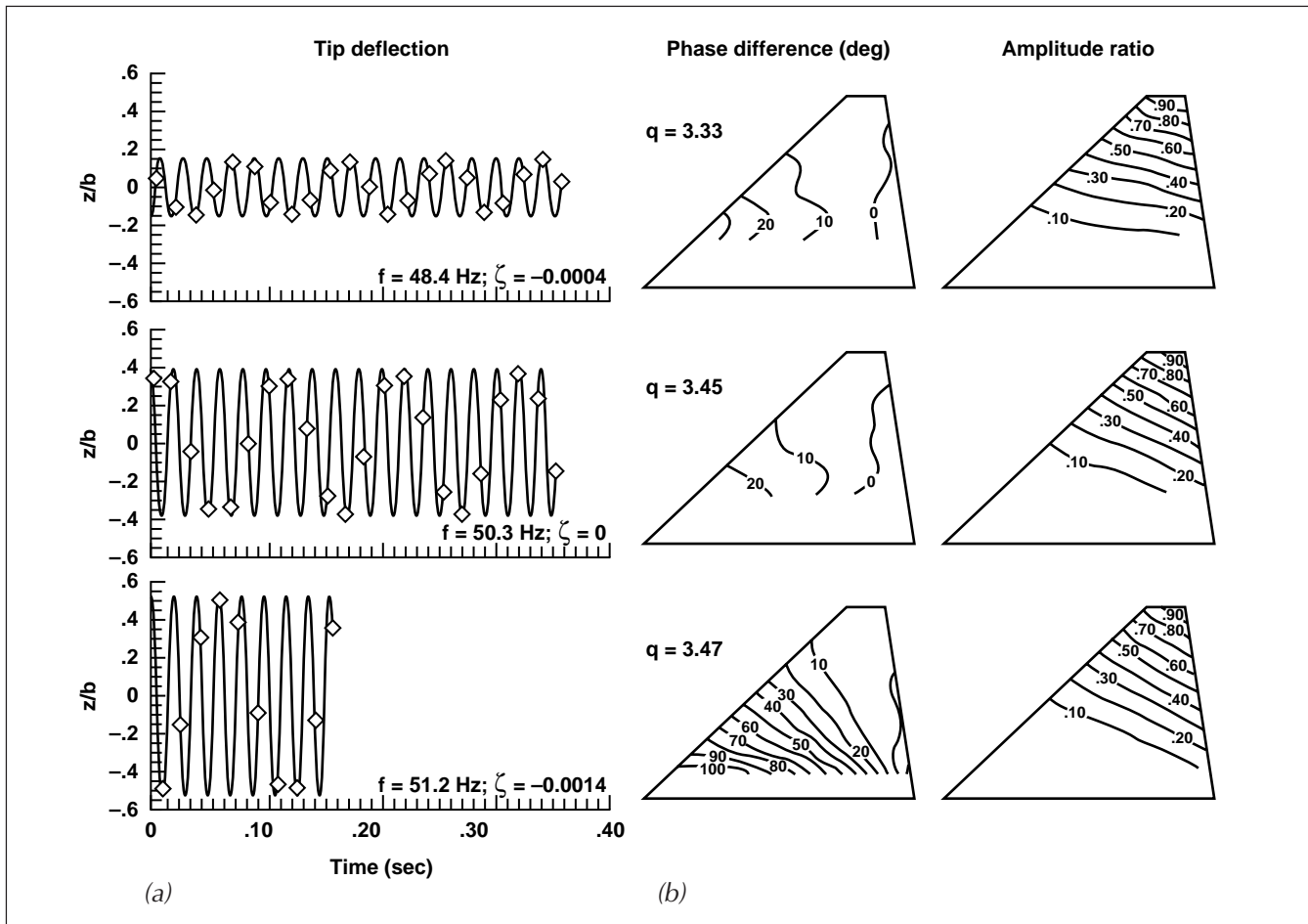


Fig. 2. Deflection of wingtip trailing edge, and phase difference and amplitude ratio with respect to tip trailing edge.

extension of this work is to apply PSP and photogrammetry to tests of helicopter rotor blades.

Point of Contact: E. Schairer/L. Hand
(650) 604-6925/1646
eschairer@mail.arc.nasa.gov
lhand@mail.arc.nasa.gov

Visualizing Wind-Tunnel Experimental Data

Samuel P. Uselton, Glenn Deardorff, Leslie Keely, Yinsyi Hung, Arsi Vaziri

A new software tool that displays data collected during wind-tunnel tests and that supports interactive analysis of those data has been developed at Ames Research Center. The tool, called exVis, allows visualization and interaction methods frequently used in analyz-

ing computational results to be applied to experimentally collected data. This product is a step toward developing a unified environment for analyzing data from multiple sources. The ability of researchers and engineers to display and interact with data from a variety of sources within a single visualization environment will increase the understanding gained from the data and reduce the time required.

The initial product, exVis 1.0, was developed for data collected

using a pressure-sensitive paint (PSP) system. The exVis software package reads a Flexible Image Transport System (FITS) format file produced by the PSP data-acquisition system which contains pressure values, and displays these data as an image in a window ("ImageViewer" shown at left in the figure (see Color Plate 9 in the Appendix)). The image can be displayed using a gray scale or a pseudocolor mapping of data to screen intensity.

Users can select tools that allow the selection of a "slice" of data from the image along a line segment. This slice is then graphed in a separate window ("GraphViewer," at the right in the figure) that shows how the coefficient of pressure varies along the length of the slice. Several slices can be selected from the same image and graphed on the same axes, or different slices (or sets of slices) can be graphed in separate windows. Multiple ImageViewers can each display an image, with selected slices graphed together or separately. The ImageViewer and GraphViewer can each be queried interactively to show the data value at the cursor; the GraphViewer also displays the corresponding location in the ImageViewer. The user can change the sizes and positions of ImageViewers and GraphViewers.

Previously selected slices or graphs can be deleted, and a graph can be printed via postscript. A user can save the current status and restore the program to that state at a later time. An on-line help feature is also included.

Although exVis was developed specifically with PSP data acquisition in mind, it is sufficiently robust to work with other scalar data that are provided in FITS format, and could be easily adapted for data provided in other two-dimensional array formats. ExVis 1.0 was completed in July 1996 and integrated with other Ames-developed software for use in a wind-tunnel test (September 1996).

Point of Contact: S. Uselton
(650) 604-3985
uselton@nas.nasa.gov

Surface Tension Effects on Skin Friction Measurements

G. Ziliac, A. Celic

The Fringe-Imaging skin friction technique (FISF), which was originally developed by Monson and Mateer at Ames Research Center and recently extended to three-dimensional flows, is the most accurate skin-friction measurement technique currently available. The principle of the FISF is that the skin friction at a point on an aerodynamic surface can be determined by measuring the time-rate-of-change of the thickness of an oil drop placed on the surface under the influence of the external air boundary layer. Lubrication theory is used to relate the variation in oil-patch thickness to shear stress.

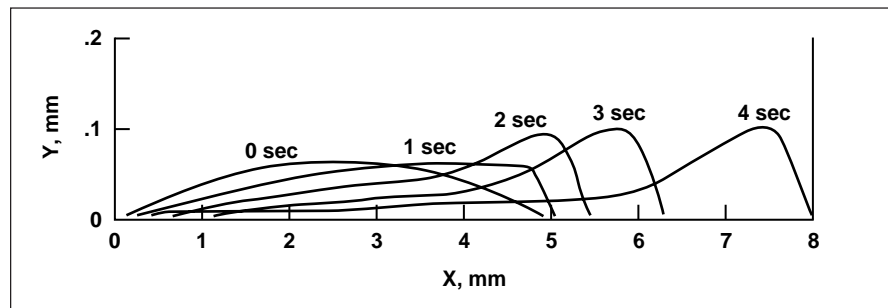


Fig. 1. Oil-drop profile evolution.

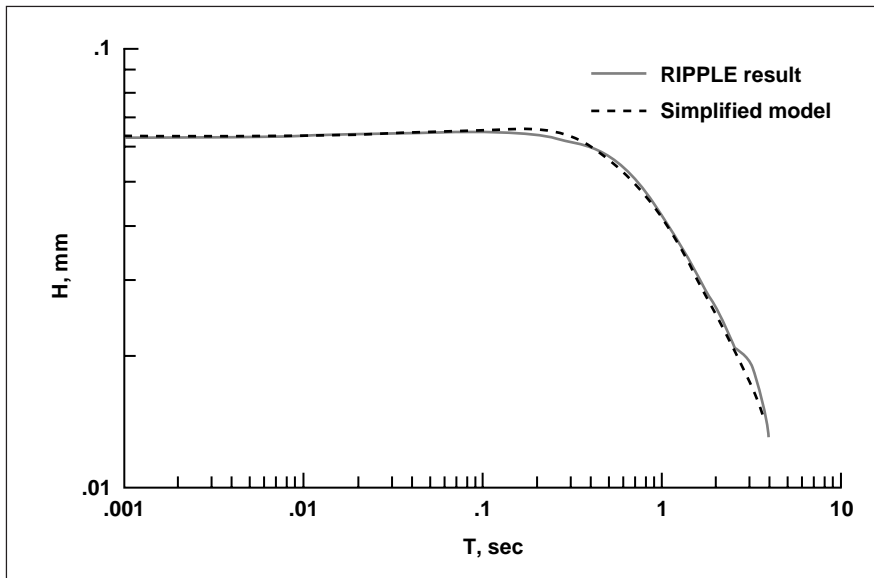


Fig. 2. Oil-drop thickness at $X = 3$ mm.

The uncertainty of FISF measurements is estimated to be as low as 4%, yet little is known about the effects of surface tension and wall-adhesion forces on the measured results.

A modified version of the free-surface Navier-Stokes solver RIPPLE, developed at Los Alamos National Laboratories, was used to compute the time development of an oil drop on a surface under a simulated air boundary layer. RIPPLE uses the Volume of Fluid (VOF) method to track the surface and the Continuum Surface Force (CSF) approach to model surface tension and wall-adhesion effects.

The figures show the development of an oil drop over a period of about 4 seconds. The profile of the drop (first figure) rapidly changes

from its initial circular-arc shape to a wedge-like shape. The close agreement between the oil-drop thickness computed using RIPPLE and the results obtained with a greatly simplified numerical model of oil-drop flow (solution of Squires oil-drop equation which does not include surface tension and wall-adhesion effects) proves that surface tension will have a negligible effect on FISF results (second figure).

Point of Contact: G. Zilliac
(650) 604-3904
gzilliac@mail.arc.nasa.gov

Fullerene Gear Design, Simulation, and Visualization

Albert Globus

Ames Research Center has designed and computationally investigated a series of atomically precise gears based on fullerene chemistry (see first figure). These gears are approximately 1 nanometer in diameter and can turn at up to 100 gigahertz according to computer simulations. Long-range goals include the design and validation of programmable molecular machines that can replicate and build useful aerospace products. This work will require massive computer power as nanotechnology research moves from “what if” to “how.” The current simulations help in understanding these computational requirements. If successful, molecular nanotechnology could revolutionize aeronautics and space technology by producing materials with radically improved strength-to-weight ratios and active materials filled with atomically precise machines that react to the environment and that can self-repair.

Hypothetical nanotechnology materials based on diamond chemistry have great potential, but at present no clear path can be seen for their synthesis. In contrast, fullerenes (closed-cage carbon molecules) are now routinely produced in the

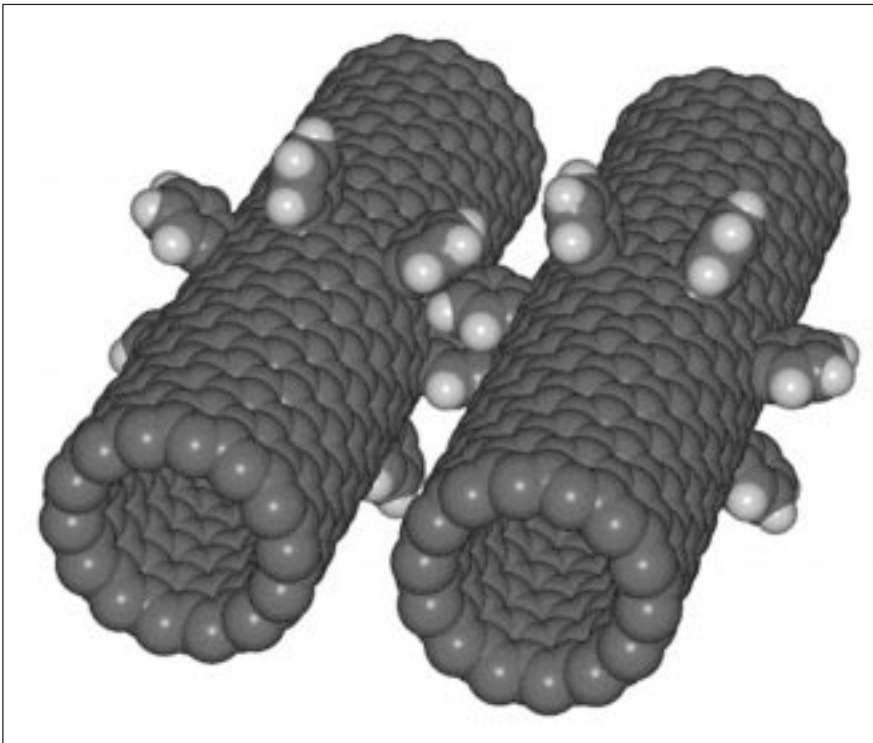


Fig. 1. Hypothetical carbon nanotube gears. Each gear is approximately 1 nanometer in diameter. Simulations suggest this system can rotate at up to 100 gigahertz.

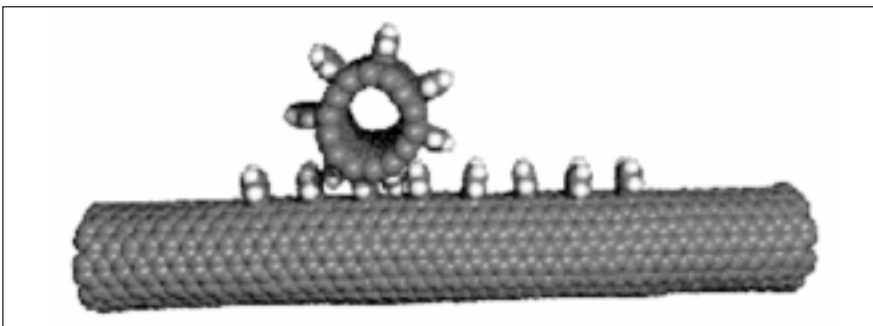


Fig. 2. Hypothetical rack-and-pinion system built from functionalized fullerene nanotubes.

laboratory. The carbon form called C-60 (a molecule with 60 carbons arranged in a soccer-ball-like configuration) is produced commercially, and carbon nanotubes have been produced in bulk, some over 100 microns long. It is possible to add a wide variety of molecular fragments to C-60 and other fullerenes. In particular, benzyne will react with the C-60 under mild laboratory conditions to form appended structures similar to gear teeth.

A series of videos has been made including gear synthesis steps, favorable operating conditions, various gear configurations, a rack-and-pinion system (see second figure), and tooth slip conditions, which are all based on molecular dynamics simulations run on parallel computers. Each gear consists of a carbon nanotube with several O-benzyne fragments added to form gear teeth. Molecular dynamics simulations suggest that when one gear is rotated, intermolecular forces cause the second gear to rotate at up to 100 gigahertz without slippage or fragmentation.

Point of Contact: A. Globus
(650) 604-4404
globus@nas.nasa.gov

GLOBAL CIVIL AVIATION/
ENVIRONMENTAL COMPATIBILITY

Civil Tiltrotor Noise Abatement Approaches

William A. Decker,
Rickey C. Simmons

A civil tiltrotor regional transport operating from vertiports near urban and business centers offers considerable potential for relieving conventional airport runway congestion. Flight operations near urban areas must also minimize noise effects while providing for all-weather schedule reliability. Conversion from airplane-mode flight to a helicopter-like landing while minimizing noise presents both a challenge and an opportunity for tiltrotor aircraft. The introduction of worldwide aircraft position information with the Global Positioning Satellite system provides an economic guidance source to support the desired low-noise, all-weather operations.

Initial tiltrotor noise-abatement landing approach profiles were constructed based on actual noise measurements of the XV-15 tiltrotor research aircraft. Instead of a conventional landing approach which intercepts and tracks down a 3-degree glideslope, two alternative profiles were constructed, both featuring an initial 3-degree descent which changes to a steep 9-degree descent close to the landing spot (first figure). Based on the XV-15 noise data, the steeper final approach path offers good potential for reducing noise while providing better clearance of obstacles near

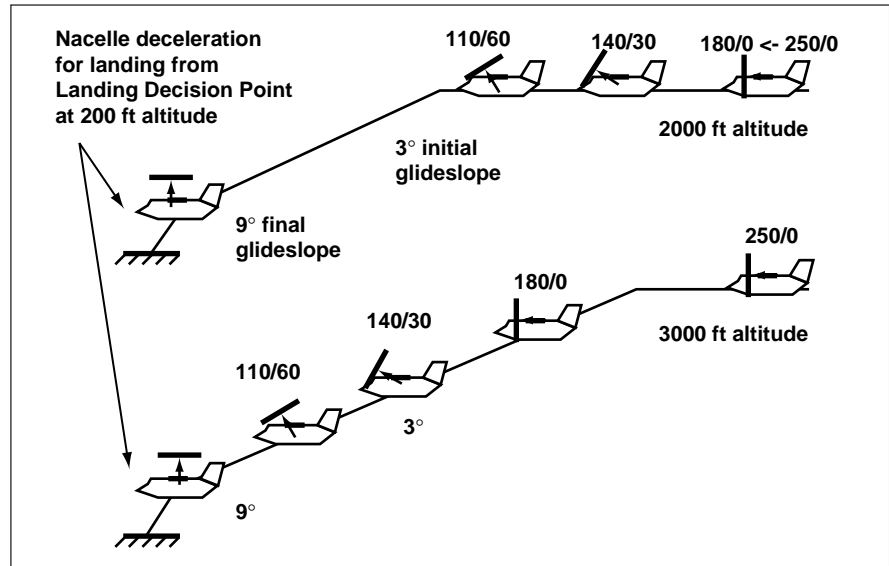


Fig. 1. Tiltrotor noise-abatement approach profiles with two-segment flightpaths. Altitude (flightpath angle), airspeed, and nacelle angle (for example, 110/60°) are specified as functions of distance from landing.

the vertiport. Depending on the terrain and airspace constraints associated with nearby conventional airports, the initial approach segment involved conducting either a level-flight conversion toward the helicopter-mode landing configuration, or performing all of the conversion in descending flight. Both approach profiles carefully specified airspeed, descent rate (flightpath position) and proprotor tilt angle based on the distance from the landing spot.

Cockpit displays and control features have been developed to help guide pilots to reliably and easily fly these complex approach profiles in all-weather conditions. As illustrated in the second figure, the displays were adapted from modern

electronic display formats for transport aircraft. Pursuit guidance using flightpath vector symbols, adapted from military head-up display designs, has been developed for tiltrotor use and applied to the panel-mounted electronic displays.

The unique large-motion cueing capability of the Vertical Motion Simulator (VMS) at Ames Research Center contributed to piloted evaluations of approach profiles and displays. Use of a visual scene based on the San Francisco Bay Area, developed in the VMS SIMLAB, contributed to the evaluation scenario and provided geographic rationale for the complex approach flightpath. Eleven pilots representing NASA, the FAA, British CAA, and the rotorcraft industry



Fig. 2. Pilot's view on approach to urban vertiport. Electronic cockpit displays provide guidance for complex noise-abatement approach profiles.

evaluated the approaches and displays, and provided comments for further refinement.

Point of Contact: W. Decker
(650) 604-5362
bdecker@mail.arc.nasa.gov

XV-15 Blade-Vortex Interaction Noise

C. W. Acree, Megan S. McCluer, Cahit Kitaplioglu

As part of the continuing In-Flight Rotorcraft Acoustics Program, flight tests of the XV-15 tiltrotor were completed and wind-tunnel tests are under way. Program objectives are (1) to use the NASA Ames YO-3A acoustic research aircraft to measure blade-vortex interaction (BVI) noise from rotorcraft in flight and to make compari-

sons with similar wind-tunnel measurements, (2) to use these comparisons to better understand BVI noise, and (3) to determine how to minimize BVI noise on rotorcraft.

During the flight portion of this test, the YO-3A fixed-wing aircraft used a wing-tip-mounted micro-

phone to measure BVI noise generated by the XV-15 tiltrotor. Four flights were performed with the YO-3A and XV-15 flying in close formation, as shown in the figure. The flight conditions and microphone location were chosen to measure the most prominent BVI noise. The starboard wing-tip microphone of the YO-3A was positioned 20 degrees below the right rotor hub of the XV-15 and offset to the right to pick up BVIs occurring at a rotor azimuth of 150 degrees (see figure). The distance between the starboard wing-tip microphone and the rotor hub was 3 rotor diameters (75 feet). Target flight conditions included advance ratios of 0.165 and 0.185, tip Mach number of 0.69, a rotor weight coefficient of 0.0111, and descent rates of 300–1100 feet per minute.

The results of the flight test were used to determine equivalent test conditions for a series of tests of the XV-15 rotor in the National Full-Scale Aerodynamics Complex



Fig. 1. YO-3A and XV-15 in formation flight.

(NFAC) 80- by 120-Foot Wind Tunnel test section at Ames Research Center. A single (right-side) rotor was mounted on the Rotor Test Apparatus (RTA), and microphones were placed in locations geometrically identical to the relative positions of the YO-3A microphones and XV-15 rotor during flight. The data from the NFAC tests have been compared with the flight data to validate the wind-tunnel test and the measurement methods. Although very good qualitative agreement was achieved, good quantitative agreement has yet to be demonstrated. In particular, the ability to match wind tunnel with flight will likely require very good characterization of the flight operating conditions to enable matching of the exact test condition in the wind tunnel.

Point of Contact: C. Acree
(650) 604-5423
wacree@mail.arc.nasa.gov

Tiltrotor Aeroacoustic Model

Larry Young

NASA conducts tiltrotor research programs in order to meet national requirements for military and civilian tiltrotor aircraft. This research requires moderate-to-large-scale wind-tunnel testing of tiltrotor models. Such testing provides the data necessary to confirm aeroacoustic prediction methods, and to investigate and demonstrate advanced civil tiltrotor and high-speed rotorcraft technologies.

In 1991, NASA established that it had a requirement to gain an

improved understanding of the aeroacoustic characteristics of tiltrotor aircraft and, therefore, initiated the development of two hardware-compatible test rigs: an isolated-rotor test stand and a full-span model (dual rotors with a complete airframe representation). These two test stands are inclusively called the Tilt Rotor Aeroacoustic Model (TRAM). The isolated rotor test stand is not a stand-alone unit, but is instead intended to be composed chiefly of major subassemblies of the full-span configuration.

The TRAM will be used as a test bed for testing moderate-scale tiltrotor models in two different test configurations in different research facilities: (1) isolated rotor testing at the Duits-Netherlands Windkannel (DNW) in The Netherlands; and (2) isolated rotor and full-span testing at the National Full-Scale Aerodynamics Complex (NFAC) at Ames Research Center.

A checkout test of the TRAM isolated-rotor test stand was con-

ducted in the NFAC N246 Model Preparation building at Ames. The checkout testing included the acquisition of hover data—including rotor airloads data—for a 1/4-scale set of proprotor blades using the NFAC NPRIME data-acquisition system. Key test-stand capabilities being checked out include a rotating amplifier system (RAS) developed by the Nationaal Lucht-en Ruimtevaartlaboratorium (NLR) and the Monitoring Front-End Data System (MFEDS) real-time safety-of-flight monitoring system. A considerable amount of infrastructure buildup—including armor-plate shielding and control room installation—was required in the N246 building to enable TRAM functional testing.

The full-span version of the TRAM test stand is also being concurrently developed. Fabrication of full-span model development is under way (see figure). A new generation rotor-control console for



Fig. 1. Full-span TRAM fabrication and assembly.

the isolated rotor test and the full-span model is also in development.

The 1/4-scale TRAM rotors and airframe are based on the design of the V-22 Osprey tiltrotor aircraft. The TRAM test stand will also be an advanced technology demonstrator platform for the Short Haul Civil Tiltrotor (SH(CT)) program, a sub-element of the Advanced Subsonic Technology (AST) initiative. Both Boeing and Sikorsky Aircraft have been contracted by the NASA SH(CT) program to develop interface hardware to test a new generation of small-scale, advanced proprotors on the TRAM test stand.

Point of Contact: L. Young
(650) 604-4022
lyoung@mail.arc.nasa.gov

Predicting and Analyzing Rotorcraft Noise

Roger C. Strawn, Rupak Biswas,
Lenny Olikier

Aerodynamic noise is a major problem for future civil tiltrotor designs. Noise is a particular problem during landing when the rotor-wake system is pushed up into the rotating blades. The resulting blade-vortex interaction (BVI) noise can be unacceptable in urban environments. All four of the major U.S. helicopter companies have active research programs with the objective of reducing tiltrotor and helicopter BVI noise.

Three things are required in order for rotor designers to systematically reduce BVI noise: (1) an improvement in the accuracy of far-field noise predictions; (2) the ability

to analyze those predictions in a way that identifies the sources of the offending noise; and (3) control of rotor-blade motion in ways that reduce the noise. Researchers at Ames Research Center have recently developed new acoustic prediction and analysis tools that directly address the first two of these three objectives.

The new acoustic prediction scheme combines computational fluid dynamics (CFD) with Kirchhoff integration methods. The CFD methods compute the nonlinear aerodynamics and acoustics close to the rotor blades, and the Kirchhoff integrations carry the acoustic information to the far-field in a computationally efficient manner. These CFD/Kirchhoff methods run on the IBM SP-2 parallel computer to facilitate the computation of time-accurate acoustic information over large regions of space. Computer audio and visual rendering (see figure) of the resulting far-field

acoustic propagation allows rotor designers to “see and hear” the noise in the far-field. Computer animations of the far-field noise propagation convey much more information than can be obtained from typical rotor-noise experiments, in which the data are limited to those picked up by a few far-field microphones. In addition to the new prediction and visualization tools, the CFD/Kirchhoff analysis can be modified to highlight the sources of noise on the Kirchhoff surface. This allows a rotor designer to pinpoint the origins of the far-field noise and to modify the blade trajectories to minimize the blade-vortex interactions.

The new prediction and analysis tools will have applications to a variety of helicopter and tiltrotor geometries.

Point of Contact: R. Strawn
(650) 604-4510
rstrawn@mail.arc.nasa.gov

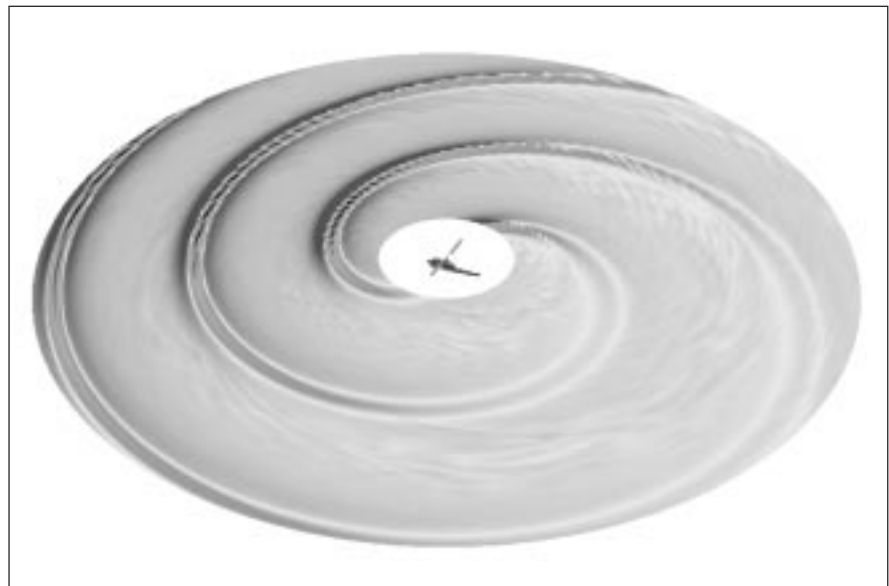


Fig. 1. Computed acoustic pressure contours for the AH-1 Cobra helicopter.

Airframe Noise Measurements: Atmospheric Pressure

W. Clifton Horne, Julie A. Hayes,
Michael E. Watts, Paul H. Bent

With the trend toward quieter, higher bypass-ratio engines in commercial transport aircraft, airframe noise is a significant problem during approach and landing. In support of the Noise Reduction Element of the Advanced Subsonic Technology (AST) Program, an aeroacoustic test of an unpowered, 4.7%-scale McDonnell Douglas DC-10 was conducted in the NASA Ames 40- by 80- Foot Wind Tunnel (see figure). Acoustical measurements included streamwise traverses of four microphones, far-field measurements with directional microphones using parabolic reflectors, and noise-source location with a 40-element phased microphone array. Aerodynamic measurements included steady and unsteady wing-surface pressures and model incidence.

The primary objectives of this test were to (1) assess the feasibility of extrapolating wind-tunnel airframe noise measurements for comparison with full-scale flight-test results, (2) locate prominent noise sources with the acoustic array, and (3) evaluate prototype noise-reduction concepts on a realistic transport configuration.

Measurements supporting all of the primary test objectives were obtained. In particular, acoustic images of airframe noise sources on the high-lift system and landing gear were obtained. This was achieved using the Microphone Array Phased



Fig. 1. DC-10 model in the Ames 40- by 80-Foot Wind Tunnel.

Processing System developed at Ames Research Center. This system used high-performance graphical workstations in the control room to process the array data and display results during the test. The system processed 200 frequencies at each data point within 30 minutes, thus allowing all test data to be processed during the test (as much

as 3 months of posttest processing were required in previous tests). The processing system was designed to fully support existing remote access wind-tunnel capabilities.

Studies of flap-edge fences designed to reduce noise emanating from the flap edge showed broadband noise reduction levels of

3–4 decibels. Correlation of the noise signals on a far-field microphone with the unsteady pressure signals on the model aircraft surface was effective in locating the source of the airframe noise.

Point of Contact: C. Horne
(650) 604-4571
chorne@mail.arc.nasa.gov

Airframe Noise Measurements: Pressures to 4.7 Atmospheres

W. Clifton Horne, Stephen M. Jaeger, Mahendra Joshi, James R. Underbrink

Airframe noise, primarily attributable to the landing gear, leading-edge slat, and trailing-edge flap, is known to be a significant component of the approach and landing noise of commercial transport aircraft. The NASA Advanced Subsonic Technology (AST) Noise Reduction Technology Program is sponsoring several measurement and prediction programs in order to reduce airframe noise by 4 decibels below 1992 levels. Because of the expense of flight tests, an important element of this research is the application of new measurement technology, such as the multisensor phased acoustic array, on tests of small-scale wind-tunnel models and then scaling and extrapolating these measurements to full-scale. The physics of aerodynamic noise generation and the effect of geometric scale are highly complex and not

well understood. Therefore, acoustic measurements, over a range of scale factors (or Reynolds numbers), are required to identify the important noise sources on full-scale aircraft and to determine the scaling laws that will permit accurate full-scale predictions from small-scale tests.

Recent successful tests by Ames and Boeing using a multielement phased microphone array in closed, untreated test sections suggested that useful airframe noise measurements could be obtained in the Ames 12-Foot Pressure Wind Tunnel (PWT) for variable Reynolds number testing. Feasibility tests of a Boeing 52-element array in the 12-Foot PWT were planned in two phases. An initial study of the operational feasibility was planned with the test section empty except for a survey strut, model ground plane, and calibration noise sources. If this initial study proved to be successful, a second demonstration of aeroacoustic measurements of a 4.7%-scale DC-10 was planned in conjunction with McDonnell Douglas to acquire the first variable Reynolds number airframe noise measurements. The results would be compared with atmospheric measurements acquired from the same model in the 40- by 80-Foot Wind Tunnel at Ames with a 40-element phased-array designed and assembled at Ames.

The first feasibility test demonstrated that the microphone-array system (sensors, cabling, signal acquisition and processing, and computer networking) could be

accommodated with existing facility support infrastructure. Several aeroacoustic noise sources were located with the array, associated with support struts and the trailing edge of the semi-span ground plane. The second test utilizing the 4.7%-scale DC-10 aircraft model was then undertaken. During this second test, the Boeing array acquired noise measurements to 60 kilohertz, corresponding to about 3 kilohertz full-scale, and identified noise sources at atmospheric pressure which corresponded closely with sources identified in the previous 40- by 80-Foot Wind Tunnel test (see figure (see Color Plate 10 in the Appendix)). In addition, noise measurements were obtained for pressures up to 4.7 atmospheres. Preliminary evaluation of these measurements show that the relative strength of the noise sources varies with Reynolds number in a complex and as yet unpredictable manner, stressing the need for large-scale, high-Reynolds-number validation of noise-prediction methods.

Point of Contact: C. Horne
(650) 604-4571
chorne@mail.arc.nasa.gov

REVOLUTIONARY TECHNOLOGY LEAPS/
INNOVATIVE TECHNOLOGY AND TOOLS

X-36 Pioneers Advanced Aerodynamics and Flight Controls

Rodney Bailey, Mark Sumich

The X-36 project is pioneering the development of advanced aerodynamics and flight control technologies that will permit the concurrence of low radar observability, agility, and supersonic speed in a single design. Prior to the X-36 technologies, these features were mutually exclusive. The flight evaluations of the X-36 aircraft, a joint NASA/McDonnell Douglas project, are currently under way at the Dryden Flight Research Center.

The project began in February 1994 after several years of research and concept development in the Ames facilities by both Ames and McDonnell Douglas engineers.

The project involves the design, fabrication, and flight evaluation of two unmanned aircraft. The 10-foot-span flight articles are about 18 feet long and 3 feet high and weigh 1250 pounds.

Features of the X-36 include multifunction wing trailing edge control surfaces, combined ailerons, split ailerons and flaps, wing leading edge flaps, and all moving canards. The aircraft has neither vertical nor horizontal aft tail surfaces. The aircraft (shown in the figure) is naturally unstable in both the pitch and yaw directions, with artificial stability provided by the control laws utilizing both aerodynamic and propulsion forces.

The flight testing at Dryden will evaluate real-time stability margin and will determine aerodynamic, stability, and control data on the configuration using the parameter-identification derivative.

Point of Contact: R. Bailey
(650) 604-6265
rbailey@mail.arc.nasa.gov



Fig. 1. X-36 Tailless Fighter Agility Research Aircraft prepares for flight at the Dryden Flight Research Center.

Closed-Loop Neural Control of Rotorcraft Vibration

Sesi Kottapalli

A study on identification and control of rotorcraft hub loads (vibration) using neural networks has been initiated at Ames Research Center. Neural control simulation covers both identification and control of hub loads, where a metric is used to represent the hub load components. The closed-loop controller must be computationally efficient, it must converge quickly (in six iterations or less), and gradient-based methods must not be used.

The program objective is to implement closed-loop neural control of rotorcraft vibration in a wind tunnel in two phases: (1) conducting neural-control simulations using existing individual blade-control wind-tunnel test data, and (2) implementing closed-loop neural control during a future full-scale rotorcraft wind-tunnel test (contingent on first-phase results being sufficiently promising).

The identification (plant modeling) procedure, which involves the use of a two-hidden-layer radial basis function neural network, has been completed. The procedure has been extended to multi-input, multi-output applications. A simple, straightforward-to-implement neural-control technique, the "direct inverse" method, was selected, successfully applied, and found to

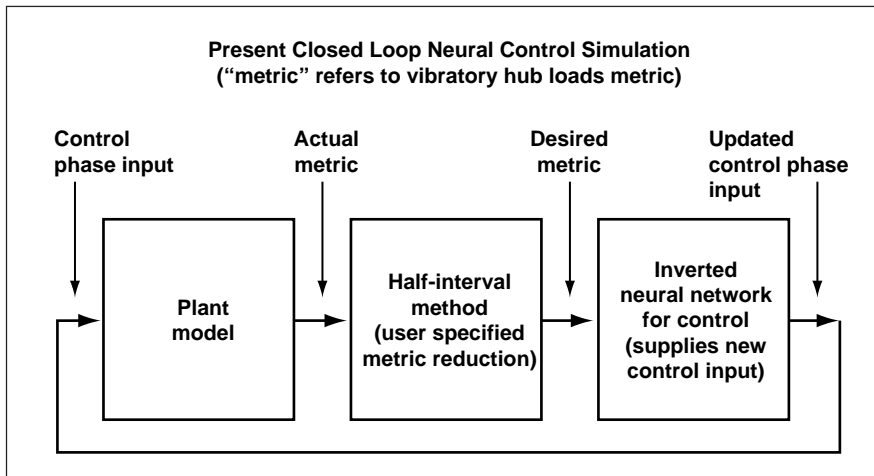


Fig. 1. Inverted neural network for vibration control.

be robust. The present approach (see the figure) has the following essential ingredients: accurate plant modeling, halving of the metric in order to accelerate controller convergence, “inverted-axes” control modeling, and a feedback iterative loop. A back-propagation neural network used in the control step has been successful. Current results show that a 66% reduction in baseline rotor vibratory hub loads is achievable in only four controller iterations. A limited-scope comparison of the results from the present neural-control procedure with those from a one-step deterministic controller showed that the two control methods are comparable, with neural control being more robust.

Point of Contact: S. Kottapalli
 (650) 604-3092
 skottapalli@mail.arc.nasa.gov

Coupled Navier–Stokes and Optimizer Analysis of a Transonic Wing

Roxana M. Greenman,
Samson Cheung, Eugene L. Tu

Numerical optimization can be used as a means of studying the effects of the geometric parameters on the aerodynamics of a wing. Different types of aerodynamic numerical-optimization techniques that have been researched in recent years have been found to need improvement. New optimization tools must be developed to provide efficient means for improving the design process and understanding the flow physics. The overall objective is to develop the necessary tools needed to help, using computational fluid dynamics for the design of advanced wings through the inclusion of new, promising optimization

modules to the code OVERFLOW. The object is to demonstrate the use of a numerical-optimization routine to understand the significance of different geometric parameters on the aerodynamics of a wing.

This study demonstrated how one optimizer package is used to study the flow physics of a transonic wing. This numerical-optimization routine is integrated with a grid generator and a validated Navier–Stokes flow solver. The effects of wing sweep angle, root and tip twist angles, dihedral, and angle of attack on the lift-to-drag ratio are studied using surface-pressure contours and pressure distributions. The results show that when lift-to-drag ratio is increased using single design variable optimization, the resulting lift coefficient falls below the original value. The angle of attack must be increased in order to preserve the original lift coefficient with the modified geometry. A better way to find the optimal configuration with the highest lift-to-drag ratio is by first optimizing with multiple design variables (see the figure (see Color Plate 11 in the Appendix)), then including the angle of attack in the design loop with lift constrained to the original value. This method showed an improvement of 2.4% (with constant lift) in the lift-to-drag ratio.

Point of Contact: R. Greenman
 (650) 604-3997
 rgreenman@mail.arc.nasa.gov

Parallel Unstructured Mesh Adaption

Rupak Biswas, Leonid Oliker,
Roger Strawn

Computational methods to solve large-scale realistic problems can be made more efficient and cost effective by using them in conjunction with dynamic mesh adaption procedures that perform coarsening and refinement to capture interesting solution features. Such adaptive procedures evolve with the solution, and they provide scientists a robust and reliable methodology to obtain solutions on adapted meshes that are comparable to those obtained on globally fine grids but at a much lower computational cost. In addition, with the popularity of distributed computing, parallel unstructured mesh adaption procedures are absolutely imperative.

An efficient solution-adaptive procedure has been developed for the simultaneous coarsening and refinement of unstructured tetrahedral meshes. An innovative data structure, which uses a combination of dynamically allocated arrays and linked lists, allows the mesh connectivity to be rapidly reconstructed after individual points are added and/or deleted. The data structure, based on edges of the mesh rather than the tetrahedral elements, not only enhances the efficiency but also facilitates anisotropic mesh adaption. This scenario means that each tetrahedral element is defined by its six edges rather than by its four vertices. Each edge, in turn, maintains a list of all the elements that share it. Thus, elements that need to

be modified can be rapidly identified when an edge is inserted or deleted. Regions of the mesh that need to be adapted are identified by marking the edges based on an error indicator. The adaption procedure for each element is determined from a binary pattern that depends on which of its six edges are marked. The edge data structures and pattern marking ensure that the refinement and coarsening procedures can be performed efficiently.

The parallel mesh adaption procedure has been used to model the high-speed impulsive noise for a UH-1H helicopter rotor in hover. A coarse mesh is initially generated and additional points are dynamically added to capture the acoustic wave and the shock near the tip. Mesh coarsening is used to remove unnecessary points from regions with smooth solutions; thus, existing grid points are redistributed in a more efficient manner. A close-up of the final grid and pressure contours in the plane of the rotor after three adaption steps is shown in the figure (see Color Plate 12 in the Appendix). Results show excellent agreement with experimental microphone data for far-field acoustic pressure. Parallel speedup depends on the fraction of the mesh that is adapted. When 33% of the mesh was refined, a speedup of 43.2X was obtained on 64 processors. The speedup improved to 51.5X when 60% of the mesh was refined.

Current results demonstrate significant gains in computational efficiency when the parallel solution-adaptive method is compared to its fixed-grid counterparts.

These improvements are necessary for future high-fidelity simulations of realistic problems in unsteady environments.

Point of Contact: R. Biswas
(650) 604-4411
rbiswas@nas.nasa.gov

Load Balancing Adaptive Unstructured Meshes

Rupak Biswas, Leonid Oliker,
Andrew Sohn

Mesh adaption is a powerful tool for efficient, unstructured-grid computations, but it causes load imbalance among processors on a parallel machine. A novel method has been developed to dynamically balance the processor workloads with a global view. A dual graph representation of the initial computational mesh keeps the complexity and connectivity constant during the course of an adaptive computation. It is a portable system for efficiently performing large-scale adaptive calculations in a parallel message-passing environment.

The first figure depicts the framework used for parallel adaptive scientific computations. Mesh adaption, repartitioning, processor assignment, and data remapping are critical components of the framework that must be accomplished rapidly and efficiently so as not to cause a significant overhead to the numerical simulation. The unstructured mesh is first partitioned and mapped among the available processors. A solver then runs for several iterations, updating solution

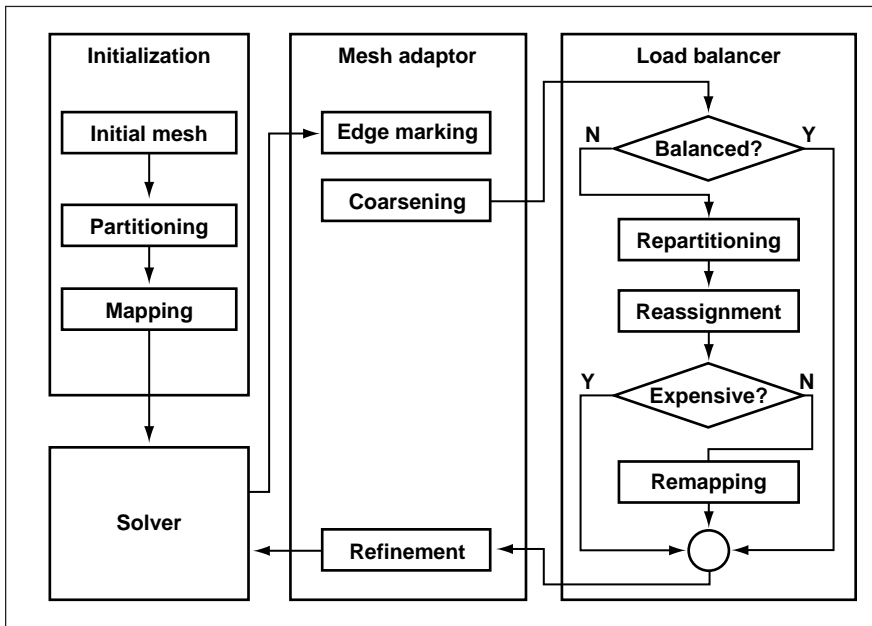


Fig. 1. Framework for parallel adaptive scientific computation with load balancing.

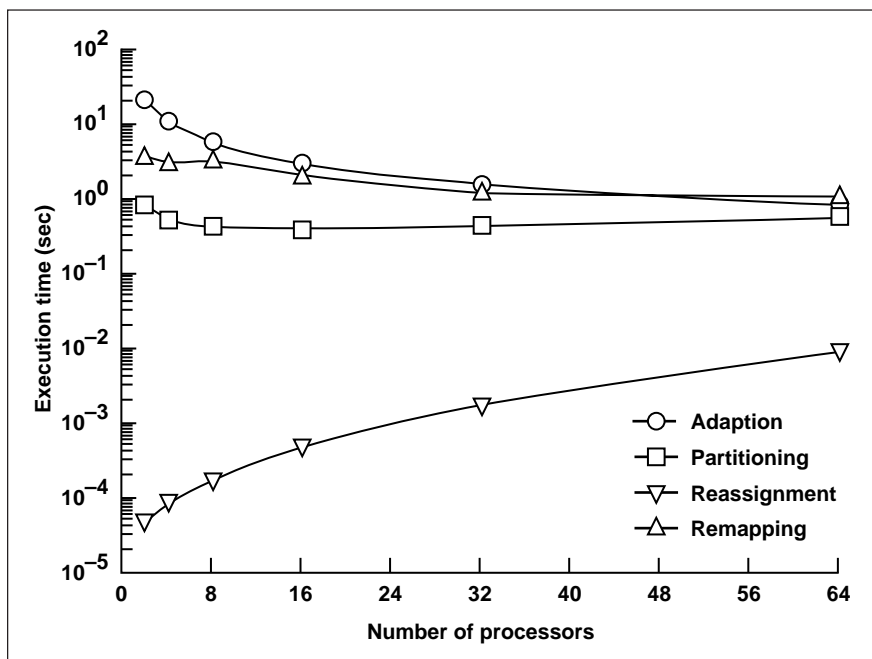


Fig. 2. Anatomy of total execution time.

variables. After an acceptable solution is obtained, the mesh adaption procedure is invoked. It first targets edges of the mesh for coarsening and refinement based on an error indicator computed from the numerical solution. The old mesh is then coarsened, resulting in a smaller grid. Since edges have already been marked for refinement, it is possible to exactly predict the new mesh before actually performing the refinement step. Program control is thus passed to the load balancer. If a quick evaluation step determines that the new adapted mesh will be unacceptably load balanced, a repartitioner divides the mesh into subgrids. The new partitions are then assigned to the processors in a way that minimizes the cost of data movement. If the remapping cost is less than the computational gain that would be achieved with balanced partitions, all necessary data are appropriately redistributed; otherwise, the new partitioning is discarded. The computational mesh is then actually refined and the numerical calculation is restarted.

An extensive study with a computational mesh used to simulate a UH-1H helicopter rotor blade acoustics experiment indicated that the load-balancing scheme is effective for large-scale scientific computations on distributed-memory machines and scales excellently with the number of processors. The second figure shows how the total execution time was spent in each module of the framework when the mesh was refined to be more than five times larger than the original.

The processor reassignment times are almost negligible compared to the other times. The repartitioning time is generally independent of the number of processors. Both the adaption and remapping times gradually decrease as the number of processors is increased. These sample results show that none of the individual modules will be a bottleneck on massively parallel machines.

Point of Contact: R. Biswas
(650) 604-4411
rbiswas@nas.nasa.gov

Initial Release of the Field Encapsulation Library

Steve Bryson

Computational fluid dynamics (CFD) simulations are a new way of designing and evaluating aircraft designs on a computer. CFD simulations are computed at many points, forming a three-dimensional grid in space. The variety of grid types can greatly complicate the task of using computer graphics visualization to investigate the CFD simulations (see the figure (see Color Plate 13 in the Appendix)). Visualization algorithms can depend very strongly on the type of grid; an algorithm written for one grid type may not work on another grid type. This problem is particularly acute when developing a general-purpose visualization system for CFD. The objective of the Field Encapsulation Library (FEL) project is to solve the grid-dependence

problem by implementing a library that provides a grid-independent approach to CFD data access. Using FEL, a single visualization algorithm can work on a variety of grid types. Very high performance data access is an additional objective in order to support interactive visualization, which allows intuitive exploration of the simulated flow phenomena. Another objective of FEL is to provide programmers with the ability to access, organize, and manipulate field-type data on many types of numerical grids at the same time.

FEL was fully implemented and released for structured multizone and unstructured grid types, proving the grid-independence concept. Data access times averaging 0.0002 second per access were measured. These capabilities allow the development of high-performance visualization algorithms that will work for all supported grid types. FEL has been integrated into the Virtual Windtunnel as well as other individual visualization systems. The concepts behind FEL were presented at Visualization '96, an IEEE peer-reviewed conference held in October 1996 in San Francisco, California.

FEL is an example of a "horizontal product," a set of software libraries that can be used in a variety of applications, significantly reducing the time required to implement a new visualization system.

Point of Contact: S. Bryson
(650) 604-4524
bryson@nas.nasa.gov

RANS-MP: Portable Parallel Navier–Stokes Solver

R. Van der Wijngaart,
Maurice Yarrow

Efficient, cost-effective solution of flow problems of interest to the aircraft industry requires competitively priced hardware and maintainable, portable software. The current generation of parallel computers provides that hardware, and standard system software such as the message passing interface (MPI) library provides half of the software solution. The other half comes from application programs that employ algorithms that are tolerant of differences in specific machine parameters, most notably the speed with which the processors in a parallel computer can exchange data. The Reynolds-averaged Navier–Stokes with multipartitioning (RANS-MP) program has been specifically designed to meet these requirements.

The newly developed RANS-MP flow solver program employs the advanced, bidirectional, multipartition algorithm. This method limits data movements between processors to a minimum, rendering it insensitive to the peculiarities of different parallel computers. RANS-MP uses the widely available MPI, which means it can run efficiently on most of today's parallel machines. It also employs a pilot

version of MPI's companion input/output (I/O) library MPI-I/O, which allows efficient scheduling of previously prohibitively expensive parallel read and write operations.

The first figure shows the performance of the program on the Ames Research Center IBM SP-2 parallel computer in terms of millions of points updated per second by the flow solver. The problem is that of viscous flow around an aircraft wing. A good measure of the quality of a parallel program is its scalability, which is defined as the improvement in performance as more processors are added to the computation. The figure indicates that, even for a relatively small grid of fixed size of 200,000 points, the scalability is quite good (heavy dashed curve). Performance is even better if the problem size is allowed to grow with the number of processors employed (heavy solid curve). For reference, the ideal speedup curve (thin solid line) is also shown.

The second figure indicates the improvement in performance of using the MPI-I/O library over that of the standard, nonparallel I/O library on the SP-2, where a gain of up to a factor of 30 in write speed can be observed.

Although RANS-MP primarily targets cache-based systems that make up the bulk of the latest high-performance computing architectures, care has also been taken to provide good performance on more traditional computers such as the Cray C90 and the NEC SX-4. There-

fore, the code must be written to allow efficient vectorization, the main source of performance improvement on such machines. When the wing problem is solved on the C90, RANS-MP attains a respectable 45% of the maximum possible performance of the machine.

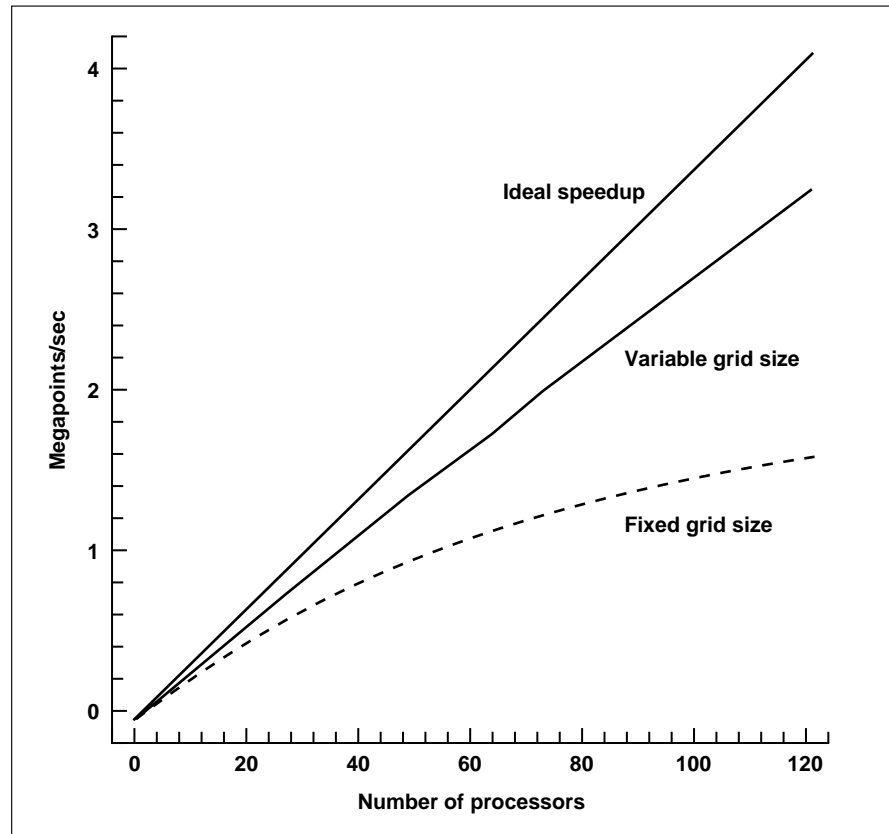


Fig. 1. Millions of points updated per second on IBM SP-2.

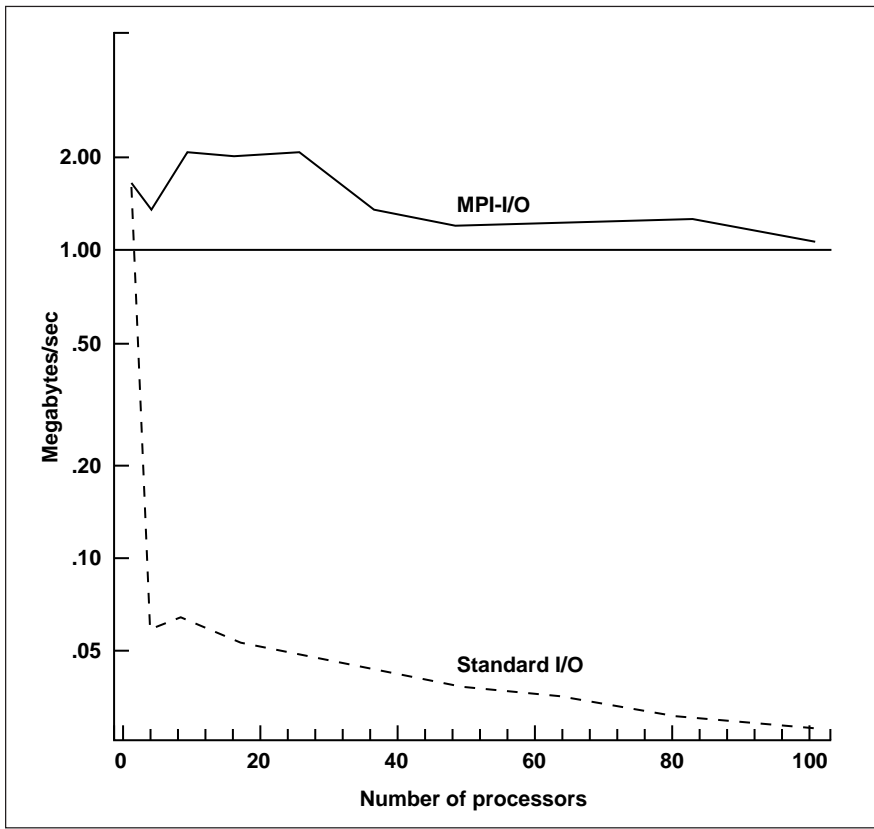


Fig. 2. Write speed in megabytes per second for MPI-I/O and standard I/O on IBM SP-2.

Measurements show that more than 99% of all computational statements are executed in vector mode.

Point of Contact: M. Yarrow
(650) 604-5708
yarrow@nas.nasa.gov

Parallel Tools for Parallel and Distributed Computer Systems

**D. DiNucci, M. Frumkin, R. Hood,
H. Jin, L. Lopez, R. Papasin,
C. Schulbach, J. Yan**

Software tools have been developed that accelerate the development of Grand Challenge Computational Aeroscience applications for massively parallel processing systems. These software tools and associated research focus on areas critical to understanding and using computer systems capable of

trillions of floating point operations per second, including: (1) performance tuning, visualization, and analysis; (2) parallel debugging; and (3) programming paradigms and environments.

In the first area, an integrated performance-tuning environment is developed around the Automated Instrumentation and Monitoring System (AIMS). (See the first figure.) AIMS is a software tool that automatically instruments parallel FORTRAN and C programs, monitors their execution on parallel architectures, and displays and analyzes their performance. Dynamic variation of system parameters and overall performance are automatically captured during execution and subsequently displayed on the color screen of a workstation. A key feature of AIMS is that it provides source-code click-back, allowing the user to relate trace events with specific statements in the application program. AIMS also supports tracking and visualization of interprocessor data movements. In addition to providing trace information, AIMS has been used to investigate the possibility of regenerating program trace information from statistics collected during program execution.

The Numerical Aerodynamic Simulation trace visualizer (NTV) is a related tool that provides an alternative to the visualization kernel (VK) of AIMS. Whereas VK provides dynamic visualization of programs, NTV provides static, zoomable views. Another product, Ben, is a library of visualization routines that can be used to develop visualization capabilities in other software tools

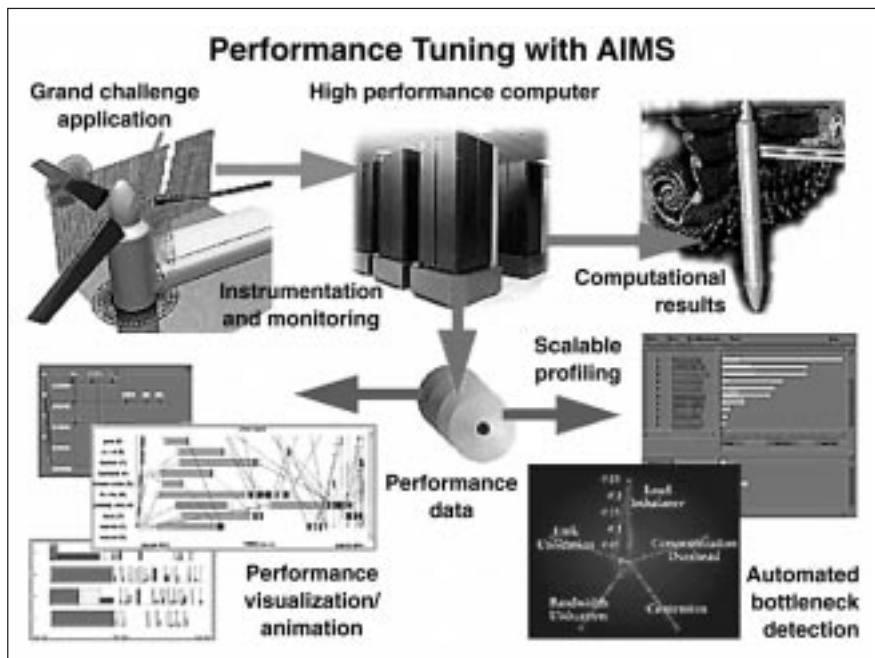


Fig. 1. AIMS software toolkit for automatically instrumenting parallel programs, monitoring their execution, and displaying and analyzing their performance.

and products. AIMS is available for the IBM SP-2 (message passing interface (MPI)) and on workstation clusters (parallel vertical machine (PVM) and MPI). NTV supports AIMS traces as well as native traces from the IBM SP-2.

The second area involves the development of a debugger for use on parallel and distributed computer systems. The portable parallel/distributed debugger (p2d2) (see the second figure) is a system using a client/server model that is portable across target machines and communication libraries. This system allows the architecture- and operating system-dependent code to be located in a server while the client-side code remains highly portable. It was designed with scalable user

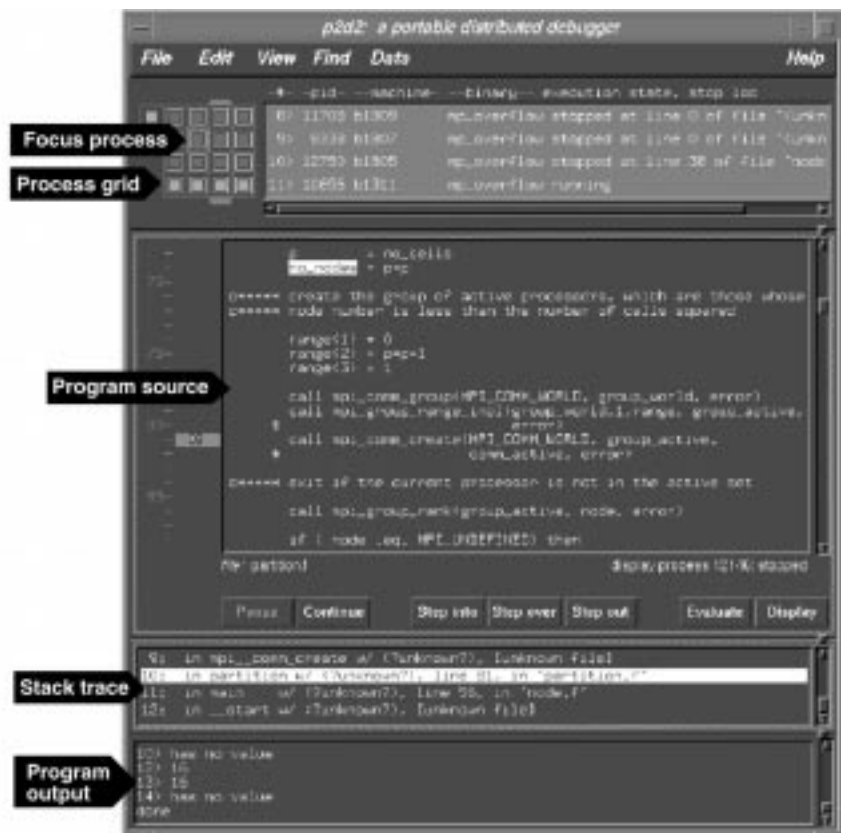


Fig. 2. p2d2 being used to debug the running program `mp_overflow`.

interface elements in expectation that users will want to debug computations involving many (16 to 256) processes. p2d2 is currently available on the IBM SP-2 (for MPI). Development of support for PVM has also been completed.

In the third area, programming paradigms and environments, the Cooperative Data Sharing System (CDS) has been developed to provide an efficient, portable, and simple system for creating processes and communicating between them in cluster, message-passing, and shared-memory environments. This setup allows the user to specify the semantics required of each communication so that it can execute with near-optimal performance on any target architecture: shared-memory, message-passing, or cluster. The CDS application user interface consists of two layers: a kernel level (CDS1), with objectives of minimality, orthogonality, portability, efficiency, and utility; and a user level (CDS2) built upon CDS1, with the sole objective of providing a useful user interface without interfering with the desirable characteristics of CDS1. CDS1 is available on SUN Solaris and Silicon Graphics Inc. Challenge Array systems.

Point of Contact: C. Schulbach
(650) 604-3180
cschulbach@mail.arc.nasa.gov

Numerical Aerodynamic Simulation Parallel Benchmarks 2.2

**William Saphir,
R. Van der Wijngaart,
Alex Woo, Maurice Yarrow**

The Numerical Aerodynamic Simulation (NAS) Parallel Benchmarks 2.2 (NPB2.2) bring a new era of integrity to the performance claims of the vendors of high-performance parallel computers. NASA is an immediate beneficiary of these benchmark tools, as is the scientific and engineering community at large, since evaluation of high-performance computers can now be based on objective performance criteria rather than vendor hyperbole. The NPB2.2 also stand out as excellent source code models for the development of future parallel versions of simulation programs for the aerospace industry.

NPB2.2 consist of source code versions of seven computational fluid dynamics applications and kernels that were originally given as "paper and pencil" specifications. In their original form, they gained wide acceptance as measures of parallel computer performance, but vendor implementations were machine-specific and proprietary. The current source code versions, however, have been specifically designed to run on modern parallel computers that support the commonly available message passing interface (MPI). They are available from the World Wide Web, and have been designed to be extremely easy to use. Data generated by these benchmarks are now available for a wide variety of parallel computers from numerous

vendors, and are readily viewable at the NASA NPB Web site.

New to NPB2.2 are the IS integer sort kernel and a vastly improved FT Fast Fourier Transform kernel. Unlike the other kernels that measure floating-point performance, the IS code does integer operations only and measures raw processor power. It also provides a strenuous test of the speed of the communication network of a modern parallel computer. The new FT program, no longer limited to 128 processors, has had its floating-point performance improved. The three application benchmarks known as BT, LU, and SP solve equations of viscous flow, each with a different algorithm. The remaining two kernels solve a multigrid problem and a so-called "embarrassingly parallel" problem. The suite provides a comprehensive test of the capabilities and relative performance level of a parallel computer, making the task of assessing high-performance computers for NASA laboratories easier than ever before.

Point of Contact: M. Yarrow
(650) 604-5708
yarrow@nas.nasa.gov'

Large-Scale Parallel Semiconductor Simulation

Subhash Saini

At the present time, several technologies are pressing the limits of the semiconductor-based computer industry, including the 0.1-micron foreseeable limit of the photolithography process, quantum

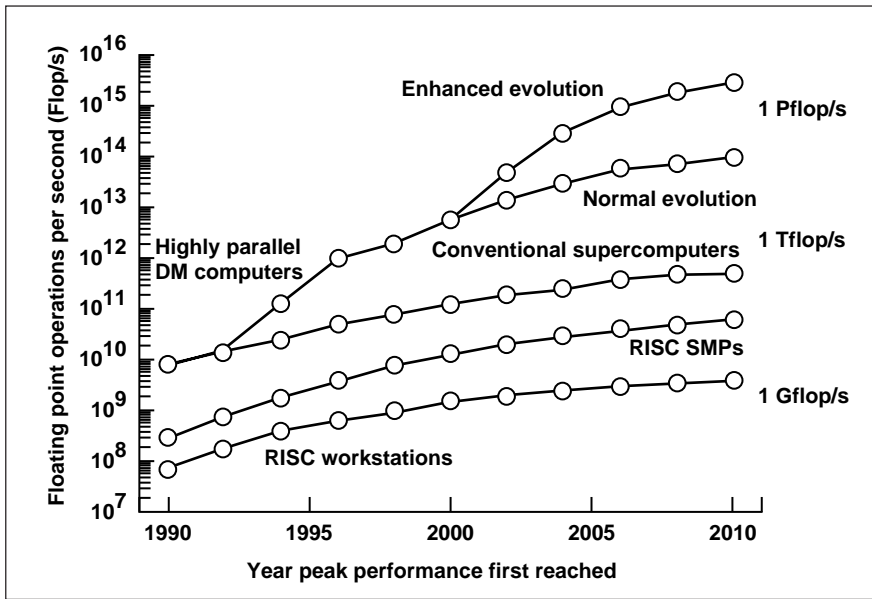


Fig. 1. High-performance computing technology roadmap.

effects, heat dissipation, the skyrocketing cost of manufacturing plants, and others. NASA requirements for high-performance computers are different from those of mainstream industry. For many applications, such as the High-Performance Computing and Communication (HPCC) remote exploration and experimentation (REE) project, NASA requires low-powered, ultracompact, high-performance computers that are resistant to radiation damage. By the year 2010, many important future NASA missions will rely on petaflops computer systems. Applications of interest to NASA that will most likely require petaflops computing include multidisciplinary optimization of commercial aircraft designs, propulsion systems, large-eddy and the direct numerical simulation of turbulence; computation of the radar scatter signature of aircraft bodies; full-scale simulation of the Earth's

atmosphere and climate; and the design, manufacture, and operation of smart nanorobots for space exploration.

A roadmap for the high-performance computing industry has been developed and is presented in the figure. Current consensus is that petaflops computing systems will be feasible in 20 years using advanced semiconductor technology. Ames Research Center has instituted a new program in semiconductor process and device modeling to ensure that NASA will be able to meet future requirements of petaflop computing. In spite of the seemingly obvious need for highly parallel computing as a simulation and design tool in this arena, so far any utilization of parallel systems has been rare. The principal impediments include access to parallel testbeds, as well as the availability of usable software and parallel computing expertise. A

strategy for implementing parallel adaptive unstructured-grid technology for semiconductor device modeling has been developed. This strategy addresses the important issues, such as load balancing. Also studied were the scaling properties of several algorithms, such as fast multipole expansions (FME) to determine the trade-off between FME and long-range molecular dynamics methods in terms of computational cost. Both these methods are used in device modeling.

Point of Contact: S. Saini
 (650) 604-4343
 ssaini@mail.arc.nasa.gov

REVOLUTIONARY TECHNOLOGY LEAPS/
 SUPERSONIC TECHNOLOGY

Nonlinear Aerodynamic Shape Optimization of High-Speed Research Configurations

Susan Cliff, James Reuther, Ray Hicks

The overall goal of this research is to develop an aerodynamic shape optimization technique that is based on nonlinear computational fluid dynamics (CFD) methods and control theory techniques; eliminates the dependence on a large number of CFD solutions; and can be effectively used to optimize aerodynamic shapes to yield superior aerodynamic performance. In support of the high-speed research (HSR) program, the specific objective is to apply these methods to

candidate configurations to assess their capabilities and simultaneously enhance the aerodynamic performance of the vehicle.

The aerodynamic design for supersonic cruise of high-speed commercial transport aircraft is an extremely difficult problem because of the complex flow fields and the need to efficiently integrate the major components of the vehicle (i.e., the fuselage, wing, and engine nacelles) while satisfying numerous structural and operational constraints. Past design efforts have relied upon linear theory methods. Unfortunately, the near-field interactions of the components are nonlinear and the use of linear theory-based design methods provides only limited design guidance. Furthermore, the level of cruise aerodynamic performance achievable with linear design methods is insufficient to ensure an economically viable configuration.

The role of CFD in the aerospace industry today is primarily that of an analysis tool used in the final stages of the design process. Although this tool has proved very beneficial, to make full use of the power of CFD it must be incorporated into the framework of an automated design process. Past efforts to accomplish this objective have proved extremely difficult for applications involving complex aircraft configurations because of the computational expense associated with the thousands of CFD solutions that are required to gain an understanding of aerodynamic design space and its related optima.

Traditional aerodynamic shape optimization methods use finite

differences to obtain the necessary gradient of an aerodynamic objective function (for example, drag) with respect to the design variables. Thus, if N is the number of design variables used for the shape design, then N flow solutions are required to obtain the gradient during each design cycle. Through the use of control theory-based methods, a set of adjoint equations are formulated that reduce the computational requirement down to the equivalent of two flow solutions, independent of the number of control variables. The result is a computational savings of greater than an order of magnitude. Furthermore, since the gradient calculations are no longer dependent on the number of design variables, the shape of complex configurations can be optimized using a large number of design variables.

Using the nonlinear design/optimization code named SYN87 and its predecessors OPT3D and OPT67, which combine Euler flow solvers with constrained and unconstrained numerical optimization algorithms, five successful aerodynamic designs have been accomplished. The first four designs have been validated through wind tunnel testing. The most recent application of this automated aerodynamic design process, which used SYN87 and the adjoint gradient computations, was focused on the Mach 2.4 HSR Technology Concept Airplane (TCA). The cruise aerodynamic shape of this configuration (shown in the figure (see Color Plate 14 in the Appendix)) was optimized to obtain the minimum drag subject to a large spectrum of realistic geometry

constraints, including wing spar depth, wing leading edge bluntness, landing gear box size and location, fuel volume, passenger cabin dimensions, and floor attitude. The optimization procedure used up to 140 independent design variables distributed over the wing and fuselage and focused on wing thickness and camber and fuselage camber and area distribution. Over 200 design iterations were executed in the overall design process, and they yielded very significant performance gains relative to the baseline. These performance gains were validated through numerous detailed Euler and Navier–Stokes analyses. Hardware is currently being fabricated for a wind-tunnel test to experimentally validate the results.

This design/optimization approach represents some of the first successful attempts to use the power of CFD as a true design tool applied to complex aircraft configurations with a large realistic spectrum of constraints. In addition, the large performance gains achieved clearly demonstrate the advantage of using nonlinear design methods to enhance aerodynamic performance.

Point of Contact: D. Bencze
(650) 604-6618
dbencze@mail.arc.nasa.gov

Surface Operations Behavioral Evaluation Interim Testbed for High-Speed Research

Mary K. Kaiser

The eXternal Vision System (XVS) element of the high-speed research (HSR) program is examining issues associated with building a high-speed civil transport (HSCT) with no forward-looking windows. Forward visibility would be provided by a synthetic vision system, generally conceived as displaying visible light camera imagery with superimposed symbology. This design concept presents numerous engineering and human factors challenges, including the adequacy of the XVS display for control, navigation, and obstacle detection; integration of the XVS display with the side windows (which are optical); and crew coordination in an XVS-equipped flight deck.

Surface operations may present particular challenges to an XVS-equipped aircraft because vehicle control is primarily vision-based (compared to many phases of flight in which the pilot relies heavily on instrument information) and because artifacts such as sensor-offset parallax become more severe when the aircraft is close to the ground.

To examine these surface operations issues in a high-fidelity testbed, the HSR program is constructing a near-full-scale testbed, the Surface Operations Research Evaluation Vehicle (SOREV). The SOREV is scheduled to be operational in late FY97. In the interim,



Fig. 1. The SOREV. Externally mounted cameras feed the forward and inboard displays at the rear driver station. An outboard side window is configured to simulate the side window visibility planned for the HSCT.

Ames has worked with industry partners at Boeing and Honeywell to equip a full-size Ford van (shown in the figure) with an XVS system located at a rear driver station. The rear station has two XVS displays (forward and inboard) and an optical window with the visibility angles specified by the Reference H design of the HSCT. The cameras can be mounted at several locations on the vehicle, creating parallax similar to that anticipated with aircraft mounted camera systems. Transport delays in the camera/display system can be introduced, and the impact on driver control and situational awareness can be examined. Although its overall fidelity is somewhat limited, the SOREV is proving to be a useful testbed for

“first looks” at critical human factors issues associated with the XVS and surface operations.

Point of Contact: M. Kaiser
(650) 604-4448
mkaiser@mail.arc.nasa.gov

REVOLUTIONARY TECHNOLOGY LEAPS/
ACCESS TO SPACE

Propulsion Checkout and Control System

Ann Patterson-Hine

The Propulsion Checkout and Control System (PCCS) was part of the Integrated Propulsion Technology Demonstrator (IPTD) task supported by the X-33 program. The objective of the IPTD was to predict and evaluate potential improvements in ground and flight propulsion-system operations in efforts to reduce turnaround times and to cut cost-risk factors. The IPTD consists of liquid-oxygen and liquid-hydrogen propulsion modules, a remote interface unit that is a prototype of Rockwell's X-33 Phase II propulsion system avionics-to-control-center interface, and a prototype control center at Marshall Space Flight Center's (MSFC's) Advanced Engine Test Facility.

The task, which was completed in FY96, achieved the following: (1) on-board diagnostic/prognostic algorithms for the propulsion system of the Reusable Launch Vehicle were demonstrated to be capable of trending and analyzing a historical database; (2) playback of IPTD data on valve actuations identified early performance degradation of the 12-inch prevalve in the main propulsion system that otherwise would have been undetectable; (3) the diagnostic/prognostic algorithms are the first known application of predictive Integrated Vehicle

Health Management to an operational cryogenic testbed; and (4) testability models developed by using a software tool set from QualTech Systems, Inc. were used in positioning the IPTD sensors.

The design models were automatically converted to real-time code that monitored sensor data and that worked with the Langley smart-sensor routines to identify off-nominal conditions to the operator. This successfully demonstrated Rockwell's approach to reducing software development costs by reusing design models and software for operational vehicle code.

Point of Contact: A. Patterson-Hine
(650) 604-4178
apatterson-hine@mail.arc.nasa.gov

Space Science Enterprise



Overview

NASA's Space Science Enterprise seeks answers to fundamental questions about the origin of the Universe, the origin and evolution of galaxies and planetary systems, the origin and distribution of life in the Universe, and the connections between the Sun, Earth, and heliosphere. Through our primary mission in astrobiology (the study of the living Universe), Ames provides pioneering research, technology development, and flight projects that promote fundamental discoveries about the origin, evolution, and distribution of life within the context of cosmic processes. Research is conducted to:

- Determine the abundance and distribution of biogenic compounds that are conducive to the origin of life
- Identify locations in the Solar System where conditions conducive to life have existed
- Survey and begin surface explorations of the most fascinating and accessible planetary bodies
- Discover the origin, evolution, and fate of the Universe, galaxies, stars, and planets
- Survey cosmic rays and interstellar gas as samples of extrasolar matter
- Explore the frontiers of the heliosphere
- Search for planets and planetary formation around other stars

Exobiology and Astrobiology

Ames has been recognized as a world leader in astrobiology and exobiology (search for extraterrestrial

life) since the inception of these disciplines. Research at Ames focuses on revealing how life begins, on what processes govern its evolution, on what destiny may be realized, and on how often life may have emerged on other planets. When coupled with Ames' pioneering research on the dynamics of galaxies, molecular gases and clouds, planetary systems, and the Solar System, our study of life is facilitated by understanding the cosmic environment within which life evolves. Ames conducts studies of biologically important materials in geologic samples and in extrasolar matter; provides theoretical insights for addressing major issues in life's evolution; plays a key role as NASA's expert in matters of planetary protection; and helps to focus the science for future Mars missions on issues related to the possibility of the independent origin of life on Mars.

One of the most important questions in exobiology and astrobiology is how living systems emerge from molecular chaos. Highlighted in this report are exobiological simulations that revealed several new and important basic principles governing the ability of peptides to acquire ordered structures, to self-catalyze, and to give rise to a simple mechanism for transmitting signals from the external environment to the interior of a protocell.

The role of comets in the origin of life is also featured. Comets, which can be considered the fossils of the protoplanetary nebular processes, retain within their icy nuclei clues about the beginning of the Solar System. Ames reported an important finding this year on the

composition and properties of interstellar and cometary ices that may have profound implications for our understanding of the origin of life.

Planetology

Ames conceived and initiated 7 of the 11 planetary missions that have flown since 1972, including the Mars Pathfinder. The Galileo probe made history on December 7, 1995, with its entry into the atmosphere of Jupiter, the first time a spacecraft entered the atmosphere of an outer planet. Plunging into Jupiter's swirling storm clouds at 106,000 miles per hour, the probe descended 400 miles through turbulence, violent winds, and clouds, transmitting data for almost an hour before the communications system succumbed to the intense Jovian environment. Results from the probe's descent are reported below.

Ames also recently completed a comprehensive study of the Solar System which fully models the entire range of bombardment, transport, and mixing effects by which highly absorbing "primitive" interplanetary material pollutes, and redistributes material in, an initially pristine icy system such as Saturn's rings. Surprising findings are described in this report.

Of all the planets in the Solar System, Mars is most like Earth, especially in that its weather and climate are dynamically similar to Earth's and in that its history may have included life. Research highlighted in this report includes a new finding on the structure of the Martian regolith and its role in the Martian climate; the results of Ames research on the nature of the Martian

oxidants—a primary obstacle to uncovering the biological history of Mars; and a unique concept, the *Pascal Mission*, to use Mars as a natural laboratory for the study of factors that control a planet's climate system.

Astrophysics

As NASA's lead Center in airborne astronomy, Ames pioneered and developed astrophysics and has the world's only capability for making astronomical observations from the stratosphere. Development was begun this year on the Stratospheric Observatory for Infrared Astronomy (SOFIA), the infrared telescope of which will gather almost an order of magnitude more light than its predecessor and achieve a five-order-of-magnitude improvement in capability. Ames astronomers, who also contribute directly to space-based infrared science, won the right to the most observation time on the premier infrared space mission of the decade—the European Infrared Space Observatory. These and the highlights described below are presented more fully in later sections of this report.

Ames and the University of Tokyo produced the Mid-Infrared Spectrometer on the Japanese Infrared Telescope mission which obtained infrared spectra of more than 10,000 objects and has yielded interesting new information on the character of the interstellar material. Results obtained this year confirm that two types of interstellar material—grains and certain polycyclic aromatic hydrocarbons (PAHs)—are mixed in a constant ratio throughout different interstellar regions of the

Galaxy, hinting at common evolutionary processes. A complementary Ames study on PAHs revealed that a new type of PAHs, hydrogen PAHs (H-PAHs), found at the boundary of the Orion Nebula and Orion Molecular Cloud, are absent in higher-radiation environments. Results presented in this report indicate that different chemically active regions in planetary nebulae and molecular clouds are defined—at least in part—by the characteristics of the radiation environment.

Protoplanetary nebulae, the birthplaces of planets and planetary systems, are distributed throughout the Universe. The "primary accretion" process—the process by which the first sizeable objects (comets, asteroids, etc.) formed from solids that entered a given protoplanetary nebula as micron-sized dust motes—is one of the major unsolved problems of the origin of planetary systems. A new insight, achieved this year upon completion of a new model of turbulence and damping by particles in the midplane of a protoplanetary nebula, challenges certain theories of accretion dynamics.

Ames researchers recently completed the most comprehensive theoretical computation of the potential energy surface and dipole moment for hot water in sunspots of the Sun and in the spectra of selected cool stars, revealing that sunspot atmospheres are much cooler in the shallow layers than had been predicted by previous models. These results and other potential applications of the model are highlighted in this report.

The final stages in the life of a star somewhat more massive than

the Sun was studied by Ames researchers and colleagues from the University of Hawaii and the University of Wyoming. The results provide an important insight into understanding how the structural evolution of the nebula, through interacting winds, might provide the conditions necessary for molecular survival.

Also described in this issue is a remarkable "hands-on" educational software package developed by Ames that allows students of all ages to perform simulated observations of planets around other stars, as if they were the astronomers, and then to analyze the data to determine the habitable properties of the planets. Included in the package is a description of Ames' proposed Kepler mission, the only currently practical method for finding Earth-sized planets around other stars.

Space Technologies

To support the Space Science Enterprise, Ames scientists and engineers develop, validate, and verify enabling, cutting-edge, high-payoff technologies for conducting future space science and exploration missions at substantially reduced costs. Cost reduction is achieved principally by using information technology to develop advanced flight- and ground-system autonomy technologies. The following highlights are reported more fully in later sections.

An executive system for intelligent autonomous spacecraft, planned for the Deep Space One mission, was prototyped this year. Deep Space One will autonomously navigate to asteroids and comets and will be able to achieve its mission in

the face of a wide variety of faults, including total loss of command and control from Earth.

Live tests of a key component of the Automatic Telescope Project were successfully completed. The primary objective is to provide advanced scheduling and automation infrastructure so that the benefits and performance of single-user automatic telescopes can be made available to a large community of users, with no additional people in the loop. The benefits will be a dramatic reduction in telescope operating costs and an increase in both scientific productivity and ease of use.

Ames' Assisted Space System Experimental Testbed (ASSET) project is an Internet-based global spacecraft control network that provides operational support of a variety of low-cost missions and a high-risk, low-inertia testbed for validating spacecraft autonomy strategies. This year ASSET enabled rapid experimentation with revolutionary autonomy technologies in a real-world, complex space system in support of the New Millennium program concerning the data distribution, principal investigator interfacing, beacon operations, ground-system automation, and fault management.

Ames has developed WaveLab, a powerful suite of wavelet algorithms that can be used to characterize the physical processes underlying complicated temporal and spatial variations, removing unwanted observational noise from data, compressing data with insignificant loss of information, and probing computer models for physical processes with large

dynamic range. WaveLab is available at no cost to the public on a World Wide Web site maintained at Stanford University.

Significant progress has been made in understanding and improving the operation of two of the main components of a pulse-tube cryocooler for use in spacecraft. In addition, Ames developed a star sensor that can be mounted in a cryogenic vacuum vessel to serve as a guide star-tracker for the Gravity Probe B relativity mission.

Remote Analysis of Martian Surface Materials

D. Blake, P. Sarrazin, D. Bish,
D. Vaniman, S. Chipera, S. A. Collins,
T. Elliott

A miniaturized x-ray diffraction and x-ray fluorescence (XRD/XRF) instrument for exploring the Mars surface is being developed; the instrument will minimize the uncertainties inherent in remote mineralogical and geochemical analyses. The instrument has been named CHEMIN, in reference to its role as a simultaneous chemical and mineralogical analyzer. A functioning prototype of this instrument uses a copper X-ray tube, transmission geometry, and an energy-selective charge-coupled device (CCD) operating in single-photon counting mode to collect simultaneous XRF and XRD data.

The ultimate use of this instrument will be in obtaining combined XRD and XRF data from planetary samples. Such an approach will greatly improve the accuracy of remote petrological analyses by constraining the number of possible mineralogic interpretations of the data. For example, although the Viking landers provided very useful XRF data on the Martian regolith, the complex chemistry reported (particularly the mixed-anion suite that includes sulfur and chlorine, as well as oxygen) allows a wide range of mineralogic interpretations. Since remote XRF has yielded proven results, the focus is on preliminary tests in obtaining quantitative

XRD data from the prototype CHEMIN instrument.

X-ray diffraction is the most direct and accurate analytical method for determining the presence of mineral species, because the data obtained by this method are fundamentally linked to crystal structure. Other methods, based on chemical or spectral properties, are derivative and subject to much greater uncertainties. Moreover, significant progress has been made in the last decade in the development of quantitative XRD of multicomponent mixtures.

The Rietveld method, which fits the entire observed diffraction pattern with a pattern calculated using the crystal structures of the constituent phases of the model mineral system, shows great promise for mineral analysis. This method can provide rapid quantitative estimates of mineral abundance, as well as compositional, unit-cell parameter and structural data on individual minerals. In addition, recent advances in quadratic goal programming allow solution of simultaneous linear equations using

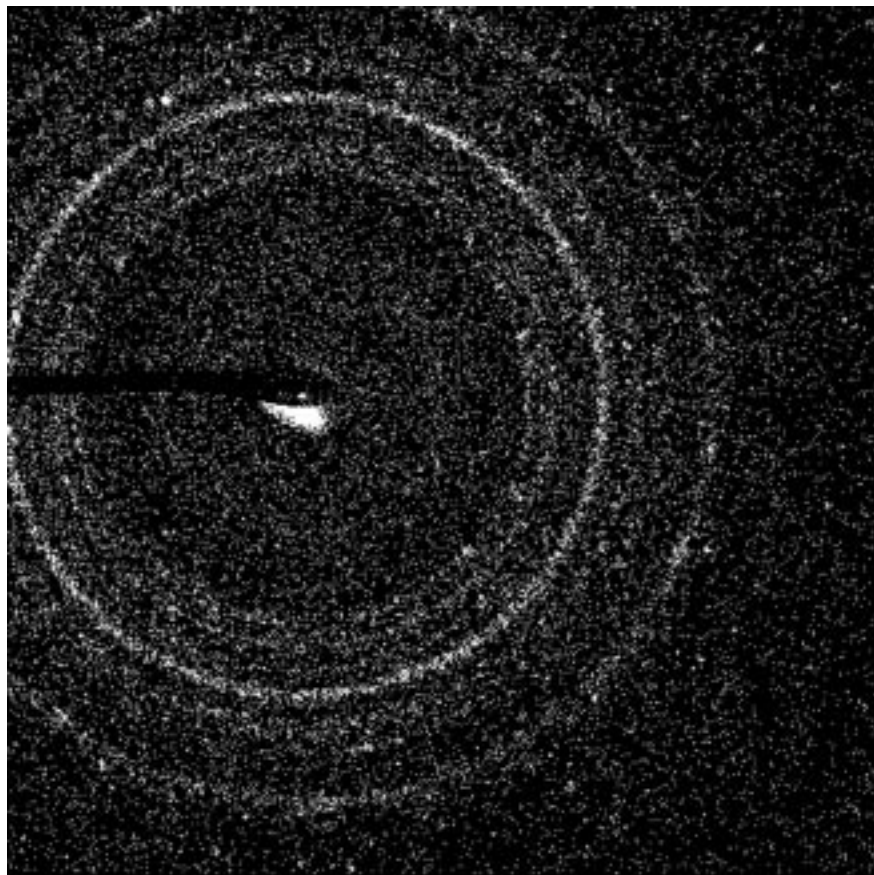


Fig. 1. Two-dimensional image of basalt diffraction pattern obtained with the CHEMIN instrument using only monoenergetic copper-characteristic radiation. The rings correspond to lattice spacings within individual minerals making up the basalt.

chemical and mineralogic data. Use of these techniques with combined bulk-sample XRD and XRF data makes possible extraction of considerable information on individual mineral compositions.

To test the capabilities of CHEMIN against realistically complex samples, Rietveld analysis was used to determine mineral abundances from CHEMIN-derived diffraction patterns of a basalt. This sample was chosen as representative of a rock type that is known to be abundant on the Martian surface, and also one that fits the generic mineralogy of all of the Mars meteorites identified so far (including the ALH84001 meteorite purported to contain evidence of primitive Martian bacteria).

XRD and XRF data were obtained from a sample of terrestrial basalt with the prototype CHEMIN instrument using repetitive 30-second counts. After accumulation of numerous 30-second-count datasets, the data were analyzed on a pixel-by-pixel basis. X-ray powder diffraction rings were generated by

Table 1. Rietveld quantitative analysis of basalt sample

Mineral	Weight, %
Forsterite	7.5
Albite	28.9
Anorthite	17.5
Augite	4.7
Magnetite	1.9
Phlogopite	0.1
Florapatite	1.6
Sanidine	37.9

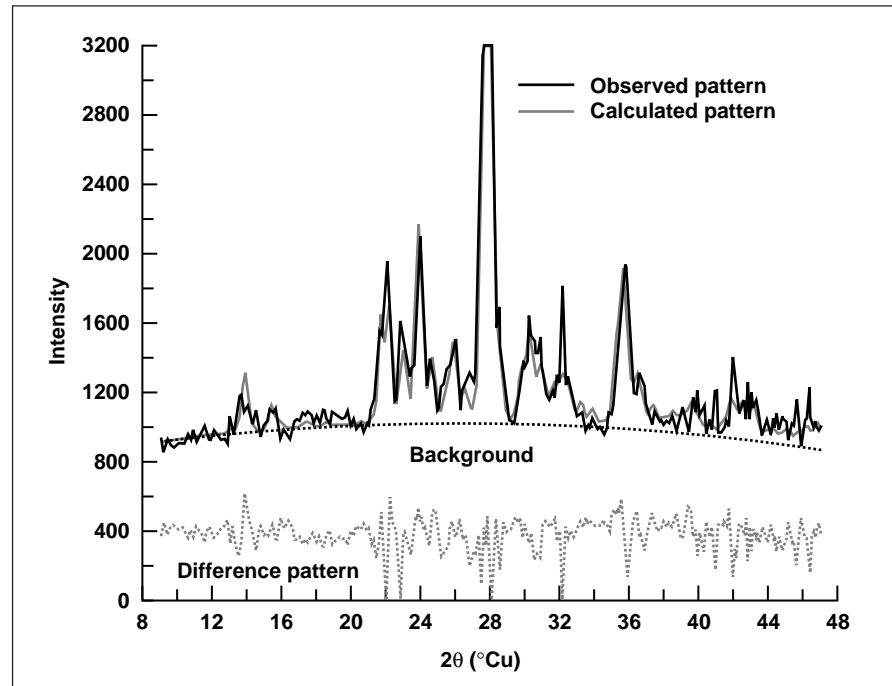


Fig. 2. Rietveld refinement of the diffractogram obtained by summing x-ray intensities shown in Fig. 1 radially around the central beam. The patterns are evaluated by least-squares fitting between model and actual results.

plotting the two-dimensional distribution of those pixels containing copper-characteristic radiation (first figure). The powder rings were then integrated to generate conventional 2θ -versus-intensity powder-diffraction patterns (2θ is the angle between the diffracted beam and the entering beam). The resulting XRD data were used as input to Rietveld refinements. The results of the analysis are shown in the table and in the second figure. Despite the complexity of the basalt sample and the significant limitations of the prototype CHEMIN instrument, the Rietveld analysis is surprisingly good, with a calculated pattern that

agrees well with the observed pattern. In addition, the resulting mineral analysis agrees well with optically determined modes for this sample. This level of success has only recently been obtained, and considerable improvement in the CHEMIN results are anticipated in the near future.

The CHEMIN instrument has been proposed for a number of space missions, and an XRD/XRF capability is included in instrument suites proposed for Mars landers and rovers by several working groups.

Point of Contact: D. Blake
(650) 604-4816
dblake@mail.arc.nasa.gov

Stable Isotope Biogeochemistry of Hydrothermal Systems

David J. Des Marais

Hydrothermal systems probably existed in any rocky planet which was sufficiently large to accumulate substantial internal heat from radioactive decay and which also possessed a significant crustal inventory of water. Hydrothermal systems provide the liquid water, nutrients, reduced conditions, and chemical energy necessary to support life. Therefore NASA's astrobiology and solar system exploration programs should include a search for hydrothermal systems in other planets.

The stable isotopic composition of the elements oxygen (O), hydrogen (H), sulfur (S), and carbon (C) in minerals and other chemical species can indicate the existence, extent, conditions, and processes (including biological activity) of hydrothermal systems. The reactions between hot water and rock-forming minerals allow the isotopic ratios $^{18}\text{O}/^{16}\text{O}$ of deuterium to hydrogen (D/H) of the minerals to equilibrate with this water, causing isotopic changes which can be used to detect fossil systems and to delineate their areal extent. These isotopic changes can indicate fluid composition, alteration temperatures, water-rock ratios, and so forth. The $^{18}\text{O}/^{16}\text{O}$ values of hydrothermal silica and carbonate

deposits tend to increase with declining temperature and thus help to map temperature gradients within hydrothermal systems. The $^{13}\text{C}/^{12}\text{C}$ values of carbonates and ^{13}C -depleted microbial organic carbon increase along the thermal gradients of thermal spring outflows, principally because of the outgassing of relatively ^{13}C -depleted carbon dioxide (CO_2). Hydrothermal waters can differ in their D/H contents because of their variety of sources, which can include seawater or rainwater, which falls over ranges in elevation and geographic location. Therefore, measurements of D/H values in hydrothermal minerals can help to decipher the origins of the fluids. The $^{34}\text{S}/^{32}\text{S}$ and $^{13}\text{C}/^{12}\text{C}$ values of fluids and minerals reflect the origin of the S and C, the partial pressure of O_2 , and also the nature of key oxidation-reduction processes. For example, a wide range of $^{34}\text{S}/^{32}\text{S}$ values is consistent with equilibration below 100°C between sulfide- and sulfate-bearing minerals, and can be attributed to sulfur metabolizing bacteria and *not* to nonbiological processes. Depending on its magnitude, the difference in the $^{13}\text{C}/^{12}\text{C}$ value between carbonate minerals and coexisting organic carbon can be attributed either to equilibrium at hydrothermal temperatures or, if the difference in the ratio exceeds 1%, to organic biosynthesis (see figure).

The observations of hydrothermal mineral assemblages and coexisting organic carbon in Yellowstone National Park indicate that both temperature gradients and microbial communities can indeed be documented through measurements of their oxygen and carbon

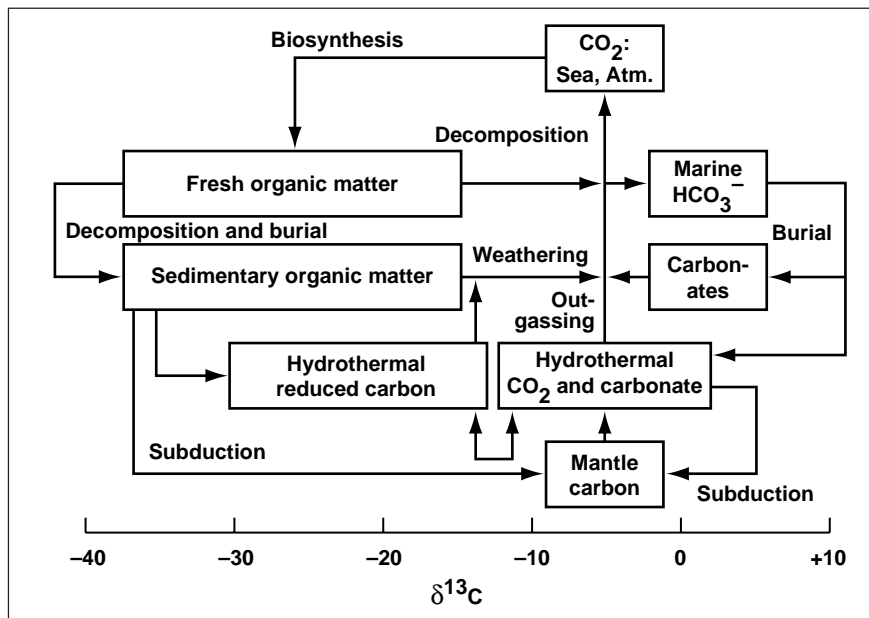


Fig. 1. Carbon isotopic composition of crustal carbon reservoirs, with special emphasis on hydrothermal systems. The horizontal axis depicts variations in $^{13}\text{C}/^{12}\text{C}$ values in parts per thousand, with lower values to the left. Boxes and arrows depict carbon reservoirs and processes linking the reservoirs, respectively. The isotopic composition of hydrothermal carbon species can be affected both by mantle carbon and by contamination from crustal sources of organic and carbonate carbon.

isotopic compositions. Parallel measurements are now being made in rocks from an ancient (400-million-year-old) hydrothermal system in Queensland, Australia.

Point of Contact: D. Des Marais
(650) 604-3220
ddesmarais@mail.arc.nasa.gov

Fossilization Processes in Thermal Springs

Jack Farmer, Sherry Cady,
David J. Des Marais

Stromatolites are laminated biosedimentary structures that form when communities of microorganisms either entrap sedimentary grains, or induce the precipitation of minerals through their metabolic processes. Fossil stromatolites provide a primary source of information about the early biosphere on Earth, and have also been identified as important targets in the exploration for a fossil record on Mars. These megascopic biosedimentary structures are rich storehouses of paleobiological information and often contain not only the fossilized remains of the microorganisms which produced them, but also biochemical and isotopic signatures that directly link them to life processes.

Thermal springs are highly productive microbial factories that provide an important glimpse into the nature of the primitive biosphere. In recent years, the microbial communities and stromatolites of thermal springs have assumed a prominent place in studies of primitive biospheres. During the

early history of Earth, it is likely that hydrothermal systems were widespread owing to higher internal heat flow, and to the thermal energy invested by large impacts. Thus, hydrothermal environments are regarded as key environments for the origin and early evolution of terrestrial life, a view that also receives support from the universal tree of life derived by comparing the nucleic acid base sequences in the RNA of living organisms. The patterns of early branching suggest that the common ancestor of all living organisms was an extreme thermophile, that is, a microorganism that preferred living at temperatures above 80°C (176°F).

The fossil record of thermal-spring deposits is virtually unknown, and no subaerial systems have yet been recognized in the ancient geological record of Earth. In order

to create a framework for recognizing such deposits in the Precambrian record, the authors have been carrying out studies of modern thermal-spring systems in Yellowstone National Park, along with ancient deposits from localities in western North America and Australia.

In FY96 studies of modern thermal springs led to several discoveries that have helped refine the understanding of stromatolite morphogenesis and fossilization processes at high temperatures. Columnar geysersites (see first figure), are high-temperature subaerial splash deposits that form around the vents of siliceous thermal springs. The structures thus formed resemble many Precambrian stromatolites. Columnar geysersites were first studied in the late 1970s and determined to be abiogenic (that is,

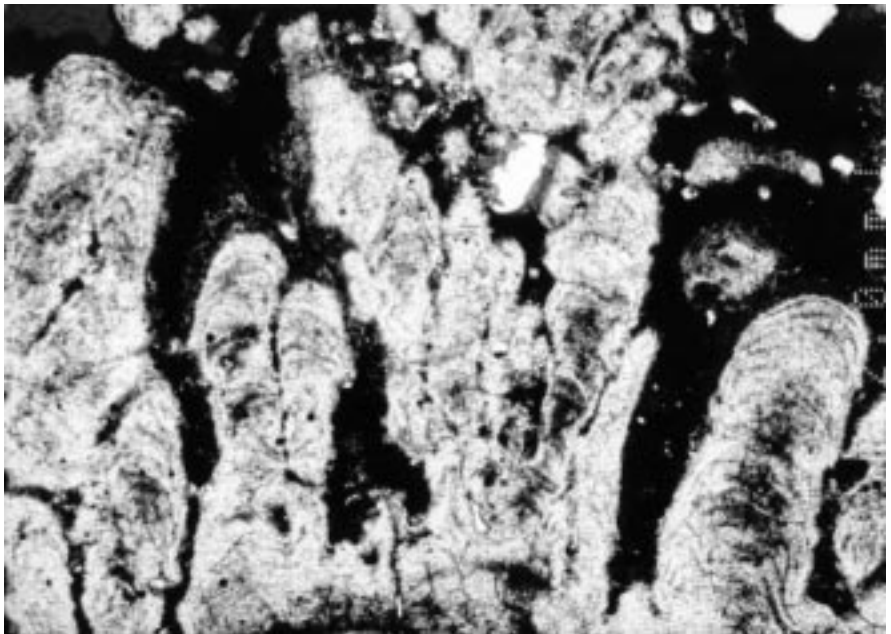


Fig. 1. Thin-section view of columnar stromatolites (geysersites) formed around high-temperature vents of silica-depositing springs in Yellowstone National Park; columns are about 3 mm high.

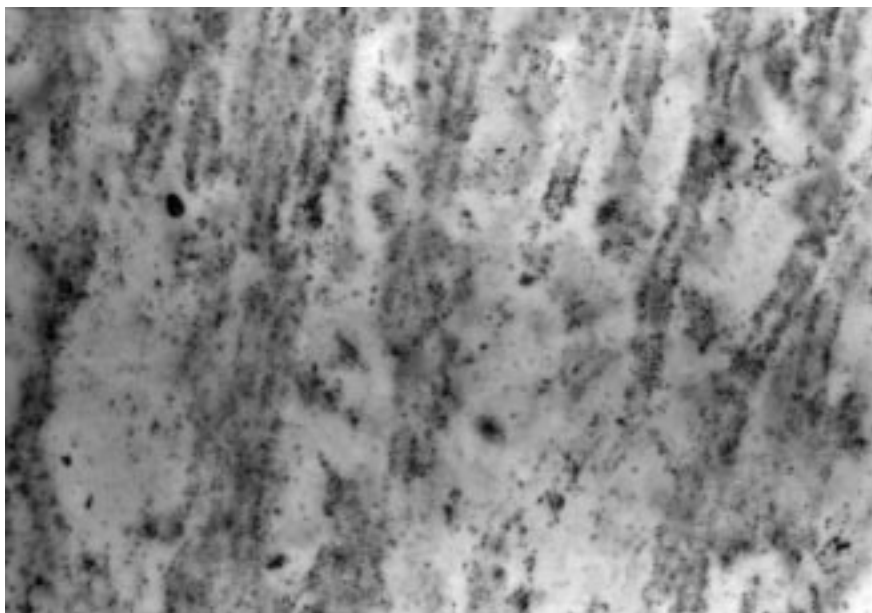


Fig. 2. Thin-section view of fossilized microbes from 350-million-year-old siliceous thermal-spring deposits discovered in the Drummond Basin of northeast Queensland, Australia; individual filaments are about 20 μm in diameter.

not produced by living organisms). Since that time, some authors have questioned the biogenicity of the oldest fossil stromatolites, suggesting that they were also formed inorganically. But studies of modern geysers have shown conclusively that these deposits are actually formed in the presence of thin biofilms of thermophilic bacteria and archaeobacteria, and that the geysere microstructure reflects a significant biogenic contribution.

In FY96 the first detailed paleontological studies of ancient subaerial thermal-spring deposits in northeast Queensland, Australia, were also completed. These 350-million-year-old deposits are precise analogs for the modern subaerial systems that have been studied in Yellowstone.

Observations were made of the primary biofabrics and microfossils that are preserved in these ancient deposits, despite extensive textural reorganization during diagenesis (second figure).

Point of Contact: J. Farmer
(650) 604-5748
jfarmer@mail.arc.nasa.gov

Molecular Biomarkers for Stromatolite-Building Cyanobacteria

Linda L. Jahnke, Roger E. Summons, Harold P. Klein

Life began on early Earth in an environment devoid of free molecular oxygen (O_2). It is clear that the rise of O_2 as a consequence of the evolution of oxygenic photosynthesis had a profound effect not only on the subsequent progression of biological evolution but also on Earth's geological history. Although oxygenic photosynthesis evolved within the cyanobacterial lineage, evidence for this event's timing remains obscured within the molecular and rock records. One potential help in resolving this issue resides in the complex organic molecules that can be extracted from ancient sedimentary rocks. These molecules, called biomarkers, are the remnants or molecular fossils of ancient microorganisms. The carbon skeletons of such fossil molecules can survive structurally intact for billions of years, and organic geochemists are working to identify them in ancient organic sedimentary materials. The challenge is to understand the link between such molecular fossils and their "living" counterparts, the biomarker molecules synthesized by contemporary bacterial groups. Understanding the function and influence of environmental factors on the synthesis of such biomarker molecules in the source organism can then provide a basis for interpretation of this ancient organic record.

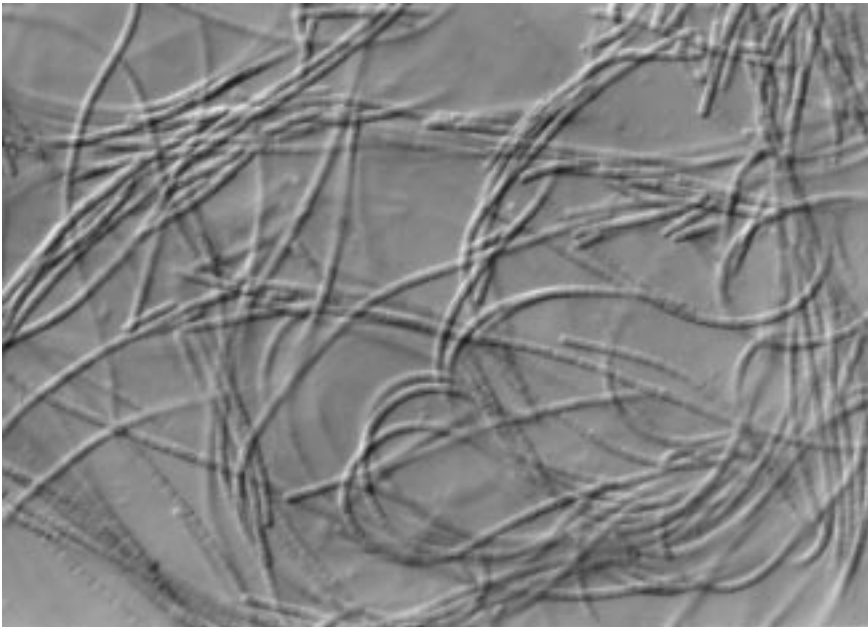


Fig. 1. Photomicrograph of a *Phormidium* (filament width 1.5 μm) isolated from a Yellowstone microbial mat.

Extant cyanobacteria are a diverse group of prokaryotic microorganisms found in a wide variety of modern environments. We have focused our study on the types of cyanobacteria involved in the construction of microbial mats and their fossilized equivalents, stromatolites. These laminated, organo-sedimentary structures are among the most common fossils in the geological record. Important biomarkers for identification of cyanobacterial input to sedimentary organic matter are a group of straight-chain hydrocarbons (alkanes) having 17 to 20 carbons (C_{17} - C_{20}) with midchain, branched methyl groups such as 7-methylheptadecane (C_{17}). These methylalkanes are specific to

cyanobacteria, are resistant to biodegradation, and form some of the oldest known biomarkers, having been isolated from Proterozoic rocks dated at 1.7 billion years ago. More recently, we have identified another class of methylated alkane having two methyl branches at carbons 7,11 or 7,10 in a cyanobacterium, *Phormidium luridum*. We found that these dimethylheptadecanes (DMA) were only synthesized when the cyanobacterium was grown with low levels of dissolved inorganic carbon (DIC). Cells grown with DIC levels equivalent to atmospheric levels of carbon dioxide (CO_2) (0.03%) contain DMA, whereas cells grown with 1% CO_2 have only a straight-chain n-heptadecane. We have carried out a screening of a variety

of cyanobacteria to determine the extent to which this low DIC-DMA synthesis phenomenon occurs. To date, we have screened 6 marine and 12 freshwater strains of cyanobacteria. None of the marine cyanobacteria, including several *Synechococcus*, three *Oscillatoria*, and a *Pseudanabaena* were able to synthesize DMA. This was also true for a variety of cyanobacteria (*Gloeocapsa*, *Synechococcus*, *Oscillatoria*, *Pseudanabaena*) isolated from the hot spring, microbial mats in Yellowstone National Park. Two other Yellowstone isolates, *Chlorogloeopsis* and *Fischerella*, did synthesize dimethylalkanes, but these compounds differed in carbon chain length and methyl group positions, and were synthesized under both high and low DIC conditions. The only cyanobacteria found to be capable of dimethylheptadecane synthesis were four *Phormidium* types isolated from siliceous hot springs (see first figure). Like *Phormidium luridum*, the Yellowstone *Phormidium* contained high levels of DMA when grown under low DIC conditions.

The *Phormidium* are responsible for the formation of a type of columnar stromatolite, the Conophyton (conical-formed microfossils). Conophyton were one of the most distinctive groups of stromatolites which disappeared near the end of the Precambrian. The *Phormidium* mats in Yellowstone provide a surviving "primitive" analog for



Fig. 2. Silicifying *Phormidium* mat (width 12 inches) showing *Conophyton* structure, Weeds Pool, Yellowstone National Park.

study of the *Conophyton*s (second figure). DMA are found only in Precambrian oils, and disappear from younger organic sediments just as the *Conophyton* stromatolites disappear from the rock record. The environmental factors controlling dimethylalkane synthesis in the

Yellowstone *Phormidium* mats may provide important insights for interpretation of the organic molecular fossil record.

Point of Contact: L. Jahnke
(650) 604-3221
ljahnke@mail.arc.nasa.gov

Earth-Threatening Comets Leave Tell-Tale Dust Trails

Peter Jenniskens, David Morrison

Over its geologic history, Earth has been bombarded by a continuous shower of large asteroids and comets, some of which led to large-scale extinctions. Unlike other dangers, impacts of larger bodies can affect mankind as a whole and pose a threat to modern civilization. The first step toward avoiding such impacts is to know where the potential impacting objects are. Most large asteroids can be found by dedicated searches using large telescopes, because they have a short orbital period and come close to Earth frequently enough to be detected. However, that is not the case for comets with long orbital periods, which come back to the inner parts of the solar system only once every 200–100,000 years. And some 2 to 10% of all such impacts are thought to be due to these long-period comets.

Researchers are studying the possibility of using the meteoroid particles in the path of these comets as a means of detecting their presence. From numerous accounts of amateur observers, they know that some meteor streams show brief episodes of high activity: the meteor outbursts. At such times, Earth crosses relatively recent ejecta of particles, which evaporate in Earth's atmosphere in the flashes of light that are called meteors. Most intriguing are the outbursts that occur at times unrelated to the return of the comet to perihelion, and it is

suspected that these might be associated with long-period comets. It remained unclear whether the outbursts were caused by a trail of dust in the path of these comets or by clouds of dust in orbits with a shorter orbital period. No observations made with standard meteor observing techniques had been successful, until FY96.

It was proposed that the planetary motions affect the orbits of particles, causing Earth to periodically traverse the trail of dust. The return of one such stream in November of 1995 was predicted. Conditions would be favorable to measure the orbital period of the particles over Europe and Africa, where it was night at the expected time of the event, and the point from which the meteors radiated would be high in the sky, allowing good viewing. A network of photographic and image-intensified TV systems was set up in Andalusia, Spain, operated principally by amateur observers of the Dutch Meteor Society.

The outburst did indeed occur and was confirmed by many observers in Europe. Meteor rates increased briefly to five meteors per minute. Most of the meteors were too weak to be photographed. A rare color image is shown in the figure (see Color Plate 15 in the Appendix). Ten meteors were recorded from multiple sites and triangulation of their paths allowed the reconstruction of the orbit of the particles. The particles had a long orbital period, confirming that this meteor outburst was due to a trail of dust in the wake of a long-period comet. Identification was made of 14 such streams that produce occasional outbursts

and techniques are being developed to find more in order to study their properties.

Point of Contact: P. Jenniskens
(650) 604-3086
peter@max.arc.nasa.gov

Capturing Cosmic Dust on Mir

**Kenji Nishioka, Ted Bunch,
Mark Fonda, Glenn Carle,
Sherwood Chang, James Ryder,
Janet Borg**

As part of exobiology's effort to solve the quintessential question of how life started on Earth, it is necessary to have information concerning the prehistoric origin and evolution of biogenic elements and compounds from the interstellar medium that coalesced into the solar system. Interplanetary and cosmic dust particles (IDPs/CDPs) are believed to have survived from that early period largely unchanged; as a result, they may shed light on the chemical pathways taken by the biogenic elements and their compounds in moving from their origins in stars and the surrounding media to their incorporation into planetary bodies such as Earth. Thus the interest to capture contamination-free cosmic dust particles.

Ames Research Center, the SETI Institute, and Lockheed Martin Missiles and Space have developed ultrapure aerogel, containing about one part per million carbon, for contamination-free capture of CDPs in Earth orbit. This group joined with the University of Paris's Institute for

Astrophysical Studies and flew a CDP-capture experiment early this year (October 1995 to February 1996) as part of the European Exposure Facility's Comrade experiment on the Russian Mir space station. Two small capture cells/modules each 9 by 5 by 1.5 centimeters thick were flown, recovered, and returned to Ames on March 25, 1996. One of the two aerogel capture modules was exposed from early October 1995 until early February 1996; the second capture module was exposed for only 10 days during the Orionids shower in October 1995. These capture cells were the first aerogel experiments to fly on Mir. The results of preliminary analyses of the capture modules are summarized below. Strict procedures were followed in handling the modules to ensure that any changes detected, including contamination, would be a result of the environment around Mir, from shipping of the modules (packing material), or from captured particles.

Physical (visual) examinations of the modules were done in a 10,000 class clean room. When the module covers were removed, the integrity of the module/aerogel was verified; it had survived shipping, launch, orbital exposure, and recovery without apparent structural problems, except for stretching of the platinum retainer wires. This probably resulted when entrained air in the aerogel could not escape quickly enough to equalize the internal pressure and the rapidly decreasing external pressure during launch, thus causing the aerogel to bulge and the wires to stretch. The cosmetic surface blemishes on the

aerogel surface reported in the 1995 Research and Technology Report, appeared noticeably darker and rougher, whereas the clear unblemished surfaces appeared unaffected in the recovered modules; this was later confirmed by microscopic examination. These initially blemished areas are probably susceptible to ozone oxidation.

While in the clean room, surface and subsurface aerogel samples were taken from the modules for analyses. Organic chemical analyses of the aerogel surface samples showed high contamination levels (2%) of dioctyl adipate, a plasticizer. This was unanticipated, and there are no reports of this contaminant as an orbital experiment concern in the literature. Additional samplings from the modules confirmed the high contamination levels. Interior samples showed that the contamination did not migrate and was confined to the surface.

An automated microscopic scanning system at the University of California at Berkeley was used to scan the modules for impacts. Several candidate impact points with tracks were found and are being analyzed by an x-ray probe technique at Brookhaven National Laboratory. Preliminary x-ray fluorescence spectra results from the x-ray probe of a track failed to detect particulate matter at the end of the track. But, the “chondritic” elements calcium (Ca), iron (Fe), nickel (Ni), manganese (Mn), titanium (Ti), and chromium (Cr) were found in the track and could indicate the breakup of a pyroxene particle; however, small amounts of lead (Pb), zinc (Zn), copper (Cu), strontium (Sr), and zirconium (Zr) were also found,

strongly suggesting the possibility of an orbital debris particle or other source of contamination.

Valuable insights were gained into the manufacturing, fabrication, and use of aerogel for building a successful IDP/CDP capture instrument from this flight experiment. Aerogel is robust and holds together even under IDP/CDP impact, and under launch and ground handling loads. Also, aerogel does not appear susceptible to the migration of surface contaminants. But as expected, the experiments gave rise to new questions. For example, where did the high concentration of dioctyl adipate come from? Do particles, especially at the micron or tens of micron size, survive capture, and how will these micron-size particles and their tracks be found and analyzed cost effectively?

Point of Contact: K. Nishioka
(650) 604-0103
knishioka@mail.arc.nasa.gov

Simple Peptides at Water-Membrane Interfaces

Andrew Pohorille, Christophe Chipot

Even the simplest protocell must have had the capability to catalyze the chemical reactions needed for its survival and growth and to communicate with its environment. These functions must have been accomplished by simple molecules that could have been present in a protobiological milieu. One such group of potential early catalysts and signaling molecules were the

peptides—possible precursors of enzymes and receptors. Unfortunately, short peptides typically have disordered structures in aqueous solution and, therefore, do not appear to be suitable for the desired cellular functions. However, at water-membrane, water-oil, or water-air interfaces, many of these peptides, depending on their sequence, can acquire a broad range of well-defined secondary structures, such as α -helix, β -strand, or β -turn. A crucial, common characteristic of these interfaces is that a nonpolar phase is adjacent to water.

The ability of small peptides to organize at aqueous interfaces was examined by performing a series of large-scale molecular dynamics computer simulations of several peptides. The peptides were composed of two amino acids, nonpolar leucine (L) and polar glutamine (Q), in a variety of environments; they differed in the size and sequence of the amino acids. Among the molecules studied were the dipeptides LL, LQ, QL, and QQ. Although these peptides were too short to form a secondary structure, they are very good models for use in examining the conformational preferences of the peptide backbone as a function of the sequence and the environment. The studies of L/Q peptides were extended to include two heptamers, of sequence LQQLLQL and LQLQLQL. The sequences were designed to maximize the interfacial stability of the α -helix and β -strand conformations, respectively, by exposing polar side chains to water and nonpolar side chains to a nonpolar phase.

Finally, a transition of an undecamer (11 residues), composed

entirely of leucine residues, from a disordered structure in water to an α -helix in a nonpolar phase, representing the interior of the membrane, was investigated. This is the first time that the complete folding of a peptide in solution was accomplished in computer simulations.

The simulations revealed several basic principles governing the sequence-dependent organization of peptides at interfaces. Understanding these principles allows for determining how peptides could have performed protocellular functions.

Short peptides tend to accumulate at interfaces and acquire ordered structures, provided that they have a proper sequence of polar and nonpolar amino acids. The specific identity of amino acids appears to be less important, which is a desirable protobiological property. The dominant factor determining the interfacial structure of peptides is the hydrophobic effect, which is manifested at aqueous interfaces as a tendency for polar and nonpolar groups of the solute to segregate into the aqueous and nonpolar phases, respectively. The resulting structures are called amphiphilic. Exceptions from this tendency are observed only when intramolecular hydrogen bonds are formed in the nonpolar phase without completely removing polar side chains from water, a unique feature of interfacial systems.

Based on the results for folding the LQQLQL heptamer to an α -helix at the water surface, it is proposed that, whenever possible, peptides fold at interfaces through a series of amphiphilic intermediates. Transitions between these intermediates involve changes not only in

backbone angles but also in conformations of side chains. Once folded, the peptides form structures that are suitable for polymerization and have the potential for catalytic activity.

If peptides consist of nonpolar residues only, they insert into the

nonpolar phase. As demonstrated by the example of the leucine undecamer, such peptides fold into an α -helix as they partition into the nonpolar medium (see the two figures). The folding proceeds

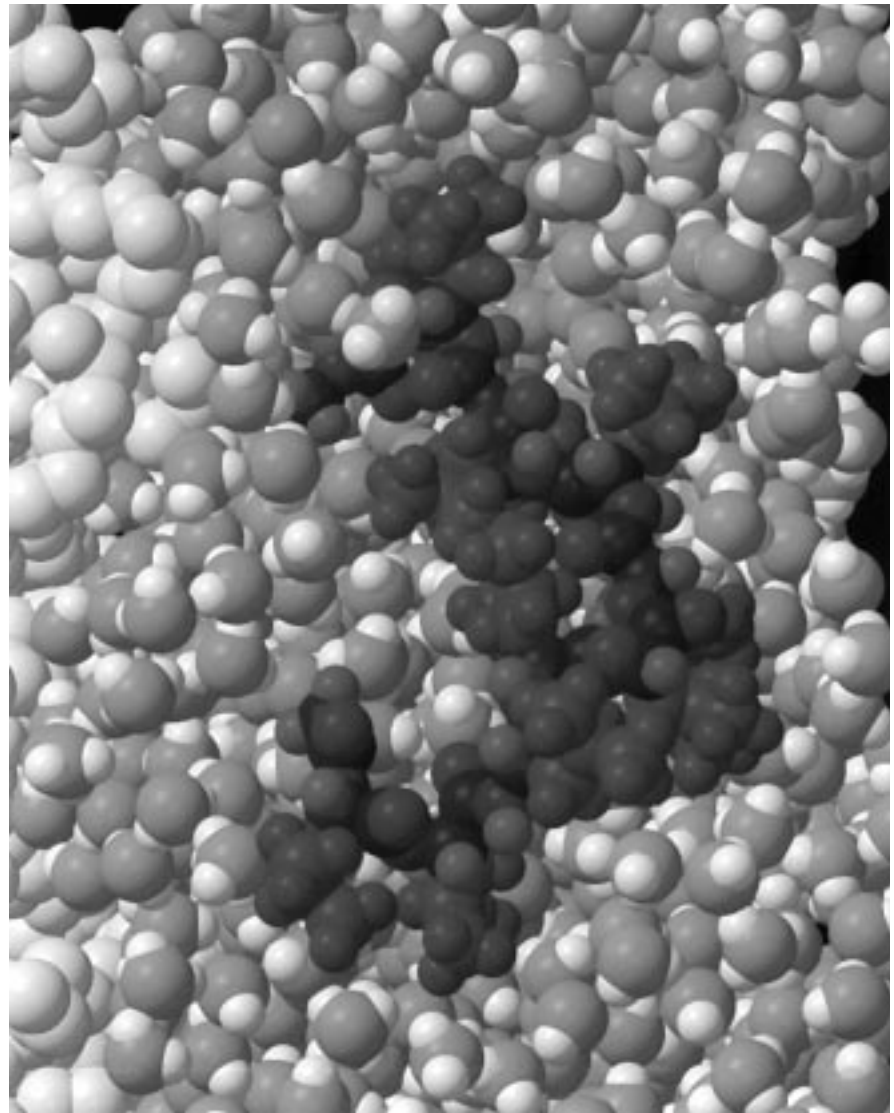


Fig. 1. Polyleucine undecamer interacting with the water-hexane interface at $t = 0$ nanoseconds. The center of mass of the peptide is located approximately 11 angstroms from the water-hexane interface. In water, the structure of the peptide is disordered. The atoms of the polyleucine are dark gray, the oxygen and hydrogen atoms of water are medium gray and white, respectively, and the CH_2 and CH_3 segments of hexane are light gray.

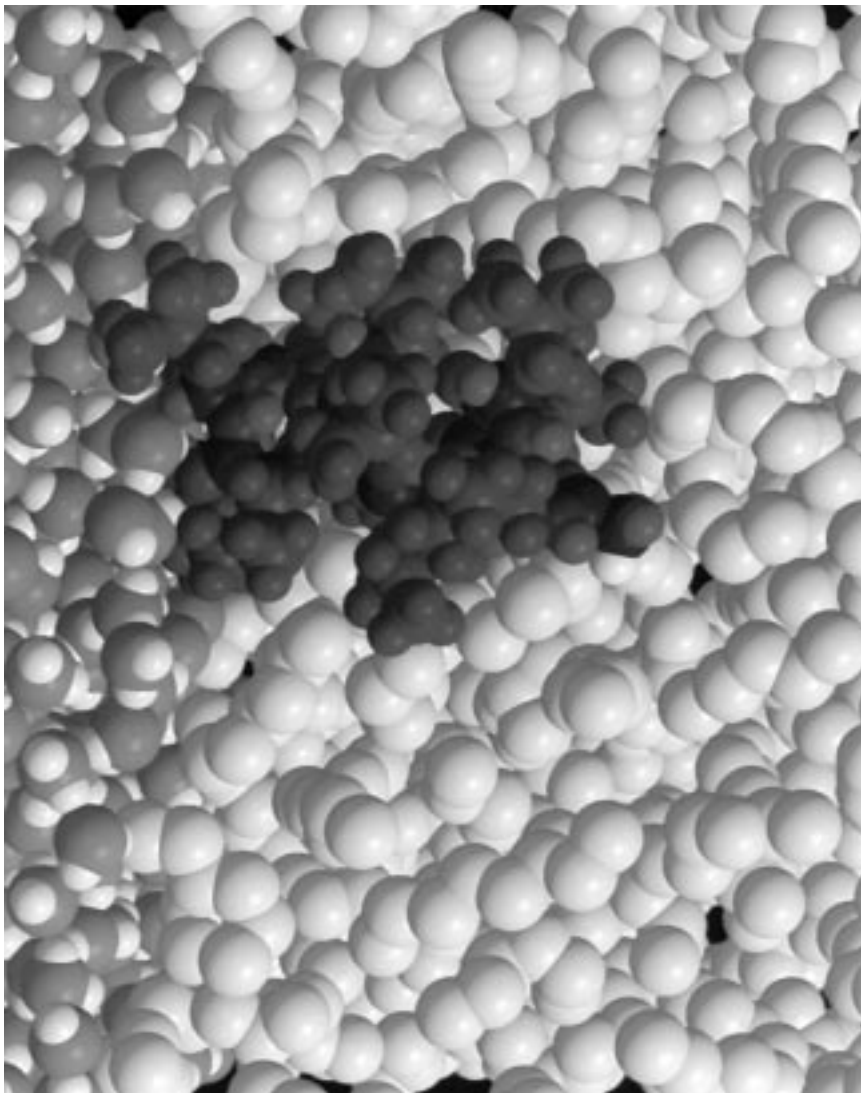


Fig. 2. Polyleucine undecamer interacting with the water-hexane interface at $t = 40.2$ nanoseconds. The peptide has folded into an α -helix, and the peptide backbone vector makes an angle of about 20° with the normal to the water-hexane interface. The color scheme is the same as described in Fig. 1.

through an intermediate conformation, called a 3_{10} -helix, which remains in equilibrium with the α -helix. Once in the nonpolar environment, the peptides can readily change their orientation with respect to the interface from parallel

to perpendicular, especially in response to local electric fields. The ability of nonpolar peptides to modify both their structure and orientation with changing external conditions may have provided a

simple mechanism for transmitting signals from the environment to the interior of a protocell.

Point of Contact: A. Pohorille
 (650) 604-5759
 apohorille@mail.arc.nasa.gov

Silicon-Micromachined Gas Chromatography System

**Thomas Shen, James Suminto,
 Frank Yang, Daniel Kojiro,
 Glenn Carle**

The development of gas chromatographic equipment for planetary atmospheric probes and soil gas or pyrolytic analysis was required for both the Viking mission to Mars and the Pioneer Venus mission. A gas chromatography (GC) instrument was used for the Pioneer Venus mission. However, future missions, such as the Mars Exploration Missions and missions to probe the atmospheres or moons of the outer planet, will require further reductions in equipment weight, volume, and power requirements.

NASA is in a very dynamic mode at this time. A massive effort is under way to revolutionize the technical approach to spacecraft and robotic exploration. The Discovery Program is the first of these new approaches. Other programs following it include New Millennium, Micro-spacecraft, and Nanoinstruments. All of these enterprises have in common the requirement for better, faster, cheaper. Clearly, current technology will not likely be feasible for future space studies.

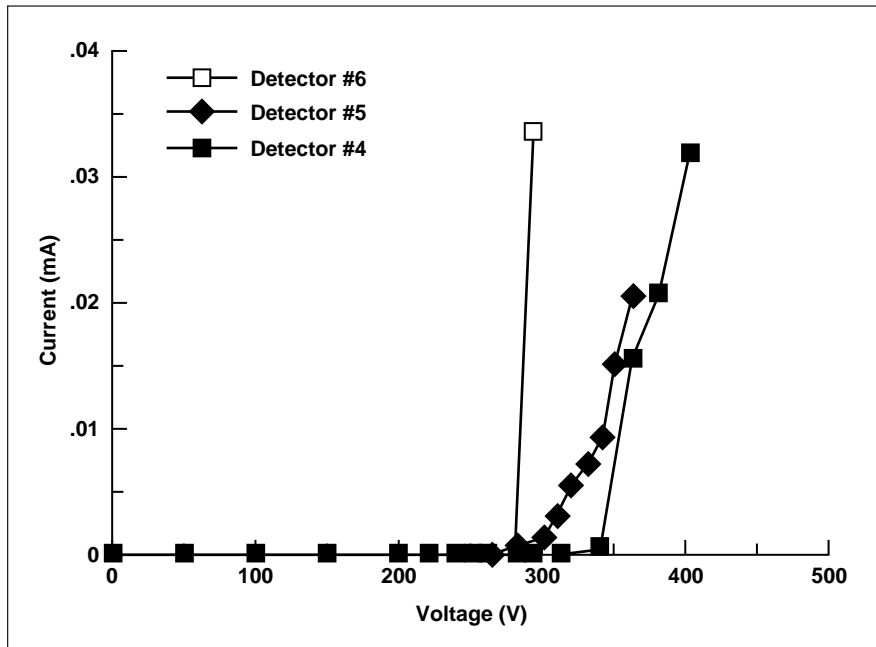


Fig. 1. Discharge curves of micromachined chips.

A silicon-micromachined GC system in which the detector and column are integrated into a small piece of silicon has been studied by several researchers. The problem is that no sensitive detector has been designed and tested. A proposal was made to use the metastable ionization detector principle, and replace the radioactive material with the glow discharge method, which has not been studied on the silicon-micromachined GC system. A very narrow discharge distance can be produced and controlled, a helium ionization detector can be produced, and a highly sensitive analysis can be obtained (concentrations below the parts-per-million level can be detected) through a micromachined silicon wafer. In addition, a column

on the chip with the new in-house-developed highly efficient silicon polymer material (U.S. patented) will be modified and coated to separate most chemical components. This small and highly sensitive GC system will be able to meet future mission requirements.

In this first year of the project, several micromachined chips with different electrode designs were prepared and tested. The preliminary devices were produced by Micro-Tech Scientific Inc. Several chips have been evaluated. The discharge curves of these chips are demonstrated in the figure.

Point of Contact: T. Shen
(650) 604-5769
tshen@mail.arc.nasa.gov

Nitrogen Sources and Sinks on Early Earth

David P. Summers

One important form of fixed and reduced nitrogen on early Earth is ammonia. However, current geochemical evidence points to a nonreducing atmosphere which contains nitrogen (N_2) instead of ammonia. One source of ammonia involves the formation of nitrite (NO_3^-) which can then be reduced to ammonia by ferrous iron (Fe^{+2}). It has also been suggested that this cannot be an important source of ammonia since nitrite can react with ammonia (to make nitrogen).

Whether this is true, however, depends on how the kinetics of the reactions involved compare with the speed of other sources and sinks for both ammonia and nitrite. If the reaction of nitrite with ammonia is slow compared with other processes that make and destroy ammonia, then it will not be important. Any evaluation of the importance of various sources and sinks of nitrite and ammonia, and of whether ammonia is likely to be present in significant amounts, requires an analysis of all the kinetic processes affecting those species.

Using a kinetic analysis of rate data that had either been measured at Ames or were already published in the literature, a kinetic analysis was performed to establish what the concentrations and rates might have been in the early ocean. Plausible sinks/sources for nitrite and ammonia on early Earth are: the reduction of nitrite to ammonia, the reaction of nitrite with ammonia, photochemical destruction of either nitrite or

ammonia, and destruction at hydrothermal vents. The photochemical destruction of nitrite depends on trace species that can react with photo-generated hydroxy radicals and on the amount of ultraviolet light, neither of which is known for certain to have existed on early Earth. Furthermore, the product of photolysis, nitric oxide (NO), is the same compound that nitrite (and hence ammonia) is formed from. Therefore, values for rates of photochemical destruction probably represent only an upper limit. Ammonia can also be lost by adsorption into clays. However, this will be significant only when the ammonium concentration is high enough to compete with potassium and serves mostly to limit the concentration below an upper limit of 10 millimolar.

Under most conditions, the primary sink for nitrite is reduction to ammonia. Destruction at hydrothermal vents is important at acidic pH's and close to the freezing point of water. The reaction between ammonia and nitrite is not an important sink for either nitrite or ammonia. Photochemical destruction, even in a worst case scenario, is unimportant under many conditions but could be important under acidic, high carbon dioxide (CO₂) pressure, or low-temperature conditions. The primary sink for ammonia is photochemical destruction in the atmosphere. Under acidic conditions, more of the ammonia is tied up as ammonium (reducing its vapor pressure), and hydrothermal destruction becomes more important. At 25°C, pH 7.6, and 0.2 atmosphere of CO₂, nitrite and ammonia have steady-state concentrations of

3×10^{-8} and 2×10^{-6} molar, respectively. The very low nitrite concentration reflects the fact that the nitrite is reduced to ammonia before it has a chance to build up or undergo any competing processes. The concentration is such that its importance for many processes envisioned for the origin of life (like the formation of amino acids) is unclear.

This is part of a broader question of whether life would have started in the open ocean, where dilution makes the formation of more complex species difficult, or somewhere where a means of concentration species (such as with vesicles or by evaporation) is present. In general, concentration would tend to raise the concentration of all species, rather than change the relative importance of the source and sinks (except where species are not allowed to be photolyzed or swept into hydrothermal systems).

Point of Contact: D. Summers
(650) 604-6206
dsummers@mail.arc.nasa.gov

PROGRESS IN PLANETARY SYSTEMS

Planetary Rings

Jeff Cuzzi

Planetary ring and moon systems, especially the magnificent Saturn system, contain elements of processes in particle disks that provide insights into planetary formation. Saturn's rings will be a main focus of study for the Cassini mission, to be launched in October 1997. Interplanetary meteoroids

bombard planetary rings, generating ejecta which transport mass and angular momentum in systematic ways throughout the system. An exhaustive study, which fully models the entire range of bombardment, transport, and mixing effects by which highly absorbing "primitive" interplanetary material pollutes and redistributes material in an initially pristine icy system such as Saturn's rings, has been completed. The study includes careful treatment of the fate of ejecta particles as they fly about within a realistic radial profile of ring particle abundance, and also detailed radiative transfer modeling, using actual material refractive indices of the individual ring particle reflectivity as a function of wavelength and location in the rings.

The model implies (1) that with most parameters of the model constrained by other observations, it is found that the basic global brightness and color differences between the major ring regions (A-ring, B-ring, C-ring, etc.) can be understood for the first time, and in a simple way, by differential darkening caused by the infall of spectrally neutral, highly absorptive, probably carbonaceous, meteoritic material with orbits much like those of comets; (2) that the "initial," primordial composition of the rings is almost entirely water ice, but must contain a uniformly distributed, highly red, probably organic material such as is found in "primitive" bodies in the outer solar system and in Titan's organic atmospheric haze (silicates are not acceptable as coloring agents); (3) that the radial profile of ring particle color (and thus compositional) variations provides a good fit to the model

profiles for a range of exposure times which is in agreement with exposure-time estimates from bombardment effects on radial variations of ring structure; and (4) that nominal parameters for the model imply a ring age of the order of 100 million to 1 billion years, depending on the ejecta yield and the meteoroid flux, indicating that the rings may not be as old as the solar system (4.5 billion years).

Point of Contact: J. Cuzzi
(650) 604-6343
jcuzzi@mail.arc.nasa.gov

Planetesimal Formation in the Protoplanetary Nebula

Jeff Cuzzi

The “primary accretion” process—the process by which the first sizable objects (comets, asteroids, etc.) formed from solids that entered the protoplanetary nebula as micron-sized dust motes—is one of the major unsolved problems in understanding the origin of planetary systems. One key accomplishment this year was the completion of a new model of self-consistent turbulence generation and damping, by thin, dense layers of large (10-cm radius and larger) particles in the midplane of a protoplanetary nebula. Prior studies neglected the role of the particles in damping turbulence in the gas; a scheme to account for this effect has been developed and implemented. The scheme begins with the Reynolds-averaged equation for the turbulent kinetic energy. The full two-phase

equations are averaged, and new terms appear as a result of particle damping, which has been modeled using a gradient-diffusion-type approach.

In FY96, several different parameterizations for dissipation of turbulence by the gas itself, which has a major effect, were compared. A two-length scale model, a law-of-the-wall model, and two variable eddy-frequency models were explored; few really significant differences in model behavior were found between these parameterizations. Significant damping of nebula turbulence does occur, to a degree that is particle-size dependent, but the damping effect is not sufficiently strong to allow the particle layer to settle into a gravitationally unstable dense midplane layer as some prior workers had speculated. This appears to be one of the first fully coupled, physically parameterized studies of turbulence damping by mass loading—certainly this is so in the context of an orbiting disk.

Three-dimensional direct numerical simulations of particles in turbulence have been exhaustively analyzed. The Taylor microscale Reynolds number ranges from 40 to 140, and the code handles one million particles at each of 16 Stokes numbers (the Stokes number is the ratio of particle stopping time to Kolmogorov eddy turnover time). Previously, it was demonstrated that the particle size most strongly concentrated (by orders of magnitude) is in good agreement with chondritic meteoritic data. This year, it has been demonstrated for the first time that the particle density field for the most strongly concentrated particle size is a multifractal—and

that a certain key descriptor of the multifractal (the so-called singularity spectrum) is Reynolds-number independent.

Quantitatively, the density-field singularity spectrum agrees with that for turbulent dissipation, perhaps providing some profound clues toward explaining this very important process. It is now feasible to make use of extensive mathematical techniques developed for fractal analysis to predict the probability density of particle concentration at arbitrary Reynolds numbers, strengthening the applicability of these results to plausible nebulae with Reynolds numbers that are orders of magnitude higher than are achievable numerically.

Point of Contact: J. Cuzzi
(650) 604-6343
jcuzzi@mail.arc.nasa.gov

PASCAL: A Mars Climate Network Mission

Robert M. Haberle, David C. Catling, Steven C. Merrihew

Of all the planets in the solar system, Mars is most like Earth. In particular, its weather and climate are dynamically similar to Earth's. Mars therefore offers a natural laboratory for the study of the factors that control a planet's climate system. Yet the kind of observations that are needed to carry out such a study, namely long-term simultaneous measurements from a network of globally distributed surface stations, are lacking in NASA's Mars exploration program. To remedy

this, a Mars climate network mission was proposed in response to the 5th Announcement of Opportunity to NASA's Discovery Program. This mission was named PASCAL after the 17th century French scientist whose name is synonymous with the *Système International* unit of pressure.

Pressure is the key measurement of the PASCAL mission. It provides a measure of the total mass in a column of air. Given information on its horizontal and temporal variation one can infer the nature of the planet's general atmospheric circulation and climate system. Fortunately, pressure is also easy to measure, and pressure sensors do not require orientation or deployment. Thus, very simple landers can be designed that are light and robust. In effect, we are trading off the ability to make many different kinds of measurements at a few sites, for just a few measurements at many sites. This trade allows us to achieve the global coverage that is required to observe the planet's climate system while keeping the total mission cost well within the Discovery cap.

PASCAL's mission objective is to establish a network of 24 globally distributed surface stations that will measure hourly variations in pressure and temperature over a period of 10 Mars years (~18.8 Earth years). This long-term continuous presence will define the nature and variability of the planet's climate system on time scales ranging from hours to years. It will also provide a weather monitoring infrastructure for future Mars missions. In addition to network science, PASCAL will gather data on the structure of the atmosphere as each probe descends to

the surface. This aspect of the mission will be particularly valuable for future Mars orbiters which plan to aerobrake into their final orbits.

PASCAL would be launched in April of 2001 and arrive at Mars in January 2002. The 6.8-kilogram probes would be released from a spin-stabilized carrier on direct approach to Mars. To achieve global coverage, the probes would be released in salvos of eight, each separated by a propulsive time-of-arrival adjustment to allow Mars to rotate underneath. Entry descent and landing would utilize a heat shield, a parachute, and crushable material for final deceleration. One possible network configuration resulting from this deployment scheme is shown in the figure (see Color Plate 16 in the Appendix).

To ensure long lifetimes, each of PASCAL's surface stations would be powered by a Light Weight Radioisotope Heating Unit (LWRHU) coupled to a thermoelectric converter. The LWRHU also provides thermal control for the surface stations. Communication would occur through one of the orbiters of the Mars Surveyor Program (MSP). MSP plans to have orbiters at Mars beginning in September 1997 and continuing well into the next century. As a safety precaution, however, PASCAL's landers are capable of storing up to 5 Mars years of data should an orbiter not be available.

Point of Contact: R. Haberle
(650) 604-5491
rhaberle@mail.arc.nasa.gov

The Center for Star Formation

D. Hollenbach, P. Cassen

The Center for Star Formation Studies, a consortium of scientists from the Space Science Division at Ames and the astronomy departments of the Universities of California at Berkeley and Santa Cruz, conducts a coordinated program of theoretical research on star and planet formation. The Center supports postdoctoral fellows, senior visitors, and students; meets regularly at Ames to exchange ideas and to present informal seminars on current research; hosts visits of outside scientists; and conducts a week-long workshop on selected aspects of star and planet formation each summer.

The Star Formation Summer Workshop in 1996 was held at Wellesley College in Wellesley, Massachusetts, and included, in addition to the Ames scientists, about 100 astrophysicists from all over the world.

The main focus of work in FY96 was on the collapse of dense clouds to form protostars with protoplanetary disks, the evolution of these disks, which ultimately form planets, and the influence of young massive stars on the surrounding star-forming molecular cloud. D. Hollenbach, A. Tielens, and M. Kaufman modeled the thermal structure and spectra of dense molecular clouds which are collapsing to form high mass stars. A similar calculation was made by C. Ceccarelli (University of Grenoble), D. Hollenbach, and A. Tielens for clouds collapsing to form low-mass stars. When the

model spectra are compared with observations, observers can identify collapsing clouds and measure the rate at which the protostellar mass is increasing. D. Hollenbach and D. Neufeld (Johns Hopkins University) calculated the heating and ionization created when the collapsing cloud hits the protoplanetary disk. Comparisons of the models with recent radio observations of hot, ionized gas surrounding a nearby protostar made it possible to determine the rate of mass accretion onto the disk and the mass of the central protostar. K. Chick and P. Cassen developed models to explain the survival of presolar material during the formation of the solar system, as dust particles in the collapsing molecular cloud eventually incorporate into primitive meteorites.

Once formed in the collapse, protoplanetary disks around solar-type stars evolve for millions of years as they form planets. K. R. Bell and P. Cassen examined the shapes of protoplanetary disks and demonstrated how the temperature dependence of the effective grain opacity can lead to configurations in which much of the disk is shadowed from the central star. B. Pickett, P. Cassen, and R. Durisen (Indiana University) used three-dimensional hydrodynamic simulations to show how the development of gravitational instabilities in the early stages of protoplanetary disks is controlled by the radiant energy losses.

Young massive stars radiate copious amounts of ultraviolet radiation, which heats, dissociates, and ionizes the surrounding molecular cloud, and which ultimately leads to the dispersal of the cloud

and the cessation of star formation in the cloud. D. Hollenbach and H. Stoerzer modeled these processes, incorporating a large numerical code which followed the time-dependent chemistry, the thermal balance, and the transport of radiation. Their models predict the infrared spectra from such regions, so that observations can be interpreted quantitatively in terms of the rates of these destructive processes.

These theoretical models have been used to interpret observational data from such NASA facilities as the Infrared Telescope Facility, the Kuiper Airborne Observatory, and the Infrared Astronomical Observatory, as well as data from numerous ground-based radio and optical telescopes. In addition, they have been used to determine requirements for future missions such as the Stratospheric Observatory for Infrared Astronomy and the proposed Space Infrared Telescope Facility.

**Point of Contact: D. Hollenbach
(650) 604-4164
dhollenbach@mail.arc.nasa.gov**

Energetic Trapped Particles near Jupiter

John D. Mihalov

On December 7, 1995, the Galileo Probe carried experiments into Jupiter's atmosphere, near the planet's equator. The experiment complement included an energetic-particle telescope supplied by a group at the University in Kiel, West Germany. Data from this experiment could improve earlier measurements

of the innermost Jovian energetic trapped proton fluxes, made with the Pioneer 10 and 11 spacecraft, as well as provide data from the region even closer to the planet that had not yet been directly traversed by spacecraft. Beginning at 3 hours before atmospheric entry, inside the orbit of Io, and until entry, the experiment sampled the energetic trapped particle environment. Flux measurements and energy spectral and angular distribution data for energetic electrons and protons were obtained.

The electron fluxes appear to be within a factor of 3 of values obtained by earlier experiments aboard Pioneers 10 and 11, at locations where comparisons could be made. Except nearest to the atmosphere, where the energy spectrum steepened considerably, the most probable measured electron energy was about 20 and 40 million electron volts, respectively, for each of two separate electron-energy thresholds, based principally on energy-dependent responses for the experiment deduced from Monte Carlo simulations. Energetic-proton fluxes, spectra, and angular distributions were measured in three separate energy ranges in the 42 to ~131 million electron-volt energy range. The proton fluxes were observed to decrease abruptly inward from the location of Jupiter's ring, and also as Jupiter's atmosphere was approached.

Future analyses of the decreases in particle fluxes measured as the atmosphere was approached may give insight into the structure of Jupiter's near-equatorial upper

atmosphere, because the energetic particles lose energy as they interact with atmospheric constituents while they drift around the planet and bounce along the magnetic field. In addition, atmospheric interactions of the electrons are characterized by Coulomb scattering that causes diffusion of mirror points along magnetic field lines. Some energetic trapped helium, in the 62 to 136 million electron-volt per nucleon energy range, evidently was detected outside Jupiter's ring.

Point of Contact: J. Mihalov
(650) 604-5516
jmihalov@mail.arc.nasa.gov

Wavelet Software

Jeff Scargle

Wavelets are a mathematical tool for the analyzing and interpreting time series, images, and other datasets. New wavelet-based methods, developed for scientific and engineering applications, are useful for the following: (1) Characterizing the physical processes underlying complicated temporal and spatial variations; (2) removing unwanted observational noise from data; (3) compressing data with only insignificant loss of information; (4) probing computer models for physical processes that have a large dynamic range.

A powerful suite of wavelet algorithms to implement all these ideas has been developed and made publicly available under the name "WaveLab." WaveLab was a cooperative research project between

NASA Ames Research Center and the Statistics Department of Stanford University through Joint Research Interchanges, and was funded by the NASA Astrophysics Data Program and Astrophysics Software and Research Aids Program. The author collaborated with David Donoho of the Stanford and U.C. Berkeley Statistics Departments on this project. The actual software is in the form of MatLab (copyright the MathWorks, Inc.) scripts, which can be easily translated to other systems.

The World Wide Web site, maintained at Stanford (<http://playfair.Stanford.EDU:80/~wavelab/>) includes downloadable software for Unix, Macintosh, and Windows computers, complete documentation, tutorials in basic and advanced wavelet transform methods, sample data, and browser routines for exploring the sample data.

The WaveLab system has been downloaded by several thousand persons who have registered their use of this free, public-domain software, many of whom have indicated that they have already found WaveLab useful for their research, teaching, or commercial enterprises. The developers answer questions and help with user problems by e-mail.

Point of Contact: J. Scargle
(650) 604-6330
jeffrey@sunshine.arc.nasa.gov

Time-Dependent Structures in Galaxies

**Bruce F. Smith, Richard A. Gerber,
Richard H. Miller,
Thomas Y. Steiman-Cameron**

Numerical experiments on models of galaxies are yielding new insights into galactic structures and dynamics. This research is designed to examine time dependencies in the structural components of galaxies and to determine the implications for both the structural and dynamical evolution of galaxies. The results of these investigations are being used in interpreting and understanding high-resolution observations of galaxies made by the Hubble Space Telescope (HST) and other advanced observational programs. A series of numerical experiments has been made on the Cray C90 and parallel machines at the Numerical Aerodynamic Simulation (NAS) Facility at Ames Research Center to understand the nature of time-dependent processes in galaxies. These experiments probed the nature of complex motions observed at the centers of galaxies including those seen at the center of our Galaxy.

Global oscillatory modes have also been seen in the numerical experiments. These n-body experiments provided the first experimental evidence of long-lived global oscillatory motions in spherical systems. These oscillations have been identified as normal modes; the entire galaxy rings like a bell. Several modes have been identified, but two are dominant and both are spherically symmetrical. The first is nearly a homologous contraction

and expansion of the entire galaxy (the fundamental mode; a “breathing” mode), and the second has one node. A detailed study of the effects of softening in the representation of the potentials in the calculations has verified the earlier results on long-lived global oscillations.

Given that the normal-mode oscillations persist over many dynamical time scales, a natural question is: What processes could give rise to the oscillations? Among the possibilities are that (1) the oscillations could be left over from the galaxy formation process, (2) they may be initiated by interactions with neighboring galaxies, or (3) they could grow from instabilities.

These global oscillatory modes may play an important role in the structure and evolution of disk/halo galactic systems. The approach has been to assume that a significant fraction of the mass in a galaxy is in a dark halo. The halo oscillates and the luminous disk material responds to these oscillations. In the numerical experiments the disk responds to the time-varying potential by developing a ring structure that forms and disappears during each oscillation cycle (see first figure (see Color Plate 17 in the Appendix)). This pattern of response persists over time periods approaching a Hubble time (assumed age of the Universe since the big bang). The response can be understood as a resonance of the stars in an annular region where the disk epicycle frequency is the same as the halo oscillation frequency. This appearance of the ring, or annular gap, is reminiscent of some S0 galaxies (disk-like structures), such as NGC 4513. Such

systems are not uncommon and might be explained by the interaction of a disk with an oscillating halo. As the evolution proceeds a bar develops in the inner disk (see second figure (see Color Plate 18 in the Appendix)). Many galaxies, including our own, have bars in their central regions.

Point of Contact: B. Smith
(650) 604-5515
bfsmith@mail.arc.nasa.gov

Galileo Encounters Jupiter: Results from the Probe

Richard E. Young

The cone-shaped Galileo probe entered the atmosphere of Jupiter on December 7, 1995, at a speed of over 106,000 miles per hour and survived deceleration forces of 228 times Earth’s gravity. After deploying a parachute, it relayed data to the Galileo orbiter spacecraft, which was overhead, for 57.6 minutes. At the same time, the Galileo orbiter began a 2-year, 11-orbit tour of Jupiter. So far it has had close flybys of the Galilean moons Ganymede, Callisto, and Europa. The images it provides have spatial resolutions 10–100 times better than the Voyager images.

The Galileo probe project is managed by NASA Ames Research Center. Hughes Space and Communications Co., El Segundo, California, designed and built the probe. Lockheed Martin Hypersonic Systems (formerly General Electric),

Philadelphia, Pennsylvania, built the probe’s heat shield. NASA’s Jet Propulsion Laboratory, Pasadena, California, built the Galileo orbiter spacecraft and manages the overall mission.

The ratio of helium to hydrogen by mass is a key piece of information in theories of planetary evolution. For the Sun, this value is about 25%. Comprehensive analysis of results from the probe’s helium-abundance detector have shown that the helium abundance for Jupiter is near 24%, about the value for the primordial Sun.

The Jovian helium abundance indicates that gravitational settling of helium toward the interior of Jupiter has not occurred nearly as fast as it apparently has on Saturn, where the approximate helium-to-hydrogen ratio is just 6%. This indicates that Jupiter is much hotter in its interior than its neighbor Saturn, the next largest planet in the solar system. It also may cause scientists to revise their estimates of the size of the rocky core believed to exist deep in the center of Jupiter.

The abundances of several heavy elements, including carbon, nitrogen, and sulfur, are significantly greater on Jupiter than on the Sun. This implies that the influx of meteorites and other small bodies into Jupiter over the eons since its formation has played an important role in Jupiter’s evolution.

However, minimal complex organic compounds were detected, indicating that such complex combinations of carbon and hydrogen are rare on Jupiter and that the chances of finding biological activity there are extremely remote.

The winds, determined from tracking of the probe, persisted deep below the clouds, strongly suggesting that heat escaping from deep in the planet's interior drives the winds, rather than solar heating. Since all the outer giant planets exhibit strong winds, scientists hope that understanding Jupiter's winds will lead to important new insights into their unusual meteorology.

The Galileo probe apparently entered Jupiter's atmosphere near the southern edge of a so-called infrared hot spot, which is believed to be a region of reduced clouds. The probe's nephelometer (an instrument used to study suspended particles) observed only one distinct cloud layer, and that a tenuous one by Earth standards. It is likely to be an ammonium hydrosulfide cloud. Three distinct cloud layers (an upper layer of ammonia crystals, a middle layer of ammonium hydrosulfide, and a thick bottom layer of water and ice crystals) were expected. There were, however, some indications from the probe net flux radiometer and nephelometer that the probe started taking direct measurements in the bottom part of Jupiter's top ammonia ice cloud layer.

Further analysis of probe data has confirmed the preliminary report that the Jovian atmosphere appears to be relatively dry, with much less water than anticipated on the basis of solar composition and on predictions from data sent by the Voyager spacecraft that flew by Jupiter in 1979. These studies predicted a water abundance for the planet of twice the solar level (based on the Sun's oxygen content.) Actual probe measurements now suggest an

amount of water much less than that of the Sun.

The probe's instruments found much less lightning activity on Jupiter per unit area than on Earth. Lightning on Jupiter was found to be about one tenth of that found on Earth in an area of the same size. Although there is less lightning activity, the individual lightning events are, however, about 10 times more energetic than similar events on Earth.

Point of Contact: R. Young
(650) 604-5521
reyoung@mail.arc.nasa.gov

Regolith Effects on Mars' Climate

Aaron Zent

In FY96, analysis of the adsorption of water on Martian analog materials at Mars-like conditions was completed. In laboratory experiments, it was discovered that the mass of adsorbed H₂O was approximately an order of magnitude less than previously predicted. These results were used to derive new adsorption isotherms which reflect the heterogeneity of the surface sites on Martian (or any) soil.

In collaboration with Howard Houben at Ames, these new isotherms were applied to the study of the transport of water by the Martian atmosphere. It was found that the horizontal advection of water by the Martian atmosphere could not reproduce the observed patterns of atmospheric H₂O variations, but that

substantial vertical exchange between the atmosphere and the regolith could explain the results. In collaboration with Bruce Jakosky at the University of Colorado, it was found that nighttime inflections in the atmospheric temperature record at the Martian surface could be explained by the condensation of H₂O in the atmosphere, at a frost point which supports the model of diurnal H₂O exchange.

Point of Contact: A. Zent
(650) 604-5517
azent@mail.arc.nasa.gov

The Nature of the Martian Oxidants

Aaron Zent

In FY96, laboratory analysis of the ability of hydrogen peroxide (H₂O₂), complexed by the Ti⁴⁺ cation, was completed to reproduce the results of the Viking biology experiments. It was discovered that the results of the Labeled Release experiment, in which organic molecules were oxidized by a temperature-labile oxidant in the soil, could be reproduced by outer-sphere (that is, with an intervening hydroxyl radical (OH) group) peroxy-Ti complexes. The ability of inner-sphere (that is, no intervening OH group) complexed H₂O₂ to reproduce the Gas Exchange experimental reactivity and stability pattern is still being investigated.

Also explored was the role of the diffusion of H₂O₂ into the Martian regolith, and the role of

impact gardening in redistributing oxidized material through the Martian regolith. One finds that for reactive half-lives of the order of 100,000 years, diffusion will carry the oxidant into the upper 20 meters of the Martian regolith; also impact cratering will stir this material throughout the upper 100 meters of the regolith, necessitating deep drilling if unoxidized material is to be recovered.

Point of Contact: A. Zent
(650) 604-5517
azent@mail.arc.nasa.gov

A Thermo-Acoustic Oxidant Sensor

Aaron Zent

In FY96, an investigation was begun into the feasibility of using a thermo-acoustic oxidant sensor to identify and quantify the nature of atmospherically produced oxidants in the Martian atmosphere. A series of selective chemical coatings, including lead sulfide, metal phthalocyanines, and peroxidase are placed on chemiresistors and surface acoustic-wave devices. The mode of measurement for the chemiresistors is resistivity change owing to bonding between the measure and the coating; for the acoustic-wave devices it is mass changes of the same coating. Sensitivity to hydrogen peroxide, ozone, and carbon monoxide is demonstrated.

In collaboration with Dr. Marc Madou of the University of California at Berkeley, flight electronics for this experiment are being developed. In the coming year, the crosstalk and

effect of background gases on the proposed array of coatings will be investigated.

Point of Contact: A. Zent
(650) 604-5517
azent@mail.arc.nasa.gov

PROGRESS IN ASTROPHYSICS

Astrobiology in the Astrochemistry Laboratory

Louis J. Allamandola, Scott Sandford, Max Bernstein, Robert Walker, Dave Deamer

The Ames Astrochemistry Laboratory has made major contributions to the understanding of the composition and properties of interstellar and cometary ices. This is done by studying laboratory analogs of cometary and interstellar ices. An important application of this work to the origin of life is reported here. Since comets are considered to be a major source of the molecules brought onto primitive Earth before life began, their organic composition is of central importance to questions concerning the origin of life.

Cosmic ices contain the very simple molecules, water (H₂O), methanol (CH₃OH), carbon monoxide (CO), carbon dioxide (CO₂), molecular hydrogen (H₂), ammonia (NH₃), and formaldehyde (H₂CO), as well as more complex species. Ultraviolet irradiation of these ices produces other simple species such as H₂, H₂CO, CO₂, CO, methane (CH₄), formyl radical (HCO), and more complex organic molecules known as amides, nitriles, amines,

ketones, aldehydes, and polymers which are of particular interest from a prebiotic perspective. The ready formation of these complex organic species from simple starting mixtures and the ice chemistry that ensues when these ices are warmed suggest that interstellar ices and comets may have played an important part in the origin of life.

In addition to cometary ices raining a rich inventory of potentially important prebiotic molecules down onto early Earth, the compounds in cometary ices may also have played a role in early membrane production. Formation of membranes is considered a critical step in the origin of life, for they are required to isolate and protect the interior workings of a cell from the surrounding medium. Within the confines of a membrane, conditions such as acidity can be moderated and held at a different value from that in the surrounding medium, nutrients can be concentrated, and so on. Although it is uncertain where membrane formation falls in the sequence of events leading up to the origin of life, it is considered an absolutely crucial step. When the most complex organic molecules produced by irradiation of the simple mixed molecular ices are placed in water, water-insoluble droplets form naturally. This self-organizing, lipid-like behavior is similar to that found for the organic components of the Murchison meteorite. The figure shows micrographs of these nonpolar droplets. Both photographs are of the same field of view, with the upper photograph taken in normal light (yellowish cast) and the lower in fluorescent

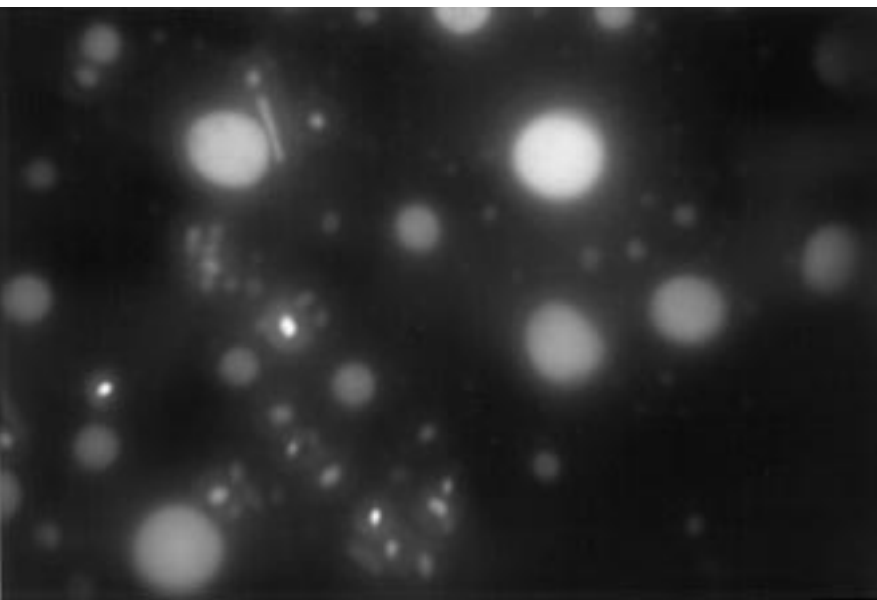
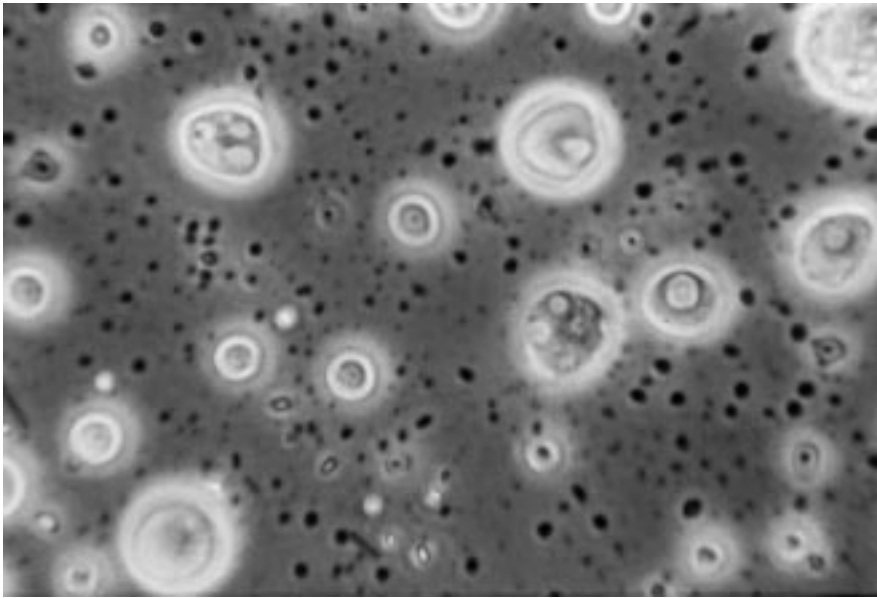


Fig. 1. Photomicrographs of the water-insoluble droplets formed when a few drops of water are placed on the most complex molecules produced by irradiation of an interstellar and cometary ice analog. Both photographs show the same field of view, with the upper photograph taken in natural lighting and the lower in fluorescence stimulated by ultraviolet. Taken together, these photographs show that the self-organizing droplets form naturally from these materials and that they also trap luminescent materials in their structures.

emission stimulated by a black light (ultraviolet light). The upper photograph shows the presence of two distinct phases, liquid water and insoluble droplets. Several of the self-organized droplets show intriguing structures suggestive of cell walls. In comparing the upper and lower photographs, it is interesting to note that all of the larger and many of the smaller droplets have trapped blue photoluminescent material also produced by the original ice irradiation. The ability to trap energy receptors within these structures is also considered a critical step in the origin of life, for it provides the means to “power” the protocell, as photosynthesis does today in plants.

Point of Contact: L. Allamandola
(650) 604-6890
allamandola@ssa1.arc.nasa.gov

Spectrum Synthesis of Hot Water in Sunspots and Selected Cool Stars

Duane F. Carbon, David Goorvitch

The objective of this research is to define the energy distribution of late-type stars so that their physical state is better known. Better information about their physical state will then lead to improved abundance determinations and energy standards. Very recently, Partridge and Schwenke of Ames Research Center completed an elaborate theoretical computation of the potential-energy surface and dipole moment function for H_2O . They have used their results to predict the positions and

strengths of nearly 308 million $^1\text{H}^1\text{H}^{16}\text{O}$ lines. This line tabulation is the most complete now available. It extends to sufficiently high excitations so that the spectra of M-stars (cool red stars) may be modeled with greater accuracy than ever before provided the predicted line parameters of Partridge and Schwenke are themselves accurate.

Synthetic sunspot spectra have been computed using the Partridge and Schwenke H_2O line list and the sunspot umbral models. In order to test the new line list, a careful comparison of these synthetic spectra and of published high-resolution sunspot atlases has been carried out. This comparison shows that the new H_2O line list successfully predicts the sunspot H_2O spectrum and that it can specify where further improvements in the line tabulation are necessary. In addition, as part of this study, it is demonstrated that sunspot atmospheres are much cooler in their shallow layers than predicted by the models and that the most recent line tabulation for the OH molecule is seriously in error.

Using the new H_2O tabulation, the extent to which hot stellar water blankets the H (1.65 microns), K (2.20 microns), and L (3.45 microns) passbands for selected K- and M-star model atmospheres and, thus, the energy distribution of these stars, is also investigated.

Point of Contact: D. Carbon
(650) 604-4413
dcarbon@nas.nasa.gov

A High-Altitude Site Survey for SOFIA

Michael R. Haas, Leonhard Pfister

The Stratospheric Observatory for Infrared Astronomy (SOFIA) will have a 2.5-meter telescope mounted in the aft section of a Boeing 747 SP for use in making astronomical observations at wavelengths between 0.3 and 1600 microns. This study investigates the meteorological conditions above 41,000 feet and finds that there are significant weather patterns at these altitudes which can adversely affect airborne astronomy.

Experience has shown that high-altitude cloud cover and water-vapor overburden are the most important meteorological factors affecting the quality of astronomical observations at typical flight altitudes. To determine acceptable home base sites for SOFIA, these factors must be measured over broad geographic regions, since a typical flightpath covers hundreds of kilometers. The only source of such data is satellites which provide global coverage of Earth over an extended period of time.

This study gathers the best available satellite data, shows that they corroborate airborne experience, and demonstrates that they are consistent with well-known global circulation, convection patterns, and upper-tropospheric/lower-stratospheric dynamics. Part (a) of the figure (see Color Plate 19 in the Appendix) shows the total frequency of cloud occurrence as measured by the Stratospheric Aerosol and Gas Experiment (SAGE II). This instrument uses a limb occultation

technique, so it has good vertical resolution, but relatively poor horizontal resolution. The cloud-frequency data have been vertically integrated above 41,000 feet and averaged over the three summer months (June, July, and August) for a 6-year period. Part (b) of the figure shows the total frequency of cloud occurrence for summer as measured by the High-Resolution Infrared Radiation Sounder (HIRS) sensors on polar orbiting National Oceanic and Atmospheric Administration satellites since June, 1989. Since this satellite is nadir-looking, this dataset has much better horizontal resolution, but a significantly higher minimum optical depth and poorer vertical resolution.

Water vapor is the principal molecular absorber throughout much of the infrared. Its strong vertical stratification at altitudes below the tropopause is one of the primary motivations for conducting airborne observations from the stratosphere, where the water-vapor overburden is relatively small and constant. Furthermore, the negative temperature gradients just below the tropopause allow rapid vertical transport of moisture. When combined with low, upper tropospheric temperatures, this results in the formation of extended, thin sheets of cirrus clouds. Part (c) shows the average tropopause height for the summer season, and part (d) shows the water-vapor overburdens in precipitable microns as inferred from the Microwave Limb Sounder (MLS) for the summers of 1992 and 1993. Although the positive temperature gradient above the tropopause strongly increases the vertical stability of the atmosphere and

places a lid on the rapid vertical transport of moisture in Earth's atmosphere, there are clearly large variations from this simple model.

The largest variations in high-altitude weather over the United States occur in the summer because the tropopause is near 41,000 feet. Moreover, different portions of the United States lie in different meteorological regimes in terms of large-scale circulation and the potential for convection. The eastern Pacific is dominated by the downward motion associated with the mid-Pacific upper-level trough, and by generally lower sea surface temperatures. East of a line extending from northern Mexico along the Rockies into Canada, there is upward motion associated with the continental upper-level ridge. Warm moist air from the Gulf of Mexico, and to a lesser extent from the Gulf of California, promotes convection east of the Rockies and in northwestern Mexico. Moffett Field, the site selected for SOFIA operations, is well within the regime of downward motion which results in lower upper-level cloudiness and lower water-vapor overburdens.

Point of Contact: M. Haas
(650) 604-5511
mhaas@mail.arc.nasa.gov

Kepler Mission Educational and Public Outreach Software

David Koch

In response to the strategic goals of finding other habitable planets

and conveying this objective to students and the public, an educational software package has been developed and distributed publicly.

Experience with educators has shown a demand not just for information, but also for science data that students could analyze. This has been a difficult challenge, since in general the latest data from airborne and space-borne experiments almost always requires sophisticated data processing and an "educated eye" to glean the subtle effects being observed. However, the observations to be performed by the *Kepler Mission*, which has been proposed to the Discovery Program, to detect Earth-sized planets are based on a straightforward principle that can be easily understood even by upper elementary students. An interactive software package has been developed that allows the students to both perform simulated observations as if they were the astronomers and then to analyze the data to determine the habitable properties of the planet.

The *Kepler Mission* has been proposed as a Discovery Mission to search for habitable planets. The purpose of the mission is to continuously and simultaneously observe 160,000 stars for evidence of planetary transits. When a planet passes in front of its star it causes the star to dim. When a second transit of the same duration and with the same brightness change occurs, the exact orbital period can be predicted. When additional transits are seen, one has a high confidence that a planet has been detected. From the period, the orbital distance of the planet from its star can be calculated and the characteristic temperature of the planet estimated. From the

change in brightness the planet size can be calculated, and the mass and surface gravity can be estimated.

The software package has several components, including the following:

1. A description of the latest results in the search for planets beyond our own solar system;
2. A description of a habitable planet, one where liquid water may be found on the surface;
3. A description of the various methods, including the capabilities and limitations of the different detection techniques;
4. A description of the *Kepler Mission*, the only currently practical method for finding Earth-sized planets;
5. An interactive *Kepler Mission* simulator;
6. A biography of Johannes Kepler, a description of his three laws of planetary motion, and information on his life and times.

The software is written in Hyperstudio™ for the Macintosh, and the Hyperstudio™ player is included. The software can be downloaded from the *Kepler Mission* web site (WWW.kepler.arc.nasa.gov). When compressed, the entire software package with the player is 1 megabyte and will fit on a single high-density disk; thus it is easy for teachers to copy it and carry it into the classroom. Use of the software does not require an Internet connection.

Point of Contact: D. Koch
(650) 604-6548
dkoch@mail.arc.nasa.gov

Mid-Infrared Studies of Diffuse Interstellar Material

Thomas L. Roellig

Infrared observations of the emission from material located in the diffuse regions of space between the stars can provide important information on its composition and energy state. This information is crucial to our understanding of star formation and galactic evolution. Unfortunately, such observations are very difficult, largely because this emission is very weak and is easily drowned out by infrared radiation emitted from the telescope optics. Furthermore, many of the most interesting regions in the infrared spectrum are obscured by absorption in Earth's atmosphere.

As a result, a telescope in space cooled to temperatures only a few degrees above absolute zero is needed for these investigations. Such a telescope, optimized for infrared studies of diffuse regions, was flown in 1995 in a NASA/Japanese Space Agency collaboration—the Infrared Telescope in Space (IRTS) infrared survey mission. The Mid-Infrared Spectrometer (MIRS), an instrument developed and operated jointly by NASA Ames and the University of Tokyo, was attached to the IRTS and operated over wavelengths ranging from 4.6 to 11.7 microns. This is an ideal spectral region for investigations of infrared emission from solid material, since it covers many of the diagnostic stretching and bending modes of candidate interstellar material. The IRTS/MIRS telescope/instrument combination achieved

sensitivities that were orders of magnitude better than any instrumentation previously used for diffuse mid-infrared emission studies.

The first data from the MIRS have now been analyzed and have yielded interesting new information about the interstellar material. The observed mid-infrared interstellar emission was found to be concentrated almost solely in a few emission bands (see the figure). This was

true both for those regions located within the plane of the galaxy and for those regions above the galactic plane. The remarkable similarity of the spectra from the different regions indicates that there is little chemical differentiation between these regions. The spectral features themselves are indicative of emission from a class of hydrocarbons—polycyclic aromatic hydrocarbons (PAHs). In the scenario envisaged to

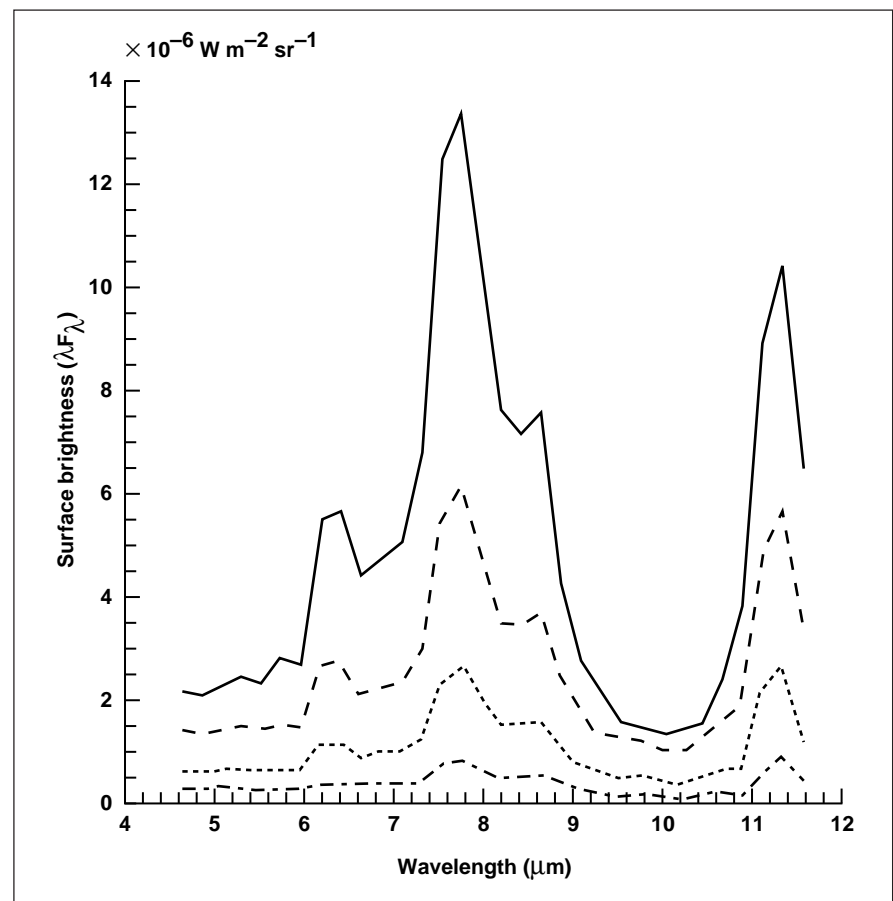


Fig. 1. Spectra obtained from the Mid-Infrared Spectrometer on the Infrared Telescope in Space mission. For all spectra, the galactic longitude was approximately 50° . The different lines correspond to different galactic latitudes, b . The solid line indicates emission from $-0^\circ 40' < b < 0^\circ$, the dashed line emission from $1^\circ < b < 2^\circ$, the dotted line emission from $2^\circ < b < 3^\circ$, and the dot-dashed line emission from $3^\circ < b < 5^\circ$.

operate in the interstellar medium, these molecules absorb ultraviolet photons and then emit this energy in the infrared. The spectra obtained by the MIRS show that the mid-infrared emission from the diffuse regions in the galaxy can be attributed almost solely to this material. The MIRS data also show that the previously unexplained excess emission observed in the mid-infrared by the earlier Infrared Astronomical Satellite (IRAS) mission can be attributed to these emission bands.

Interestingly enough, a comparison of the spatial distribution of these mid-infrared emission features with the emission at the much longer wavelength of 100 microns observed with the Infrared Astronomical Satellite mission indicates a very close correlation. Since the 100-micron emission is not expected to arise from PAHs, but instead from much larger grains of solid material, this tight spatial correlation must mean that these two different kinds of interstellar materials are mixed in a constant ratio throughout the different interstellar regions in the galaxy.

Point of Contact: T. Roellig
 (650) 604-6426
 troellig@mail.arc.nasa.gov

Infrared Observations of G0.18-0.04

Janet P. Simpson, Sean W. J. Colgan, Angela S. Cotera, Edwin F. Erickson, Michael R. Haas, Mark Morris, Robert H. Rubin

Radio images of the center of our Galaxy show a number of features that are unique in the Galaxy and that are very difficult to explain. Some of these are demonstrated in the figure, which is a 20-cm Very Large Array radio image by F. Yusef-Zadeh and M. Morris, overlaid with contours showing the locations of the Galactic Center molecular clouds. A quarter of a degree from the Galactic Center

there is a long thin "Arc," also called the Straight Filaments, that crosses the Galactic Plane at right angles. The length and thinness of the synchrotron radiation emitting Arc (and other arcs not in the figure), suggest that the Galactic Center region has a strong magnetic field; however, the excitation and source of the relativistic electrons emitting the synchrotron radiation is not known.

The Galactic Center H II region, G0.18-0.04, also called the "Sickle," is located where the Arc crosses the Galactic plane. The Sickle appears to be the ionized edge of the dense molecular cloud whose contours are shown in the figure. In the past, the source of ionization of the Sickle has

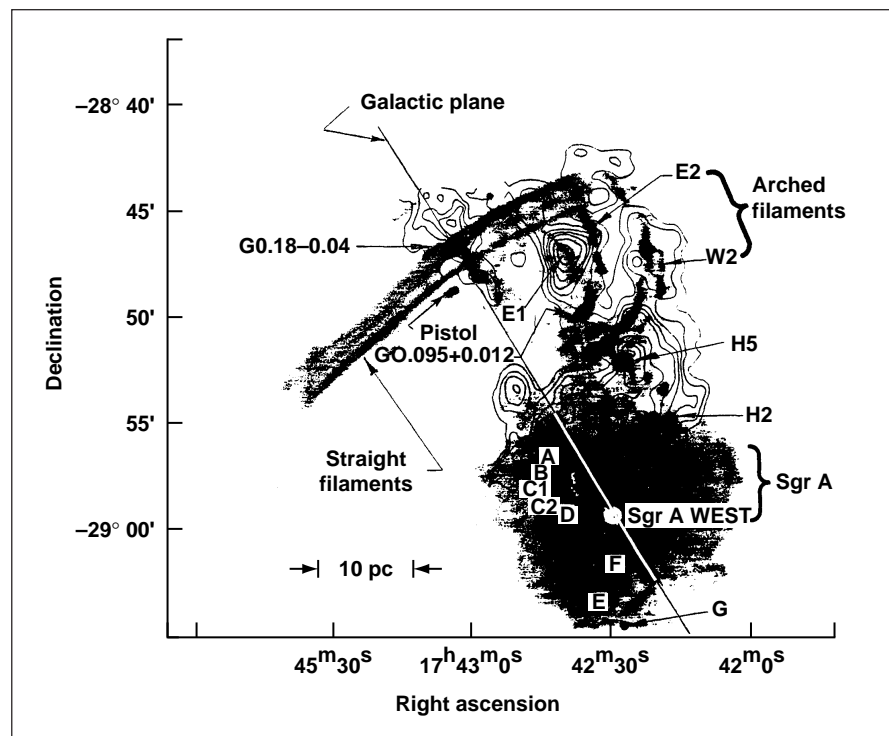


Fig. 1. The 20-cm Very Large Array radio image, overlaid with contours showing the locations of the Galactic Center molecular clouds. Sgr A is the Galactic Center. G0.18-0.04 (the Sickle) and the Pistol are labeled.

been ascribed to both the interaction of the cloud with the magnetic field of the Arc and to the hot stars in the adjacent star cluster, AFGL 2004, also known as the “Quintuplet Cluster.” There is a smaller region of thermal gas known as the “Pistol”; the star cluster AFGL 2004 lies between the Sickle and the Pistol. Because of the great obscuration toward the Galactic Center, it is not possible to see these regions at wavelengths visible to the eye; instead, one must use infrared and radio telescopes to view the region. The objective of this study is to ascertain the relative locations of the stars, the ionized and molecular gas, and the sources of gas excitation and dust heating.

Far-infrared lines of C+, N+, N++, O0, O++, Si++, and S++ were measured with the Cryogenic Grating Spectrometer on the Kuiper Airborne Observatory. For the H II region, electron densities for both the O++ and S++ zones were estimated, and abundance ratios were calculated for O++/S++, N++/O++, N+/N++, N+/O++, Si+/S++, and S++/H+. For the less excited gas in the interface region between the H II region and the molecular cloud, the incident photon flux and densities were estimated from the C+ and O0 lines and the far-infrared continuum.

Near-infrared images of the region were taken by A. Coteri as part of her Stanford University Ph.D. thesis (1995), supported by a NASA Graduate Student Research Fellowship at Ames. From the 1.65 and 2.1 micrometer photometry of stars in the field and from the Hydrogen Br gamma images, the extinction to the region could be estimated. The

extinction is fairly uniform over the region and is consistent with a location in the Galactic Center. There is no indication of the dense molecular cloud that had previously been suggested by other researchers to lie between Earth and the region in the images of the star field. The previous suggestion of excitation of the Sickle by interaction of the molecular cloud with the magnetic field required that the cloud, which recedes at 25 kilometers per second away from Earth, produce the observed 20- to 120-kilometers-per-second ionized gas in the H II region by running into the magnetic flux tubes of the Arc. Thus, both the Arc and the ionized gas would be on the far side of the cloud from Earth in this scenario. Since the near-infrared measurements of the stars and the ionized gas demonstrate that the gas must be on the near side of the cloud, this early suggestion cannot be correct.

The observed lines were compared with predictions of models of slab H II regions ionized by a cluster of luminous stars. This comparison indicates that the source of ionization of the Sickle is probably the hot stars of the AFGL 2004 cluster, but the Pistol has a lower ionization than its proximity to the cluster would suggest. More likely, the Pistol is ionized by the extremely luminous star that the Ames researchers found to be located near the center of its arc. Since the positions at some distance from AFGL 2004 have higher ionization than is predicted by the models, it is likely that there are additional hot stars scattered throughout the region. The low excitation lines and far-infrared continuum from the molecular cloud

and interface region between the cloud and H II region are also consistent with heating and excitation by the same stars. The electrons in the Arc probably originate in the ionized gas of the H II region and are excited to relativistic energies by magnetic reconnection of the magnetic field lines of the Arc and the molecular cloud.

Point of Contact: J. Simpson
(650) 604-1613
simpson@cygnus.arc.nasa.gov

New 3.405-Micron Interstellar Emission from Organic Hydrocarbons

Gregory C. Sloan, Jesse D. Bregman

Polycyclic aromatic hydrocarbons (PAHs) are a form of organic hydrocarbon identified by their complex spectral emission in a rich variety of astronomical sources. This spectrum includes several emission features between 3 and 13 microns, originally described as the unidentified infrared emission features. Louis Allamandola and his Ames collaborators identified the carriers of this spectrum by their laboratory analysis of PAHs. These molecules typically consist of 20-50 carbon atoms arranged in a flat matrix of aromatic rings, with hydrogen atoms bonded to the carbon on the edge. The C-H bonds produce most of the spectral features observed from the ground; stretching modes produce features at 3.3 microns and nearby; bending modes produce features at 8.6 microns and in the

11.2–12.7-micron region. These organic molecules may represent more than 15% of all interstellar carbon, so a better understanding of their composition would give us insight into the evolution of interstellar carbon material. Because PAH spectra are seen in so many sources, a better understanding of the emission mechanisms would make them very powerful probes of the interstellar medium.

PAH spectra are observed typically at the edge of ionized regions. One such region, the Orion Bar, is a transition region between the Orion Nebula, ionized by the ultraviolet energy from the Trapezium, and the molecular cloud to the southeast. These transition regions have strong gradients in ultraviolet flux decreasing from the ionized zone to the molecular region. The Bar presents the observer on Earth with an edge-on geometry which makes it an excellent laboratory to study how PAH emission varies with excitation conditions.

The 3-micron PAH emission in the Orion Bar was observed using a long-slit spectrometer at the United Kingdom Infrared Telescope in October 1995. These spectra allow one to trace the strength of the 3.29-micron PAH feature, which dominates the spectrum and arises from a ground-state aromatic C-H stretch; the weaker features observed at 3.40 and 3.51 microns; and the underlying emission plateau which stretches from 3.3 to 3.6 microns. These features peak on the ionization front, and drop in strength into both the ionized and molecular regions. The features decrease into the ionized region because the harsh

ultraviolet field is destroying the PAHs there. They decrease into the molecular region because the ultraviolet flux which excites the spectral features is being attenuated by the high optical depths of the neutral and molecular gas in the Bar. In general, these features decrease into the molecular region exponentially, with a $1/e$ scale height of approximately 10 arcseconds. However, the PAH plateau, and the 3.40- and 3.51-micron features show a layer of enhanced emission roughly 10 arcseconds behind the ionization front, right where emission from H_2 also peaks. This enhancement is especially noticeable in the 3.40-micron emission feature.

A careful analysis of both the shape and the strength of the 3.40-micron feature reveals that it actually consists of two spectrally and spatially distinct components. The main component peaks at 3.395 microns and behaves spatially very similarly to the PAH plateau and the 3.51-micron feature. The secondary component peaks at 3.405 microns, and its emission is concentrated 10 arcseconds behind the ionization front, again, right where the H_2 emission peaks.

The spectral properties can be interpreted in terms of recent laboratory analyses of PAHs at NASA Ames by Bernstein, Sandford, and Allamandola and by Joblin, Tielens, Allamandola, and Geballe. Joblin et al. analyzed PAHs with attached methyl sidegroups, which contain aliphatic C-H bonds and produce an emission feature close to the position of the secondary component, 3.405 microns.

Bernstein et al. analyzed what they describe as H-PAHs, or PAHs with additional H atoms attached to the carbon on the periphery of the PAHs. These atoms convert aromatic C-H bonds to aliphatic C-H bonds, producing an emission feature at 3.395 microns, as well as the PAH plateau and emission feature at 3.51 microns. In fact, their laboratory spectrum of hexahydropyrene provides the closest match yet attained to the astronomical PAH spectrum.

The evidence is growing that the 3.40-micron feature arises from an aliphatic C-H bond. Both of the components at 3.40 microns that we have identified arise from such a bond, although the bond resides in different carriers. Based on the differences in spatial behavior between these components, it appears that the methyl sidegroups are easily destroyed beyond the molecular hydrogen emission layer, whereas the H-PAHs survive right up to the ionization front.

Point of Contact: J. Bregman
(650) 604-6136
jbregman@mail.arc.nasa.gov

PROGRESS IN SPACE TECHNOLOGIES

Assessment of the Cassini Command and Data Subsystem

Edward A. Addy

Formal methods have been promoted as an effective means of developing software that requires a high degree of assurance. Yet to date, formal methods have not significantly affected software development practices. The difficulty of maintaining the fidelity of the formal model with the system as the system undergoes changes in requirements and specifications during development has contributed to its failure to influence the developmental practices. The goal of this project is to determine if the use of

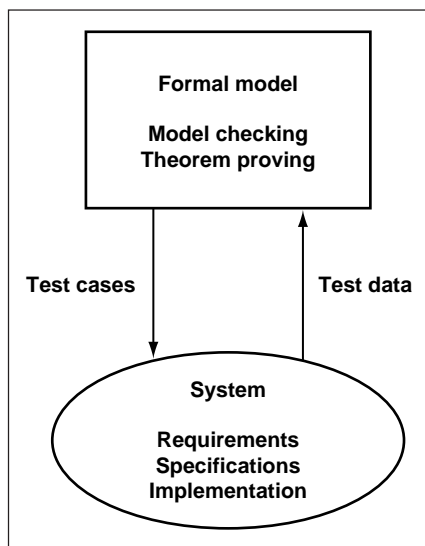


Fig. 1. Use of theorem-proving in generating test cases to maintain formal model fidelity during system development.

theorem-proving within a formal model can be used to generate test cases for testing the actual system being modeled. The union of formal models with test-case generation will help to alleviate the difficulty of maintaining fidelity, and will provide useful information in the form of test cases to the development team.

The functioning of the scheduler and interrupt handler through analysis of the Cassini Command and Data Subsystem (CDS) source code has been used as a case study. A formal model of this part of the CDS software was created, using the formal specification language, Prototype Verification System (PVS), which is based on a classic, typed higher-order logic. The PVS system includes support tools and a theorem prover. This follows on from previous research in which formal model checking was used to generate test cases for the actual system. The test data and the model checking have been used jointly to maintain the fidelity of the model with the actual system as it is being developed. This project has used theorem-proving within the formal model in a similar fashion, to generate test cases for the CDS and to increase the fidelity of the model to the CDS, as illustrated in the figure.

The source code from the Cassini CDS related to the scheduler and interrupt handler functions was analyzed. The formal modeling process identified that the millisecond interrupt was not functioning properly. The development team modified the scheduler, improving its performance and eliminating the potential for improper memory

allocation. A preliminary PVS model of the scheduler and interrupt handler functions has also been developed.

Point of Contact: E. Addy
(304) 367-8353
edward.addy@ivv.nasa.gov

Automatic Telescope Project

John Bresina

The primary objective of the Automatic Telescope Project is to provide advanced scheduling and automation infrastructure so that the benefits and performance of single-user automatic telescopes can be made available to a large community of users, with no additional people in the loop. In addition, Web-based assistance is provided for "service observing," which is becoming the dominant operations mode for large-scale, sophisticated telescopes. The benefits are a dramatic reduction in telescope operating costs and an increase in both scientific productivity and ease-of-use. The Associate Principal Astronomer (APA) enables electronic request submission, automatic loading and scheduling, and electronic data return, all under the control of a single astronomer (see the figure for an illustration of the architecture). The advanced loading and scheduling techniques provide fair allocation of telescope time and support high-quality data collection.

The APA software tools have been extensively tested by G. Henry at Tennessee State University (TSU)

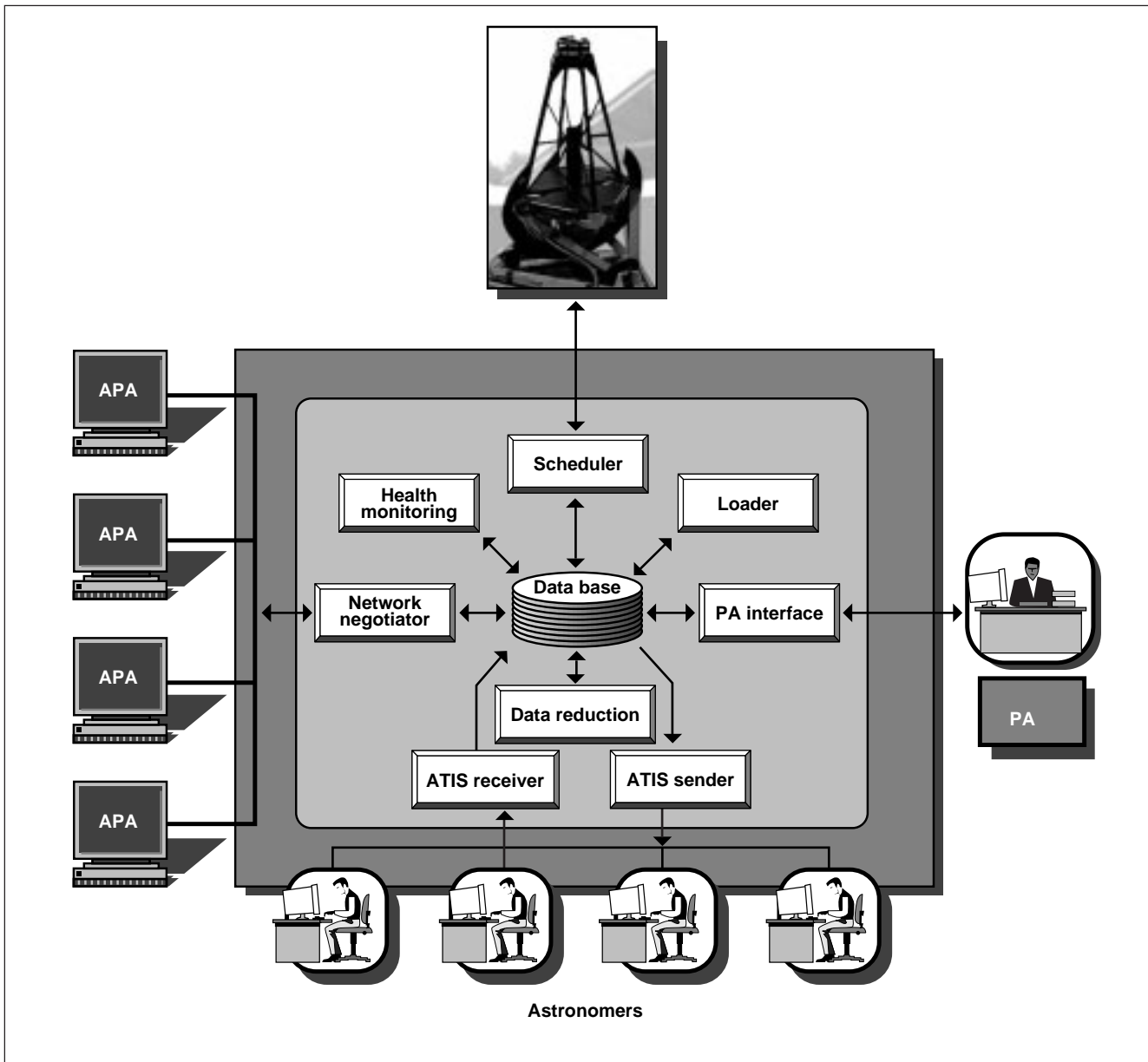


Fig. 1. Associate Principal Astronomer architecture.

and by the Fairborn Observatory staff. The scheduler has been executing nightly since January 1996 for Fairborn telescope T8. The loader has been undergoing nightly testing for the same telescope since April 1996, and the Service Observing Associate (SOA) is undergoing

testing on the UK Infrared Telescope (UKIRT). There was enthusiastic reception of the APA from UKIRT, the Hands-On-Universe project, the Four College Telescope, and UK's New Generation Astronomical Telescopes Project. John Davies carried out a successful "live test"

of the SOA at UKIRT and demonstrated the system to senior staff of the multinational Gemini project (and others).

Point of Contact: J. Bresina
(650) 604-3365
bresina@ptolemy.arc.nasa.gov

Guide Star Tracker for Gravity Probe B Relativity Mission

John H. Goebel

The guide star tracker for the Gravity Probe B (GPB) Relativity Mission is used to define the inertial reference frame against which the relativistic effects of a satellite in a polar Earth orbit can be measured. The tracking telescope is cooled to superfluid helium temperature

(1.87 kelvin) in order to accommodate the gyroscope readout detectors of the Superconducting Quantum Interference Device (SQUID). Because both the gyroscope and guide telescope are rigidly mounted together in the liquid-helium-cooled portion of the satellite, the starlight sensing detectors and preamplifier electronics must function without disturbing either the gyroscopes or the telescope wavefront. Tracking accuracy of the order of 10 milliarcseconds is required, implying that

thermal disturbances must be kept to a minimum.

The Space Technology Branch has contributed to the star sensor development effort for GPB by assisting in the design, construction, development and testing of the photodiode and cooled electronics. This effort is a collaboration with scientists and engineers at Stanford University, Marshall Space Flight Center, Goddard Space Flight Center, Ames Research Center, Lockheed-Martin Corporation, and various suppliers of component parts.

A photograph of the Revision B hybrid electronics circuit for the star sensor that is mounted in the cryogenic vacuum vessel is shown in the figure. The sensor has been demonstrated to meet the requirements for functioning in the cryogenic environment by operating at a somewhat elevated temperature of 70 kelvin with a power dissipation not exceeding 2 milliwatts. Operation of the sensor at temperatures down to 30 kelvin has been demonstrated at power dissipation less than 1 milliwatt.

Point of Contact: J. Goebel
(650) 604-3188
jgoebel@mail.arc.nasa.gov

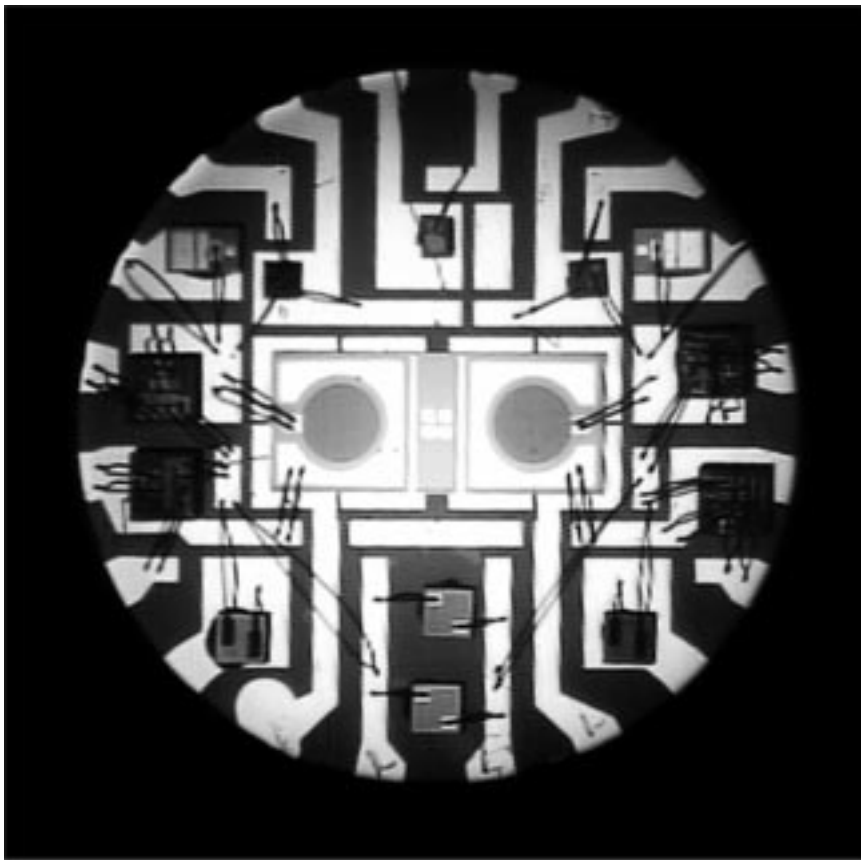


Fig. 1. Revision B Hybrid Circuit. This circuit is 0.400 inches in diameter and includes two circular silicon photodiodes and four square silicon field effect transistors. Light from the guide star is focused on the detectors which convert the light to electrical current which in turn is amplified by the transistors. The circuit is thermally isolated from the cryogenic environment so that it can operate at an elevated temperature of 70 kelvin.

Pulse-Tube Cryocooler Development

Peter Kittel

Pulse-tube coolers have unique advantages over the other coolers that are usually considered for NASA space missions. Because they have

no moving parts in the cold part of the cooler, they have inherently very long lifetimes and very low levels of vibration. However, they are a relatively new technology and require further development to achieve the thermal efficiency of more mature coolers such as Stirling coolers. The first figure shows the main components of a pulse-tube cryocooler.

The compressor (at room temperature) provides an oscillating gas pressure which moves gas into and out of the cooler. The regenerator consists of a tightly packed bed of fine screens that absorb any temperature oscillations in the gas. The compressor end of the regenerator is at room temperature and the other end is cold. The pulse tube isolates the cold junction from the orifice and reservoir at room temperature. A properly adjusted orifice creates a special relationship between the pressure oscillations in the pulse tube and the gas flow such that heat is drawn from the cold junction and deposited at the orifice.

In FY96 great progress was made in understanding and improving the operation of two of the main components of the cooler—the regenerator and the orifice.

For the screen mesh in the regenerator to adequately absorb temperature oscillations in the gas passing through it, it must have a large surface area and a large mass. These requirements suggest a large number of very fine screens and a high impedance to the gas flow. The regenerator must not be too restrictive, because this would reduce the pressure and flow available for cooling at the pulse tube. It is crucial to find the best compromise between

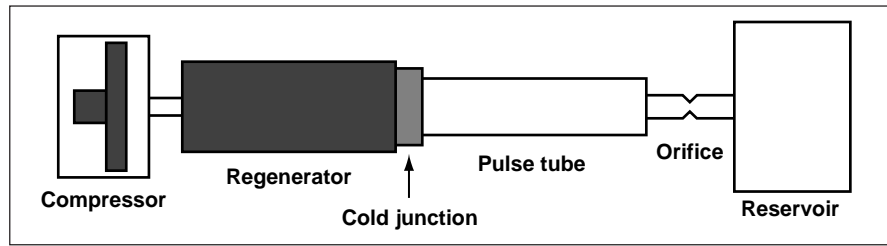


Fig. 1. Components of a pulse tube-cryocooler.

absorbing temperature oscillations and allowing adequate flow.

The behavior of this region of the cooler has been difficult to predict; measurements of pressure drop with oscillating flow have disagreed with predictions based on steady-flow data. Therefore, measurements were made to characterize the screen mesh of the regenerator under oscillating flow

conditions that were similar to those that would exist in actual use. These measurements showed that the pressure drop at frequencies near 60 cycles per second was 20–30% less than that predicted from steady-flow data. These improved data (shown in the second figure) will allow much better optimization of the regenerator screens.

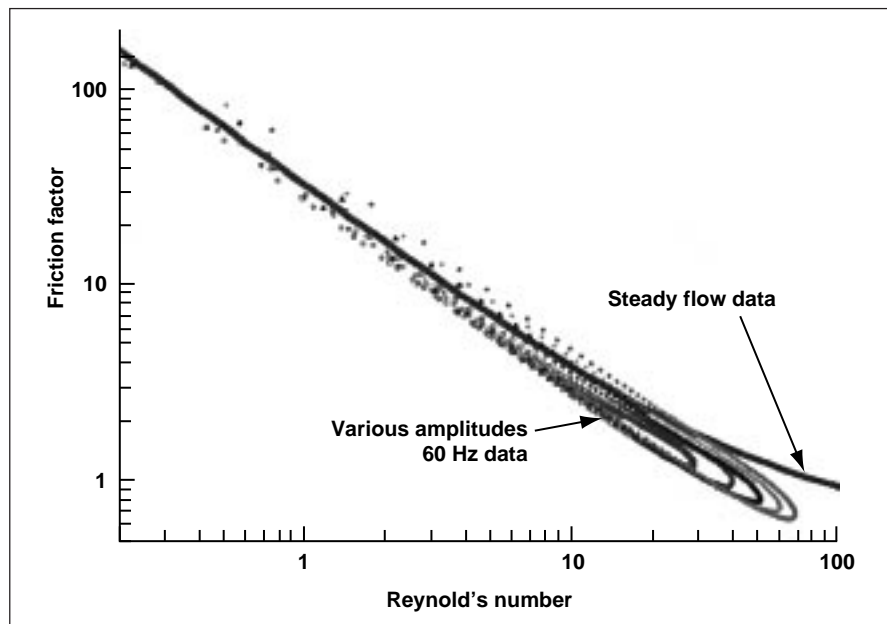


Fig. 2. Pressure drop in a 325-mesh regenerator. Solid curve is steady-flow data. The data points are the instantaneous pressure drop during 60-cycle runs for a variety of amplitudes.

The orifice serves to adjust the relationship between oscillating gas pressure and gas flow in the pulse-tube section. An analysis of the system shows that much more cooling power could be obtained if sufficient adjustment of this relationship could be achieved. However, the range of adjustment available from a simple orifice is not enough to allow the utilization of the extra cooling power that the system is capable of. What is needed is a device that has “inertance” in addition to the dissipation of the orifice. To use an electrical analogy, the “resistance” represented by the orifice needs to be replaced by a device with “inductance.” A device with the inertance needed turns out to be a long narrow tube; typically it would be 2-3 millimeters in diameter and several meters long.

Preliminary testing has been performed with such an inertance tube in place of the orifice, and the cooler performed considerably better than it did with the orifice; this shows that the analysis is on the right track. More improvement is expected as understanding of the operation of the inertance tube is gained and its parameters are optimized.

Point of Contact: P. Kittel
(650) 604-4297
pkittel@mail.arc.nasa.gov

Automated Space System Experimental Testbed Project

Christopher Kitts

The Automated Space System Experimental Testbed (ASSET) project is an Internet-based, justified-operations control system for small satellites. The project’s objective was to establish a global spacecraft control network in order to (1) provide operational support for a variety of low-cost missions, and (2) provide a high-risk, low-inertia testbed for validating spacecraft autonomy strategies.

The operational system provides an automated link between a variety of users (including principal investigators, students, operators, and the public) and a multitude of spacecraft payloads. The ASSET system is capable of accepting goal-level experimental parameters and planning and scheduling system and spacecraft activities, and of conducting mission and health-related tracking, telemetry, commanding operations with the spacecraft, and delivering the experimental data to the original experimenter. To do this, the ASSET system components include a central mission control center, geographically distributed ground stations, a variety of spacecraft, Internet and HAM radio communications links, and numerous payload components.

ASSET provided an unparalleled opportunity for rapid experimentation with revolutionary autonomy technologies in a real-world, complex space system. The initial ASSET implementation is supporting the

New Millennium Program Autonomy Technical Integration Experiments concerning data distribution, principal investigator interfacing, beacon operations, ground system automation, and fault management.

Point of Contact: C. Kitts
(650) 604-0149
kitts@ptolemy.arc.nasa.gov

Amphion and Meta-Amphion

Michael Lowry

Most of today’s programming problems involve a programmer building special domain-oriented software libraries (modules that perform a specific function) for every domain. Then users must make software program calls to these modules in order to get the work done. The correctness of these programs is difficult to prove. Amphion automates the use of these software libraries. It enables a user to state a problem in an abstract, graphical visual programming notation, rather than requiring the user to construct a solution by manually composing software components. Amphion then automatically generates a program consisting of calls to the library components to solve a specific problem. Moreover, as part of this generation process, which is done through automatic theorem-proving, Amphion produces a mathematical proof that the program is correct. Formal mathematical methods are

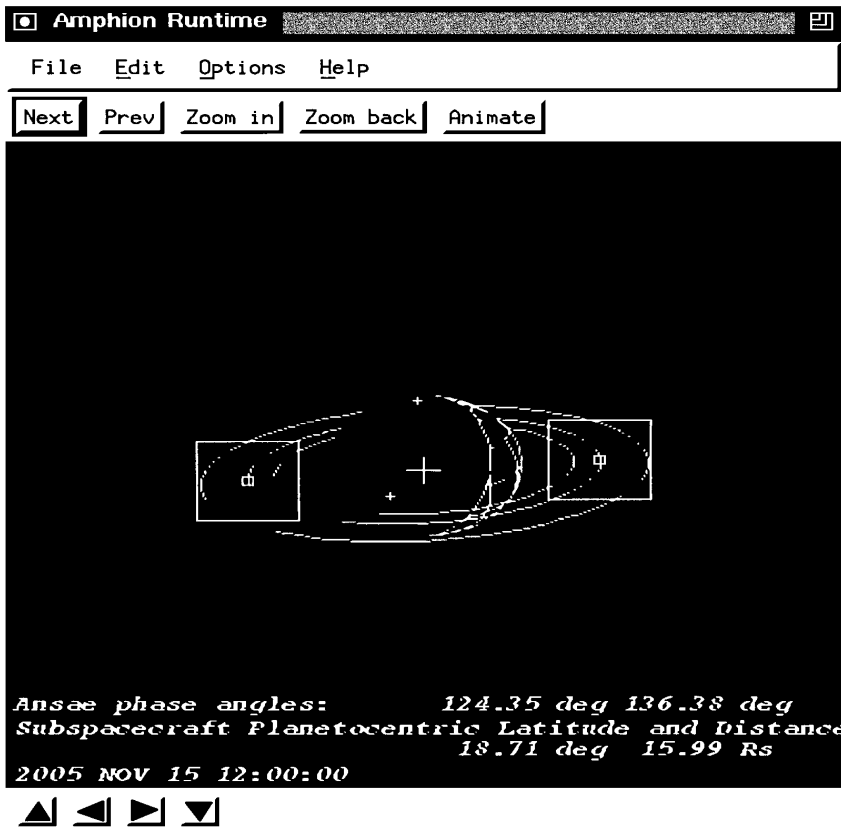


Fig. 1. Amphion-generated science-opportunity visualizer for the Cassini Mission.

applied for program verification. If performed manually, this formal proof is costly and only becomes cost-effective for safety-critical systems.

Meta-Amphion is a system that will enable software-library developers to create and maintain their own specialized Amphion systems. In essence, Meta-Amphion is the next-generation application-generator technology. Using Amphion, it takes on average an order of magnitude less time for a user to develop a domain-oriented problem specification than to manually generate and debug a program. Equally important, a user does not need to learn the

details of the components in a software library. This removes a significant barrier to the use of NASA's software libraries. The figure shows a snapshot of a science-opportunity visualizer for the Cassini Mission. The code for the visualizer was generated automatically by Amphion.

The benefit of Meta-Amphion is to enable the widespread development of specialized Amphion systems, thus realizing the dual benefits of automated formal methods and domain-specific automatic programming. Meta-Amphion is the set of tools and infrastructure needed to elevate programming from the

code level to the declarative, specification level. The generic Amphion system is nearly mature, having gone through an extensive alpha/beta version that has already been tested by customers.

Point of Contact: M. Lowry
 (650) 604-3369
 lowry@ptolemy.arc.nasa.gov

Focal-Plane Sensor Array Development for Astronomy in Space

Mark E. McKelvey,
 Robert E. McMurray, Jr.,
 Craig R. McCreight

A team at Ames Research Center is evaluating the suitability of a number of detector and readout-device technologies for space-infrared astronomy applications. This program aims to foster development of focal plane array (FPA) detector technology that will allow reliable background-limited infrared (IR) astronomy from space-based platforms such as the Space Infrared Telescope Facility (SIRTF). Advances in microelectronics to provide operation of low-noise, low-power devices in the radiation environment found in Earth orbit are keys to the success of this program.

Evaluations of state-of-the-art Impurity Band Conduction (IBC) focal plane detector arrays produced by several manufacturers are continuing for applications in the 5–30-micron wavelength range. These detectors rely on a thin, highly doped IR-active layer to provide

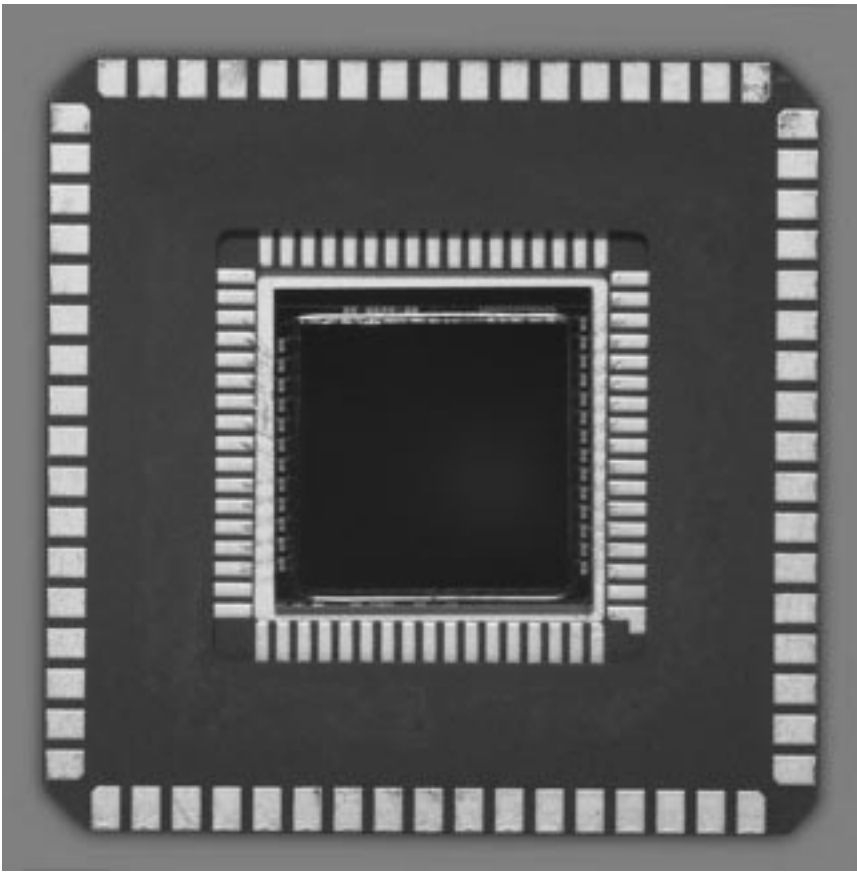


Fig. 1. 256×256 element infrared detector array.

high quantum efficiency from a small detector volume, minimizing the ionization cross section for cosmic ray events. A high-purity blocking layer prevents excessive dark current, despite the high doping levels in the IR-active layer. IBC arrays also exhibit wider spectral response than alternative photoconductor (PC) architectures, without many of the performance anomalies associated with PC devices. IBC architectures are well suited to modern epitaxial fabrication methods, and the technology has progressed to the point where large-format hybrid FPAs that are

sensitive to IR wavelengths as long as 28 microns can be reliably produced.

Work in FY96 was concentrated on evaluating the performance of large-format (to 256×256 detector elements; see figure) state-of-the-art IBC detector arrays in simulated on-orbit radiation environments, using the 76-inch Crocker Cyclotron on the campus of the University of California at Davis to provide a high-energy proton beam for device testing. These tests, in collaboration with astronomers from Cornell University and from the University of Arizona, have shown a marked

difference in radiation-damage susceptibility between similar arrays from different manufacturers. This damage is manifested as dose-dependent activation of dark current that could be of crucial importance to the Wide-Field Infrared Explorer (WIRE) or SIRTf science missions. The results of the Ames tests are being fed directly back into the manufacturing process in order to help advance the state of the art.

Improved IBC devices from a joint Ames/Santa Barbara Research Center development are presently being evaluated. These 256×256 arrays utilize a simplified unit cell architecture and new sampling techniques to achieve read noise levels as low as 12 equivalent electrons. These devices are prototypes for the flight detectors to be used on the SIRTf Infrared Array Camera (IRAC). The Ames group will continue to play an important role in the definition and execution of the IRAC detector acceptance and qualification test program.

Other recent efforts involve hardware and software upgrades to the suite of test instrumentation maintained in the detector laboratory. Recent upgrades have allowed easier manipulation of the data files collected from these large-format detector arrays. A project is presently under way to enhance the capability of the data acquisition system to handle arrays as large as 1024×1024 elements. Continuous software development has provided improved test flexibility, automation, and repeatability. Work on maturing IBC technology and improved readouts, along with other sensor technologies

in ongoing efforts, will enhance overall IR focal-plane performance in NASA space- and ground-based applications.

Point of Contact: M. McKelvey
(650) 604-6643
mmckelvey@mail.arc.nasa.gov

Intelligent Execution for Autonomous Spacecraft

Barney Pell

An executive system is an event-driven and goal-oriented agent that coordinates run-time activity among a set of components involved in a control system. As such, it provides a language and a framework in which software designers can express how planning, control, diagnosis, and reconfiguration capabilities are to be integrated into an autonomous system. It can request and execute plans involving concurrent activities among subsystems, in the presence of uncertainty in the success, timing, or outcomes of activities. A smart executive provides a language for expressing goal-decompositions and resource interactions. When interpreting this language at run-time, the executive automates the decomposition of goals into smaller activities which can be executed concurrently, thus automating aspects of the labor-intensive sequencing function in spacecraft operations.

This task investigates the development of increasingly intelligent execution systems, their role in autonomous control systems, and their practical application as an enabling technology for autonomous

space missions. We are currently grounding the research by developing the smart executive, part of the Remote Agent (RA) being developed for the Deep Space One (DS1) mission, part of NASA's New Millennium Program (NMP). DS1 will autonomously navigate to asteroids and comets and will be able to achieve its mission in the face of a wide variety of faults, including total loss of control from Earth.

As an integrating technology, an executive enables each software component to be expressed independently, but it controls the interactions among those components so that the overall activity of the system achieves global constraints as dictated by a high-level plan. This dramatic increase in modular software design reduces development and integration costs and increases software reuse both within and across missions. The goal-directed task-decomposition automates much of the labor-intensive sequencing process in spacecraft operations. This capability also enables a new generation of adaptive controllers, in which different control modes are developed that are switched by a smart executive based on feedback from the environment.

The DS1 mission will validate the smart executive and the entire RA in the context of actual space flight. The architecture will serve as the baseline for the next generation of space missions, and will be deployed to a wide variety of manned and unmanned spacecraft; it will also increase the level of autonomy in other control systems, such as aircraft and factories.

FY96 accomplishments include completion of the rapid prototyping effort in November 1995, demonstration of the prototype, and presentation of the smart executive to the NMP in the December 1995 Technology Readiness Review, which accepted the RA architecture to be developed for the DS1 mission.

Point of Contact: B. Pell
(650) 604-3361
pell@ptolemy.arc.nasa.gov

New Millennium Program Deep Space 1 Flight Software Program Management

Scott Sawyer

The New Millennium Program's Deep Space One (NMP DS1) Flight Software team comprises staff from Ames and the Jet Propulsion Laboratory (JPL) (which also includes individuals from the Air Force Phillips Laboratory, TRW, Carnegie-Mellon University, and Thinkbank, Inc.). The team is developing flight software (FSW) for the first mission of the New Millennium Program (NMP). The Ames team (along with part of the JPL team) is dedicated to developing and testing the "Remote Agent" architecture of the FSW. The remote agent (RA) integrates rule- and model-based fault detection, isolation, and recovery; advanced planning and sequence management capabilities; and a system executive that serves as an autonomous agent controlling and coordinating the satellite's behaviors during normal

and abnormal operations. The RA is capable of responding autonomously to system and payload faults and malfunctions, establishing contact with ground operations personnel when necessary, and replanning portions of the mission onboard to accommodate unanticipated changes in spacecraft performance or objectives. The DS1 mission will be the first ever to fly an onboard autonomous agent flight system.

Program management objectives are (1) managing Ames and JPL team personnel; (2) defining development schedules, descope options, and contingency plans when necessary; (3) preparing and presenting status reviews and briefings to program management, Center management, and review boards; (4) making budget and workforce projections; and (5) acquiring the necessary resources to allow the team to accomplish its goals. Technical objectives include flight/ground interface design, RA design oversight, and the performance of engineering duties related to autonomous systems such as defining command and telemetry system requirements, fault protection system policies, and FSW validation policies.

Successful development of an RA FSW architecture for NMP DS1 will identify new avenues of research which will guide the growth and development of the next generation of “thinking” spacecraft. The RA architecture will be expanded to be used in a wide variety of manned and unmanned vehicles. By carefully selecting applications projects to accompany

the research, Ames can effectively focus the research efforts on practical problems at the cutting edge of technology.

Point of Contact: K. Swanson
(650) 604-6016
kswanson@mail.arc.nasa.gov

Human Exploration and Development of Space Enterprise



Overview

NASA's Human Exploration and Development of Space (HEDS) enterprise brings the frontier of space fully within the sphere of human activity. Ames supports the HEDS enterprise by conducting research, managing spaceflight projects, and developing advanced technologies. An objective of these efforts is to seek knowledge of physicochemical and biological phenomena that can be fully explored only at very low gravity levels. This objective embraces the quest for knowledge of the role and influence of gravity in living systems—one of the elements of NASA's astrobiology activities. A second objective is to develop technologies for advancing human exploration of space and achieving routine space travel. A complementary objective is to apply knowledge generated in pursuit of these objectives, where feasible, to enrich life on Earth. During FY96, numerous research and technology efforts that addressed the following goals of the HEDS enterprise were accomplished:

- Increase knowledge of nature's processes using the space environment.
- Advance human exploration of the solar system.
- Achieve routine space travel.
- Enrich life on Earth through educational, commercial, and technological opportunities in space.

New knowledge and an increase in the understanding of nature's processes related to the influence of gravity on living systems are

acquired by a two-pronged approach: (1) Research is conducted on the ground and in space over a range of gravitational levels and with a variety of biological specimens; and (2) specialized equipment and advanced technologies are developed to support life-sciences research on the ground and in space. The knowledge thus acquired is then integrated and disseminated by using information technology.

In this report, new life-sciences research findings are presented; for example, new biochemical assays of bone collagen degradation, which are useful tools for monitoring bone mineral loss (a major biomedical problem of long-duration human spaceflight). Other research shows that both cerebral blood flow velocity and cerebral oxygenation decrease prior to fainting. This finding improves our understanding of the typical orthostatic intolerance and fainting observed in many astronauts following spaceflight. Additional work has focused on understanding the process of dual adaptation (or separate adaptations to two mutually conflicting sensory inputs) as it applies to the altered gravity environment. These studies should provide greater insight into the processing of altered gravitational inputs directly relevant to an astronaut's ability to function well in space.

Technological advances described in this report have numerous applications in the medical and biomedical fields. The Virtual Environment Surgery Workbench, in combination with software originally developed for an Ames spaceflight experiment with rodents, has

attracted much interest from reconstructive surgeons, and this tool is expected to decrease the training time of a skilled craniofacial reconstructive surgeon from 20 to 10 years. In addition, this technology may soon offer doctors in the emergency room real-time, high-fidelity, three-dimensional information so that accurate diagnoses and potential reconstructive alternatives can be quickly determined.

Neural net software development has resulted in another medical technology aimed at increasing the capability of neurosurgeons. The software enables a robotic probe to “learn” a patient’s brain characteristics, making it easier for a surgeon to locate the exact position of a tumor after surgery is under way and the normal swelling of brain tissue complicates the process.

In the ongoing effort to develop methods to monitor vital blood constituents, a prototype system that has application to astronaut health, space life sciences, and Earth-based medicine has been created. Concentrations of ions in flowing blood plasma can now be measured by a computer-controlled data-acquisition system known as the Blood Flow Ion Analyzer. Liver-function support systems are direct beneficiaries of this technology, as there is a specific need to continuously monitor and control ion concentrations of processed blood plasma.

A spinal compression harness designed as a potential aid to astronauts in combating back pain during spaceflight is also of interest to orthopedic therapists. The harness allows doctors to perform magnetic resonance imaging while positioning

the patient in the characteristic supine position but with loads added to the spinal column simulating those that occur naturally in the upright posture. Such imaging capability will provide a greater range of diagnostic data for doctors who treat the millions of people who suffer back pain.

Another recent Ames project involving telemedicine, Spacebridge to Russia, linked three U.S. hospitals and a university with two medical centers in Moscow via the Internet. Ames is responsible for developing the technical architecture as well as providing direction in setting up the Internet connections and the motion video consultation and video teleconferencing features. These capabilities have already enabled telemedicine consultations among all test users, and plans are under way to utilize the system as an educational tool for hospitals.

As part of the HEDS goal to explore the solar system, Ames has actively pursued life-support methodologies relating to atmosphere regeneration, water purification, recycling from waste materials, and food production. The work has given birth to new concepts of reducing spacecraft power and weight requirements.

Research in the unique environment of space requires specialized equipment to operate within microgravity and assure that the research conducted does not pose a health or safety risk to the human crews. One such piece of equipment developed during the past year is the standard interface glovebox, which is now flying aboard the Mir station. This device was designed to provide an enclosed workspace that contains

particulates, odors, and the kinds of chemicals and biological specimens required by life scientists.

To help astronauts achieve maximum productivity during the particularly crucial first days of flight, researchers at Ames have been working on ways to reduce the space adaptation syndrome. Autogenic-Feedback Training (AFT) seems to be effective in controlling motion sickness under a variety of conditions, including spaceflight. The AFT exercise technique can also be used to control blood pressure and thus ameliorate postflight orthostatic intolerance.

Lower-body negative pressure equipment specifically developed as a potential countermeasure for the debilitating effects of long-term human spaceflight has been modified to provide a variety of loading levels on the lower body. In combination with a treadmill, the equipment has applications both as a countermeasure to the atrophy of the musculoskeletal system during spaceflight and as a rehabilitative tool for treating patients suffering spinal trauma on the Earth.

The use of a device that combines resistive exercise with aerobic training is described. Presently, cardiovascular exercise is emphasized during Space Shuttle missions; however, research with the “SX-1 Variable Resistance Exercise Device” suggests that astronauts may be able to maintain muscle size and strength while also maintaining bone density during spaceflight.

It is vitally important that the results of HEDS research be quickly disseminated to the public, that is, the commercial sector and the

educational and scientific communities. To this end, life-sciences spaceflight data are being published in the scientific and popular literature and archived in the National Space Science Data Center at the Goddard Space Center. Ames is also actively engaging teachers and students to promote science education of our nation's youth.

Biochemical Markers of Bone Metabolism in a Rat Spaceflight Model

Meena Navidi, Jeanne Wren,
Sara Arnaud

Newer biochemical assays of bone collagen degradation products in urine are useful tools for monitoring bone loss (a major concern of spaceflight) and the effects of countermeasures to prevent bone loss in human adults. The results reflect the collective metabolic activities of bone resorption in the entire skeleton, a process that is activated by exposure to a head-down tilt, bed-rest spaceflight model. These techniques have yet to be applied to small-animal models of weightlessness. Through histologic methods, the decrease in new bone formation in the rat tibia during spaceflight is well documented. Recently, increases in osteoclast number and resorption were observed in highly localized areas in the proximal tibia. Ground-based models of juveniles of the same species show morphologic changes consistent with reduced bone formation in unloaded hind limbs with no evidence for increased resorption. The mature rat, exposed to the same ground-based model with unloaded hind limbs for 28 days, reveals less bone mineral content in the femur, compared with ambulatory controls. This apparent bone loss is thought to be caused by increased resorption as well as

depressed formation, but no histologic or biochemical measurements support this idea.

To evaluate bone resorption, an assay that measures deoxypyridinoline (Dpd), a product of the breakdown of collagen crosslinks in bone was used. This assay is currently regarded as one of the most specific and sensitive markers of bone resorption. The 24-hour excretion of Dpd in two-month-old juveniles was more than seven times

higher than in six-month-old mature animals (see the figure). This age difference reflects growth rates that average 2-3 grams per day in juveniles and are stable and essentially zero in mature animals. Exposure to the spaceflight model for 14 days reduced Dpd excretion, whereas it remained unchanged in the control juveniles. In contrast, mature rats showed increases in Dpd excretion after 14 days exposure to unloading, as shown in the figure.

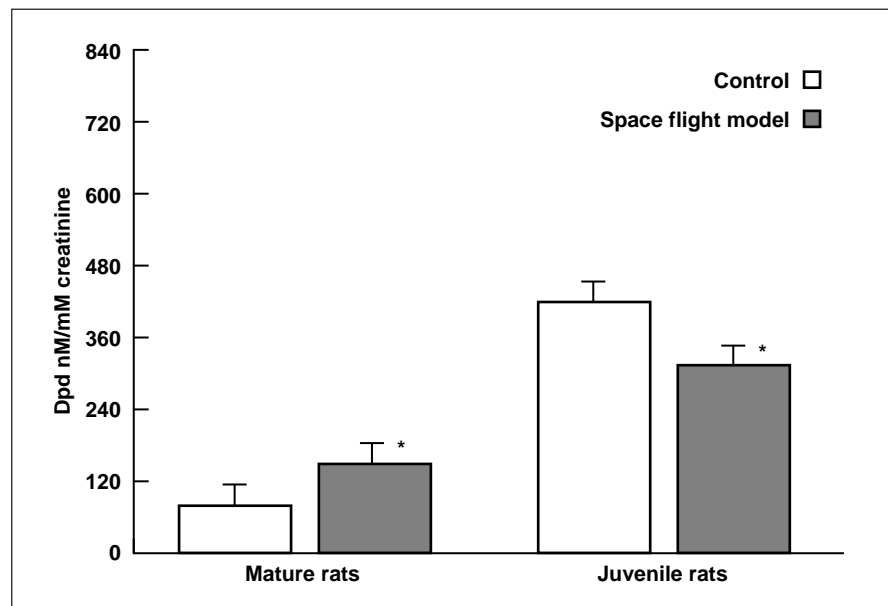


Fig. 1. The 24-hour excretion of deoxypyridinoline in the urine of juvenile and mature rats prior to and 14 days after exposure to a spaceflight model in which the hind limbs were unloaded. Note the higher excretions ($p < 0.05$) in the young animals than in the mature animals, and the opposite responses to the model at each age.

These results illustrate the marked, age-dependent differences in the response of the skeleton to a weightless environment. Results in the mature animals, who at six months of age have acquired 96% of the bone they will have in their lifetimes, are similar to the increases observed in human adults. There is an increase in bone resorption after unloading the skeleton, a situation favorable to bone loss unless accompanied by an increase in bone formation. Alkaline phosphatase, a circulating marker of bone formation, was unchanged in this study. The opposite result, suppression of high resorption rates in juveniles, could be related to depressed growth hormone or a growth factor during exposure to the model. While it is clear that the adaptation of the skeleton to microgravity requires site-specific changes in the rates of formation and resorption in weight-bearing bones (to modify bone structure for new loads), there also appears to be a systemic response reflected in bone marker assays that quantifies overall skeletal metabolism.

Point of Contact: M. Navidi
(650) 604-5755
mnavidi@mail.arc.nasa.gov

Cerebrovascular Responses Prior to Fainting

**Kana Kuriyama, Toshiaki Ueno,
Richard E. Ballard,
Donald E. Watenpugh,
Suzanne M. Fortney,
Alan R. Hargens**

Reduced orthostatic tolerance, commonly observed after spaceflight, occasionally causes fainting during standing. Prefainting conditions are usually manifested by symptoms such as a sudden drop of heart rate or blood pressure that is followed by loss of consciousness if standing is continued. Although the cerebrovascular system may play an important role in postflight fainting, there have been few reports concerning cerebral hemodynamics prior to fainting. This study was therefore undertaken to investigate cerebrovascular responses by measuring cerebral blood-flow velocity and cerebral tissue oxygenation prior to fainting, using lower-body negative pressure (LBNP) as an orthostatic stress.

Seven healthy male volunteers were exposed to supine LBNP in steps of 10 millimeters Mercury every 3 minutes until prefainting symptoms were detected. Blood pressure and heart rate were measured with an automatic finger-cuff device. Cerebral blood-flow velocity

within the middle cerebral artery was measured with transcranial Doppler sonography. Cerebral tissue oxygenation was monitored using near-infrared spectroscopy over the forehead.

During the initial stages of LBNP stress, when blood pressure decreases and heart rate is elevated, these cardiac responses are caused by blood pooling in the legs. But as LBNP continues, cardiac insufficiency occurs prior to fainting. This study focused on the 2-minute period prior to the fainting endpoint when LBNP was stopped. In a typical subject, blood pressure continued to decrease gradually as fainting was approached (see the figure). Heart rate decreased rapidly in the final 30 seconds, signifying cardiovascular insufficiency just prior to fainting.

The new finding of this study is that both cerebral blood-flow velocity and cerebral tissue oxygenation decrease prior to fainting. The decrease of cerebral blood-flow velocity can be explained as a decrease of cerebral blood flow or a dilatation of the middle cerebral artery. The decrease of cerebral tissue oxygenation can be explained as a decrease of cerebral blood flow or less likely, a decrease of cerebral tissue metabolism. Therefore, it is probable that cerebral blood flow decreases just prior to fainting.

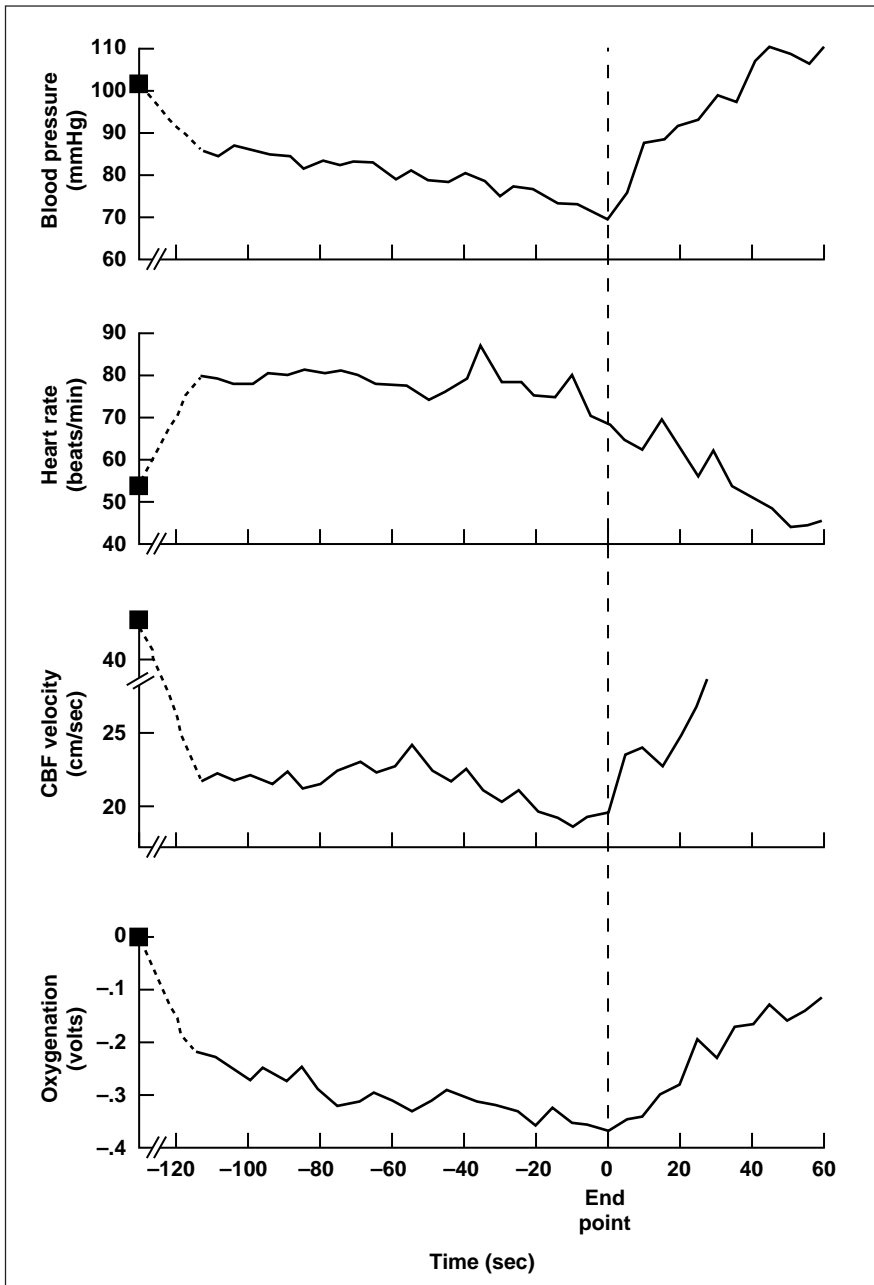


Fig. 1. Blood pressure, heart rate, cerebral blood-flow (CBF) velocity, and cerebral oxygenation with emphasis on the final 2 minutes prior to lower-body negative pressure (LBNP)-induced fainting. Baseline values of each measurement (n) represent supine data obtained just before starting LBNP protocol.

In conclusion, during LBNP-induced fainting, cardiac insufficiency primarily occurs, resulting in the failure of cerebrovascular circulation. This study improves the understanding of postflight fainting in astronauts and may aid in the development of preventive methods.

Point of Contact: A. Hargens
 (650) 604-5746
 ahargens@mail.arc.nasa.gov

Chronic Exposure to Hyper-G Suppresses Otolith-Spinal Reflex in the Rat

Nancy G. Daunton,
 Merylee Corcoran, Robert A. Fox,
 Li-Chun Wu

As part of an ongoing effort to understand the neural mechanisms underlying adaptation to altered gravity, behaviors reflecting the function of gravity receptors (otolith organs) in the inner ear (for example, air-righting reflex, orientation) of the rat have been studied following chronic hyper-gravity (hyper-G) exposure and found to be considerably altered. In addition to the behavioral data, morphological studies conducted by Ross in conjunction with the behavioral studies have shown that there is a reduction in numbers of synapses on otolithic hair cells in the utricular maculae of animals exposed to the same chronic hyper-G conditions. These behavioral and morphological findings suggest that the sensitivity or gain in the otolithic system may be

decreased following chronic hyper-G exposure.

One way to evaluate the gain or sensitivity in the otolithic system is to use the “free-fall” response, which is an otolith-spinal reflex elicited by a sudden brief vertical-linear acceleration or drop. Using electromyographic (EMG) techniques, this response has been demonstrated in a number of muscles in animals and humans. The earliest component of this response is dependent on intact otolith organs and does not habituate over trials.

The otolith-spinal reflex response to sudden free-fall was used to monitor sensitivity or gain in the otolithic system following chronic exposures to hyper-G. The investigators hypothesized that the amplitude of the early EMG response would be lower in animals exposed to hyper-G than in animals experiencing only the normal 1-G environment.

A free-fall apparatus was developed that allows the animal, in a prone position, to be dropped suddenly over a 40-centimeter distance and then gently stopped by pairs of “soft springs.” This device provides a sudden, vertical-linear-accelerative, free-fall stimulus to the animal being tested. Animals were instrumented with EMG electrodes in the gastrocnemius muscle of the hindlimb. The EMG response, along with acceleration of the animal, was recorded during 10 drops for each animal. The animals were tested within 3.5 to 9 hours following chronic (7 to 14 days) exposures to hyper-G produced by centrifugation on the Ames Research Center 24 Foot-Diameter Centrifuge.

Analysis of the data showed that in animals exposed to hyper-G, the majority of responses (61%) to the free-fall stimuli were of very low amplitude (suggesting low sensitivity or gain), while normal, control animals had very few (13%) low-amplitude responses (see the figure). Furthermore, a significantly higher percentage of responses were low amplitude in animals exposed to 2.8 G than in those exposed to 2.0 G. This suggests greater loss of sensitivity or gain with centrifugation at higher G levels. In all cases animals exposed only to the rotational component of centrifugation had response amplitudes similar to those seen in normal control animals that were not exposed to centrifugation.

The results of this study suggest that chronic exposure to increased gravitational conditions leads to a decrease in the sensitivity or gain of the gravity-sensing (otolith organ) portion of the vestibular system. Furthermore, a greater degree of suppression is produced by exposures to higher G levels. This decreased sensitivity may underlie the deficits in otolith-mediated behaviors seen following chronic hyper-G exposure and may be related to the reduced numbers of synapses found in otolith organs under the same conditions. The critical next question is whether the free-fall response will be increased following chronic exposure to microgravity. If that is the case,

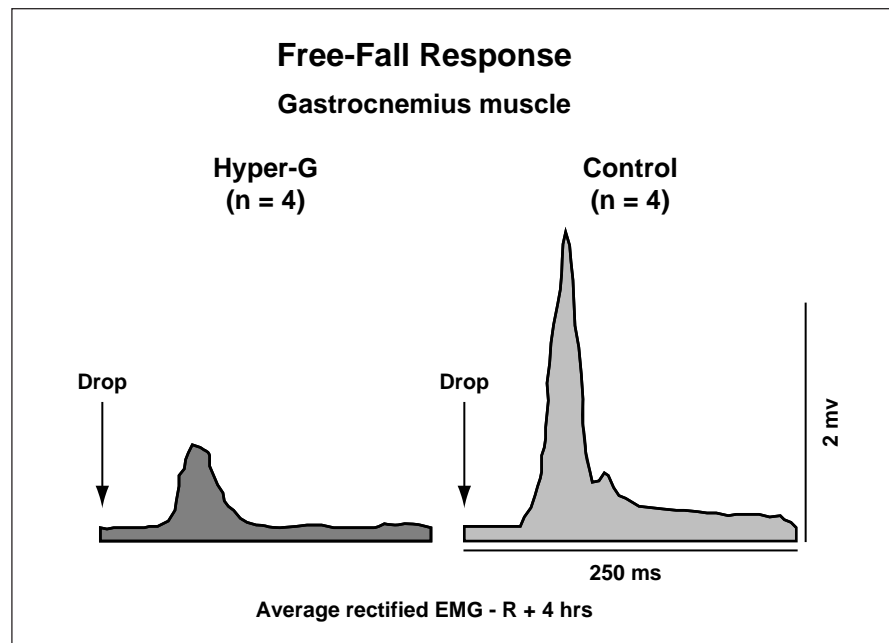


Fig. 1. Average rectified electromyographic (EMG) response from four animals exposed to 2 G for 7 to 12 days and from four control animals, showing reduced amplitude of average response in hyper-G animals as compared with control animals.

important evidence will be obtained on how the otolith organ system is modified to subserve optimal vestibulo-spinal function (orientation, postural control, locomotion) in altered gravitational environments.

Point of Contact: N. Daunton
(650) 604-4818
ndaunton@mail.arc.nasa.gov

“Dual Adaptation” to Space-Related Sensory Rearrangements

Robert B. Welch

A series of studies is examining the process of “dual adaptation” in a variety of atypical sensory environments representative of those likely to be experienced by astronauts. The term “dual adaptation” refers to the acquisition of separate, relatively independent adaptations to two (and perhaps more) mutually conflicting sensory environments resulting from repeated alternation between exposure and adaptation to one of the sensory environments and exposure and adaptation to the other environment. Evidence of dual adaptation is seen in a progressive decline in (1) the perceptual and/or behavioral interference that occurs at the initial transition between the two sensory conditions, (2) the amount of exposure necessary to produce asymptotic adaptation, and/or (3) the amount of adaptation acquired after a given amount of exposure. During FY96, three investigations of dual adaptation were completed.

The first investigation, conducted by R. B. Post (University of California, Davis) and R. B. Welch (NASA Ames Research Center), measured perceived movement of a stationary visual stimulus during head movements, known as “apparent concomitant motion” (ACM). ACM was measured both before and after exposure periods in which subjects performed voluntary head oscillations while viewing a spot that moved in conjunction with the head. During these intervals, subjects looked at the spot as it moved alternately in the same direction as the head was moving during either 0.25 or 2.0 hertz head oscillations, and then in the opposite direction as the head at the other frequency. After a period of exposure, the visual stimulus came to be perceived as stationary only if it was caused to move in the same direction as that viewed during adaptation at the same frequency of head motion. Thus, these results confirmed the presence of dual adaptation of ACM in which the stimuli used to identify the prevailing sensory environment were those associated with head-movement frequency.

In the second investigation, conducted by R. B. Welch (NASA Ames Research Center), B. Bridgeman and J. A. Williams (University of California, Santa Cruz), and R. Semmler (University of Clausthal, Germany), two experiments examined the possibility that the human vestibulo-ocular reflex (VOR) is subject to dual adaptation, as well as “adaptive generalization,” which is the ability to adapt more readily to a novel sensory rearrangement as a result of prior dual-adaptation training. In Experiment

One, subjects actively turned the head during alternating exposure to (a) the visual-vestibular rearrangement (target/head gain = 0.5), and (b) the normal situation (target/head gain = 0.0). These conditions produced both adaptation and dual adaptation of the VOR, but no evidence of adaptive generalization when tested with a target/head gain of 1.0.

Experiment Two, in which exposure to the 0.5 gain entailed externally controlled (that is, passive) whole body rotation, resulted in VOR adaptation, but no dual adaptation. As in Experiment One, no evidence of adaptive generalization was found. It was concluded that it was the absence of a salient discriminative cue in the passive rotation experiment that prevented dual adaptation from occurring.

In the third investigation, conducted by R. B. Welch and N. Daunton (NASA Ames Research Center), R. Fox (San Jose State University), and M. Corcoran and L. Wu (NASA Ames Research Center), albino rats underwent four, 7-day periods of continuous 2-G exposure, by means of centrifugation, which alternated with four, 7-day periods of normal gravity (1 G). Before and after each 7-day period, subjects were measured on (a) their righting reflex when dropped suddenly from an initially supine position into a vat of water 40 centimeters below (“air righting”), and (b) swimming behavior after striking the water. Latency to the occurrence of air-righting was found to be subject to a form of dual adaptation. Specifically, animals that were repeatedly tested showed a significant improvement in mean

speed of air righting (+47%; $p = 0.008$), while control animals who received 2-G exposure, but were only tested on righting (and swimming) after the last of the 7-day exposure periods, showed only a marginally significant ($p = 0.12$) 25% improvement in mean air-righting speed.

Point of Contact: R. Welch
(650) 604-5749
rwelch@mail.arc.nasa.gov

TECHNOLOGY APPLICATIONS TO
HUMAN HEALTH

Virtual Environment Surgery Workbench

Muriel D. Ross

The research and development of a virtual environment (VE) surgery workbench was undertaken by the Biocomputation Center in FY96. This workbench will be used for training reconstructive surgeons and for patient-specific planning of complex craniofacial and other reconstructive surgeries. The virtual environment technology will be useful to the Human Exploration and Development of Space (HEDS) Enterprise for training astronauts for long-term missions in space. It will provide VE simulation capability during space-flight to help astronauts respond appropriately to unanticipated emergencies.

The Immersive WorkBench (Fakespace, Mountain View, CA), is used for displays (shown in the figure (see Color Plate 20 in the Appendix)). This workbench is large

and permits several individuals to see the visualization projected above the table top in three dimensions. Special glasses are required (see the figure). The images are greatly enlarged so that a novice can see details readily. The images can then be reduced in size to attain a more true-to-life size for further practice. This workbench will be used as interactive, VE tools are developed for training and planning purposes. Also, displayed images can be sent to remote sites over a network. The goal is to have interactive displays so that researchers and surgeons at remote sites can see identical three-dimensional (3-D) images and interact with them.

In the Biocomputation Center, unique software has been developed that permits detailed, 3-D reconstruction of the face and skull of patients from computerized tomography (CT) scans. The Visible Human Dataset provided by the National Institutes of Health was used to reconstruct the face and skull of a 57-year-old female. In the reconstruction of the face, even tiny wrinkles around the mouth can be seen, and deeper wrinkles and the texture of the skin are realistic. Because of the level of detail possible, a laser scan to record the face prior to surgery is no longer needed. The images are rendered with high fidelity.

The face and skull of an infant patient was generated from formatted CT scans in about 20 minutes using the newly developed software and a Silicon Graphics Onyx RE2 workstation. The infant had premature closure of a skull suture on the right and of part of the anterior fontanelle (commonly known as the

“soft spot”). The images of the skull clearly show the extent of fusion of the bones. Without surgical intervention, the right side of the head would not grow properly, the head and face would be deformed, and the brain would be compromised. Because of the high fidelity of the viewed images, surgeons have declared the software ready to use as a diagnostic tool. The goal is to have even more complex reconstructions completed within 15 minutes, or less, making it possible for doctors in emergency rooms to have a patient scanned and see the trauma in 3-D within minutes. In addition, work is beginning that will make it possible to port the software to less expensive workstations, promoting wider availability of the technology.

A necessary part of the software development is the ability to cut out, to remove, and to insert pieces of bone elsewhere, then to computationally restore the soft tissues so that the new face can be molded to the new skull for viewing prior to surgery. Software has been developed to do this using a model grid system. The software will be incorporated for use with an actual skull as the next step in software development. The software will be generally applicable, for example, in reconstructive surgery utilizing skin to recreate a breast in a mastectomy patient.

The value of the training aspects of the technology should not be underestimated. It takes as many as 20 years to train a highly skilled craniofacial reconstructive surgeon. If training in a simulator reduces this amount by half, 10 productive years will be added to a surgeon’s professional life. Furthermore, use of

simulator technology greatly reduces the cost of training. It is cheaper to practice on a computer than to participate in surgery on a patient and learn in this prolonged way. Also, new approaches to surgery can be quickly incorporated into a simulation to increase capability in new surgical techniques.

The VE technologies that are being developed will reduce medical costs, shorten the time necessary to train surgeons, and permit better preplanning of surgery. They also will improve the quality of life for the patient by producing a better outcome when surgery is first carried out. As these beneficial VE technologies are transferred to the public, NASA also benefits from these applications that are useful to the HEDS Enterprise and to long-term spaceflight.

Point of Contact: M. Ross
 (650) 604-4804
 mross@mail.arc.nasa.gov

Noninvasive Estimation of Pulsatile Intracranial Pressure Using Ultrasound

Toshiaki Ueno, Richard E. Ballard,
 John H. Cantrell, William T. Yost,
 Alan R. Hargens

Exposure to microgravity causes a blood shift toward the head that may elevate intracranial pressure (ICP). As widely observed in patients with brain tumors or hemorrhage, elevation of ICP may cause headache, nausea, or vomiting. These conditions strongly suggest that elevated ICP in microgravity may

cause or exacerbate similar symptoms during spaceflight. In addition, recent clinical reports suggest that elevated ICP impairs regulation of blood flow in the brain and normal

neural activity. Consequently, ICP is a critical parameter for understanding physiologic adaptation to microgravity. However, the magnitude and time course of altered ICP

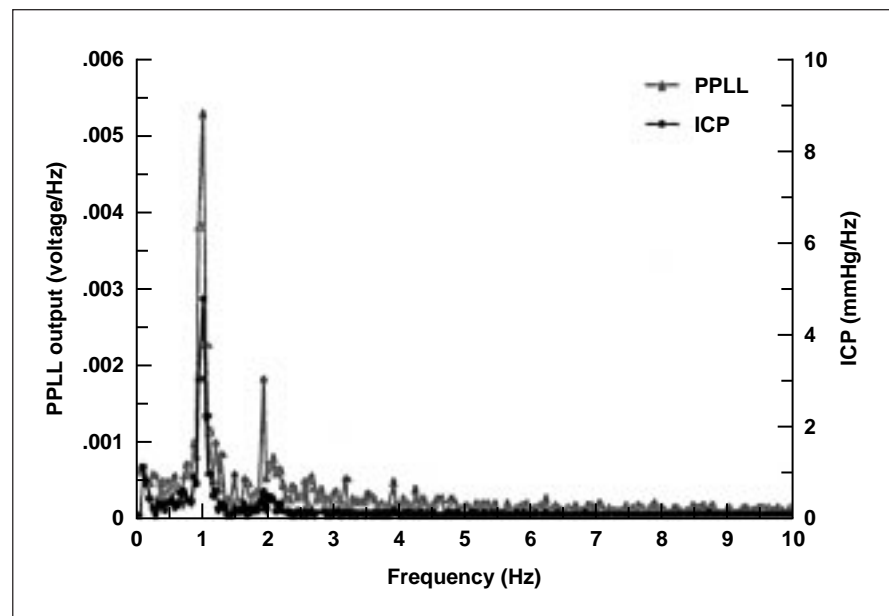
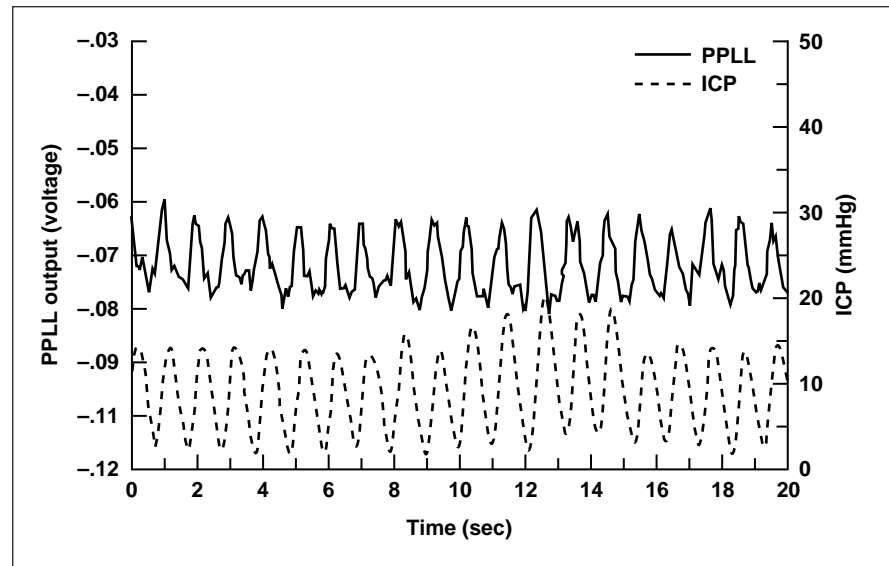


Fig. 1. Results of cadavera study. Typical waveforms in the pulse phase locked loop (PPLL) output and ICP are shown as a solid line and a dash line, respectively. ICP pulsations were generated manually by infusing saline into the ventricle at a rate of 1 cycle/second (1 hertz). The units of the PPLL output are voltages. The results of frequency analysis are superimposed.

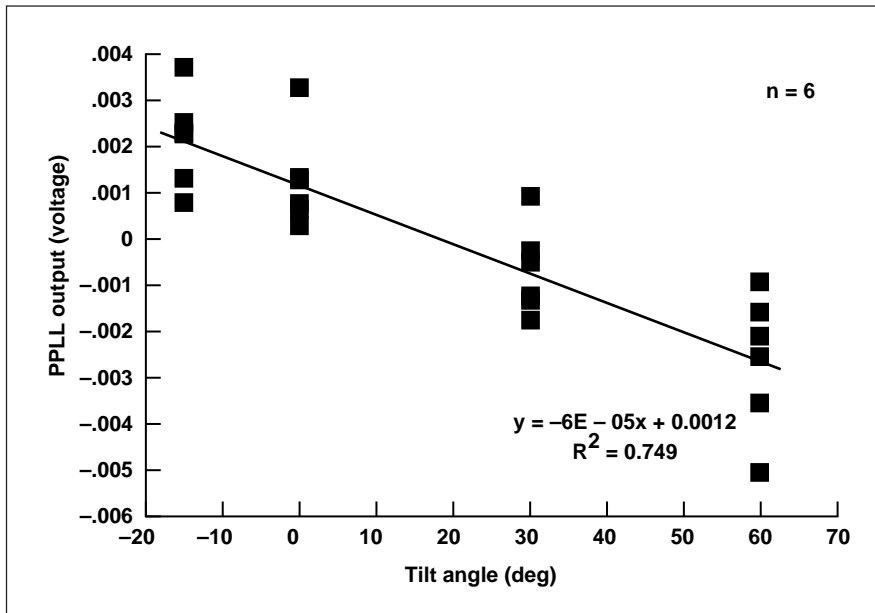


Fig. 2. Results of tilt study (n = 6). Amplitudes of pulsatile changes in the PPLL output are shown against the tilt angles. A linear regression line is superimposed.

are still unknown, primarily because of the invasiveness of currently available techniques.

A new ultrasound device to measure skull movements that occur with altered ICP has been developed and refined. The principle of this device is based upon pulse phase locked loop (PPLL), which enables the detection of changes in distance on the order of micrometers between an ultrasound transducer on one side of the skull and the opposite inner surface of the cranium. Although the skull is often assumed to be a rigid container with constant volume, many researchers have demonstrated that cranial bones move in association with changes in ICP. In the typical operation, the instrument transmits a 500 kilohertz ultrasonic tone burst through the cranium via a

transducer placed on the head. The ultrasonic wave passes through the cranial cavity, reflects off the inner surface of the opposite side of the skull, and is received by the same transducer.

In the first experiment, changes in cranial distance in three cadavera (ages 85–90) were measured with the ultrasound device, while pulsatile changes in ICP were generated by infusing saline into the lateral ventricle. To correlate the non-invasive measurement with ICP directly, a fiber-optic, transducer-tipped catheter was inserted into the intracranial space. In the second experiment, changes in cranial distance in six healthy volunteers (ages 18–31) were measured while they were placed in 60 degree, 30 degree head-up tilt, supine, and

10 degree head-down tilt positions. ICP was not measured directly. In both of the experiments, an ultrasound transducer was taped securely to the lateral head above the right ear.

In the cadaver study, frequency analysis (fast Fourier transformation) revealed that cranial pulsations were clearly associated with ICP pulsations (see the first figure). In the tilt study, the magnitudes of cranial pulsations were linearly correlated to tilt angles as shown in the second figure.

The ultrasound device has sufficient sensitivity to detect cranial pulsation associated with cardiac cycles. As previously reported, the amplitude of ICP pulsations is closely related to intracranial compliance. In other words, when intracranial fluid volume and pressure increase, arterial pulsation produces a higher amplitude ICP pulsation. Increased amplitude of ICP pulsations will be manifested by larger fluctuations in distance across the skull. Accordingly, by analyzing the magnitude of cranial pulsations, absolute estimates of ICP during spaceflight are possible.

Point of Contact: A. Hargens
(650) 604-5746
ahargens@mail.arc.nasa.gov

MRI-Compatible Spinal Compression Harness

Richard E. Ballard,
Donald E. Watenpaugh,
Iwane Mitsui, Klaus P. Fechner,
Douglas S. Schwandt, Alan R. Hargens

Sixty to eighty percent of the population of the United States experiences back pain during their lives. While noninvasive imaging systems such as magnetic resonance imaging (MRI) and computed tomography scanners have been used as diagnostic tools for studying back pain and orthopaedic injury, these imaging devices require patients to lie down, thus eliminating any effect of axial loading on the body that occurs in upright posture. As a result, these imaging systems often provide diagnostic data of limited use, particularly to disorders related to loading and unloading of the spine.

The MRI-Compatible Spinal Compression Harness (a patent recently filed by NASA Ames) is designed to produce gravity-like axial compressive loads on the body, thus increasing the effectiveness of existing diagnostic imaging systems for detecting spinal disorders. In addition, the spinal compression device will help researchers study the physiology and biomechanics of intervertebral discs and causative mechanisms of back pain in patients on Earth and astronauts in space.

The spinal compression apparatus is lightweight, compact, and inexpensive, and fits into existing diagnostic equipment without costly modifications (see first figure). In its present configuration, the device consists of a nonmetallic footplate

connected to shoulder pads, and alternatively to a head cap, by nylon webbing and elastic cords. Pulling the webbing through plastic buckles allows adjustment of cord tension, and thus compression level. The amount of compression is measured by nonmetallic force sensors that are currently being manufactured by a commercial partner. Alternative features of the device include a helmet-like headgear with adjustable elastic straps to provide neck compression, a saddle to distribute compression to the seat, and other attachments that allow static and dynamic compression of specific body segments or joints. A space-related benefit of the device includes the potential to compress the spine

and alleviate back pain in astronauts during spaceflight, when spinal length increases between 4 to 7 centimeters.

In a recent pilot study, four healthy male subjects (age: 33–52; weight: 72–113 kilograms) were fitted with the spinal compression harness and placed in supine posture within an MRI scanner. Each subject's spine was imaged without compression (control condition) and again at 25% and 50% body weight compression (the lumbar spine bears about 50% body weight in upright posture). Three of the subjects underwent an additional compression level of 75% body weight (see the second figure). Longitudinal distance between T7/T8 (thoracic

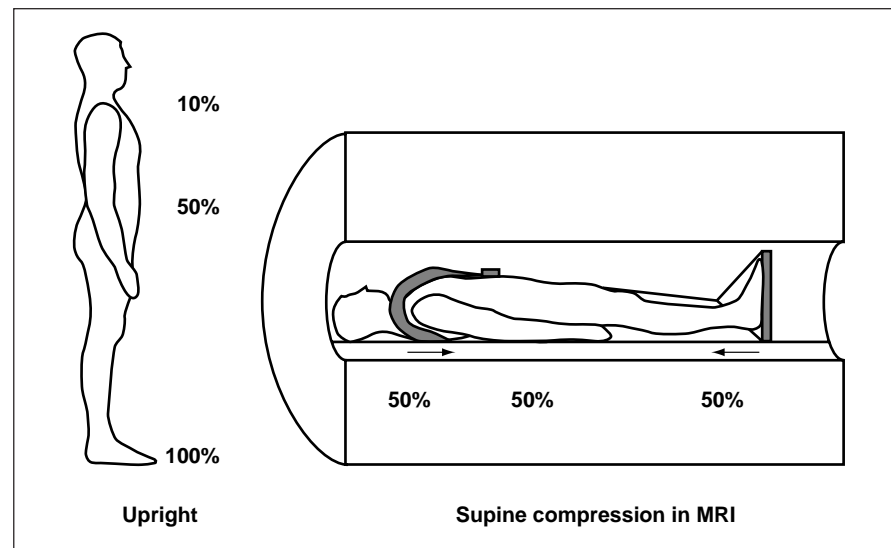


Fig. 1. Percentage of body weight locally supported during upright posture (left) and supine compression in MRI (right). In upright posture, a gradient of weight-bearing exists from the head to the feet, whereas the harness for MRI compresses tissues uniformly between the sites of compression. Thus, loads are adjusted to the specific tissue to be scanned under load (for example, the lumbar spine typically experiences 50% body weight in upright posture).

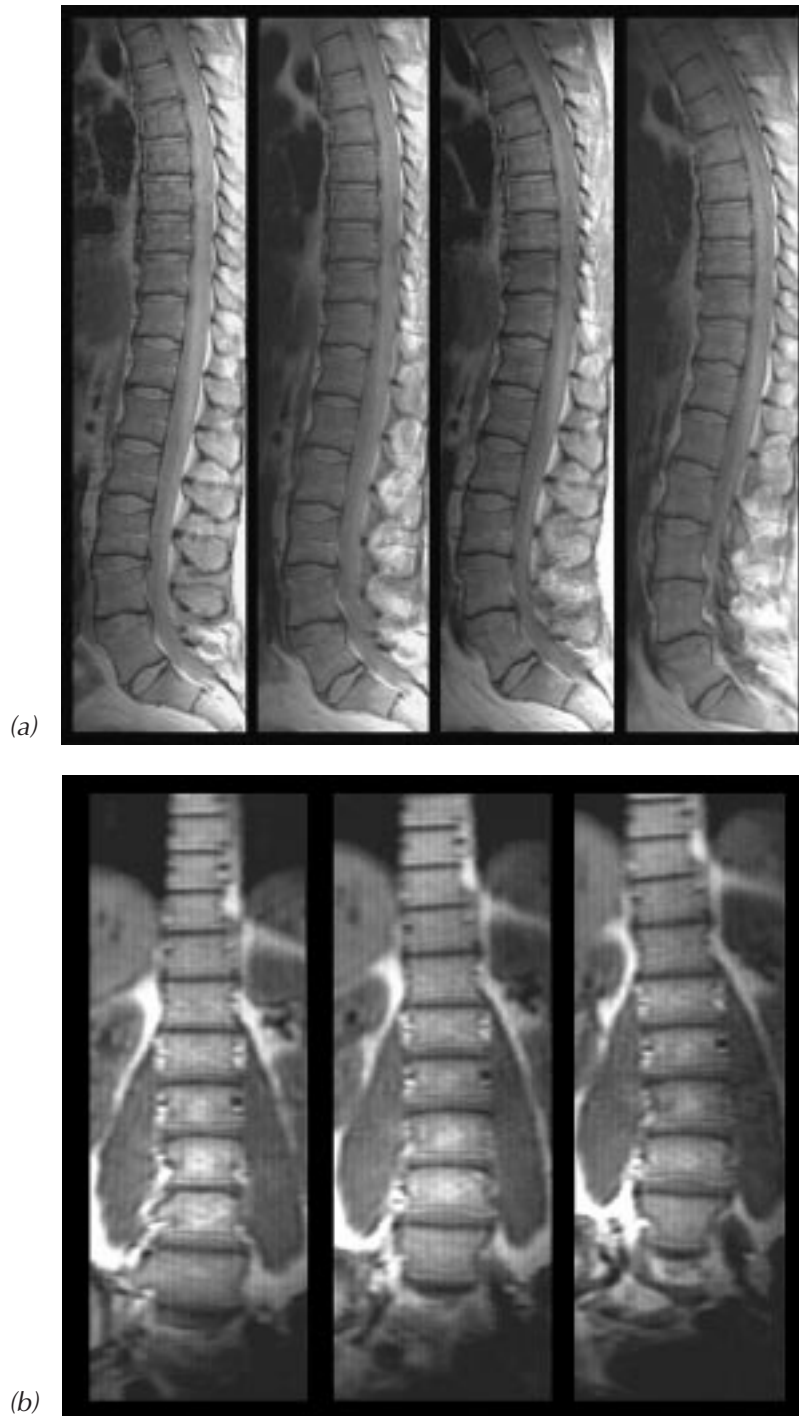


Fig. 2. Side view (a) and front view (b) of a spine during MRI with graded compression. Note the increase in curvature with increased load. This particular subject had a slightly bulging disc on the posterior side of L3-L4 (third visible disc from the bottom) which was accentuated by compression. BW = body weight.

level) and L5/S1 (lumbar/sacral level) discs decreased by 3.2 ± 0.8 millimeters (mean \pm SD) with 25% body weight compression, 5.6 ± 1.1 millimeters with 50% body weight compression, and 6.8 ± 1.2 millimeters with 75% body weight compression. The distance reduction was attributed to decreased disc thickness and increased spinal curvature.

While further development and validation of this technology are necessary, these results indicate that the spinal compression harness is capable of loading the spine effectively during supine MRI, and thus may be a valuable tool for studying effects of gravity-like loads on the spine. Previously this capability has not been available to researchers or clinicians.

Point of Contact: A. Hargens
(650) 604-5746
ahargens@mail.arc.nasa.gov

Near-Infrared Spectroscopy to Monitor Forearm Muscle Oxygenation

Gita Murthy, Alan R. Hargens

Muscle pain can be caused by repeated and constant exertion of a specific muscle. Such exertion may increase muscle pressure, reduce blood flow and muscle oxygenation, and cause muscle fatigue and pain. Low levels of prolonged muscle contraction of the forearm muscles are common in many work settings and may cause fatigue. Crew operations in the Life Sciences

Glovebox on the Space Station is one such work environment. The purpose of this study was to determine whether forearm muscle oxygenation decreases significantly at low levels of contraction. Nine male and female subjects participated in the study. Each subject was seated as shown in the first figure.

Muscle oxygenation was measured noninvasively using a near-infrared spectroscopy technique. The spectroscopy probe was

placed over the forearm muscle and gently secured with an ace wrap. Subjects were asked to contract their forearm muscle maximally three times. After 1 minute of data collection during relaxed posture, subjects contracted their forearm muscle once again for 1 minute, during four different load applications (randomly ordered). Loads were imposed by weights that were placed on the knuckles and allowed the subjects to work at 5, 10, 15, and 50% of

maximum voluntary contraction. At the end of the minute, the load was removed and a 3-minute recovery period followed. At the end of the protocol, with the spectroscopy probe still in place, subjects were required to exercise their forearms to exhaustion such that very little muscle oxygenation was recorded. This procedure is necessary to obtain a functional zero level for each subject. The data were normalized to a relative scale between the physiologic minimum (0%) established during the exhaustive exercise and the spectrophotometer output during relaxation (100%).

After 35 and 40 seconds of contraction, muscle oxygenation leveled off at below baseline levels and remained at that level throughout the 1-minute contraction period. Muscle oxygenation decreased from 100% during rest to $89 \pm 4\%$ (SE), $81 \pm 8\%$, $78 \pm 8\%$, and $47 \pm 8\%$ at 5, 10, 15, and 50% maximal forearm contraction, respectively (see the second figure). Muscle oxygenation decreased significantly at 10, 15, and 50% of maximal contraction compared to resting values.

This study shows a significant reduction in muscle oxygenation even at levels as low as 10% maximal contraction. Muscle deoxygenation during muscle contraction may play an important role in the development of muscle fatigue and pain associated with repetitive tasks, especially in confined environments such as in a glovebox. There are no simple, easy to use instruments that can noninvasively measure muscle oxygenation in deep and superficial

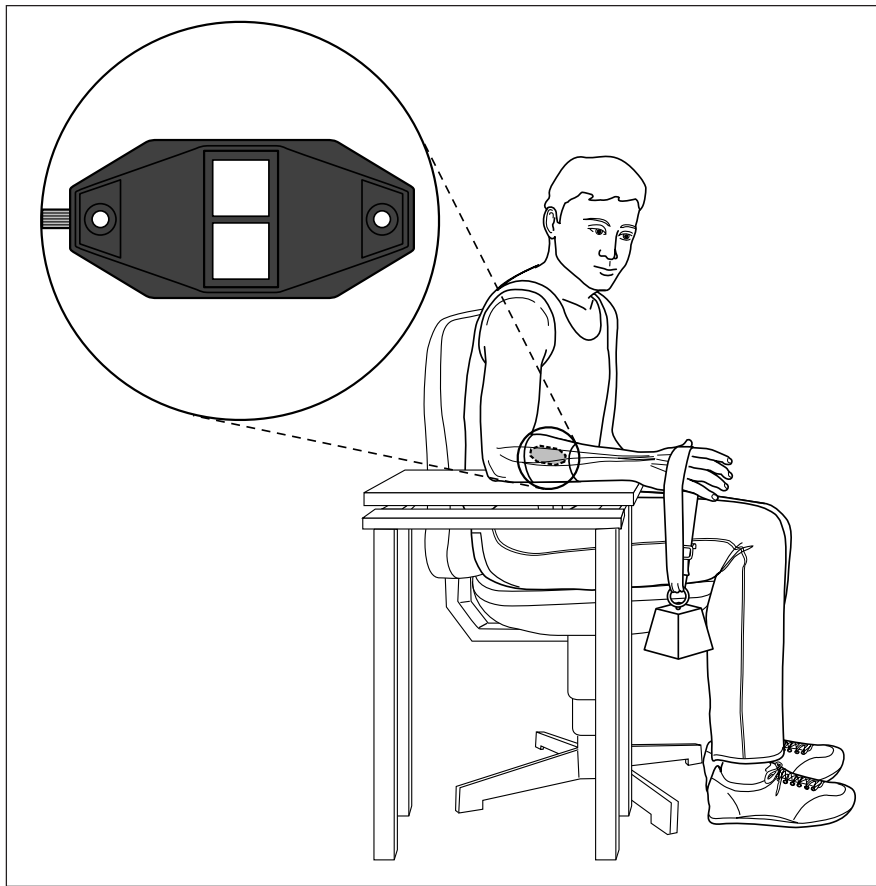


Fig. 1. Subject posture during the study. The inset shows the spectroscopy probe that measures muscle oxygenation.

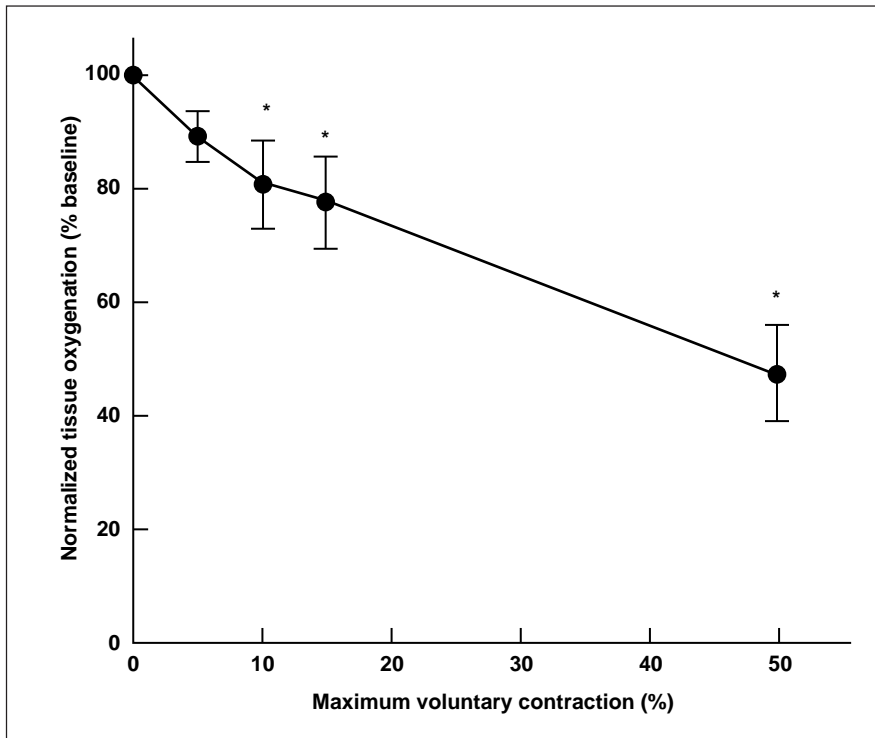


Fig. 2. Muscle oxygenation decreases with increasing load on the forearm muscle.

working muscles. Thus, the spectroscopy device may provide an important tool to study muscle fatigue and pain and to improve the designs of workstations in space.

Point of Contact: A. Hargens
(650) 604-5746
ahargens@mail.arc.nasa.gov

BIONA 1—Blood Flow Ion Analyzer

John W. Hines, Christopher J. Soms

Liver support systems will benefit from continuous monitoring and control of the ion concentrations of processed blood plasma. To measure the concentrations of ions in flowing blood plasma, a prototype, computer-controlled data acquisition system, the “Blood Flow Ion Analyzer” (BIONA 1), has been designed. BIONA 1 monitors plasma ion concentrations, displays them as a function of time, and saves the data to a file for later analysis. The sensors are miniaturized, catheter-type, ion-selective electrodes that

have membranes selective to only one ionic species. Since the porcine liver cells decrease the plasma calcium over time, requiring the addition of Ca^{2+} -enriched buffers, the initial ion of interest is Ca^{2+} . Monitoring the pH and temperature of the blood plasma is also desired and can be implemented with future prototypes.

To measure concentrations with ion-selective electrodes, a reference electrode that provides a concentration independent potential is needed. The potential of the ion-selective electrode (indicator electrode) depends on the concentration of the ion for which it is selective. The difference between reference and indicator potential can then be related to the ion concentration; a process called calibration. Ion-selective electrodes need to be calibrated before the first use and recalibrated after certain periods of time to minimize the amount of error generated by drift and changes in sensitivity (potential change per decade change of concentration).

The BIONA 1 system prototype allows semiautomatic electrode calibration. Computer-controlled solenoid valves are used to temporarily reroute blood plasma away from the sensor flow path to a bypass flow path during calibration. One end of the sensor path, its inlet, is then connected to a syringe with a calcium chloride buffer solution, and the other end, to a waste container. This allows injection of buffer solutions for calibration without contaminating the blood plasma with buffer. After the buffers have been injected and calibration is finished, the inlet of the sensor path

is reconnected to the blood plasma flow while its outlet is still routed to the waste container. This results in the removal of buffer solution from the sensor path by the blood plasma flow. After a few seconds (flow-rate dependent), all buffer has been replaced by plasma. The sensor outlet is then switched back and the electrode tube is completely reconnected to the blood plasma flow. The prototype is currently limited to a plasma flow rate of approximately 100 cubic centimeters per minute.

The electrode signal is amplified by a high-input impedance amplifier and acquired by a data acquisition PCMCIA card and a laptop computer. The same card also outputs

digital signals to control (turn on/off) the solenoid valves.

The solenoid valves require a 12-volt DC power supply (at least 6 watt) that is provided by a wall transformer. The amplifier circuit is powered by two AAA batteries for isolation purposes. To reduce the electromagnetic interference with the sensor signal, the box is copper clad to provide shielding. Shielding, however, is only effective if the box is grounded, which can be accomplished by connecting the box with a ground wire to earth ground (for example, from an outlet). A schematic of the BIONA 1 system is provided in the figure.

This technology development represented a diverse collaborative effort between researchers and technologists at the Center for Emerging Cardiovascular Technologies (a National Science Foundation-sponsored program managed from North Carolina State University), and a team at the University of North Carolina at Chapel Hill and other affiliates in the Research Triangle, and at Case Western Reserve University in Cleveland, Ohio. A prototype Sensor Array for monitoring physiological ions in a hepatic bioreactor was demonstrated in a joint development activity with the Department of Surgical Research and the Liver Support Group at the Cedars-Sinai Hospital in Los Angeles, California.

Point of Contact: J. Hines
 (650) 604-5538
 jhines@mail.arc.nasa.gov

Intelligent Controller for Neurosurgery

Robert Mah

In preparation for neurosurgery to remove tumors, magnetic resonance imaging (MRI) scans are usually taken to locate the tumor and its positional coordinates. However, during the surgical operation to access the tumor, the brain swells and the location of the tumor shifts. As a result, the neurosurgeon must rely on experience to search for the tumor interface using surgical tools and tactile feedback. (Brain tumors typically have a

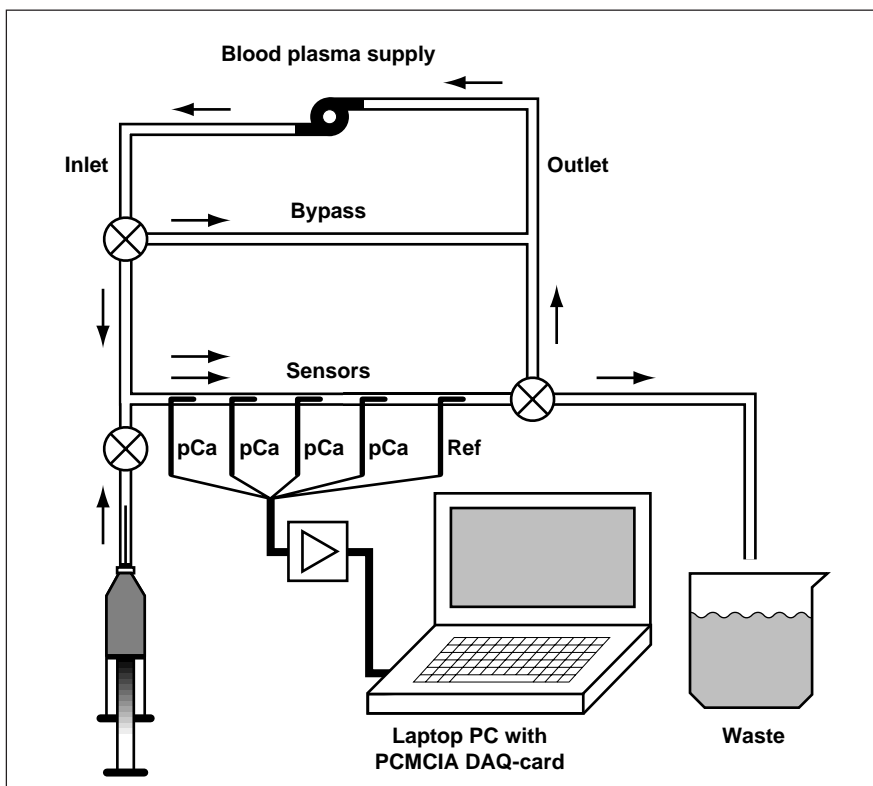


Fig. 1. Blood Flow Ion Analyzer (BIONA 1) system diagram.



Fig. 1. Robotic neurosurgical hardware testbed.

different density than normal brain tissue). During this procedure, an artery can accidentally be severed by the surgical tool which can lead to death.

A simple robot that can “learn” the physical characteristics of the brain may give surgeons more precise control of surgical instruments during delicate brain operations. The procedure utilizes a robotic smart probe that “learns” the brain’s characteristics by using neural net software. The probe, equipped with tiny sensors, enters the brain, gently locating the edges of tumors while preventing damage to critical arteries. Potentially, the neurocontrolled robot, making slow, very precise movements during an operation, will be able to “feel” brain structures better than any human surgeon.

This research has contributed to the design of an intelligent robot that can improve the safety, accuracy, and efficiency of neurosurgery. This technology is expected to have direct spinoffs to the general field of surgery. In FY96, the NASA/Stanford Neurosurgical Computational Testbed was developed (see the figure). World-wide press coverage (major television stations, major newspapers, and radio stations) was received and an invention patent is pending.

Point of Contact: R. Mah
(650) 604-6044
rmah@mail.arc.nasa.gov

Center for Health Applications of Aerospace Related Technologies (CHAART)

Byron Wood, Louisa Beck, Sheri Dister, Brad Lobitz

The Center for Health Applications of Aerospace Related Technologies (CHAART) was initiated at the beginning of FY95 by NASA Headquarters' Life and Biomedical Sciences and Applications Division (Code UL), within the Office of Life and Microgravity Sciences and Applications. The goal of CHAART is to promote the application of remote sensing (RS), geographic information systems (GIS), and related technologies to issues of human health. Fiscal year 1996 began with the First Cyril Ponnampereuma Symposium on Remote Sensing and Vector-Borne Disease Monitoring and Control, held in Baltimore, Maryland, on November 28–30, 1995. The symposium, hosted by NASA and the Third World Foundation (TWF), was attended by national health representatives from Brazil, Cameroon, China, Indonesia, Malawi, Malaysia, Mexico, Myanmar, Namibia, Nigeria, Rwanda, and Zimbabwe. The goal of the symposium was to develop RS/GIS-based, health-related research proposals from Third World countries. The CHAART staff gave tutorials on RS and GIS and led panel discussions to define country-specific issues.

As part of the new Memorandum of Understanding (MOU) between NASA and the Centers for Disease Control and Prevention

(CDC), the CHAART staff worked intensively with CDC personnel in Atlanta, Georgia, to develop collaborative projects. As a result of these discussions, the CHAART staff organized and taught two workshops on the uses of RS for public health applications. These workshops were conducted at CDC Headquarters in Atlanta (May 6–7, 1996), and at CDC's facility in Ft. Collins, Colorado (May 27–30, 1996). Recommendations for future NASA/CDC collaboration were generated at these events. As part of the NASA/National Institutes of Health (NIH) MOU, the CHAART staff also spent the year working with researchers funded through the NIH. These researchers received supplemental funding through a joint NASA/NIH call, and used these funds to integrate RS/GIS into their ongoing research on disease. CHAART directly assisted Dr. James Maguire (Brigham and Women's Hospital at Harvard Medical School), who is studying leishmaniasis in Teresina, Brazil, and Dr. Rita Colwell (University of Maryland), who is studying cholera in the Bay of Bengal.

In other activities, CHAART also worked closely this year with TWF personnel to identify 10 visiting foreign scientists whose research or jobs involve human diseases. These scientists will spend two months at CHAART during FY97 learning how to integrate RS/GIS into their studies on human health. Two of CHAART's staff are on the Advisory Board of the Pan American Center for Earth and Environmental Studies. This center, established at the University of Texas, El Paso, as a Minority University Research Center, was awarded a \$6.5 million grant from the Mission

to Planet Earth Enterprise to support environmental research in the Southwest.

CHAART also provides RS/GIS support to Dr. Uriel Kitron (University of Illinois, Champagne-Urbana), who is funded by NIH to study the distribution of Lyme disease in the Upper Midwest.

Point of Contact: B. Wood
(650) 604-4187
blwood@mail.arc.nasa.gov

Telemedicine Spacebridge to Russia

Steve N. Kyramarios

NASA's newest telemedicine project, entitled Spacebridge to Russia, is a collaborative effort between NASA and the Space Biomedical Center for Research and Training in Moscow, and establishes a testbed to evaluate Internet telemedicine in both operational and educational settings. The project connects the Clinical Hospital of the Ministry of the Interior in Moscow and the Moscow State Medical School sites with Baylor Medical Center, Fairfax Hospital, Latter Day Saints Hospital, and Yale Medical School through the multicast backbone (MBONE).

The goal of this project is to provide medical telecollaboration and electronic patient record production and review through the Internet. The program will help NASA develop a permanent telemedical system that provides medical support for its astronauts and other personnel involved in the

joint spaceflight program with Russia. In addition, the experience gained from this effort will provide insight into the potential of medical practice over the National Information Infrastructure and the Global Information Infrastructure.

This telemedicine testbed is between three clinical hospitals in the United States (U.S.) (Fairfax Hospital, Falls Church, Virginia; Latter Day Saints Hospital, Salt Lake City, Utah; and Yale University, New Haven, Connecticut) and two medical centers in Moscow (Clinical Hospital of the Ministry of Interior and the Space Biomedical Center for Training and Research at Moscow State University). UNIX-based Silicon Graphics Inc. multimedia workstations are located at each site and are linked to the Internet. The workstations incorporate Internet tools including a graphical user interface (GUI) on the World Wide Web, and the MBONE toolset for video conferencing. It is estimated that several hundred clinical consultations will be conducted between the clinical sites in the United States and Russia.

In addition to engineering the technical architecture, Ames Research Center has contributed to the project by providing technical leadership and implementation in Internet connectivity, motion video consultation, and video teleconferencing. These capabilities have enabled telemedicine consultations in a "grand round" format for unique case presentations. In addition, an educational program organized by Baylor Medical Center in Houston, Texas, is developing a series on recent advances in cardiology under the direction of Dr. Michael

deBakey, the world famous heart specialist. The educational program includes live multicast video and web-based medical imagery. Clinical consultations are prepared at each site using a standard format that includes motion video, data transfer, still photography, and video teleconferencing capabilities. Cases are made available to the reviewing hospitals through a Web server. Each site provides clinical coordination of the cases on a rotating basis.

Point of Contact: S. Kyramarios
(650) 604-4950
skyramarios@mail.arc.nasa.gov

PROGRESS IN IMPROVING SPACE
TRAVEL

Advanced Life Support/ Human Exploration and Development of Space Enterprise Activities

Dick Lamparter, Mark Kliss

The Ames Research Center (ARC) Advanced Life Support Branch carries out research and development of new technologies that will advance the human exploration and development of space. These activities will reduce life cycle costs, improve operational performance, promote self-sufficiency, and minimize expenditure of resources for future space exploration. Significant opportunities for Earth application of the developed technologies are available, including:

Atmosphere Regeneration: Data on the influence of water on the

adsorption of carbon dioxide and trace contaminants show significant reduction in capacity of sorbents and the possibility of elution back into the cabin environment. New materials and operating procedures will help mitigate this safety problem. New knowledge of adsorption processes has led to a method of in situ resource utilization of oxygen for Mars missions. Experimentally validated, the process is likely to fly on the Mars In Situ Propellant Production/In Situ Resource Utilization (ISPP/ISRU) Precursor experiment in 2001. The data being developed on materials have given insight into process modifications that will reduce power and space requirements. This research program supports contamination aspects of flight experiments.

Recovery of Resources from Waste Materials: Not currently recycled, human and food wastes are key elements for advanced life-support systems that approach self-sufficiency. Both Supercritical Water Oxidation (SCWO) and incineration processors have been developed and are currently under evaluation. Key issues being addressed include waste preparation and process feed and product stream cleanup, with a special focus on acid gases and other trace contaminants produced. A prototype incinerator will soon be delivered to the Johnson Space Center (JSC) for evaluation in an extended manned chamber test. The U.S. Navy has expressed interest in SCWO technology for its potential to reduce hazardous liquids to carbon dioxide and water while ships are deployed at sea.

Food production: Activity in this area is leveraged off prior research. In collaboration with the National Science Foundation, a unit to produce fresh food at the South Pole is being developed. The analysis of dietary requirements, crop mix, and multicropping in growth chambers has application to the Human Exploration and Development of Space (HEDS) objective of providing self-sufficiency. Experience in dealing with crews in remote environments is applicable to NASA. Information generated from this program is being formatted as part of the development of the JSC chambers.

These activities form the basis for an important technology transfer to native communities in Alaska where health hazards exist because of poor rural sanitation. Code STR has established cooperative agreements with the state, university, and local communities to apply the NASA-developed technology and systems analysis capability toward improving health, through diets and treatment of water and solid waste streams.

Point of Contact: M. Kliss
(650) 604-6246
mkliss@mail.arc.nasa.gov

Mir Hardware—Stepping Stone to Station

**Bonnie P. Dalton, James Connolly,
Gary Jahns, Paul Savage**

The Mir program has not only allowed the performance of biological experiments under long-term microgravity exposure (for example, 90 to 145 days), but also has provided a realistic view of experiences during the International Space Station program in terms of operations and hardware preparations. In contrast to the Spacelab profiles, in which major flights occurred every 2 to 3 years, Mir flights and the associated planning, hardware

and experiment development, and pre/postflight processing have occurred three times annually and have typically been initiated no earlier than 1.5 years prior to launch. As a result, hardware has been developed very rapidly, with applications to interim flights a principal objective (until the International Space Station is fully functional).

During the past 2 years, an insect habitat and a standard interface glovebox (SIGB) have been developed for use on Mir. The insect habitat was built with the assistance of Lockheed Martin Engineering and Sciences Company and other contract support.

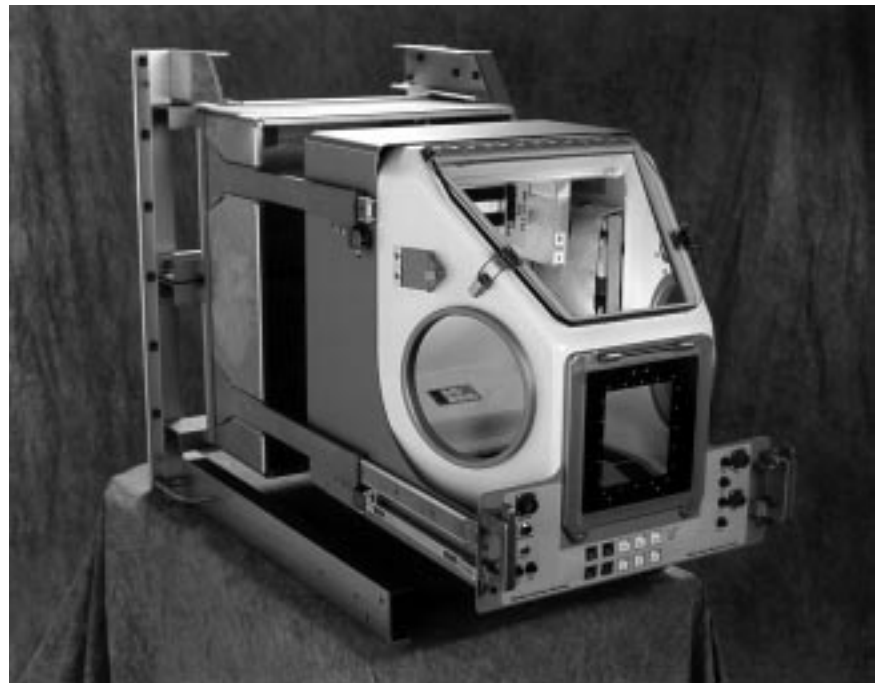


Fig. 1. Microgravity glovebox for Mir.

The SIGB was designed to provide a fully enclosed workspace for the execution of in-flight science procedures. The SIGB utilizes sliding rails and latches adapted from the Johnson Space Center's standard interface rack (SIR), allowing it to fly in virtually any existing or future space platform. The work surface of the unit is approximately 1 square foot and the work volume is 2.3 cubic feet. Bounded by a fiberglass shell consisting of five layers of epoxy resin, it is finished with white urethane for easy cleaning. Airflow within the unit is modeled after a laminar flow hood. The air filtration system provides a net negative pressure of 0.1 to 0.6 inch water with respect to ambient. All portions of the SIGB airflow system maintain negative pressure with respect to ambient in all operational modes. The filtration system has been designed to provide full containment of spills for specific chemicals (used in biological fixative preparations), including Campbell's Fixative, paraformaldehyde, and Russian variant solution. Access for operation is through attached gauntlet ports. The SIGB, ready for mounting in the Space Transportation Service vehicle, is shown in the figure.

The insect habitat, known as the Beetle Kit, was designed for a NASA-5 increment experiment entitled "Effects of Gravity on Insect Circadian Rhythmicity" that will study the Tenebrionid beetle. The hardware incorporates an automated circadian timing system (CTS). Since previous spaceflights have shown a notable effect on the CTS of both

vertebrates and invertebrates, it is anticipated that the ability to perform long-term measurements on Mir will greatly enhance the scientific community's knowledge of this subject. The Beetle Activity Module (BAM), the hardware housing the insect and the timing system, is an adaptation of an existing item of Russian hardware with expanded capabilities. Housing 32 beetles, the BAM is self-contained, and includes both a treadmill and a timing system. Food consists of a small quantity of dry oatmeal. Movement of a beetle on the treadmill indicates the insect's activity during portions of its circadian rhythms. Data collected from the flight experiment and from ground-based centrifuge studies at Ames Research Center will help determine if the CTS exhibits adaptation during long-term exposure to altered gravitational fields and whether that exposure changes the sensitivity of the CTS to flight.

In summary, Ames' participation in the Mir program resulted in the development of important hardware used for long-duration investigations and the methodology for rapidly building and qualifying the hardware. Additionally, Ames' participation has served as a vital educational stepping stone toward ensuring the success of activities onboard the International Space Station.

Point of Contact: P. Savage
(650) 604-5940
psavage@mail.arc.nasa.gov

Wireless Network Experiment for Space Shuttle/Mir

Richard Alena

The Wireless Network Experiment (WNE) was a risk-mitigation experiment designed to demonstrate the feasibility of using wireless networks aboard the International Space Station. The customer was the Shuttle/Mir Science Program at the Johnson Space Center (JSC), which is under the Space Station Program. The WNE consisted of a set of three computers that could communicate via the wireless radio network system, as shown in the figure. A network monitor program graphed network throughput in real time as the computers were moved through the habitable volume. This experiment was successfully conducted onboard both the Space Shuttle and Mir Space Station during the docked space transport system-76/Mir 21 flight.

The current International Space Station data system baseline does not provide adequate support for payloads and onboard computer systems. Adding additional cabled network resources is prohibitive in terms of cost and weight. A wireless network allows portable computing resources to be brought up to the Space Station and installed with minimal effort and, at low-cost, support a significantly augmented data processing capability for payloads and crew.

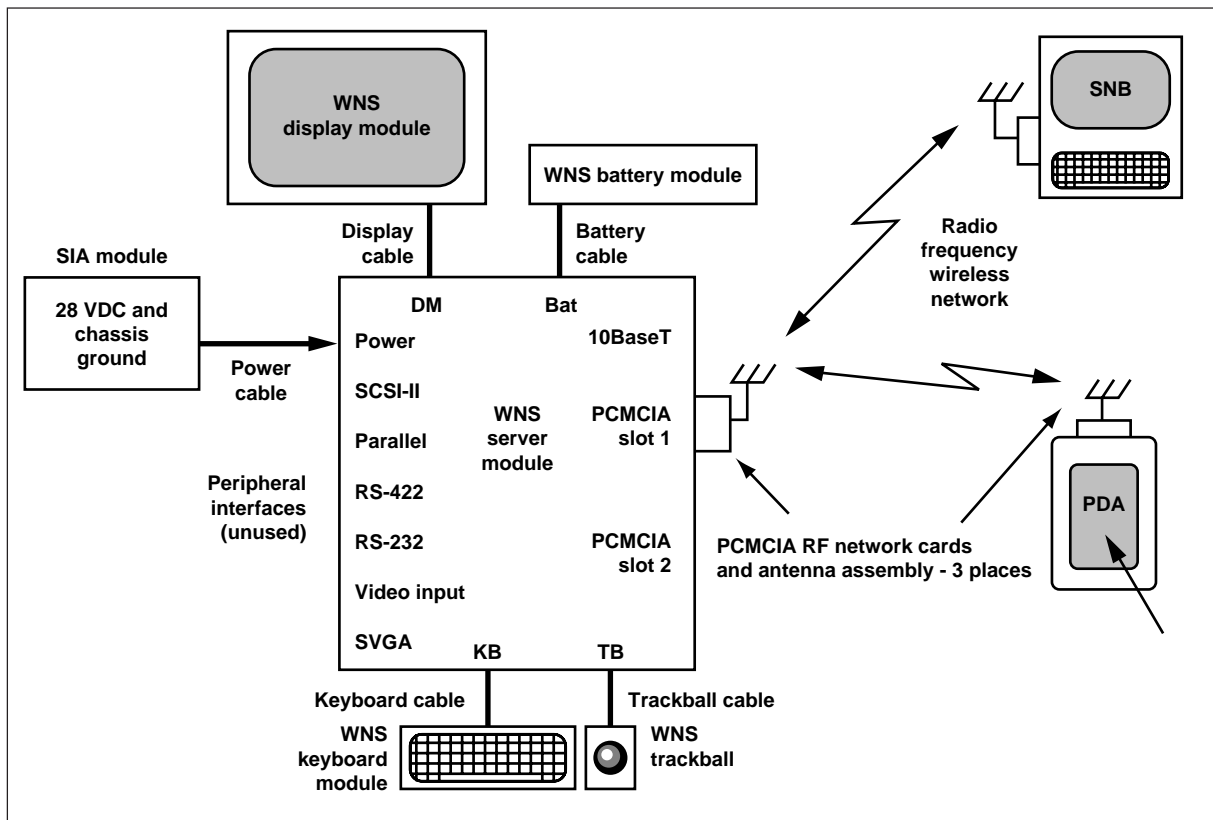


Fig. 1. Schematic of the Wireless Network Experiment (WNE) system.

The WNE was conducted in March 1996. Demonstration of the next-generation (Web-based) data system concept to NASA and JSC astronauts and engineering managers was made in May 1996. The post-flight testing and preliminary report were completed in August 1996.

Point of Contact: R. Alena
 (650) 604-0262
 ralena@mail.arc.nasa.gov

Engine Diagnostic Filter System

Tarang Patel

The project objective was to develop posttest data analysis tools for potential deployment as real-time and in-flight instruments for the next generation rocket engines for space vehicles. Analysis was made on the exhaust plume data collected from the Space Shuttle main engines. The analysis capability is to give indications of engine erosion and its potential source inside the motor.

The real-time analytic capability is unique in its ability to identify the principal eroding metal species under way in an engine during engine operation. Such health monitoring activity can be used to shut down an engine test prior to a potential catastrophic failure. This step could lead to a possible in-flight capability, under research, which would be used for onboard diagnosis for health management, and could represent a safety check for the space vehicle crew. A much more immediate benefit of the posttest analysis is that it provides engineers,

involved in engine tear-down activity following a test, a real indication of whether such an expensive task is necessary.

This project was the world's first use of plume spectroscopy to produce realistic, quantified estimates of metal erosion from a rocket engine. During recent routine testing of a main Space Shuttle engine at the Stennis Space Center, the analysis tools coupled to data from a diagnostic instrument were able to determine metal erosion taking place and pinpoint the event of a catastrophic failure. The methods used in the analysis were even able to extract silver and copper lines, despite the fact that they were swamped in the rich hydroxyl grouping (OH) structure of the spectrum.

Point of Contact: T. Patel
(650) 604-4721
maumau@nas.nasa.gov

Formal Lightweight Approaches to Validation of Requirements Specifications

Steve Easterbrook

The objective of this research was to evaluate the use of formal methods as a tool for independent verification and validation (IV&V) of software requirements specifications (SRS) for spacecraft flight software. Formal methods allow an IV&V team to test SRS for properties such as consistency, completeness, safety, and correctness. The research

focused on lightweight methods, which can be applied to small chunks of a specification without a substantial investment in translating entire specifications into mathematical notations.

A series of case studies was conducted, applying formal modeling techniques to 'live' projects, so that the results can be fed back into the project in time to be of added value. The case studies were chosen in response to real needs on existing projects; for example, where an additional level of assurance of the correctness of the requirements was needed, over and above that obtainable through existing methods. The case studies completed in the past year related to the International Space Station. A range of different formal methods was applied, including software cost reduction, the prototype verification system, and the model checker software process improvement network (SPIN). In each case the amount of effort required to apply the method was examined, along with the types of benefits gained. This evaluation was mainly qualitative, as the baseline metrics do not exist for detailed quantitative comparisons.

The analysis conducted during the case studies provided a significant addition to the IV&V performed on the Space Station SRS. A major case study examined the requirements for the fault detection, isolation, and reconfiguration (FDIR) for the main communications bus on the space station. This study involved translation of the original prose requirements into a formal, tabular notation, and analysis of the resulting model for consistency, for

key static properties, and for correct dynamic behavior. The figure shows an analysis of the timing behavior of the FDIR requirements using the SPIN tool.

The formal methods allowed the IV&V team to quickly identify numerous weaknesses in these requirements, including ambiguous use of terminology, missing requirements, and inconsistencies in the timing requirements. These problems would normally not be detected until later in the development process, at which point the costs to correct them are significantly higher.

Results indicated that the main effort involved in applying the formal methods is in translating the prose requirements into the formal notation. However, this effort is consistent with the level of effort normally applied to performing IV&V on critical functions. In contrast, the ability to spot errors and omissions is greatly improved, as over half the issues identified in the formal analysis could not be detected during the requirements phase using existing methods. Hence, formal methods provide a cost-effective approach to analyzing requirements, provided they can be focused.

Formal methods have not yet gained widespread acceptance by software practitioners. Part of the problem has been an emphasis on adopting a baseline formal specification, from which to prove that design and implementation are correct. This project has demonstrated that a more realistic approach is to use formal methods for small pieces of modeling, especially during the early

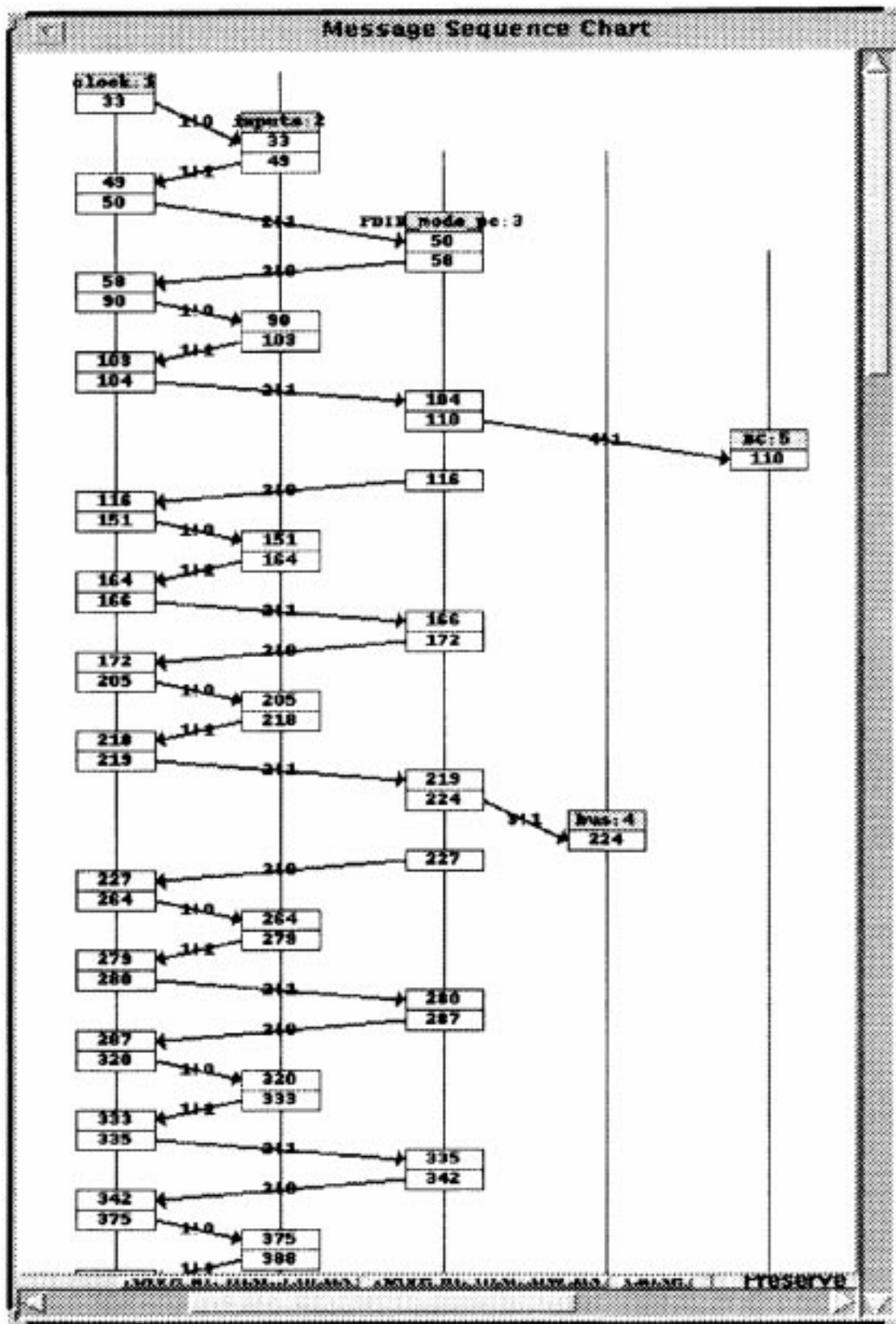


Fig. 1. A screen snapshot from the SPIN tool, showing the FDIR system (center) interacting with other subsystems (the clock, a test harness, and the hardware it controls). This analysis allows the analyst to confirm that the software will behave in the intended fashion even before it is written; that is, based solely on a statement of the requirements.

requirements stages, to answer questions that cannot be addressed in other ways.

Point of Contact: S. Easterbrook
(304) 367-8352
S.Easterbrook@ivv.nasa.gov

ASTRONAUT HEALTH/
COUNTERMEASURES

Autogenic-Feedback Training as a Potential Treatment for Postflight Orthostatic Intolerance

Patricia S. Cowings,
William B. Toscano

The goal of this research is to determine if human subjects can learn to voluntarily control blood pressure increases during a gravito-inertial stimulus (for example, tilt table), and to determine the mechanisms by which such control is effected. The training method used, Autogenic-Feedback Training Exercise (AFTE), was initially developed as a treatment for motion sickness. It involves teaching subjects to control voluntarily up to 20 of their own physiological responses simultaneously. In support of the present study, cardiovascular dynamics (derived from impedance cardiography) were measured and displayed to test participants in real time. These measures included: cardiac output, stroke volume, and an estimate of vagal tone. Tests are in progress; this report outlines the results obtained to date.

Baseline data were collected on each subject during supine, head-up tilt, and head-down tilt conditions.

Subjects were given two tests, each 50 minutes long, one test before and one test after AFTE. Physiological data were continuously recorded during both tests with the Autogenic-Feedback System-2 and impedance cardiography. The protocol for these tests is outlined as follows:

1. Supine resting baseline 10 minutes
2. Head-up tilt at 50 degrees 10 minutes
3. Supine resting baseline 10 minutes
4. Head-down tilt at -30 degrees 10 minutes
5. Supine resting baseline 10 minutes

Each subject received 6 hours of AFTE, which was administered in twelve 30-minute sessions (with subjects sitting; that is, nontilt conditions). Following a 6-minute pretest baseline, each 30-minute training session was divided into ten 3-minute trials, during which

subjects were instructed to alternately increase and decrease response levels (for example, heart rate accelerations and decelerations, peripheral vasodilatation and constriction, etc.). A 6-minute resting baseline was also collected after each session (total 42 minutes).

The purpose of these training sessions was to provide subjects with the ability to recognize bodily sensations associated with both increases and decreases in their physiological response levels and, with practice, to improve their skill in controlling these responses. Subjects eventually learn to maintain their physiological response levels at or near their own resting baseline levels and improve their tolerance to environmental stressors (for example, tilt table, conditions of microgravity, etc.).

The first figure shows a subject in the head-down tilt position. The



Fig. 1. Subject during 30-degree head-down tilt.

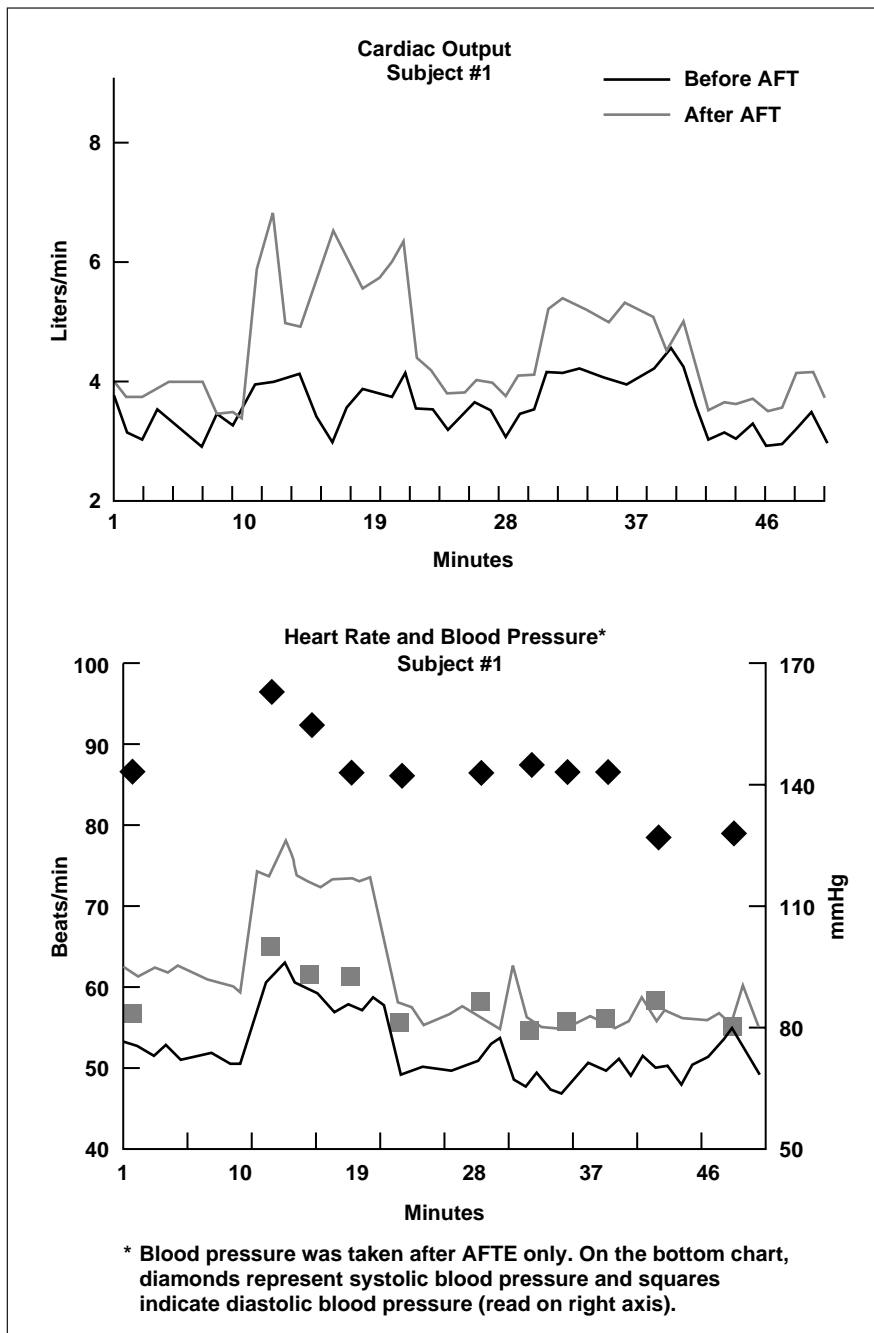


Fig. 2. Physiological responses to tilt before and after AFTE.

second figure shows physiological responses of cardiac output (top chart) and heart rate and blood pressure (bottom chart), before and after AFTE. This subject made a significant increase in both heart rate and cardiac output in response to head-up tilt (minutes 11 through 20) after eight AFTE sessions. There was no observable change in cardiac output during tilt before training.

The third figure shows the physiological data of one subject during AFTE sessions four (after almost 2 hours of training) and eight (after almost 4 hours of training). The data shown include finger pulse volume, respiration rate, heart rate, skin conductance level, cardiac output, stroke volume, central volume (actually thoracic impedance), and an estimate of vagal tone (calculated by Fast Fourier Transform in real time). Following the 6-minute baseline, subjects were instructed to produce arousal responses (constriction of finger blood volume, heart-rate and skin-conductance-level increases) but not to modify respiration or to contract muscles. More consistent control of finger pulse volume was apparent during session eight than during session four—as the subject makes the desired response at 3-minute intervals. Respiration was recorded to show that the subject was neither hypernor hypoventilating (by session eight) to influence other response changes. By session four, both heart rate and skin conductance level show evidence of learning that remained consistent through session eight. Note, however, that learned control of cardiac output, stroke volume, and vagal tone was not

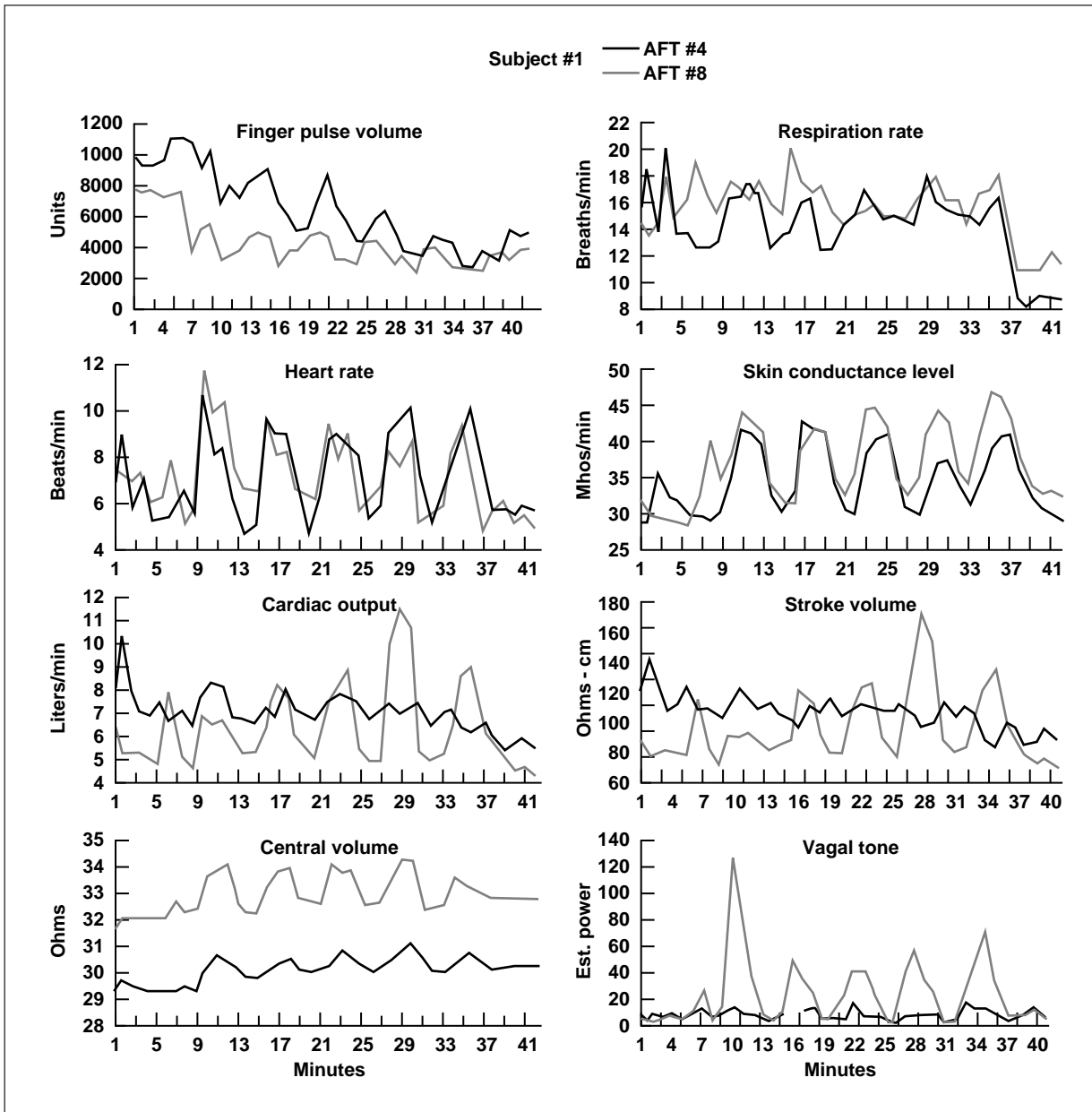


Fig. 3. Physiological responses during AFTE sessions four and eight. Note: Following a 6-minute resting baseline, subjects are instructed to produce alternating arousal (that is, constriction of blood flow to the fingers, heart-rate and skin-conductance-level increases) and relaxation responses (that is, vasodilation of fingers, decreases in heart rate and skin conductance level) at three 3-minute training trials, showing for the first time that these parameters may be subject to learned, voluntary control.

apparent until session eight, suggesting that AFTE practice is associated with observed response changes. Central volume was also modulated with instruction (that is, at 3-minute intervals) more consistently after eight sessions.

These data represent the first indication that these measures of cardiac dynamics are subject to voluntary control through learning. They show that AFTE methods may yield a powerful, potential countermeasure for postflight orthostatic intolerance that may supplement existing exercise routines utilized by crewmembers.

Point of Contact: P. Cowings
 (650) 604-5724
 pcowings@mail.arc.nasa.gov

date has lacked sufficient loads to maintain preflight musculoskeletal mass. Although treadmill exercise with bungee cords (about 2 hours per day) is the most common exercise for cosmonauts during long-duration Mir missions, biomechanical loads on musculoskeletal tissues of the lower body are only about 60 to 70% of those present on Earth. Theoretically, an integrated countermeasure for extended exposure to microgravity should combine high loads on the musculoskeletal system with normal regional distributions of blood pressure and stimulation of normal neuromuscular locomotor patterns.

Lower-body negative pressure (LBNP) exercise is an integrated countermeasure that may prevent

bed rest- and microgravity-induced deconditioning by simulating gravity. (See the figure.) The LBNP exercise device consists of a vertically oriented treadmill within a partial-vacuum chamber that is sealed around the subject's lower body. For use on Earth, supine subjects are supported by a suspension system of cables and pulleys. Suction pressure is used to pull blood and other body fluids away from the heart (thus reproducing normal upright blood pressure gradients) while simultaneously creating a gravity-like footward force.

In a recent study, it was hypothesized that daily LBNP exercise maintains cardiovascular and musculoskeletal conditioning during

Exercise for Long-Duration Spaceflight

Donald E. Watenpaugh,
 Richard E. Ballard,
 Karen J. Hutchinson,
 Jaqueline M. William, Andrew C. Ertl,
 Suzanne M. Fortney, Lakshi Putcha,
 Wanda L. Boda, Stuart M. C. Lee,
 Alan R. Hargens

Adaptation to microgravity leads to cardiovascular and musculoskeletal deconditioning to normal Earth gravity. Specific problems include muscle atrophy, bone demineralization, reduced neuromuscular coordination, and postflight reduction of orthostatic tolerance and upright exercise capacity. Presently, exercise protocols and equipment for astronauts in space are unresolved, although recent calculations suggest that all exercise in space to

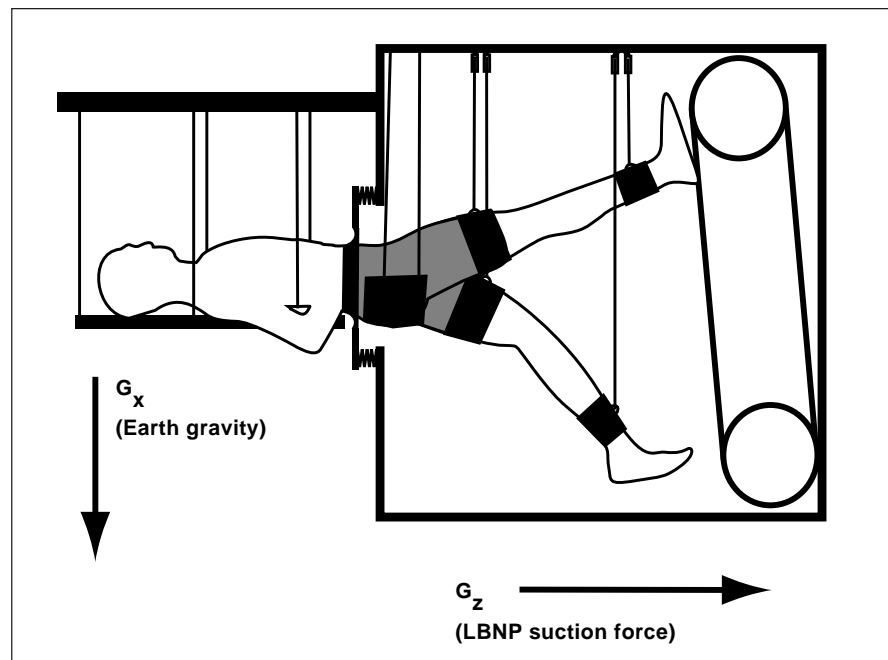


Fig. 1. Treadmill reaction force to generate body weight in supine posture equals the product of the cross-sectional area of the flexible waist seal and the suction pressure within the LBNP chamber. With exercise, inertial reaction forces against the treadmill are added to the static force.

6-degree head-down bed rest. Seven healthy male volunteers acted as their own controls, such that their responses to 2 weeks of bed rest with daily supine LBNP treadmill exercise (40 minutes of walking and running at 1.0 to 1.2 body weights of footward force) were compared to their responses to 2 weeks of bed rest with no daily exercise. The 2-week bed rest sessions were separated by 10 weeks.

Forty minutes per day of LBNP exercise preserved upright exercise capacity during 2 weeks of bed rest. Subjects' time to volitional exhaustion during their individualized treadmill tests decreased 1.72 minutes on average (10%, $p < 0.05$) after bed rest with no daily exercise; daily LBNP exercise during bed rest maintained exercise tolerance time at pre-bed rest levels. Daily LBNP exercise also maintained peak upright oxygen consumption (VO_2) at pre-bed rest levels (pre-bed rest: 59.5 ± 3.2 milliliters/minute/kilogram; post-bed rest: 56.4 ± 3.4). Mean peak VO_2 decreased significantly from 57.6 ± 2.6 to 49.8 ± 1.5 milliliters/minute/kilogram after bed rest with no exercise. Sprint speed from a standing start was maintained at pre-bed rest levels when daily LBNP exercise accompanied bed rest (pre-bed rest: 5.5 ± 0.2 meters/second; post-bed rest: 5.2 ± 0.3). However, bed rest without daily LBNP exercise significantly reduced sprint speed from 5.5 ± 0.2 to 4.6 ± 0.3 meters/second, below pre-bed rest control levels.

In conclusion, LBNP exercise improves upon current spaceborne exercise technologies by supporting

cardiovascular and musculoskeletal fitness while reducing the duration of astronaut exercise sessions.

Point of Contact: A. Hargens
(650) 604-5746
ahargens@mail.arc.nasa.gov

Keiser SX-1 Variable Resistance Exercise Device

**Jennifer Pedley, Anthony Artino,
Richard Ballard, Alan R. Hargens**

Muscle atrophy and decreased bone density are problems associated with extended exposure to microgravity. Therefore, it is vital for astronauts to exercise during long-duration spaceflight to reduce these adverse physiological changes. In collaboration with Ames Research Center and Palo Alto Veterans Administration Rehabilitation

Research and Development Center, the Keiser SX-1 resistance exercise device was developed to prevent muscle atrophy and bone weakness. Two pneumatic pistons provide variable and high resistance for the lower-body exercises, whereas a single piston allows resistance exercises for the upper body and spine. When performing the exercises, the user is secured by a harness to provide muscle isolation and proper positioning (see the first figure). The device includes an adjustable monitor that provides feedback information such as force, work, and power. Other features include strength and cardiovascular modes represented on the monitor. In the strength mode, the monitor displays the number of repetitions and the angle of the upper-body exercise levers. The cardiovascular mode conveys to the user repetitions per minute, total time of the exercise



Fig. 1. The Keiser SX-1 in an unfolded configuration.

for upper and lower body, and graphic indicators to represent the range of motion. The Keiser SX-1 is designed to fit into a standard Space Station rack. The total weight of the device is 120 kilograms (265 pounds), but the weight can be reduced to 80–100 kilograms using aluminum.

All exercises are performed in one or two positions by using the four buttons located on the handgrips. Two thumb buttons on each handgrip are capable of adjusting (1) the amount of resistance to the upper and lower extremities; (2) the leverage from a pulling to pushing exercise (that is, pulldown to a chest press); and (3) the range of motion for arms from 0 to 70 degrees (that is, row to shoulder press exercise). Maximum and minimum resistance values for the lower-body range from 1,500 to 100 Newtons and for the upper body from 1,000 to 50 Newtons. At any designated time, the user can adjust the resistance and exercise.

A user can perform resistance exercises from supine and prone positions. These exercises include: (1) bilateral chest press for strengthening the pectoralis major, anterior deltoids, and triceps; (2) bilateral row for strengthening the latissimus dorsi, rhomboids, and biceps; (3) bilateral shoulder press, supine and/or prone position for strengthening the deltoids and triceps; (4) bilateral lat pull-down, supine and/or prone position for strengthening the latissimus dorsi and biceps; (5) bilateral or unilateral leg press for strengthening the gluteals, quadriceps, hamstrings, calf muscles, and

lower back postural muscles; and (6) bilateral or unilateral hip flexion. In addition, many of the above exercises produce spinal loading that may help reduce back pain due to spinal lengthening in microgravity.

In a comparison evaluation with a standard supine leg press (SLP) device, the SX-1 demonstrated similar thigh muscle electromyographic (EMG) activities during concentric and eccentric exercises (see the second figure). With regard

to the calf muscles, gastrocnemius EMG activity was greater with the SX-1 than the SLP, while soleus EMG activity was similar or slightly lower with the SX-1 than the SLP. These results indicate that the Keiser SX-1 is capable of loading thigh and calf muscles in a manner similar to a conventional leg press device used for ground-based exercise.

Presently, cardiovascular machines are emphasized on the Space Shuttle; however, strength

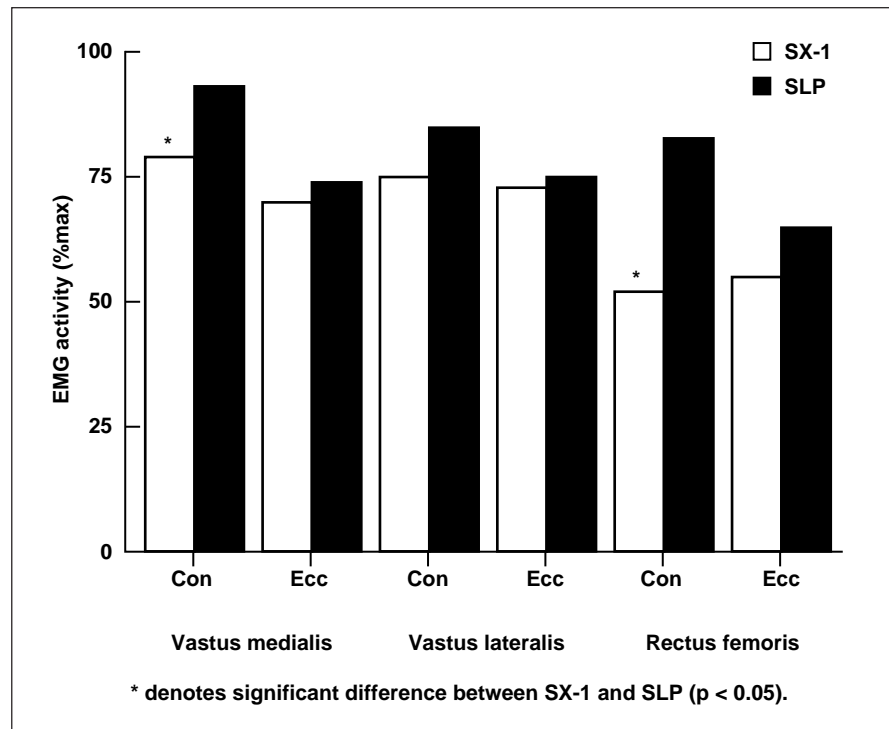


Fig. 2. Average thigh muscle electromyographic (EMG) activity in 11 subjects for the concentric (Con) and eccentric (Ecc) phases of contraction during a 10-repetition maximum leg press exercise using the Keiser SX-1 and conventional supine leg press (SLP). In general, EMG activities were similar between the SX-1 and SLP, with the exception of concentric contractions of the vastus medialis and rectus femoris. This difference is probably related to a lesser load placed on these muscles using a variable pneumatic resistance for the SX-1 as compared to a constant weight for the SLP.

training devices are an exception. Exercising on a variable-resistance device during spaceflight may be effective in decreasing the detrimental physiological effects caused by exposure to microgravity. Keiser SX-1 has the ability to combine cardiovascular and resistance training as well as spinal loading during exercise. With an appropriate high-resistance training protocol, users may be able to maintain muscle size and strength as well as bone density. The Keiser SX-1 represents an important advance toward this goal.

Point of Contact: A. Hargens
(650) 604-5746
ahargens@mail.arc.nasa.gov

Dehydration at Airline Cabin Altitude

John E. Greenleaf, Peter A. Farrell, Helmut Hinghofer-Szalkay

A contributory factor for the jet-lag syndrome in humans is total body dehydration, or hypohydration (see first figure), which is manifest by a reduction in plasma volume (hypovolemia). Exposure to prolonged chair-rest confinement and possibly to moderate altitude (alt.), as occurs in passenger airline cabins, could facilitate this dehydration. The purpose of this study was to

determine if rehydration drinks (AstroAde (AA), Performance 1 (P1), or water (H₂O)) could ameliorate the hypovolemia in 10 young men (21 to 30 years old, weighing 62 to 101 kilograms) sitting (with light activity) for 12 hours at 2800 meters (9184 feet, 539 millimeters Mercury) in an altitude chamber.

After the subjects rested for 10 hours in the chamber and consumed three normal meals (2850 kilocalories, 1400 milliliters water), their plasma volume decreased significantly ($p < 0.05$) by 9.0% (AA, alt.), 6.2% (P1, alt.), 7.4% (H₂O, alt.), and 9.0% (H₂O,

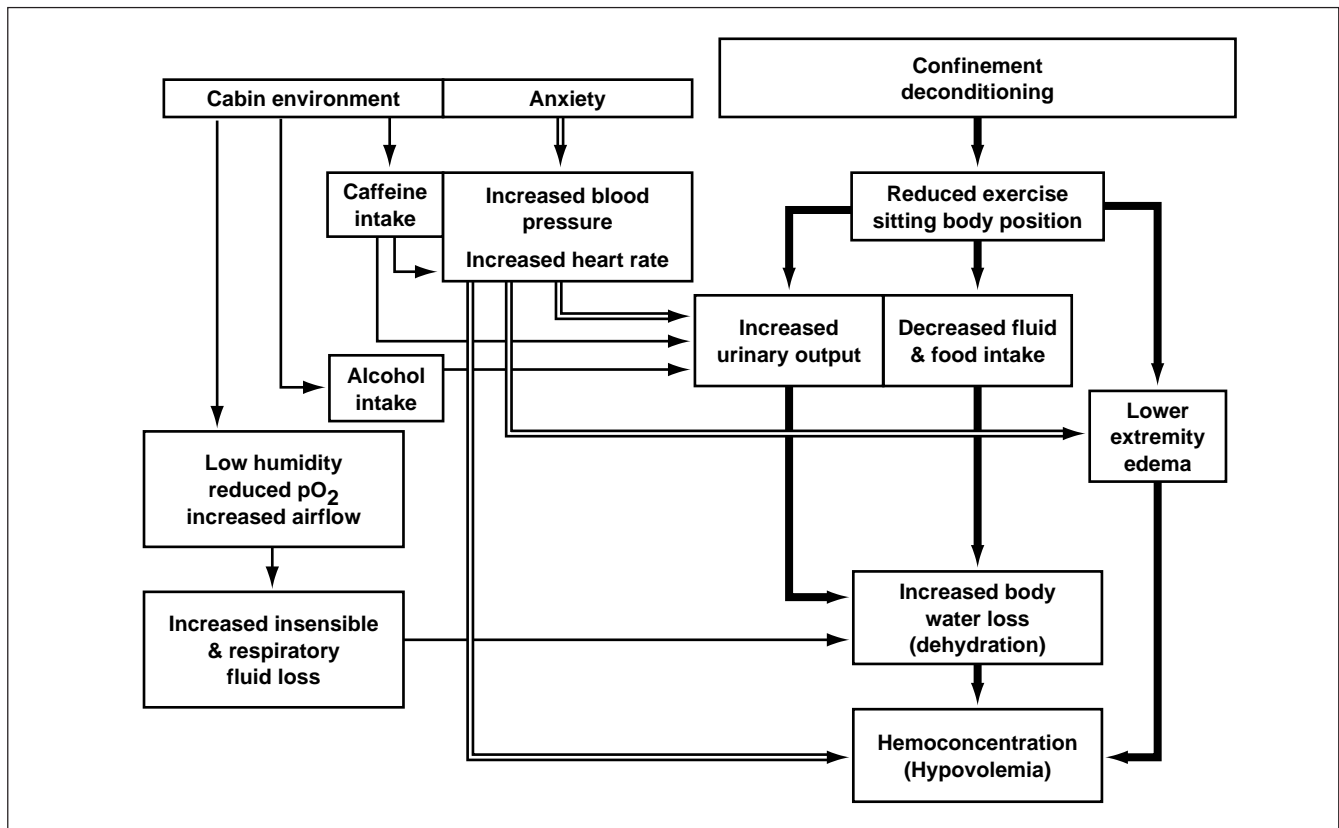


Fig. 1. Factors affecting in-flight hypovolemia.

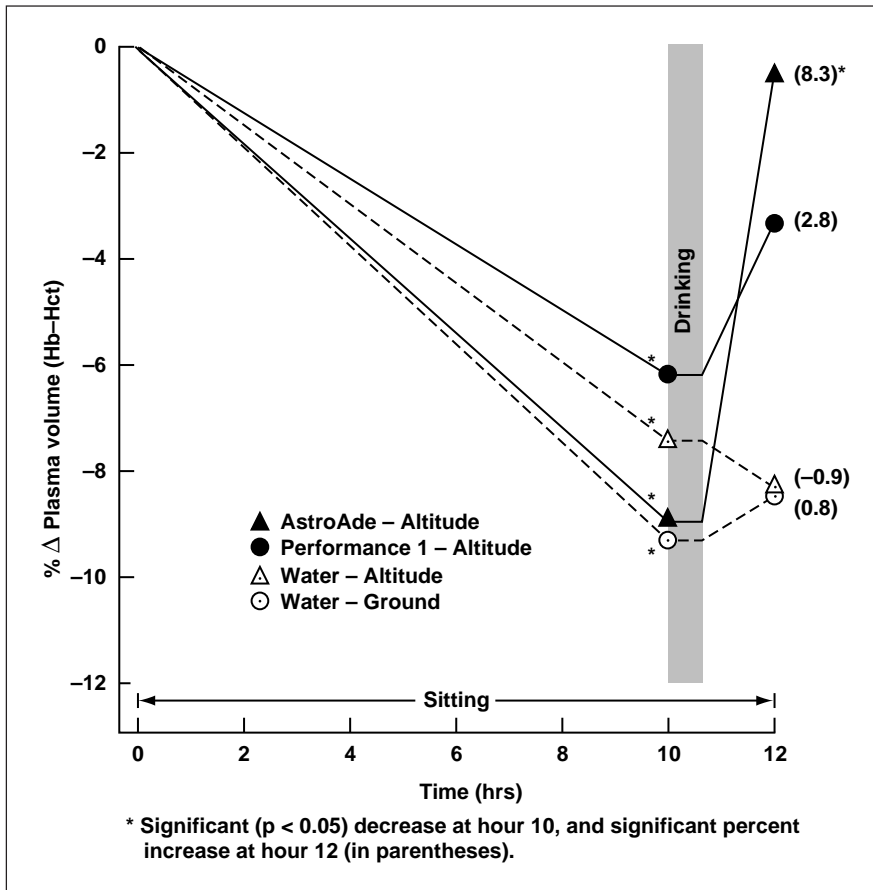


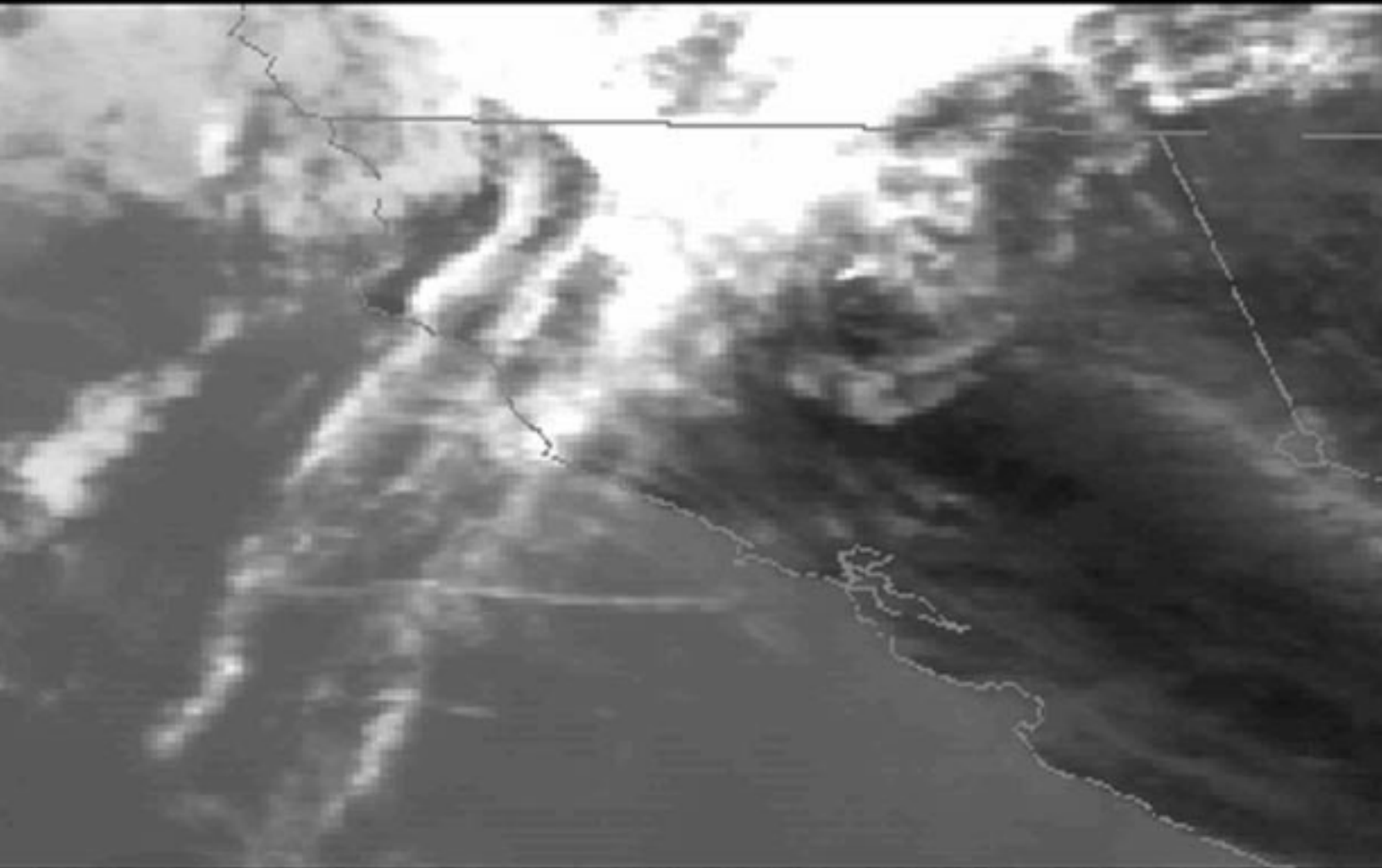
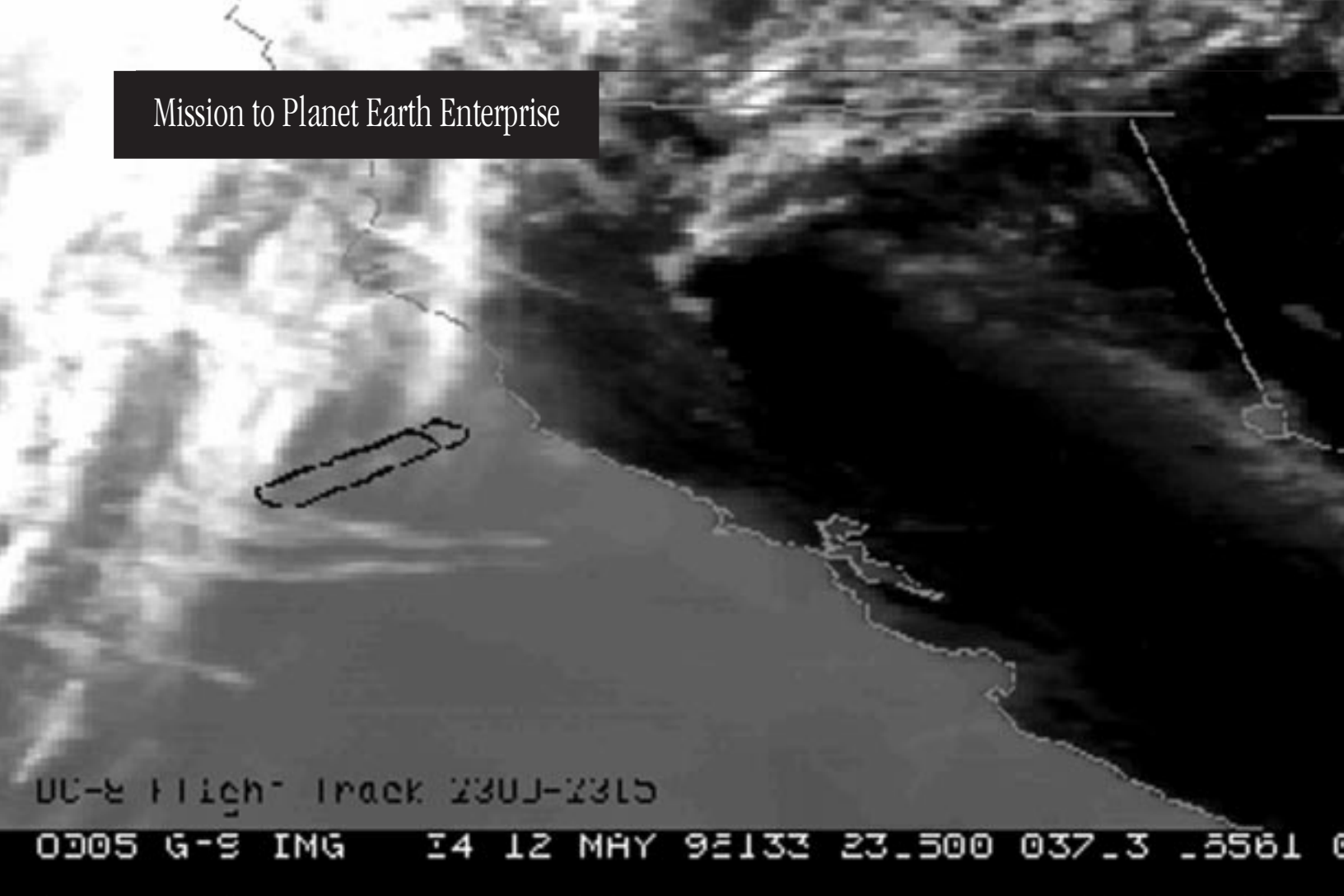
Fig. 2. Mean percent change in plasma volume at altitude and on the ground.

ground). (See second figure.) The men then drank AA, P1, or H₂O (12 milliliters/kilogram body weight, 948 milliliters at 16 degrees Centigrade). At 90 minutes (hour 120 after the 30-minute drinking period), plasma volume had increased by 8.3% (AA, $p < 0.05$), 2.8% (P1, not significant), -0.9% (H₂O, alt., not significant), and 0.8% (H₂O, ground, not significant).

These data indicate that significant dehydration and hypovolemia occur with adequate food and fluid intake during moderate (12-hour) confinement (sitting) at moderate altitude. Because plasma volume also decreased on the ground, it appears that confinement, and not the moderate hypoxia, causes the hypovolemia and hypohydration.

Point of Contact: A. Hargens
 (650) 604-5746
 ahargens@mail.arc.nasa.gov

Mission to Planet Earth Enterprise



Overview

NASA's Mission to Planet Earth (MTPE) studies the total Earth environment—atmosphere, ice, oceans, land, biota, and their interactions—to understand the effects of natural and human-induced, near-term changes on the global environment and to lay the foundation for long-term environment and climate monitoring and prediction. Ames Research Center supports the MTPE Enterprise by conducting research and developing technology to expand the knowledge of Earth's atmosphere and ecosystems. This objective is also one of the goals of NASA's astrobiology research and technology efforts, which are led by Ames. A complementary objective is to apply the knowledge gained to practical, everyday problems and to transfer the technology and knowledge to users outside NASA. Numerous research and technology efforts were accomplished during FY96, and the results address the following goals of the MTPE Enterprise:

- Expand scientific knowledge of the Earth's environmental system.
- Enable the productive use of MTPE science and technology.
- Disseminate information about the Earth's environmental system.

The research is particularly concerned with atmospheric and ecosystem science and with biosphere/atmosphere interaction. Key components of the research include the study of physical and chemical processes of biogeochemical cycling; the dynamics of terrestrial

and aquatic ecosystems; the chemical and transport processes that determine atmospheric composition, dynamics, and climate; and the physical processes that determine the behavior of the atmosphere on the Earth and other solar system bodies. Of special interest are the development and application of new technologies required to bring insight to these science topics. Significant contributions were made in three areas: analysis of critical gaseous emissions, development of models and instruments, and radiation research.

Research highlighted in this report includes focus on important environmental concerns related to stratospheric ozone depletion, perturbations in the chemical composition of the atmosphere, and climatic changes from clouds, aerosols, and greenhouse gases. Numerous state-of-the-art instruments were flown successfully, and significant data were collected for stratospheric and tropospheric research. For stratospheric experiments, the following are included: the Meteorological Measurement System (MMS), which measures pressure, temperature, and the wind vector; and a dual-channel tracer instrument for stratospheric dynamics studies (Argus).

These instruments were flown on the ER-2 aircraft for the Airborne Southern Hemisphere Ozone Experiment and for the Stratospheric Tracers Atmospheric Transport (STRAT) study. For tropospheric experiments, instruments were flown on several aircraft to measure carbon monoxide, nonmethane hydrocarbons, carbonyls, and reactive nitrogen species. Specifically,

fluxes of important biogenic gases from terrestrial ecosystems were quantified, as were contrails of subsonic aircraft and cloud effects (SUCCESS) and tropospheric aerosol radiative forcing (TARFOX).

Technology developments were realized on two fronts—modeling and instruments. Model development efforts or simulations based on developed models are presented for the following phenomena: the effect of gravity waves generated by convection or stratospheric circulation; the effects of climate and landcover interactions in the boreal biome; soil/atmosphere exchange of key trace gas species; biomass combustion and pyrogenic trace gas emissions; seasonal differentiation of microbial methane sources; a knowledge-based, interactive, graphical tool; use of supercomputer technology in ecosystem simulation; and paleoenvironment studies using pollen data and leaf area development. Newly developed instruments include: a miniaturized, lightweight, tunable diode laser spectrometer; an MMS on the NASA DC-8 aircraft to provide science-quality state variables and wind data; an airborne disaster-assessment sensor; a digital array scanning interferometer; and a fully automated, 14-channel sunphotometer to fly on remotely piloted aircraft and other platforms. Also, a new program was created (ERAST) to focus critical technology development and flight demonstration for remotely piloted vehicles.

Radiation research focuses on phenomena associated with the interaction of solar radiation with the atmosphere and solar system bodies. The high-resolution infrared spectroscopy is devoted to basic experimental and theoretical research into the absorption of radiation by gases. The purpose is to determine the molecular spectroscopic parameters needed for the design and interpretation of field measurement programs related to the environment of Earth's and other planetary and stellar atmospheres. This report also highlights experiments conducted with the Radiation Measurement System and with a new within-leaf radiative transfer model.

Using MTPE data and technology, commercial firms can expand their businesses and public-sector managers can exercise stewardship of the nation's natural resources. The enabling, productive use of MTPE science and technology is exemplified by numerous accomplishments including the effects of land-use change on the methods and assumptions currently in use to estimate the influence of land cover in Earth's carbon budgets of the northern boreal forest in Oregon. Other reported data, analyses, and technologies can be used by researchers who seek answers to key Earth science questions and by educators who teach Earth sciences.

AIRDAS—Use of Remote Sensing for Disaster Assessment and Management

James Brass, Vincent Ambrosia,
Robert Slye

Each year natural disasters in the United States cause an estimated 20 to 50 billion dollars in damage. Fires, earthquakes, floods, hurricanes, and tornadoes destroy thousands of structures, devastate resources, raise havoc with transportation and communication networks, and cause loss of life. The management of these events is costly and difficult. The consequences of these disasters are evident, and they lend themselves to monitoring, mapping, and assessment by remote sensing. The goal of this applied research project, funded by NASA's Mission to Planet Earth Enterprise and the U.S. Forest Service, is to develop, demonstrate, and transfer this technology to value-added companies and the user community. The development, based on the Airborne Infrared Disaster Assessment System (AIRDAS), a compact, multispectral scanner designed for quick aircraft integration and deployment, takes advantage of technology developed in the Silicon Valley of California and government laboratories, to collect, analyze, and communicate information to disaster management personnel. The research was performed in collaboration with Edward Hildum of Sverdrup Technology,

Robert Higgins of SIMCO Electronics, Philip Riggan and Robert Lockwood of the U.S. Forest Service, and Chien Nguyen of Raytheon.

Recent activity has involved the user community, the U.S. Forest Service, the California Department of Forest and Fire Protection, the Los Angeles County Fire Department, the Office of Emergency Services, and the Federal Emergency Management Agency to develop system requirements, review present capabilities, and make recommendations for system improvements. Major upgrades to the system, developed to fill user-driven requirements, include additional onboard real-time display capabilities, a real-time downlink capability, and improved user interface software for data exploitation. The system continues to be integrated on users' aircraft for disaster monitoring and assessment. Currently, the system resides on NASA's Lear 24, but it has also flown on P-3s, the Lear 35 and 31, the KingAir 200, and a Navajo.

The system was used in Brazil in FY96 to detect and map deforestation and fire activity, and to fly disaster monitoring missions in California, New Mexico, and Arizona. The system is currently being upgraded to provide higher-resolution datasets and to increase the telemetry capability.

Point of Contact: J. Brass
(650) 604-5232
brass@mail.arc.nasa.gov

Bay Area Digital Georesource

Edwin Sheffner, Sheri Dister,
Don Sullivan

The Bay Area Digital Georesource (BADGER) is a cooperative project among NASA, Lockheed Martin Palo Alto Research Laboratory, and a nonprofit organization called the Bay Area Shared Information Consortium (BASIC). The goal of BADGER, funded primarily by NASA's High-Performance Computing and Communication Program, is to provide NASA data and technology toward development of a system that will make digital, geospatial data of the San Francisco Bay Area available over the Internet. BADGER technology will serve as the basis for an ongoing service operated by BASIC.

BADGER contains three operational functions, all of which are designed to be performed on the Internet. First, BADGER provides a "clearinghouse" for information on the nature, location, and cost of geospatial data of the Bay Area. Geospatial data contain a distributional component, that is, data that can be represented on a map. Geospatial data include, for example, images of the surface of the Earth from ground-based cameras to satellite systems, digitized maps showing location of roads, parcels, transmission lines, and water features, and thematic maps of natural hazards or population distributions. BADGER allows users to locate geospatial data quickly. Second, BADGER provides a mechanism for public and private providers of geospatial data to

market data to users. After a user has located data of interest, he or she will be able to place an order through BADGER that will access the dataset on the server of the data provider, transmit the data to the user's machine, notify the user and the provider of completion of the transaction, and bill the user for the data delivered. Lastly, BADGER provides online applications to the user, that is, procedures by which a user can overlay and manipulate layers of geospatial data to generate an information product—fundamental, online, geographic information system functions.

Project personnel contributed to BADGER by development and implementation of the BADGER/Internet home page interface; development of secure, robust transaction protocols that allow BADGER users to access data on public and private servers; development of software for interactive location of parcels using street addresses or assessors' parcel numbers; and development and implementation of specific BADGER applications.

Two applications were demonstrated in FY96. The "Notice of Intent" application, developed for the Santa Clara Valley Water District, allows the owner/operator of a commercial enterprise to comply with a section of the clean water act by filing information electronically about the nature and destination of runoff from the site. The application completes a form and supplies three images showing the location as outlined on a digital orthophoto quad (aerial photograph) and map sheet, and an image showing the classification of the

surface area of the site as pervious or impervious. The application also calculates the percentage of land in each category. The online application, designed by BADGER and operated by BASIC, is expected to increase compliance and lower costs for the public and the agency administering the law. The second application developed by Ames staff allows users to locate a parcel in the Bay Area and display it in relation to categories of known natural hazards, for example, flood, ground motion during earthquakes, and wildfire.

BADGER is one way in which NASA data and computational technology are being used to serve commerce and real user needs, and to demonstrate the utility and practicality of the Internet.

Point of Contact: E. Sheffner
(650) 604-0021
ejs@gaia.arc.nasa.gov

Brazil/United States Environmental Monitoring and Global Change Program

James Brass, Vincent Ambrosia

This program involves a multidisciplinary team of international researchers performing cooperative studies to identify and mitigate the extent and environmental effect of deforestation and burning within the dry and wet tropical forests of Brazil. This research is performed in collaboration with Philip Riggan of the U.S. Forest Service; Joao Pereira, Heliosia Miranda, and Antonio Miranda of

the University of Brazilia; Theresa Campos of the National Center for Atmospheric Research; Robert Higgins of SIMCO Electronics; and Edward Hildum of Sverdrup Technology. The research is supported by NASA, the U.S. Forest Service, the U.S. Aid for International Development, the Instituto Brasileiro de Meio Ambiente e dos Recursos Naturais Renovaveis, the Brazilian National Space Institute, the Universities of Brazilia and Sao Paulo, and the National Center for Atmospheric Research.

Since 1992, aircraft campaigns have focused on the savannas of the central portion of Brazil. Collecting remote sensing and trace gas measurements, the campaigns have documented greenhouse gas generation, nutrient movement, and cloud condensation nuclei development in fires throughout the central Brazilian grasslands. The fire data continue to document the variability in flaming and smoldering conditions within the cerrados, with rates of spread between 0.1 and 3.0 meters per second and smoldering conditions lasting from 15 minutes to over 3 hours. Consistency in emission factors for nitrogen and carbon species continues, depending on the fuel type and condition.

The FY96 campaign focused on deforestation for the first time. Data from flights of the Airborne Infrared Disaster Assessment System over the Amazon basin and dry tropical forest documented large areas of cutting, similar to that of the Pacific Northwest of the United States. The sensor system was able to discriminate between the two major types of cutting (clearcuts and selective

harvesting), where individual high-value species are removed from the site.

Although the deforestation is important from many standpoints, the missions during August and September of 1996 concentrated on the impact of harvesting on fire occurrence and behavior. Two types of burning occur after harvesting of timber. If the area is clearcut, the resulting fire is intense and leaves a visible fire scar that can be observed using remote sensing. If the area is selectively harvested, fires occurring after the cutting are less intense and leave no telltale sign of a fire scar because the overstory left behind obscures the scar evidence.

The FY96 campaign provided the data necessary to determine the relationship between harvesting, fire activity, and greenhouse gas generation. These remotely sensed data are being analyzed and will help quantify the amount of harvesting that is occurring in each ecosystem and the resultant fire emissions. This information will be used to support the ongoing effort in Brazil to inventory the amount of greenhouse gases being produced by biomass combustion.

Point of Contact: J. Brass
(650) 604-5232
jbrass@mail.arc.nasa.gov

Carnegie/Ames/Stanford Approach Model

Christopher Potter

The Carnegie/Ames/Stanford Approach (CASA) model was developed for the study of contem-

porary patterns and processes of ecosystem trace gas exchange between the terrestrial biosphere and the atmosphere. The CASA model is unique in that it now simulates a host of trace gas fluxes (carbon dioxide (CO₂), methane (CH₄), carbon monoxide (CO), nitrous oxide (N₂O), and nitric oxide (NO)) on a scale that merges remote sensing, climate, radiation, vegetation, and soils datasets with nutrient transformation processes at the level of the soil microsite. This research was performed in collaboration with Pamela Matson of the University of California, Berkeley, Peter Vitousek of Stanford University, and Eric A. Davidson of the Woods Hole Research Center, Massachusetts.

The model has been refined over the past year to run on either a daily or a monthly time interval to simulate seasonal patterns in carbon fixation, nutrient allocation, litterfall, soil nitrogen mineralization, CO₂, CO, N₂O, NO emission, and CH₄ and CO uptake in soils. In FY96, a new global application of the CASA model, the hypothesis that variability in the ratio of N₂O:NO emissions over broad spatial gradients depends upon seasonal patterns of soil wetting and drying, was examined. It appears that gross rates of nitrogen mineralization account for major differences in gas emissions among ecosystem types. This finding has advanced the state of nitrogen (N) trace gas modeling notably by calculating indices of the global distribution of N cycling processes and estimating trace gas emissions based directly on those quantified mineralization fluxes.

The latest version of the CASA model predicts a total emission flux

of about 6 teragrams (10¹² grams) of N-N₂O per year and 10 teragrams of N-NO per year from soils worldwide (as illustrated in the figure (see Color Plate 21 in the Appendix)), exclusive of N fertilizer sources. While tropical forest ecosystems contribute over 50% of global annual N₂O emissions, cultivated areas are potentially significant sources on a regional basis. The next research goal that builds on the CASA foundation is to discern the manner by which to represent and apply *fertilized* soils and associated trace gas emissions.

Point of Contact: C. Potter
(650) 604-6164
cpotter@mail.arc.nasa.gov

Digital Array Scanning Interferometer

Steve Dunagan, Philip Hammer

A scanning interferometer, the digital array scanning interferometer (DASI), has been designed and fabricated for use in remote sensing of the ecosystem. The interferometer is based on charged-coupled-device sensor technology, providing spectral sensitivity over the range from 0.4 to 1.0 micron. Light from the ground scene is focused by means of an objective lens to an entrance slit aperture oriented normal to the scanning (flight) direction. After passing through the slit aperture, the light is collimated and divided using polarization optics into equal amplitude polarization vectors oriented along the ordinary and extraordinary axes of a

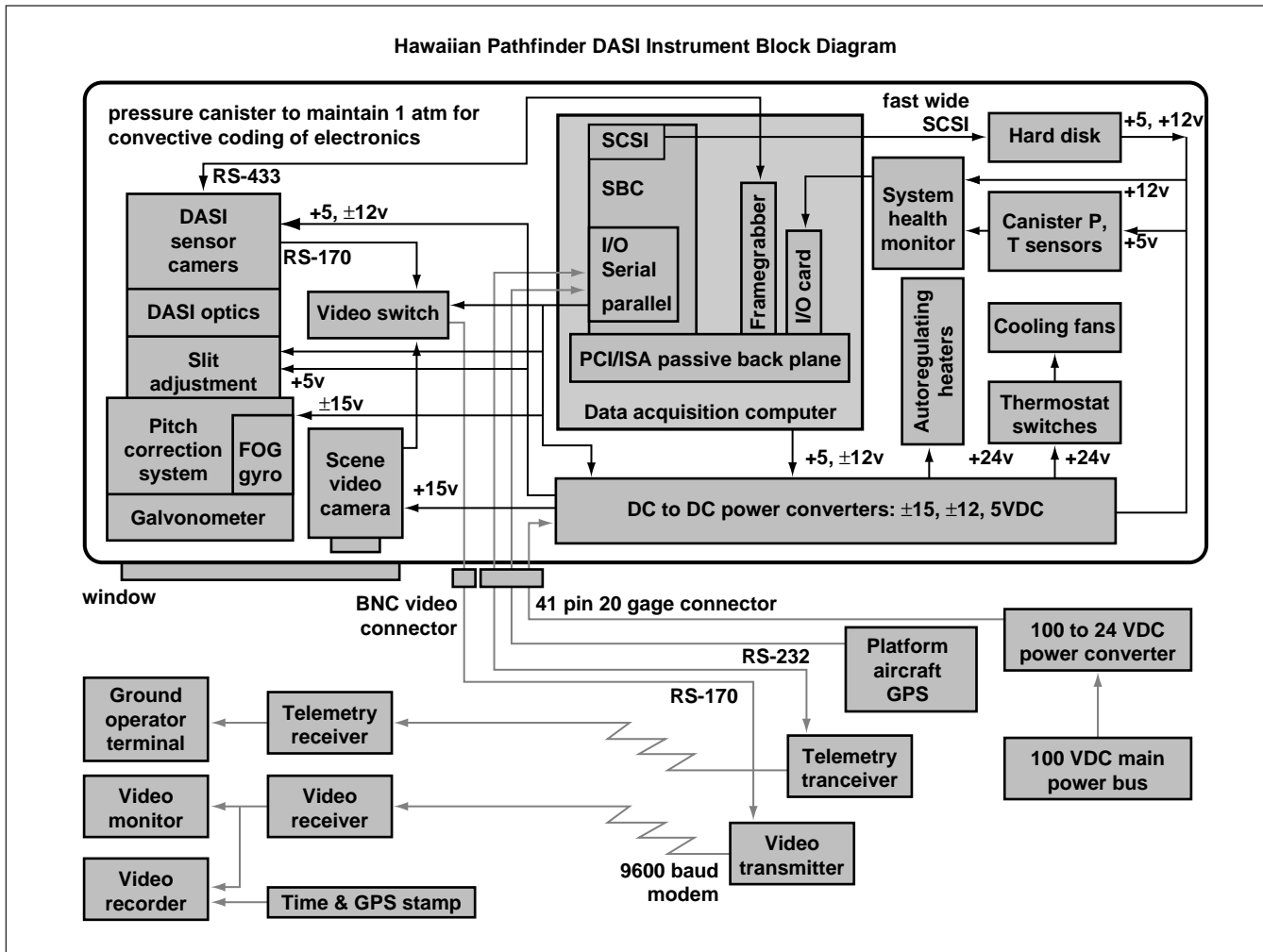


Fig. 1. Hawaiian Pathfinder DASI instrument block diagram.

Wollaston prism. The two polarization vectors are then recombined, collimated, and focused to the array detector, where an interferogram is formed. Ordinary and extraordinary rays experience a path length variation across the prism aperture. At the zero path difference location, the rays interfere constructively, regardless of wavelength, giving rise to a central peak intensity. On either side of this center burst wavelength, dependent interference gives rise to

an interferogram identical to the output of a scanning Michelson interferometer. The interferogram dimension (columns) of the array may then be Fourier transformed to yield the spectra of light originating from a ground pixel defined by the projection of the slit width and the array column width. Rows of the array provide the spatial distribution of information along the slit. Scanning the slit in the flight direction sweeps out an image hypercube.

The detector array, consisting of 240 by 750 pixels, may be configured along with the optics in several different ways to optimize spectral bandwidth and emphasize either spectral or spatial resolution. The array output is digitized at 10 bits. The primary design configuration provides a spectral range from 0.5 to 1.0 micron, with theoretical spatial resolution of 4.3 meters in the flight direction and 2.5 meters cross track

(at a 50,000-foot altitude), and theoretical spectral resolution of 13 nanometers at 0.5 micron and 50 nanometers at 1.0 micron. (Note that the interferometer samples at equal intervals in wavenumber space, resulting in a variation of wavelength resolution that scales approximately with λ^2).

The instrument has been interfaced to a data acquisition system and packaged in a pressurized container for deployment on a high-altitude, remotely piloted aircraft. The self-contained system requires less than 150 watts of power and weighs less than 10 kilograms. The data acquisition system comprises an industrial board level computer, with an Intel Pentium 100-megahertz processor, protocol control information (PCI) bus, and 256 megabytes of system random-access memory for direct memory access storage of hypercube data. A digital framegrabber and a small computer serial interface (SCSI) disk controller interface to the main computer board through a PCI passive backplane. An onboard 4.3-gigabyte hard disk permits storage of up to 16 hypercube datasets per flight. Data transfer is limited by the continuous streaming write speed of the hard disk, permitting the acquisition of 5 to 10 interferogram frames per second. A schematic diagram of the device is shown in the figure.

Point of Contact: S. Dunagan
(650) 604-4560
sdunagan@mail.arc.nasa.gov

Effect of Landuse on Regional Estimates of Coniferous Forest Water and Carbon Budgets

Joseph Coughlan, Jennifer Dungan

Geographic information systems (GISs) and ecosystem models are common tools that “scale up” measurements from ecological field experiments across landscapes, continents, and even the entire globe. Many predictions about the causes and effects of global change on the environment employ this scaling method in combination with remotely sensed data. NASA’s field experiments in grasslands (the First International Satellite Land Surface Climatology Project Field Experiment) and in northern forests (the Boreal Ecosystem Atmospheric Study) are two examples of the need to match the scale of ecological field measurements with remote-sensing data.

Remote-sensing data often come from coarse resolution (approximately 1 kilometer, or 0.63 mile) remote-sensing instruments such as the National Oceanic and Atmospheric Administration’s (NOAA’s) advanced very-high-resolution radiometer (AVHRR) and, in the future, NASA’s Earth Observing System. The mismatch between the size of the plots used in a field experiment and the size of the landscape units generated with this relatively coarse resolution data can cause scaling errors and result in an overprediction of carbon and water cycling rates. Researchers in this project are quantifying this unit-size error in a set of scaling experiments.

When moving from the plot scale (30 square meters) to climate model scale (1-degree cells), errors of up to 25 to 30% in regional water use and carbon cycling are observed for coniferous forests in the western United States.

Additionally, there is usually a mismatch between the size and shape of the units representing the landscape data used to make the regional estimates, but many researchers are unfamiliar with this error source. Project researchers have begun to document this GIS error and its effect on landscape-scale predictions made with ecosystem models. The two most common data layers are remotely sensed vegetation represented as a digital image of 1-kilometer-(0.63-mile-) long cells and large polygons mapping soil types that the GIS translates into a digital format. Unit size issues have important implications consequences for the use of soils data because soil map units usually comprise spatial units much larger in size than the vegetation map units.

In FY96, a new method was developed to control resizing of soils and vegetation units used to predict plant photosynthesis. This method reconstructs the soils data so that they are represented with “support” similar to the remotely sensed vegetation, the 1-kilometer (0.63-mile) grid cell. This reconstruction method enables researchers to conduct controlled experiments with GIS data at several spatial resolutions.

The method was implemented with a federally sponsored soils database for the state of Oregon and

a NOAA AVHRR image. The figure (see Color Plate 22 in the Appendix) shows two maps of soil water holding capacity (SWHC) for a portion of the state. The top map shows the homogeneous polygons commonly used to spatially represent soil variables. The bottom map shows the result of the new method for SWHC. Using this new map resulted in an underestimation bias of 11% in plant photosynthesis estimates for Oregon. The fact that results can vary significantly using the same model and data raises serious issues for understanding regional and global effects of climate change.

Point of Contact: J. Coughlan
(650) 604-5689
josco@gaia.arc.nasa.gov

Landsat Program

Edwin Sheffner

The Landsat Program is the longest running program to collect and distribute satellite imagery of Earth. The first Landsat satellite was launched in 1972, and the next in the series, Landsat 7, is scheduled for launch in 1998. In the quarter century of operation, the instruments on Landsat have transmitted millions of Earth images that have been employed by a broad user community for studies of global change, resource monitoring and assessment, local and regional planning, disease control, and education.

The primary program support task at Ames Research Center is to get information on Landsat to all elements of the Landsat data user

community, and to act as a repository for comments from the community on the current and future operation of the program. The task is accomplished through the use of a Landsat Program home page on the Internet. The home page was initiated in FY95; in FY96, extensive revisions and additions were made. Updated regularly with news items about the program, the page contains links to similar pages in the United States and abroad. Approximately half the users who log on to the home page are from outside the United States. An online questionnaire was also added in 1996 that will allow users to provide specific information on the program electronically.

Point of Contact: E. Sheffner
(650) 604-0021
ejs@gaia.arc.nasa.gov

Leaf Modeling

Lee F. Johnson, Chris Hlavka,
Philip D. Hammer, David L. Peterson

The proper interpretation of a land surface reflectance detected by air- or satellite-borne remote-sensing instrumentation generally requires corrections for distortions caused by the intervening atmosphere. If the signal originates from a vegetated surface, corrections for canopy and leaf anatomical structure are also needed. Although considerable progress has been made in the development of models to isolate the influence of atmosphere and canopy, less effort has been given to distortion due to leaf structure.

To address this factor, a within-leaf radiative transfer model (Leaf Experimental Absorptivity Feasibility Model, or LEAFMOD) has been developed and tested against empirical data. The model simulates the photon scattering and absorbing processes within the leaf, based upon solution of the one-dimensional radiative transfer equation, assuming a slab of leaf material with homogeneous optical properties. When run in the forward mode, LEAFMOD generates the leaf bidirectional reflectance and transmittance profiles given a specified leaf thickness, optical characteristics (scattering and absorption profiles) of leaf constituents, and concentrations of leaf constituents. In the inverse mode, LEAFMOD computes the total within-leaf absorption and scattering coefficients from the measured leaf thickness, reflectance, and transmittance. Inversion experiments with real and simulated data demonstrated that the model appropriately decouples scattering and absorption processes within the leaf.

The model produced absorption profiles for fresh leaves, with peaks at locations corresponding to the major absorption features of water and chlorophyll. Using available spectral data for grape leaves, the magnitude of the absorption coefficient profile in the visible region was strongly correlated to chlorophyll concentration determined from conventional laboratory analysis. Spectral data from a leaf-stacking and drying experiment demonstrated that absorption features related to various biochemical constituents could be identified in the dry-leaf absorption profile derived by LEAFMOD.

The model can be used to evaluate fresh-leaf spectral sensitivity to leaf chemistry, and also to investigate the influence of both leaf chemistry and leaf amount on vegetation canopy reflectance. Barry Ganapol, University of Arizona, collaborated with the Ames investigators on this project.

Point of Contact: L. Johnson
(650) 604-3331
ljohnson@mail.arc.nasa.gov

Mapping Northern Ecosystems: Applications for Circumpolar Methane Exchange

Vern Vanderbilt, Guillaume Perry, Joel Stearn

The goals of this project are to improve estimates of the areal extent of northern, high-latitude wetlands and to gain insight into the role of northern ecosystems in the global methane (CH₄) budget and, in so doing, provide improved estimates of global CH₄ exchange.

The role of northern wetlands in global atmosphere/biosphere interactions remains an unresolved but key factor in projecting climatic change in response to increasing atmospheric concentrations of greenhouse gases, such as carbon dioxide and methane. Wetlands north of 45°N represent globally significant methane sources—the organic carbon stored in the peat and soil beneath these ecosystems exceeds that of any other biome on Earth. Since climatic warming is predicted to be most dramatic in

northern high latitudes, microbial decomposition processes acting on these carbon stores will almost certainly lead to increased atmospheric loading of carbon dioxide (CO₂) and CH₄, thus potentially enhancing the greenhouse phenomenon even further.

The areal representation of boreal wetlands, the source areas for CH₄, is poorly known on regional to global scales, particularly the areal extent of bogs, fens, and open-water lakes and ponds. Various estimates of the areal extent of northern wetlands differ nearly sevenfold. These differences in global inventories lead to large discrepancies in the estimation of overall exchange of CH₄ from northern sources and sinks because emission rates from the various individual land covers (fens, bogs, open water, wetlands, and nonwetlands) can vary by a factor of more than 100:1.

The analysis of results for the Boreal Ecosystem-Atmosphere Study (BOREAS) shows that glitter, the sometimes visually blinding sparkle of sunlight from water surfaces, provides a powerful signal uniquely identifying inundated areas. These BOREAS results demonstrate that inundated areas may easily be separated from noninundated areas. It is also possible to discriminate and accurately classify fens, open water areas, and forested areas because the visually blinding glitter of sunlight off ruffled water surfaces provides a strongly angular signature reflection characteristic of wetlands. Consequently, these classifications and estimates of the areal extent of fens and open water areas are significantly more accurate than similar estimates based upon other sources

of remotely sensed data, such as the Landsat thematic mapper (TM) sensor. These encouraging results provide an order of magnitude improvement in the accuracy of estimates of the areal extent of wetlands in the BOREAS study region.

Point of Contact: V. Vanderbilt
(650) 604-4254
vvanderbilt@mail.arc.nasa.gov

Modern Ecosystems Research: Effects of Increased UV-B Radiation

Hector L. D'Antoni, J. W. Skiles

The link among these efforts is the process of stratospheric ozone depletion and the consequent increase of ultraviolet-B radiation (UV-B) in the biosphere. Given the deleterious effect of excessive UV-B in living organisms, it is imperative to establish what effects, if any, are produced by the current levels of UV-B.

Using alfalfa (*Medicago sativa* L.) as the experimental plant, several hypotheses have been tested, including: (1) production of screening pigments is stimulated by UV-B radiation; (2) node elongation is affected by UV-B radiation; (3) phenological stages (that is, flowering) are controlled by UV-B radiation; and (4) alfalfa plants grown under UV-B exclusion have higher chlorophyll concentration. In contrast with most of the work published in this area of research, these experiments were carried out with sunlight as the only source of UV-B radiation.

Plants that were grown in a growth chamber in June were transferred to a shed in the field and grown there for 6 to 8 weeks. The shed provided two chambers with identical environmental conditions except for the UV regime. Chamber 1 is fitted with a cellulose acetate screen that removes 15% of the UV band irradiance to simulate a preozone-depletion environment. Chamber 2 is fitted with a polyester screen that removes the entire UV-B irradiance band. The experiments, run the past two summers, have validated all four hypotheses and led to new questions and hypotheses. Data require intensive statistical analysis before publication.

A similar effort with the University of Mar del Plata in Argentina has resulted in several outcomes. The Antarctic spring-time "ozone hole" often reaches southern South America during the austral spring. Data show that 15 to 18 days of the three-month season have a low stratospheric ozone concentration in Ushuaia (southern Argentina), while ground-level UV-B records are concomitantly high. Negative correlation was found between stratospheric ozone concentration and UV-B irradiance at ground level. Negative correlation is higher in the wavelength range of 289 to 307 nanometers, known to damage DNA, chlorophyll, indole acetic acid, gibberelins, abscisic acid, and other important plant growth molecules.

An extended visit to Argentina resulted in the reflectance analyses and in daily measurements of solar irradiance in the 300- to 750-nanometer range in Mar del Plata (38°S) that can be compared to

those of Moffett Field, at approximately the same latitude in the Northern Hemisphere.

This research was performed in collaboration with G. R. Daleo, S. Burry, M. C. Lombardo, A. C. Mayoral, P. Palacio, and M. E. Trivi of the University of Mar del Plata, Argentina; Roy Armstrong, J. Corredor, and J. Morell of the University of Puerto Rico (Mayaguez); and Jaime Matta of the Ponce School of Medicine, Ponce, Puerto Rico.

Point of Contact: H. D'Antoni
(650) 604-5149
hdantoni@mail.arc.nasa.gov

Optimizing an Ecosystem Model for Use on Parallel/Distributed Processors

J. W. Skiles, Cathy Schulbach

The goal of this project is to update models/codes based on current ecological knowledge with state-of-the-art computer simulation technology. Such modifications will decrease execution time, enabling simulation of larger geographical areas and/or performance of more simulation experiments. Areas of emphasis are in ecology and computer science, with the expectation that techniques developed in this project will serve as a blueprint for the construction of future Earth system models that will be run on supercomputers showing how processes can be coded for distributed processing. In addition, this project is expected to enhance Ames Research Center's expertise in the

areas of information technology and ecosystem science.

As a demonstration, a grassland ecosystem model is being used to simulate the Great Plains (GP) of the United States, an area of approximately 60,000 advanced very-high-resolution radiometer pixels. Large amounts of data are necessary to initialize the model for operation on a geographical area of this size. Data required include soil types, plant community information, and weather drivers. A major undertaking is the establishment of data structures whereby the model can access correct information for a specified location, access stored soils data, calculate intermediate and state variables, and update biomass and soil-water variables on a pixel-by-pixel basis across the time frame of the simulation. All this is to be done while maintaining the biological and ecological dynamics of the ecosystem(s) being simulated.

Computer science areas of emphasis are: (1) establishing protocols for rehosting scalar code to vector supercomputers and distributed-processing supercomputers; (2) validating metrics for load balancing and processor scheduling; (3) using different types of ecological model codes (difference equation, partial differential equations, correlation equation) in the distributed environment; and (4) using automated tools to aid in the rehosting process.

Although most ecosystem models include state-of-the-art ecological concepts, they employ scalar coding that does not take advantage of the power of contemporary computing platforms.

Rehosting these codes to supercomputers entails restructuring the code itself and using available command-level instructions during compilation.

Because of weather patterns and the resultant plant communities on the GP, it is possible that some locations will have growing plants while others will not. This scenario sometimes causes a processor on a multiprocessor supercomputer to be idle while others are processing the plant growth part of the code. Activity in this project focuses on efficiently balancing the load of each processor so that none are idle, thereby decreasing the execution time for the simulation experiment.

Progress to date includes the construction of interpolation algorithms for missing data, stochastic weather generation for 31 locations on the GP, and the establishment of gaming scenarios for global change modeling, including the incorporation of increases or decreases in temperatures and precipitation and the seasonal timing of precipitation events.

Point of Contact: J. Skiles
(650) 604-3614
jskiles@mail.arc.nasa.gov

Paleoenvironmental Research

Hector L. D'Antoni

The goal of this research is to calibrate modern pollen data in terms of satellite remote-sensing data of modern vegetation, produce calibrated equations of pollen as a

function of vegetation, and use these equations to "hindcast" (as opposed to forecast) past vegetation from fossil pollen sequences obtained from stratified sediment deposits.

Many models used to predict the environmental future of Earth are driven by remotely sensed data of vegetation. Historical remote-sensing databases of vegetation reach back only a few decades. Such a time frame is not sufficient to appreciate long-term environmental processes. Paleoenvironmental data might help solve this problem. However, paleoenvironmental data are not compatible with remotely sensed data and, hence, they are of limited use for modeling.

The efforts in FY96 concentrated on the Oregon Pollen Transect, a collection of modern pollen samples from central Oregon, taken every 10 miles from Dayville in central Oregon to Newport on the Pacific coast, and crossing vegetation zones of ponderosa pine, western juniper, fir and Douglas fir, western hemlock, alder, and sitka spruce. A predictive equation of remote-sensing vegetation indices such as the normalized difference vegetation index (NDVI) was completed. Vegetation in Oregon has changed during the last 50 years, and in some localities the original floristic composition is difficult to determine from current evidence. To solve this problem, a database has been constructed with modern pollen data produced between 1930 and 1949. These data will help to recalibrate predictive equations of NDVI and other indices and, in turn, these equations will assist to hindcast Holocene (that is, the last 10,000 years) vegetation

indices that can be used in predictive models of environmental change. Thus, the data used to parameterize these models will span over 10,000 years rather than the customary few decades and will help differentiate long cycle fluctuations from meaningful trends of environmental change.

Point of Contact: H. D'Antoni
(650) 604-5149
hdantoni@mail.arc.nasa.gov

Scientists' Intelligent Graphical Modeling Assistant

Jennifer Dungan

Over the past 30 years, scientific software models have played an increasingly prominent role in the conduct of science. Unfortunately, implementation of scientific models can be difficult and time-consuming, and software engineering support available specifically for constructing scientific models is scant. Scientists' Intelligent Graphical Modeling Assistant (SIGMA), an interactive, knowledge-based, graphical software development environment, was created at Ames to fill this gap. SIGMA is designed to help scientists rapidly prototype their scientific models by simplifying construction, modification, and reuse of modeling software, and to provide a supportive computational environment for exploratory model building.

In FY96, two well-known models describing radiative transfer in vegetation canopies were added

to the SIGMA knowledge base. Sensitivity experiments were conducted with these models to investigate the relative importance of model variables in a more systematic way than is usual with traditional programming languages. In addition, two graduate students at separate universities tested SIGMA over the Internet. They were able to navigate the data flow graph for the ecosystem model, query the knowledge base for details on variables and equations, and build the rudiments of a new model.

Point of Contact: J. Dungan
(650) 604-3618
jennifer@gaia.arc.nasa.gov

ATMOSPHERIC CHEMISTRY

Airborne Natural Radionuclide Measurements in the Development and Validation of Global Three-Dimensional Models

**Mark Kritz, Stefan Rosner,
Robert Chatfield, Leonard Pfister**

As the sources, lifetimes, and atmospheric behavior of natural radionuclides (for example, ^7Be , ^{32}P , ^{210}Pb , and ^{222}Rn (radon)) are generally well understood, comparison of their observed distributions with model prediction is finding increasing application in the development and validation of the global models used to assess global change. Such comparisons, the focus of two

international workshops (December 1993 and August 1995) sponsored by the World Climate Research Programme, are a key element in the validation of the models to be used to assess the possible impact of aircraft emissions on the atmosphere in NASA's Atmospheric Effects of Aviation Program (AEAP).

Project activity in this area has been divided between the acquisition and the application of airborne radionuclide measurements for this purpose. Over the last decade, the instrumentation has flown on more than 100 flights aboard NASA aircraft, including the C-130, C-141, DC-8, and ER-2. For example, in the summer of 1994, the instrumentation was onboard the C-141 on 15 flights out of Moffett Field, acquiring a statistically significant climatology of the summertime vertical distribution of radon over northern California. This dataset found extensive application at the August 1995 World Climate Research Programme (WCRP) Workshop, and is currently being used in the validation of the NASA AEAP core model.

A more extensive set of similar airborne radon measurements was obtained over the central and western United States in the summer of 1996, flying aboard a NASA Lear jet. In addition to radon, measurements of carbon monoxide (CO), carbon dioxide (CO₂), and methane (CH₄) were made in cooperation with the National Oceanic and Atmospheric Administration (NOAA) Climate Monitoring Diagnostics Laboratory, Boulder, Colorado, and measurements of ozone (O₃) were made in cooperation with the National Center for Atmospheric Research Facility, Boulder, Colo-

rado. The combined dataset will be used by NOAA in refining their budgets of these carbon species in the northern hemisphere, and in the development and validation of at least two three-dimensional global chemical transport models.

Point of Contact: M. Kritz
(650) 604-5493
mkritz@asrc.cestm.albany.edu

Reactive Nitrogen Data from the Upper Troposphere and Lower Stratosphere

**Hanwant B. Singh, Alakh Thakur,
Peter Mariani**

NASA has launched a subsonic aircraft assessment program (SASS) to determine the effect of the current and future subsonic fleet on the Earth's environment as quantitatively as possible. A key SASS objective is to assess the effect of nitric oxide (NO) emissions from subsonic aircraft on atmospheric ozone (O₃), especially in the region of the upper troposphere/lower stratosphere. A large number of airborne studies in the free troposphere (for example, global troposphere experiment (GTE) and tropospheric ozone/stratospheric ozone (TROPOZ/STRATOZ)) and lower stratosphere (for example, the Airborne Arctic Stratospheric Expedition II) have been performed in the last decade, and a sizable body of data on reactive nitrogen species has been collected from both hemispheres. Although these data have been, to a degree, analyzed as individual datasets, no comprehen-

sive analysis and synthesis has been undertaken. Tasks in this study are to acquire, analyze, and interpret experimental data on reactive nitrogen species (along with ozone, hydrocarbons, and selected tracers) that have been collected over the last decade, with focus on the upper troposphere and lower stratosphere. The aim is to provide an overall synthesis of the present understanding of reactive nitrogen chemistry and recommendations for future field research, based on a comprehensive analysis of available data. Analysis of these data was completed in FY96 and the results are being finalized.

Point of Contact: H. Singh
(650) 604-6769
hsingh@mail.arc.nasa.gov

Airborne Autotracking Sunphotometry

Philip B. Russell, John M. Livingston, James Hanratty, Damon Ried, Jill Bauman

Atmospheric aerosols (suspensions of airborne particles comprising hazes, smokes, and thin clouds in the troposphere and stratosphere) play important roles in determining regional and global climates, the chemical composition of the atmosphere, and atmospheric transport processes. As knowledge has advanced in each of these fields, so has recognition of the importance of aerosols. As a result, national and international bodies have called for increased efforts to measure aerosol properties and effects, as a means of

improving predictions of future climate, including greenhouse warming, ozone depletion, and radiation exposure of humans and other organisms.

A fundamental measure of any aerosol is the way it attenuates a beam of light of various colors (that is, wavelengths). This attenuation is usually described in terms of the quantity optical depth. The dependence of optical depth on light wavelength is the optical depth spectrum.

The Ames airborne sunphotometers determine the optical depth spectrum of aerosols and thin clouds by tracking the sun and measuring the (relative) intensity of the solar beam in several spectral channels. The tracking head of each instrument mounts external to the aircraft cabin, so as to increase data-gathering opportunities relative to in-cabin sunphotometers and also to avoid data contamination by cabin-window effects. Each channel consists of a baffled entrance tube, an interference filter, a photodiode detector, and an integral preamplifier. The filter/detector/preamplifier sets are temperature-controlled to avoid thermally induced calibration changes. Each instrument includes an entrance-window defogging system to prevent condensation (a problem otherwise common in aircraft descents). Solar tracking is achieved by azimuth and elevation motors driven by differential sun sensors. In general, sun tracking is achieved continuously, independent of aircraft pitch, roll, and yaw, provided rates do not exceed approximately 8 degrees per second and the sun is above the aircraft

horizon and unblocked by clouds or aircraft obstructions (for example, tail, antennas).

Data are digitized and recorded by an onboard data acquisition and control system. Real-time data processing and color display are routinely provided. The science dataset includes the detector signals, derived optical depths, detector temperature, sun tracker azimuth and elevation angles, tracking errors, and time. Each instrument must maintain its radiometric calibration (including window and filter transmittance, as well as detector responsivity and electronic gain) to within 1% in each spectral channel for periods of several months to a year.

In July 1996, the first science flights of the 14-channel sunphotometer (developed under the NASA Environmental Research Aircraft and Sensor Technology Program) were made on the Pelican (modified Cessna) aircraft of the Center for Interdisciplinary Remotely Piloted Aircraft Studies during the Tropospheric Aerosol Radiative Forcing Observational Experiment.

Point of Contact: P. Russell
(650) 604-5404
prussell@mail.arc.nasa.gov

Analysis of Stratosphere/Troposphere Exchange

Leonhard Pfister, Henry Selkirk

Aircraft atmospheric sampling experiments require the support and advice of meteorologists to be successful. The purpose of this

project is to analyze meteorological fields both during and after field experiments so as to maximize the scientific return of the sampling campaigns. The emphasis in this project is to provide meteorological satellite information as it pertains to stratospheric transport and stratosphere/troposphere exchange processes.

During FY96, Ames provided meteorological coordination for the Stratospheric Tracers of Atmospheric Transport (STRAT) ER-2 sampling mission and the Tropical Ozone Transport Experiment (DC-8 mission). Three major STRAT field campaigns were undertaken. Back trajectory analyses of STRAT data yielded evidence that midlatitude cirrus shields can determine the water vapor content of the lowermost stratosphere. Some simple cloud height algorithms that can be used in real time for flight planning for the low-altitude (tropospheric) ER-2 flights have been developed. These algorithms use a combination of meteorological analyses and satellite imagery to determine the cloud altitude at any point in a satellite image.

Finally, it has been shown that the subvisible cirrus observed by the DC-8 south of Hawaii are probably due to air that originates in Micronesia and travels northward to the subtropical jet, eastward toward Hawaii, and southward—following an upper tropospheric/lower stratospheric anticyclone.

Point of Contact: L. Pfister
(650) 604-3183
pfister@telsci.arc.nasa.gov

Use of Argus in Atmospheric Studies

Max Loewenstein

The Argus instrument, a tunable-laser, infrared spectrometer, was designed to measure the long-lived tracers methane (CH_4) and nitrous oxide (N_2O) in the stratosphere up to altitudes of 30 kilometers. The ratio of these two tracers as a function of altitude provides important information on the dynamics of different regions of the stratosphere: the surf zone, the tropical pipe region, and the polar region distinguished by its strong winter vortex isolation.

In June and September 1996, the new Argus lightweight N_2O and CH_4 instrument was completed and flown on balloon launches to higher than 30 kilometers from Ft. Sumner, New Mexico (34 degrees N), the site of the NASA National Scientific Balloon Facility. In June, the instrument performed flawlessly in an engineering sense, but no reportable data resulted because of inadequate control of the diode laser mount temperatures. This control limitation was corrected in time for the September launch. In September, all aspects of the Argus instrument performed well, and ascent and descent profiles for N_2O were obtained. The methane channel is being brought up to operational status. The Argus instrument has been prepared and shipped to Juazeiro do Norte, Brazil, for use in the Orbiter Maneuvering System tropical field campaign.

Point of Contact: M. Loewenstein
(650) 604-5504
mloewenstein@mail.arc.nasa.gov

Airborne Tunable Laser Absorption Spectrometer

Max Loewenstein, James R. Podolske

The Airborne Tunable Laser Absorption Spectrometer (ATLAS) instrument was designed and built in the mid-1980s to measure stratospheric tracer fields from the ER-2 high-altitude research aircraft. During the decade of its operation, ATLAS has been used primarily to measure the nitrous oxide (N_2O) tracer field on several campaigns primarily focused on polar and midlatitude processes in the stratosphere. N_2O is a very long-lived tracer of stratospheric dynamics. Normally, chaotic-appearing observations of molecular constituents of the atmosphere such as reactive nitrogen (NO_y), carbon dioxide (CO_2), water vapor (H_2O), chloro-fluoro-carbons (CFC) and others are “smoothed” by constructing correlation diagrams of these observations plotted versus N_2O . These correlations then provide important chemical and dynamical diagnostic information on the state of the atmosphere.

The ATLAS instrument took part in the continuing Stratospheric Tracers of Atmospheric Transport (STRAT) campaigns, with field deployments carried out in October 1995 and February, July, and September 1996. The instrument continues to work flawlessly and returns very-high-quality N_2O tracer data on all flights. ATLAS N_2O data continue to be the dataset of choice for analyses carried out within the STRAT community. Data comparisons with the aircraft laser infrared

absorption spectrometer (ALIAS) and airborne chromatograph atmospheric trace species (ACATS) N₂O presented at a July 1996 STRAT workshop show that ATLAS data are of the highest quality and are true to its stated 3% accuracy.

During the Airborne Southern Hemisphere Ozone Experiment and the follow-on Stratospheric Tracers of Atmospheric Transport campaign in 1995 and 1996, a comprehensive new dataset on CO₂ and N₂O in the northern hemisphere extending from the equator to 60 degrees N was accumulated. Several important results have emerged from this new and unique dataset: Tropospheric air carrying its normal seasonal cycle and secular trend of CO₂ continuously enters the lower tropical stratosphere and is rapidly (in about one month) transported to both hemispheres. The mean age of the observed midstratospheric air is about 6 years. Pollutant exhaust gases, which will be deposited by proposed new stratospheric aircraft into the midlatitude lower stratosphere, will probably exceed the best current predictions by 30 to 100%. These results may have important implications for the influence of stratospheric aircraft on the ozone layer.

Point of Contact: M. Loewenstein
(650) 604-5504
mloewenstein@mail.arc.nasa.gov

Convectively Generated Gravity Waves

Leonhard Pfister

This work evaluates the influence of gravity waves generated by convection on stratospheric circulation in the tropics. Each convective event emits a spectrum of gravity waves with a broad variation of phase speeds. These waves will break at a variety of altitudes corresponding to these phase speeds; when they do, they will exert a force at that altitude that can affect the overall circulation of the tropical stratosphere. Understanding the nature of this force quantitatively is essential to obtaining a comprehensive picture of the transport of trace constituents such as ozone, as well as the constituents that govern ozone production and destruction. The assessment of the importance of these convectively generated gravity waves has two steps: evaluation of the amplitude and spectrum of waves from each convective system using measurements, and extrapolation of these results to global budgets using global satellite information.

This task has progressed in two areas. First, half-hourly datasets of geostationary operational environmental satellite (GOES-8) imagery for the strongly convective Panama region have been prepared for spectral analysis. The objective is to use the satellite data to establish the frequency distribution at shorter spatial and time scales than that addressed by previous satellite spectral studies. Second, two case studies of gravity waves generated by convection as observed by ER-2 aircraft measurements have been

completed. One of these, from the Stratospheric Tracers of Atmospheric Transport campaign, shows gravity waves with horizontal wavelengths of about 50 kilometers and vertical wavelengths of 5 to 10 kilometers. This result suggests that a simple "transient mountain at the tropopause" conceptual model can explain only part of the mesoscale gravity wave variance. Evidence was also found of inertia-gravity waves with horizontal wavelengths of 1000 kilometers, consistent with studies that inferred horizontal wavelengths using vertical profiles and inertia-gravity wave dispersion relationships.

Point of Contact: L. Pfister
(650) 604-3183
pfister@telsci.arc.nasa.gov

The ER-2 and DC-8 Meteorological Measurement Systems

K. Roland Chan, T. Paul Bui, Antonio A. Trias, Stuart W. Bowen, Jonathan Dean-Day

The Meteorological Measurement System (MMS) provides in situ, high-resolution meteorological parameters (pressure, temperature, and the three-dimensional wind vector). The MMS consists of three major systems: (1) an air-motion sensing system to measure the velocity of the air with respect to the aircraft; (2) an aircraft-motion sensing system to measure the velocity of the aircraft with respect to the Earth; and (3) a data acquisition system to sample, process, and

record the measured quantities. Since much of the instrumentation is attached to the aircraft at specially chosen locations, the MMS is a platform-specific instrument that cannot be transported from one aircraft to another.

The MMS is uniquely qualified to investigate atmospheric mesoscale (gravity waves) and microscale (turbulence) phenomena. Since the MMS provides quality data on atmospheric state variables, MMS data have been extensively used in almost all investigations to interpret the in situ experiments aboard the same aircraft.

Over the past decade, the ER-2 MMS has successfully participated in many missions, including the Stratospheric Tracers Atmospheric Transport missions in FY95 and FY96.

The MMS instrumentation has been modified several times. Recent significant modifications to improve the system reliability include: (1) improved navigation data using the Litton LN-100G, a lightweight ring laser gyro embedded in the Global Positioning System inertial reference system; (2) improved static pressure measurement accuracy and precision by using quartz diaphragm transducers, which have very low thermal expansion coefficients; (3) improved pitot pressure measurement, and hence true-air-speed measurement by customizing the pressure range calibration to the ER-2 flight envelope; and (4) a Rosemount open-wired, fast-temperature sensor installed forward on the fuselage, well outside of perturbed boundary layer flow,

making the temperature measurement independent of the aircraft attitude effects.

The DC-8 MMS is a new instrument, flight-tested for the first time in May 1996. The MMS performed very well during the subsonic aircraft: contrail and cloud effects special study, which also began its deployment mission in May. A preliminary set of MMS products are measurements of static pressure (p), temperature (T), the east/west component of wind (u , with east being positive), the north/south component of wind (v , with north being positive), the vertical component of wind (w , with up being positive), latitude, longitude, and pressure altitude. Analysis of the three sets of temperature data (two sets from the T_{slow} probe and one set from the T_{fast} probe) indicates that the self-consistency of the temperature measurement is within ± 0.3 degree kelvin of the MMS design specifications.

Point of Contact: K. Chan
(650) 604-6263
rchan@mail.arc.nasa.gov

Environmental Research Aircraft and Sensor Technology

Steve Wegener

Environmental research aircraft and sensor technology (ERAST) provides focus for critical technology development and flight demonstration that reduces the technical and economic risk of using remotely piloted aircraft (RPA) as a means to

collect scientific data in a timely and cost-effective manner. The ERAST sensor element addresses the science and payload aspects of RPA missions. Early focus centered on instruments for high-altitude (25 kilometers) atmospheric research. More recently, efforts have supported a wider range of science mission development activities, embracing a broader range of users. The present research is being performed in collaboration with the National Oceanographic and Atmospheric Administration, other NASA Centers, the National Center for Atmospheric Research, the U.S. Department of Energy Laboratories, several universities, and the Office of Naval Research. New concepts in RPA over the horizon (OTH) communications, key to extended missions, are being developed and tested. Research in extremely miniaturized sensor technologies holds promise for profound changes in the capability of RPAs.

The ERAST sensor element made significant contributions to the outreach in both the sensor and platform communities in FY96. The sensor element sponsored three retreats for sensor engineers during the year, which brought together a small group of experienced engineers from ERAST instrument development projects.

The ERAST sensor element demonstrated a major milestone in FY96: the ability to monitor and command RPA payloads via a satellite communications link. The airborne data system and an infrared camera aboard the Scaled Composites D2 RPA were monitored for status, the communication package was reconfigured in flight, and the

camera was commanded to acquire imagery and downlink data. This accomplishment demonstrates the ability to monitor and command platforms and payloads OTH, a capability critical for operation at distances greater than 160 kilometers from homebase. OTH communications supporting interactive research platforms will enhance operational safety and scientific productivity.

The ERAST OTH communication development effort provided the following OTH hardware capabilities in FY96:

- The telemetry interface and data system was upgraded to be compatible with the Tracking and Data Relay Satellite System (TDRSS) interface electronics. Flight tests were conducted in December 1995 and September 1996.
- TDRSS Interface electronics.
- An infrared imaging payload was developed to demonstrate the OTH capability, build expertise for remote sensing science, and foster cooperation with the Lawrence Livermore National Laboratory.
- System integration and testing demonstrated the system capability on NASA Lear jet and ERAST D2 platforms.
- A systematic approach to requesting and obtaining approval for use of radio frequency spectra for TDRSS demonstration was established.
- A "roadmap" for OTH capability for the ACE 2 was established. Extremely small sensor systems are key to placing meaningful payloads at very high altitudes. New approaches to sensor systems are being explored to reduce payload

weight, volume, and power requirements.

The ERAST sensor element sponsored a review of current atmospheric science instruments used in the Upper Atmosphere Research Program. The intention was to identify approaches where micromachine concepts might lead to significant breakthroughs required to shrink, in a revolutionary way, the weight, volume, and power consumption of today's payloads. The study (in technical review) concluded that, although some reduction was possible, reductions by a factor of ten required new measurement concepts. New work in surface acoustic wave technology suggests that sensitivities comparable to today's instruments can be achieved in shoe-box size packages. In collaboration with NASA's Mars Pathfinder project, NASA's Sensors 2000!, Sandia National Laboratories, the University of California, Berkeley, and the Jet Propulsion Laboratory, the ERAST sensor element is funding a laboratory study to demonstrate parts-per-billion measurement of carbon monoxide (CO), nitrous oxide (N₂O), water vapor, and ozone with acoustic (surface acoustic wave and flexural plate) and chemiresistive technologies. Demonstration of these results in a modular sensor array instrument is slated for FY97.

Point of Contact: S. Wegener
(650) 604-6278
swegener@mail.arc.nasa.gov

Global Emissions Inventories for Radon and the Cosmogenic Radionuclides

Mark Kritz

Natural radionuclide measurements are finding increasing application in the development and validation of global circulation and chemical tracer models. In particular, comparisons of the atmospheric radon distributions predicted by global models with radon measurements made at a surface station and aboard NASA aircraft flying in the free troposphere have been used in two recent World Climate Research Programme workshops, and by the Global Modeling Initiative component of NASA's Atmospheric Effects of Aviation Program, to identify shortcomings in the convective and long-range horizontal transport parameterizations used in state-of-the-art global atmospheric models. However, as this work has continued and progressed and models have continued to improve, there has been a growing need to review and perhaps reassess current estimates of the source functions for these radionuclides, including not only that of radon (²²²Rn) but also those of ⁷Be and other natural radionuclides.

To this end, the International Global Atmospheric Chemistry (IGAC) Program has included a natural radionuclide element in its Global Emission Inventories Activity (GEIA). The natural radionuclide panel, functioning under the GEIA/IGAC umbrella, has participants

from France, Germany, Japan, New Zealand, and the United States. Projects in FY96, performed in collaboration with Stephen Schery of the New Mexico Institute of Technology and Phil Rasch of the National Center for Atmospheric Research, included: (1) work on a global radon emissions map to replace the 1 atom/centimeter²/second global mean value currently in widespread use, and (2) initiating (as a complement to direct onsite local point surface flux measurements) a subproject to infer the global mean radon source functions using long-term observed mean atmospheric distributions of radon and the deposition at the surface of its decay product ²¹⁰Pb.

Point of Contact: M. Kritz
(650) 604-5493
mkritz@asrc.cestm.albany.edu

The Great African Plume: Tropical Carbon Monoxide and Ozone Simulation

Robert B. Chatfield

Maintenance of high concentrations of pollutants, for example, tropospheric carbon monoxide and ozone, in seemingly distant regions of the tropical troposphere is the focus of this research. Each of these compounds has a major role in controlling the oxidizing capacity of the lower atmosphere. It was thought that the source of a particularly striking accumulation of tropospheric ozone in the middle of the Equatorial Atlantic Ocean was due to biomass burning taking place in

South America or Africa. However, until this work, the roles that each played and the process for mid-oceanic, midtropospheric pollution were not clear. The work describes the origin and character of the Great African Plume from biomass burning.

A three-dimensional tropospheric chemistry model that assimilates the winds and weather that prevailed during NASA's airborne expedition, the Tropical Atmospheric Chemistry Experiment—Atlantic, has been created. The model also helps to establish important quantitative details, such as the amount of biomass-burning emission of carbon monoxide and the ability of clouds to vent material to the upper troposphere. The latter venting process creates the Upper South American Plumes and the Upper African Plume, which pollute virtually the entire southern hemisphere.

The maintenance of the concentrations of carbon monoxide and tropospheric ozone are the results of complex interplay of many natural and social phenomena that make up tropical agriculture, followed by interactions of many chemical species and meteorological processes. This project has made explicit several, while pointing out a remaining anomaly in the theory that is now widely recognized. The most visible concentration of tropospheric ozone in the mid-Atlantic appears to be caused by the Great African Plume, which extends up to about 6 kilometers. This plume arises out of a convergence of polluted material in Equatorial and Southern Africa. Pollution is then lofted in the interoceanic convergence of the

region, by processes that involve intense boundary layer mixing and convective clouds reaching to the upper troposphere. The lower tropospheric mixing process is the main source of slow, westward moving pollution episodes that produce maxima in tropospheric carbon monoxide and ozone just south of the Equator, and extend to the western tip of South America. Thunderstorm mixing of pollutants tends to lead to southeastward movement of these pollutants, and great pinwheeling plumes of carbon monoxide and ozone spin out from the central convective areas of Africa and especially South America, particularly above 8 kilometers. The model has successfully simulated aircraft observations in many details, and seems to explain more generally the satellite observations of carbon monoxide.

Most ozone in the model simulations seems to be made close to the source, over the continent, only a day or so downwind of the agricultural burning that is its source. Theory and models suggest that nitrogen oxides die out, and ozone production must then cease. Observation, however, has shown a remainder of chemically significant concentrations of nitrogen oxides in the middle and upper troposphere. It is, therefore, suggested that there is a "re-NO_x-ification" process that reproduces photochemically active nitrogen oxides, NO_x.

Point of Contact: R. Chatfield
(650) 604-5490
chatfield@clio.arc.nasa.gov

Instrument for Tropospheric Nitrogen Studies

James R. Podolske

An open path tunable infrared monitor of the atmosphere (OPTIMA) instrument is being developed to measure nitric acid (HNO₃) and nitrogen dioxide (NO₂) from the NASA DC-8 aircraft. Assessing the effect of the current fleet of commercial subsonic aircraft on the Earth's atmosphere requires detailed knowledge of the nitrogen chemistry of the upper troposphere and lower stratosphere. To date, understanding of this problem has been hampered by large uncertainties, both in the abundances of the odd-nitrogen reservoir species and in the partitioning of reactive nitrogen (NO_x) between nitric oxide (NO) and NO₂. Among the nitrogen reservoir species, HNO₃ is expected to be one of the predominant compounds. Presently, numerical models of the upper troposphere and lower-stratosphere region predict NO_x and NO_y partitioning which differs greatly from that derived from existing measurements. Current instrumentation has been shown to be inadequate for measuring HNO₃ and NO₂ with the speed and accuracy required to advance understanding in this area.

The OPTIMA instrument uses an infrared laser spectrometer coupled to an actively aligned multiple pass Herriott sampling cavity whose open absorption path between the fuselage and the inner engine pylon achieves a free-stream absorption path length of 384 meters. To further enhance the detection sensitivity of

this tunable infrared diode laser system, high-frequency wavelength modulation spectroscopy is employed. Detection sensitivity for these two gases is expected to be in the one-to-ten parts per trillion by volume range. In FY96, tests of the aircraft wing dynamics required to specify the alignment system were completed. The preliminary design of all the instrument subsystems was completed, and the final design reached the 50% level.

Point of Contact: J. Podolske
(650) 604-4853
jpodolske@mail.arc.nasa.gov

Reactive Nitrogen and Oxygenated Hydrocarbon Measurements during the Pacific Exploratory Mission

Hanwant B. Singh, W. Viezee, R. Chatfield, Y. Chen, D. Herlth, R. Kolye

The Pacific troposphere is a major region of the northern hemisphere that is relatively free of direct influences from man-made pollution. Tremendous industrial growth in Asia and North America in recent decades has the potential to significantly affect this pristine region. The Pacific Exploratory Mission-B (PEM-B) and -Tropics (PEM-Tropics), performed in collaboration with L. Salas of the San Jose State Foundation, are major contributors to the NASA Global Troposphere Experiment, designed to study the state of the perturbed and the unperturbed

atmosphere over the Pacific Ocean. These experiments aim to elucidate mechanisms by which ozone in the troposphere is formed, destroyed, and transported. To achieve this aim, data from the PEM-B mission were extensively analyzed and a new set of field measurements involving nitrogen, carbon, sulfur, and tracer species were performed during a five-week PEM-Tropics deployment. Major deployment sites for PEM-Tropics were California, Fiji, Tahiti, Easter Island, and New Zealand. Highly sensitive measurements of reactive nitrogen species, oxygenated hydrocarbons, and chemical tracers were performed by the Ames group by deploying an instrument called PANAK (PANs/aldehydes/ketones).

Point of Contact: H. Singh
(650) 604-6769
hsingh@mail.arc.nasa.gov

Subsonic Aircraft: Contrail and Cloud Effects Special Study

Owen B. Toon, Steve Hipkind, Duane Allen, Paul Bui, Roland Chan, Mike Craig, Guy Ferry, Steve Gaines, Warren Gore, Eric Jensen, Joe Jordan, Stefan Kinne, Bill McKie, Peter Pilewskie, Rudi Pueschel, Tony Strawa, Annette Walker

The subsonic aircraft: contrail and cloud effects special study (SUCCESS) program was a NASA field program that used scientifically instrumented aircraft and ground-based measurements to investigate the effects of subsonic aircraft on

contrails, cirrus clouds, and atmospheric chemistry. SUCCESS had several objectives. One was to better determine the radiative properties of cirrus clouds and contrails so that satellite observations can more reliably measure their effect on Earth's radiation budget. Study questions included determining how cirrus clouds form, whether the exhaust from subsonic aircraft presently affects the formation of cirrus clouds, and, if the exhaust does affect the clouds, whether the changes induced are of climatological significance. Several new instruments were also developed. The study also helped to better determine the characteristics of gaseous and particulate exhaust products from subsonic aircraft and their evolution in the region near the aircraft.

To achieve these experimental objectives, the NASA DC-8 and T-39 aircraft were used in situ as sampling platforms; the NASA ER-2 aircraft was deployed as a remote-sensing platform; and the NASA 757 was used as a source aircraft for studies of contrails and exhaust.

The experiment was cosponsored by NASA's Subsonic Assessment Program and the Radiation Sciences Program, which are part of the overall Aeronautics and Mission to Planet Earth programs, respectively. SUCCESS had well over a hundred direct participants from several NASA Centers, other government agencies, universities, and private research companies.

The SUCCESS project was conducted from the Kansas State University airport facilities in Salina, Kansas, from April 8, 1996, until May 10, 1996, with an extension

from May 10 until May 15, 1996, at NASA's Ames Research Center. SUCCESS coordinated with the U.S. Department of Energy's (DOE's) Atmospheric Radiation Measurements Program, which operates the Cloud and Radiation Testbed (CART) site located in Northern Oklahoma. In addition to the extensive ground-based measurements at the CART site, DOE also operated an Egret and a Twin Otter aircraft, mostly using remote-sensing instruments.

Point of Contact: S. Hipkind
(650) 604-5076
shipskind@mail.arc.nasa.gov

Stratospheric Tracers of Atmospheric Transport

Stephen Hipkind, Michael Craig

The primary goal of the Stratospheric Tracers of Atmospheric Transport (STRAT) program is the measurement of the morphology of long-lived tracers and dynamical quantities as functions of altitude, latitude, and season in order to help determine rates for global-scale transport and future distributions of high-speed civil transport (HSCT) exhaust emitted into the lower stratosphere. The observations obtained will improve understanding of broader issues involving transport of gases and aerosols in the stratosphere.

A secondary goal of STRAT is the further characterization of atmospheric photochemistry. As shown in earlier airborne campaigns, measurement of free radicals within the context of a sufficiently

large suite of tracer observations provides stringent tests for understanding the processes that control ozone photochemistry. The STRAT campaign has extended the regions and seasons for which such measurements have been taken.

The experiment made atmospheric observations with an array of instruments on the NASA ER-2 aircraft that measured long- and short-lived chemical tracers, meteorological parameters, radical species, aerosol particles, and solar radiation. The experiment consisted of six field campaigns of approximately two to three weeks each. The individual campaigns consisted of local, midlatitude flights out of Ames Research Center and tropical flights to and from the island of Oahu, Hawaii. Included in the February 1996 campaign was a coordinated flight with the NASA DC-8 aircraft during the Tropical Ozone Transport Experiment/Vortex Ozone Transport Experiment mission. In the coordinated flight, the ER-2 made measurements while flying in the exhaust plume of the NASA DC-8 aircraft.

STRAT was sponsored by NASA's Atmospheric Effects of Aviation Project, Upper Atmosphere Research Program, and Atmospheric Chemistry Modeling and Analysis Program.

Approximately 100 participants from Ames, other NASA centers, other government agencies, universities, and private consulting companies were involved in this research. The ER-2 carried a complement of 15 scientific instruments, making primarily in situ measurements with two remote-sensing instruments. Overall, 53 flights of the ER-2 used more than 260 hours of flight time.

STRAT has provided a rich dataset with seasonal coverage over two years, vertical profiles from the upper troposphere to the lower stratosphere (33,000 to 70,000 feet), and latitudinal coverage from approximately 2 degrees South to more than 60 degrees North. The analysis of these data will increase understanding of the transport and distribution of emissions into the lower stratosphere by future HSCTs. The data from the first three deployments has been published on CD-ROM.

Point of Contact: S. Hipkind
(650) 604-5076
shpskind@mail.arc.nasa.gov

Tropospheric Aerosol Radiative Forcing Observational Experiment

Philip B. Russell, John M. Livingston, Wendy Whiting

The overall goal of the Tropospheric Aerosol Radiative Forcing Observational Experiment (TARFOX) is to reduce uncertainties in the effects of aerosols on climate by determining the direct radiative effects, as well as the chemical, physical, and optical properties of the aerosols carried over the western Atlantic Ocean from the United States. Other objectives of TARFOX are (1) to perform a variety of closure studies by using overdetermined datasets to test the mutual consistency of measurements and calculations of a wide range of aerosol properties and effects; and (2) to use

the results of the closure studies to assess and reduce uncertainties in estimates of aerosol radiative forcing, as well as to guide future field programs on this subject.

An important component of the closure studies is tests and improvements of algorithms that retrieve aerosol properties and effects from satellite and aircraft radiometers. The resulting validated algorithms will permit extensions of the TARFOX results to other times and locations that have aerosol properties similar to those of the TARFOX Intensive Field Period (IFP).

NASA Ames contributed to TARFOX by supplying the Project Scientist, Project Manager, an ER-2 aircraft, and two airborne sunphotometers. The TARFOX IFP, including coordinated measurements from four satellites (GOES-8, NOAA-14, ERS-2, LANDSAT), four aircraft (ER-2, C-130, C-131, and a modified Cessna), land sites, and ships, was conducted July 10–31, 1996. A variety of aerosol conditions were sampled, ranging from relatively clean behind frontal passages to moderately polluted, with aerosol optical depths exceeding 0.5 at midvisible wavelengths. The latter conditions included separate incidents of enhancements caused primarily by anthropogenic sources and another incident of enhancement apparently influenced by recent fog processing. Spatial gradients of aerosol optical thickness were sampled to aid in isolating aerosol effects from other radiative effects and to more tightly constrain closure tests, including those of satellite retrievals.

The combined surface, air, and space datasets obtained in TARFOX will permit a wide variety of closure analyses. "Internal closure" will be assessed by comparing the quantities thus derived with those deduced from the simultaneous in situ measurements of aerosol size distribution and chemical composition. "External column closure" will be assessed by comparing aerosol extinction computed from the in situ measurements on the C-131A with those derived from the airborne sunphotometers, satellite radiometers, and ER-2 imaging spectrometers.

Such closure analyses will yield critically needed assessments and should reduce the uncertainties in derived values of anthropogenic aerosol radiative forcing. The closure analyses that use satellite optical depth and flux results will provide tests and, where necessary, improvements of satellite retrieval algorithms. The resulting validated algorithms will permit extensions of the TARFOX results beyond the TARFOX period and to other locations dominated by similar aerosols (for example, the European Atlantic coast).

Point of Contact: P. Russell
(650) 604-5404
prussell@mail.arc.nasa.gov

Fine Particle Emissions by Aircraft

Rudolf F. Pueschel, Guy V. Ferry,
Anthony W. Strawa, Duane Allen

Collections of aerosols were made with the Ames wire impactors aboard the NASA DC-8 aircraft flying in the exhaust of a Boeing 757 aircraft during the subsonic aircraft: contrail and cloud effects special study mission. Morphological analysis of scanning electron micrograph (SEM) images and energy-dispersive analysis of x-rays emitted during exposure of the particles to electrons in the SEM allowed a distinction between sulfuric acid (H_2SO_4) and soot aerosols. Size classification and integration over size distributions of both types of aerosols yielded ambient concentrations, particle surface, particle volume, and particle effective radii. This research was performed in collaboration with Jindra Goodman of San Jose State University, Steve Howard of Symtech, Sunita Verma of TMA/Norcal, and Glenn Sachse of the NASA Langley Research Center.

The ambient carbon dioxide (CO_2) concentrations, determined at NASA Langley Research Center, were $1.E-4$ to $1.E-5$ times the concentrations emitted at the engine exhaust plane. Applying these dilution factors to the soot and H_2SO_4 aerosols yielded emission indices between $0.05 < \text{EI}_{\text{H}_2\text{SO}_4} < 0.5$ grams per kilogram of fuel and $2.5E-4 < \text{EI}_{\text{soot}} < 1.4E-3$ grams per kilogram of fuel, respectively.

Relating the H_2SO_4 emission indices to the fuel-S (sulfur) content resulted in the sulfur gas-to- H_2SO_4 particle conversion of between 9 and 24%. This result is close but outside the range of 3 to 12% of sulfur oxidation that could be attributed to hydroxyl radical (OH)-limited gas-to-particle conversion. Thus, a mechanism of H_2SO_4 generation in aircraft exhaust that has yet to be determined appears to exist.

The 1990 fuel use by the commercial airline fleet amounted to $1.3E11$ kilograms. If the fuel-S content averaged 500 parts per million mass, a conversion efficiency of 20% would have led to a contribution by aircraft of $1.3E7$ kilograms of H_2SO_4 , or approximately one part in $1.E4$ of anthropogenic sulfate ion (SO_4) from other sources. If an average $\text{EI}_{\text{soot}} = 7.5E-4$ grams per kilograms of fuel is assumed, the annual emission of soot into the atmosphere in 1990 would have amounted to $1.E5$ kilograms. Compared with 24 teragrams of total anthropogenic soot emission, it follows that aircraft contributions would have amounted to one part in $1.E5$ parts of total soot aerosol.

Thus, aircraft appear to be only a minor source for both H_2SO_4 and soot aerosol. Nevertheless, the measurements reported highlight the issue of particulate (soot and sulfates) emissions from aircraft. The potential for the aircraft emissions of water vapor (H_2O), sulfur (S), and particulates to change the nitrogen oxides (NO_x) effectiveness to atmospheric ozone (O_3) changes

may be sufficiently significant to be included in models.

Point of Contact: R. Pueschel
(650) 604-5254
rpueschel@mail.arc.nasa.gov

FIRE Phase III

Peter Pilewskie, Warren Gore

Begun in 1986, the First International Satellite Cloud Climatology Project Regional Experiment (FIRE) has been an ongoing multiagency program designed to promote the development of improved cloud and radiation parameterizations for use in climate models, and to provide for assessment and improvement of International Satellite Cloud Climatology Project products. The strategy of FIRE has been to combine modeling activities with satellite, airborne, and surface observations.

The third phase of FIRE, or FIRE III, has begun with renewed efforts to understand the physical and dynamical properties of climatically important cloud systems, cirrus, and stratiform clouds. Project personnel completed the second year's work developing new solar spectral radiometric instrumentation for cloud remote sensing and atmospheric radiative flux measurements. In FY96, progress was made toward FIRE III goals by testing a prototype solar spectral flux radiometer (SSFR) at a ground site during the NASA subsonic aircraft: contrail and cloud effects special study mission. Aside from providing important information on the solar radiative properties and effects of cirrus and cirrus

contrails, the benefit of the surface deployment was the expedition of the development of the airborne SSFR, which will be flown in 1997. The team will have airborne and surface capabilities to determine the net solar spectral flux at multiple levels in the atmosphere, and can therefore determine the spectral absorption characteristics of the clear and cloudy atmosphere. Uncertainties in the amount of solar radiation absorbed by water vapor and clouds continue to be a major focus in atmospheric radiative and climate studies.

Point of Contact: P. Pilewskie
(650) 604-0746
ppilewskie@mail.arc.nasa.gov

Laboratory Spectroscopy of Carbon Dioxide in Support of Planetary Atmospheres Research

Lawrence P. Giver,
Charles Chackerian, Jr.

Spectra of planets have absorption bands caused by the molecules in their atmospheres. Measurements of these spectral features can yield information about these planetary atmospheres, such as the abundance of the absorbing molecules and the pressure and temperature of the gas. Measurement requires knowledge of absorption band absolute intensities, line positions, pressure broadening parameters, and temperature dependencies. Over the past 30 years, measurements of these parameters have been made on absorption

bands that are relevant for planetary spectra in the NASA-Ames High Resolution Spectroscopy Laboratory.

In collaboration with D. C. Benner of the College of William and Mary and NASA Langley Research Center, and L. R. Brown and J. S. Margolis of the NASA Jet Propulsion Laboratory, recent work has emphasized intensity measurements of very weak near-infrared carbon dioxide (CO₂) bands that are important for understanding the spectrum of the night side of Venus, which has a massive CO₂ atmosphere. The first intensity measurements of several of these bands were made using spectra obtained at Ames; an article reporting these measurements of bands in the 7000-per-centimeter region was published in the *Journal of Molecular Spectroscopy*. Also, measurements of the perpendicular band at 5315 per centimeter were reported at the Seventh Annual Conference on Laboratory Research for Planetary Atmospheres in Kona, Hawaii, in October 1995. Collaboration between Ames and the NASA Langley spectroscopy group resulted in a careful comparison of intensity measurements of the band at 4006 per centimeter; these results were presented at the Fifty-first Ohio State Symposium on Molecular Spectroscopy in June 1996.

As an extension of prior work on the visible spectrum of methane (CH₄), which is abundant in the atmospheres of all the outer planets, two spectra obtained at the Kitt Peak Observatory have shown that a previously unidentified absorption line in Saturn's spectrum at

6584.3 angstroms is a relatively isolated methane line.

Point of Contact: L. Giver
(650) 604-5231
giver@hires.arc.nasa.gov

Near-Infrared Remote Sensing of Cloud Liquid Water

Peter Pilewskie, Warren Gore

The 1995 Arizona Program was a multiinvestigator field experiment aimed at advancing the understanding of winter storm development, morphology, and precipitation in a mountainous region of central Arizona. From January 15 through March 15, 1995, a wide range of instrumentation was in operation in and around the Verde Valley southwest of Flagstaff, Arizona, including the Ames visible and near-infrared spectroradiometers, two Doppler radars, an instrumented aircraft, a lidar, microwave radiometers, and other surface-based instrumentation focused on the analysis of wintertime storms in this geographically diverse area. Over 25 scientists from seven institutions took part in the program.

Of special interest to the Arizona Program is the interaction of topographically induced gravity waves with the ambient upslope flow. It is hypothesized that these waves may augment the upslope-forced precipitation that falls downwind of this feature onto the Mogollon Rim. A major thrust of the program is to compare the

observations of these, and other aspects of winter storms, with those predicted with a numerical model.

The primary role of this research effort was to provide cloud remote-sensing analysis for determining cloud water thermodynamic phase, cloud thickness, and liquid water content (LWC). The unique collection of surface and in situ sensors provided valuable data toward future efforts in determining the relationships between cloud radiative properties and microphysics and investigations into the role of clouds in climate. Understanding the role of clouds in climate is predicated not only on determination of the complex manner in which radiative energy is redistributed by clouds but also on the hydrological processes that regulate the distribution of condensed water and water vapor in the atmosphere. There are fundamental gaps in the present understanding of the hydrological cycle that limit the ability to assess the present climate, let alone predict future climate, or climate response in the presence of increased greenhouse gases. Because the removal rate of condensed water depends strongly on cloud LWC, determining the distribution of LWC and its dependence on temperature are crucial toward a better understanding of cloud-climate feedback.

Analysis of the Arizona Program data continued in FY96. A new method of analyzing surface-base cloud transmission spectra, developed during the first year of this project, was useful in deriving both cloud liquid water as well as water vapor. Presently, the retrieval method derives the relative proportions of those quantities. New

analysis, based on photon path length distribution calculations, will be necessary to obtain liquid water and water vapor in absolute units. Nevertheless, the work completed during the two years of this project went far in developing this new remote-sensing technique, and will continue in the First International Satellite Cloud Climatology Project Regional Experiment. Furthermore, the instrument developed for this study, and the data acquired during two major field campaigns, were applied to other current problems in solar radiative transfer, namely, the amount of radiation absorbed in clouds, and the amount of radiation absorbed in the cloud-free atmosphere.

Point of Contact: P. Pilewski
(650) 604-0746
ppilewski@mail.arc.nasa.gov

Quantitative Infrared Spectroscopy of Minor Constituents of the Earth's Atmosphere

Charles Chackerian, Jr.,
Lawrence P. Giver

The objectives of this study are to obtain quantitative laboratory spectroscopic measurements of molecular constituents, which are of importance in understanding the "health" of the Earth's atmosphere, and, in particular, emphasize those species that are important for understanding stratospheric kinetics or are used for long-term monitoring of the stratosphere. These measurements provide: (1) line and band

intensity values needed to establish limits of detectability for as-yet-unobserved species and quantify the abundance of those species that are observed; (2) line positions, half widths, and pressure-induced shifts, which are all needed for remote and in situ sensing techniques; and (3) data on the basic molecular parameters at temperatures and pressures appropriate to the real atmosphere.

Previously, oxygen (O₂) pressure broadened spectra of the nitric oxide (NO) vibration-rotation fundamental were obtained using a flow system. These are the first such data to be recorded. These spectra will be analyzed for O₂ broadening coefficients for use in interpreting atmospheric retrievals of NO abundance. High-quality 0.005-per-centimeter resolution spectra of nitric acid (HNO₃) were obtained in the 1100- to 2700-per-centimeter spectral region. Rovibrational line intensities on these spectra will be determined to support the Open Path Trace Species Measurements in the Atmosphere experiment. Analysis for the electric dipole moment function of the ground electronic state of the hydroxyl radical (OH) molecule was completed using a very large set of relative emission lines of the Meinel system. A definitive and comprehensive compilation of rovibrational intensities for the carbon monoxide (CO) molecule in its various isotopic forms was published.

An experimental feasibility study was completed for using magnetic rotation spectroscopy (MRS) to detect free radical molecular species (in situ) in the part-per-trillion mixing ratio range. A quantitative theory

was developed to analyze the MRS results obtained as well as to predict instrumental parameters required for parts per trillion by volume detection of free radical molecular species. A multipass reflection cell inside a solenoid magnet has been constructed to achieve parts-per-trillion-by-volume sensitivity.

Infrared spectra were obtained using an interferometer and a 25-meter base-path multiple reflection cell, in the 1.8-micrometer region of the infrared red spectrum of nitric oxide for the purpose of designing a lidar-based smoke-stack detector for this molecule.

Experiments have been performed to measure line intensities of gaseous water in the 1-micrometer spectral region to help in understanding the apparent anomaly associated with absorption of solar radiation by clouds in the Earth's atmosphere.

Collaborators in this research include Chris Mahon of the Space Physics Research Institute, P. Varanasi of the State University of New York, and D. Cooper of the Stanford Research Institute.

Point of Contact: C. Chackerian
(650) 604-6300
chack@hires.arc.nasa.gov

Stratospheric Transport

**Rudolf F. Pueschel, Guy V. Ferry,
Anthony W. Strawa, Duane Allen**

The atmospheric impact of emissions by aircraft depends on how they change the steady-state abundance of constituents over background atmospheric amounts,

and on the role they play in atmospheric photochemical, dynamical, and radiative processes. Transport plays a role in this scheme, because the background concentrations of atmospheric constituents vary in space. For example, effects on column ozone of aircraft-emitted nitrogen oxides (NO_x) result from decreases in the middle and upper stratosphere and increases in the lower stratosphere and troposphere. The balance between these increases and decreases depends on the dispersion of the aircraft effluent by atmospheric transport processes, as well as the transport of long-lived species, including ozone, in the background atmosphere. Thus, one important aspect is that fraction of exhaust NO_x that would be transported from the heavily traveled flight corridors in the lower stratosphere in northern midlatitudes to the tropics, where it can be lofted to higher altitudes by atmospheric circulation. Subsequent transport back to midlatitudes would be at altitudes where the NO_x from the exhaust dominates ozone depletion.

Of interest also is the fraction of exhaust that could be transported from the flight corridors in the northern hemisphere across the equator to southern latitudes. Transport of exhaust from north to south would reduce the concentration of this fraction and mitigate the effects in the northern hemisphere.

Soot aerosol measurements were taken using the Ames wire impactor samples to document barriers to interhemispheric mixing, analogous to the stratospheric dispersion of radioactive ^{14}C tracers after the nuclear bomb tests in the 1950s and early 1960s. Because atmospheric

nuclear bomb testing was terminated in the early 1960s, the ^{14}C data permit estimates of interhemispheric mixing times that turn out to be longer than stratospheric residence times by more than one order of magnitude. This scenario explains a decade-long confinement of aircraft soot to the hemisphere into which it has been emitted.

Although there is agreement between the soot and ^{14}C datasets in horizontal interhemispheric mixing, vertical mixing between the soot aerosol emission level (12 kilometers) and the NASA ER-2 aircraft ceiling (20 kilometers) is indicated only in the soot measurements. Transport from midlatitudes to the tropics, with subsequent lofting and transport back to midlatitudes at higher altitudes, is a possibility for vertical mixing. However, since ^{14}C in the northern hemisphere does not substantiate the soot results, vertical motion due to radiometric forces of higher absorbing soot particles that could prolong their stratospheric residence times is a more plausible explanation.

This research was performed in collaboration with Jindra Goodman of San Jose State University, Steve Howard of Symtech, and Sunita Verma of TMA/Norcal.

Point of Contact: R. Pueschel
(650) 604-5254
rpueschel@mail.arc.nasa.gov

SUCCESS Irradiance Measurements

Peter Pilewski, Warren Gore

A solar spectral flux radiometer (SSFR) was deployed at the U.S. Department of Energy Southern Great Plains Cloud and Radiation Testbed during April 1996 as part of the NASA subsonic aircraft: contrail and cloud effects special study (SUCCESS). The SSFR was used to measure downwelling solar spectral irradiance in the 250- to 2500-nanometer solar spectral region, with 10- to 15-nanometer resolution. From April 12 through April 29, approximately 18,000 spectra were acquired, under a variety of meteorological conditions; a significant portion of the spectra was favorable to the study of cirrus clouds and cirrus contrails. Analysis of the solar spectral flux dataset will facilitate the study of the effects of subsonic aircraft on the surface and lower atmosphere energy budget. Simultaneous in situ observations by the NASA DC-8 will provide the micro-physical ground truth for assessment of the results.

To determine radiative properties of cirrus and cirrus contrails and their net effects on radiative energy budgets, a proper understanding of the solar radiation spectrum in the cloud-free atmosphere is needed.

A key component of the SUCCESS objectives was to obtain a better understanding of the spectral distribution of solar irradiance reaching the surface. First results from analysis of SSFR data suggest that absorption by water vapor can be determined quite accurately, and the measured spectra agree with model calculations within measurement uncertainties. These findings will help eliminate long-standing discrepancies between theory and observation and, likewise, are crucial to determining the effects of contrails on the solar energy budget.

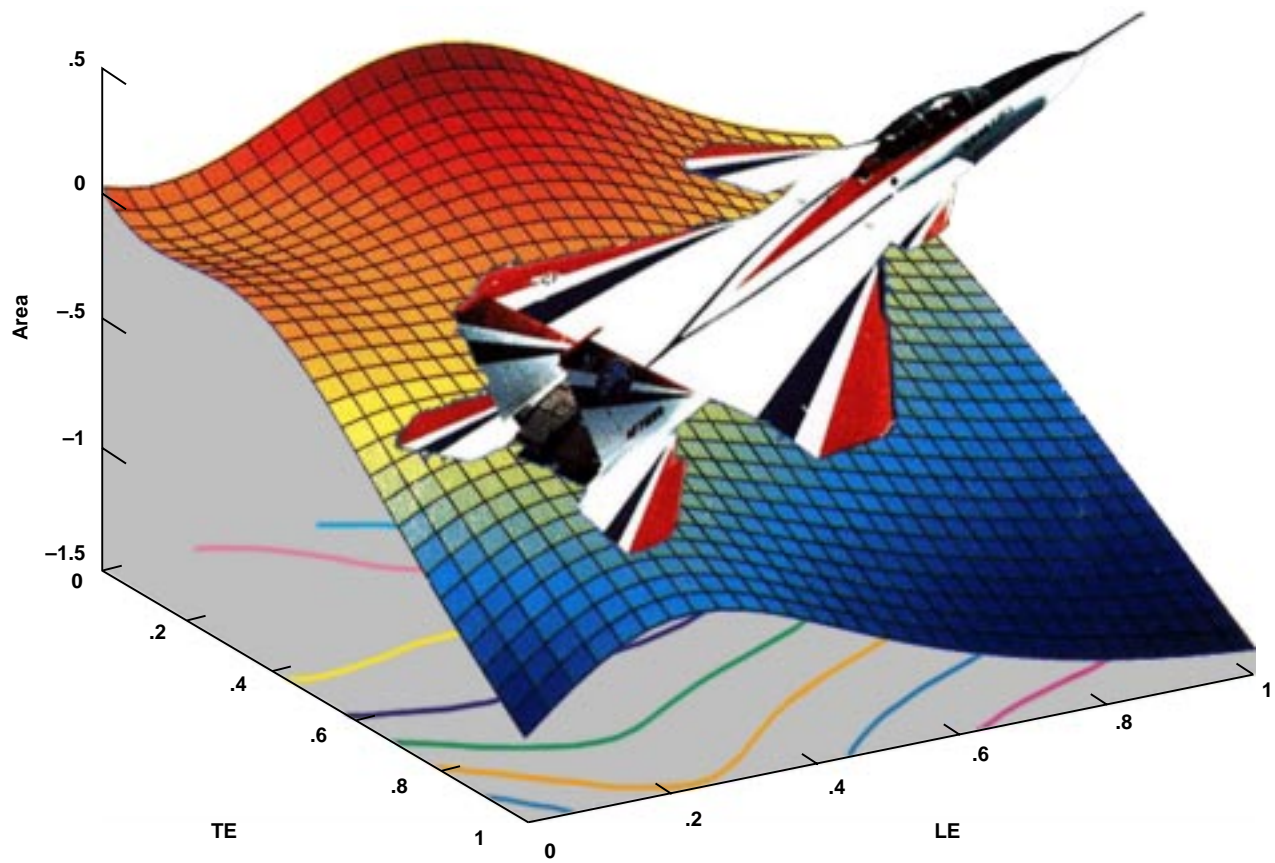
Point of Contact: P. Pilewski
(650) 604-0746
ppilewski@mail.arc.nasa.gov

Appendix

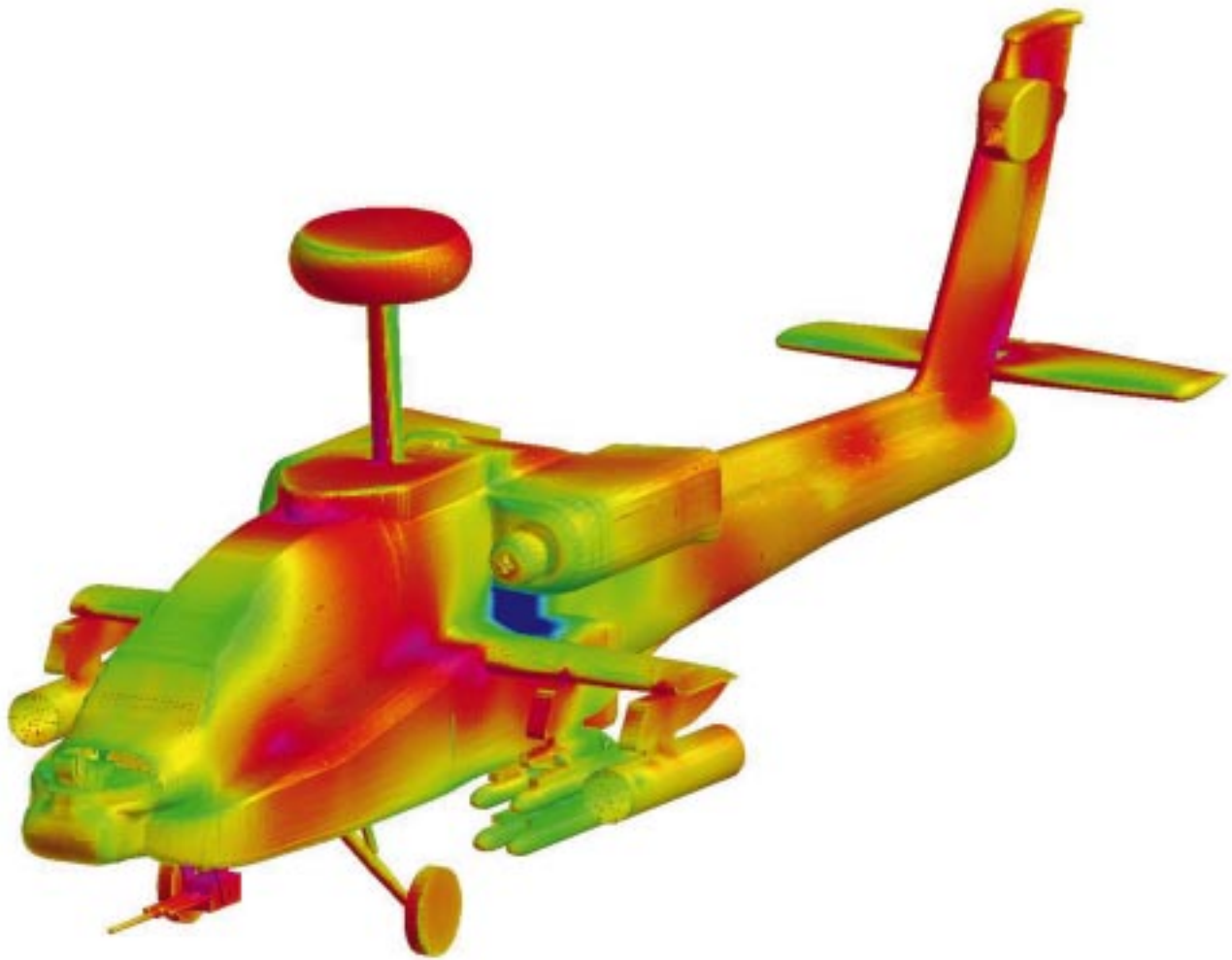
The color plates in this appendix correspond to figure citations that appear in the text. Each caption also provides the location of the figure citation.



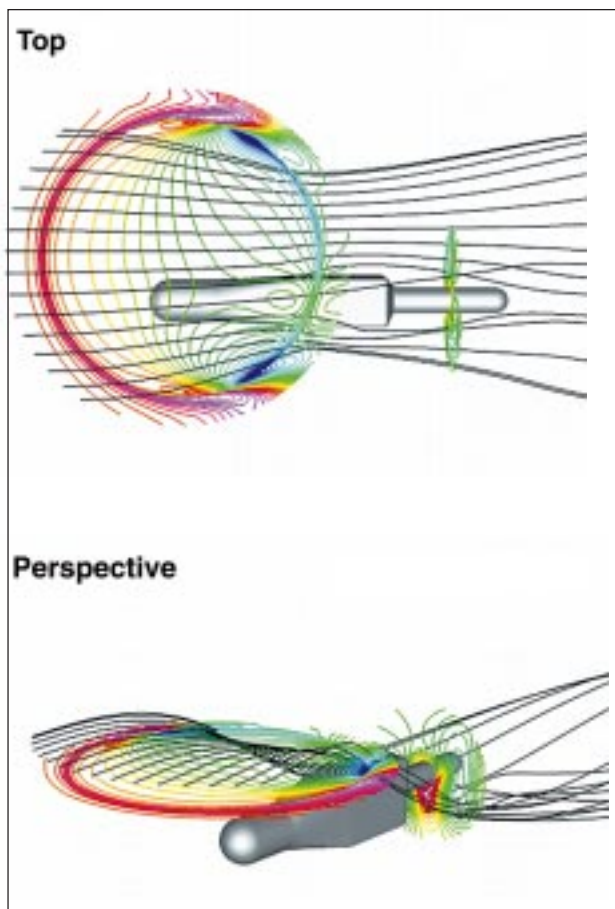
Color Plate 1. Air-traffic controllers at the Dallas/Fort Worth TRACON using FAST advisories to control arrival traffic. (Davis, p. 11)



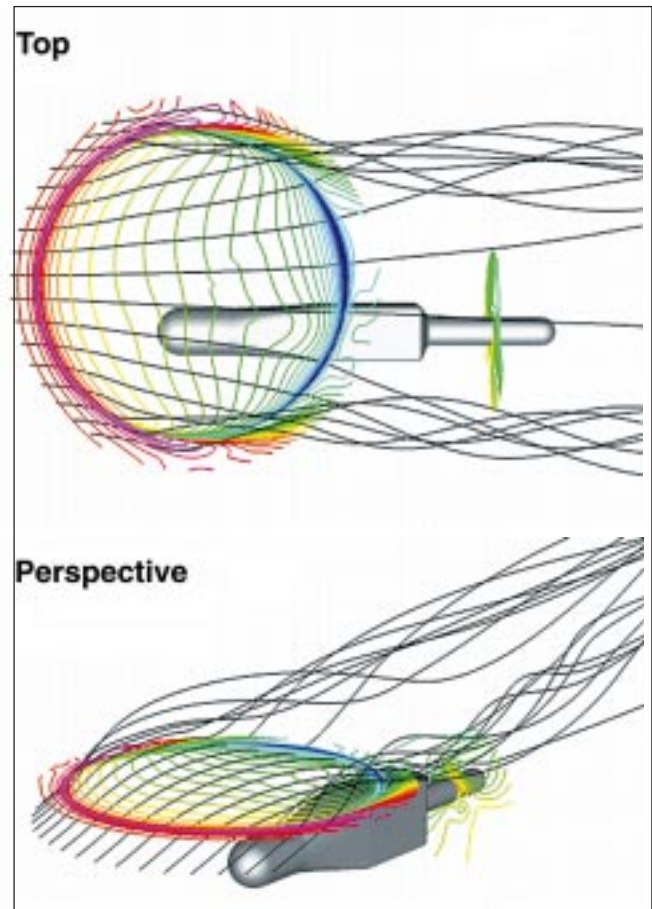
Color Plate 2. F-15 ACTIVE superimposed on aerodynamic flight envelope. (Jorgensen, p. 19)



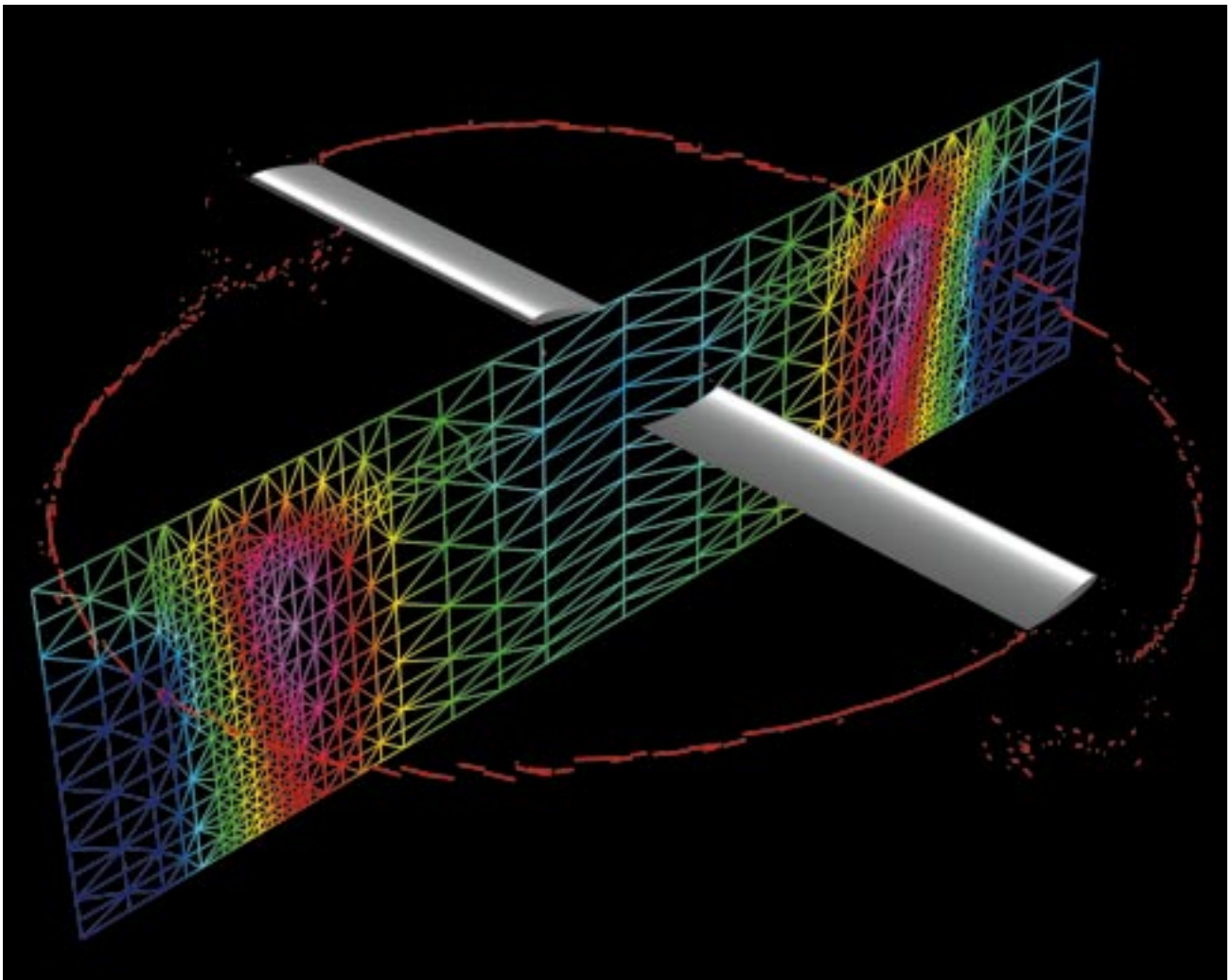
Color Plate 3. Full Apache AH-64D airframe aerodynamic loading in forward flight. (Duque, p. 36)



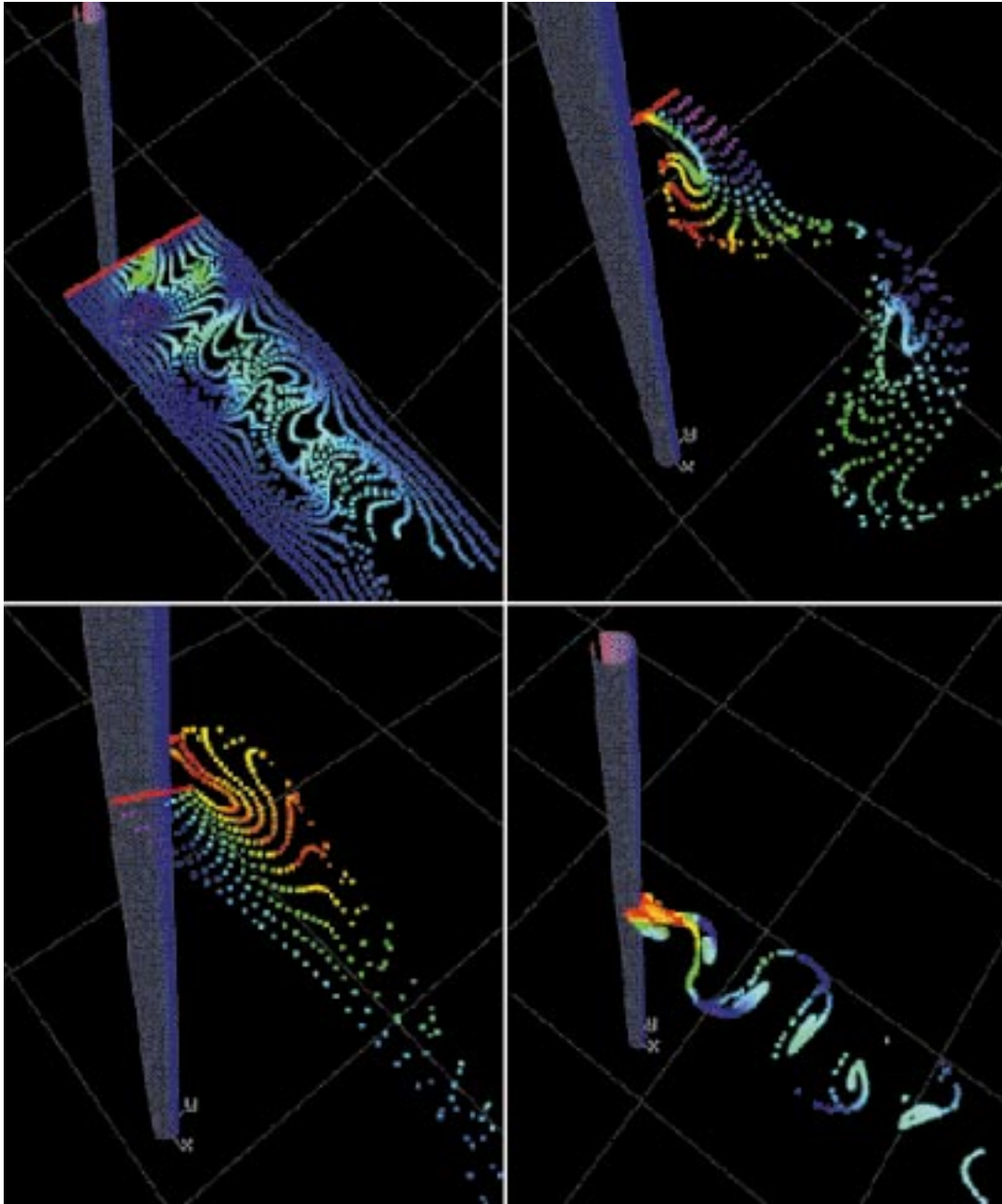
Color Plate 4. Vertical velocity contours and flow-field streamlines, 0-degree angle of incidence. (Stremel, p. 36)



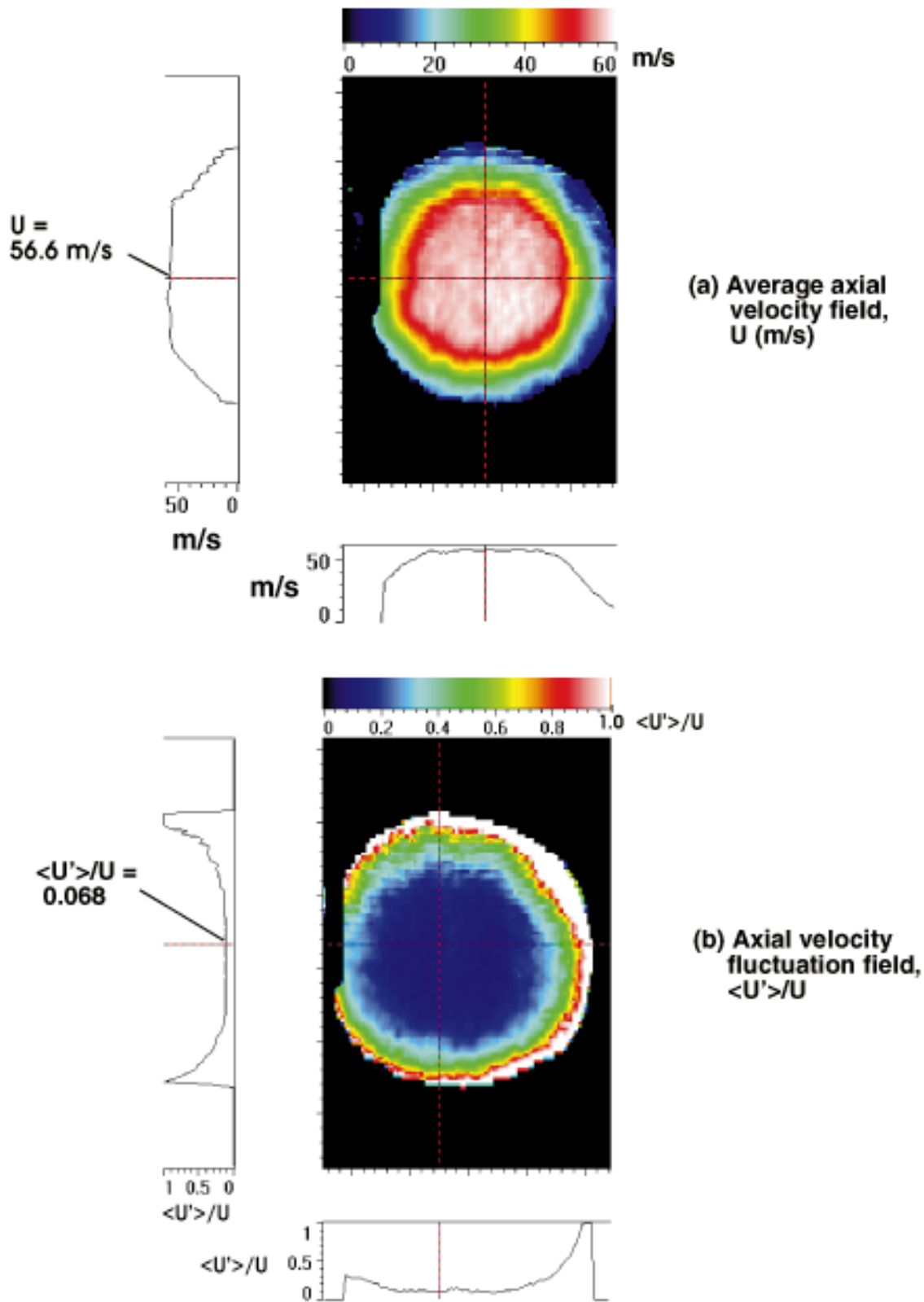
Color Plate 5. Vertical velocity contours and flow-field streamlines, 15-degree angle of incidence. (Stremel, p. 36)



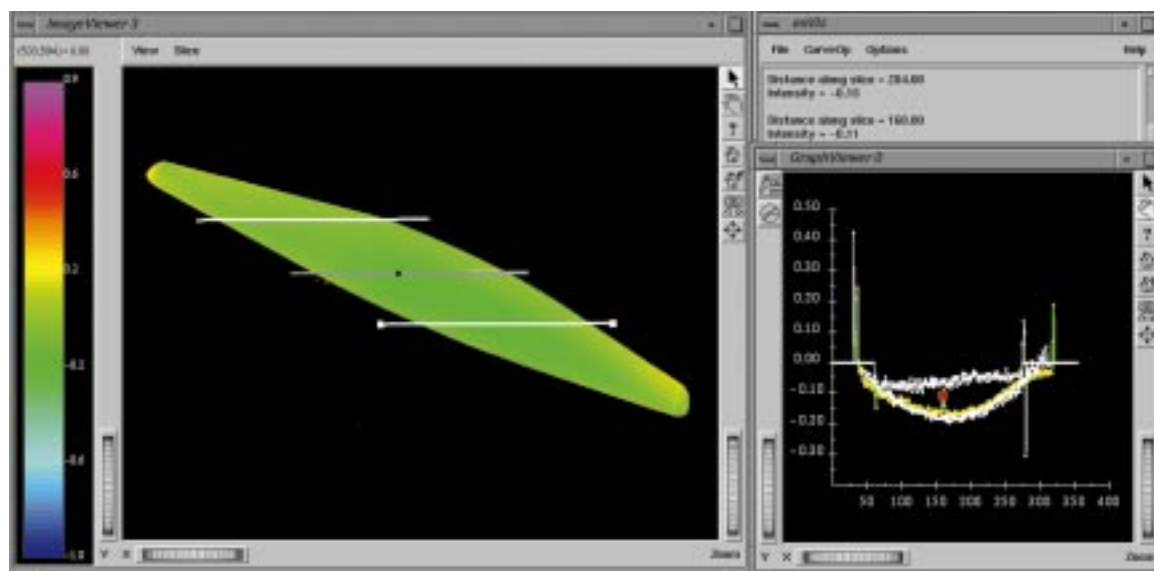
Color Plate 6. Vortex cores (red) extracted from a simulation of a helicopter rotor in forward flight. (Kenwright, p. 39)



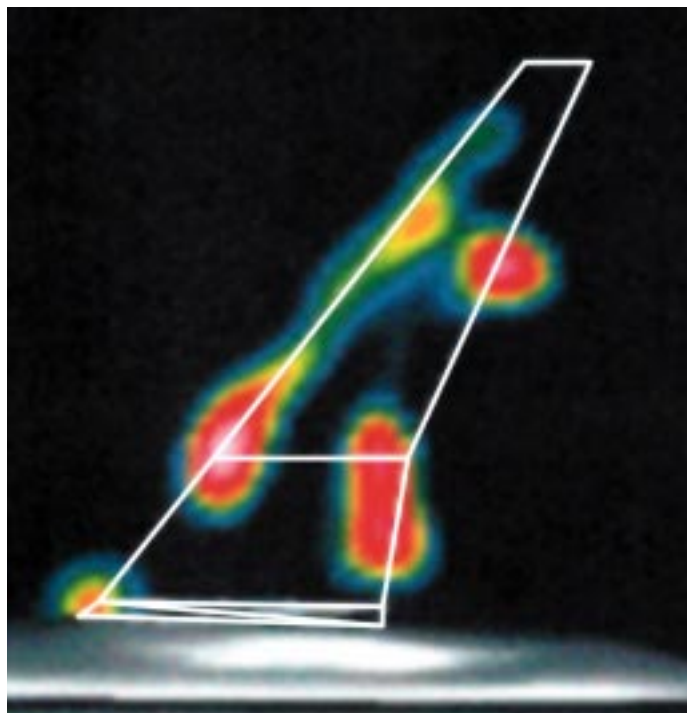
Color Plate 7. Interactive placement and visualization of streaklines in the Virtual Windtunnel permits flow features to be easily found. (Kenwright, p. 42)



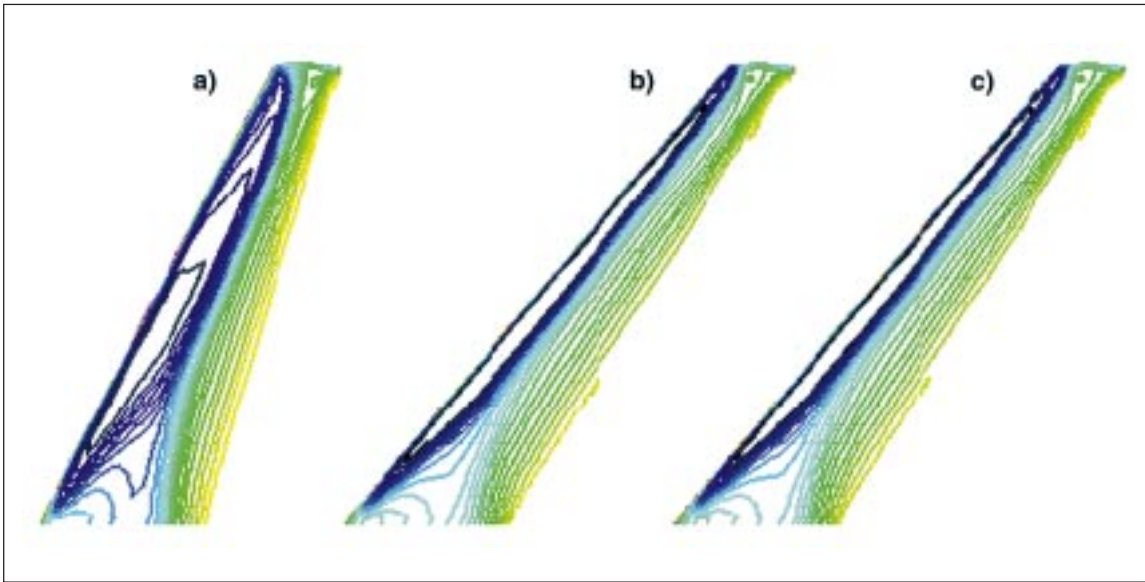
Color Plate 8. PDV measurements of axial velocity and its root-mean-square fluctuation amplitudes in a plane normal to the centerline of a low-speed, turbulent jet; the view in each image is upstream along the jet centerline. (McKenzie, p. 44)



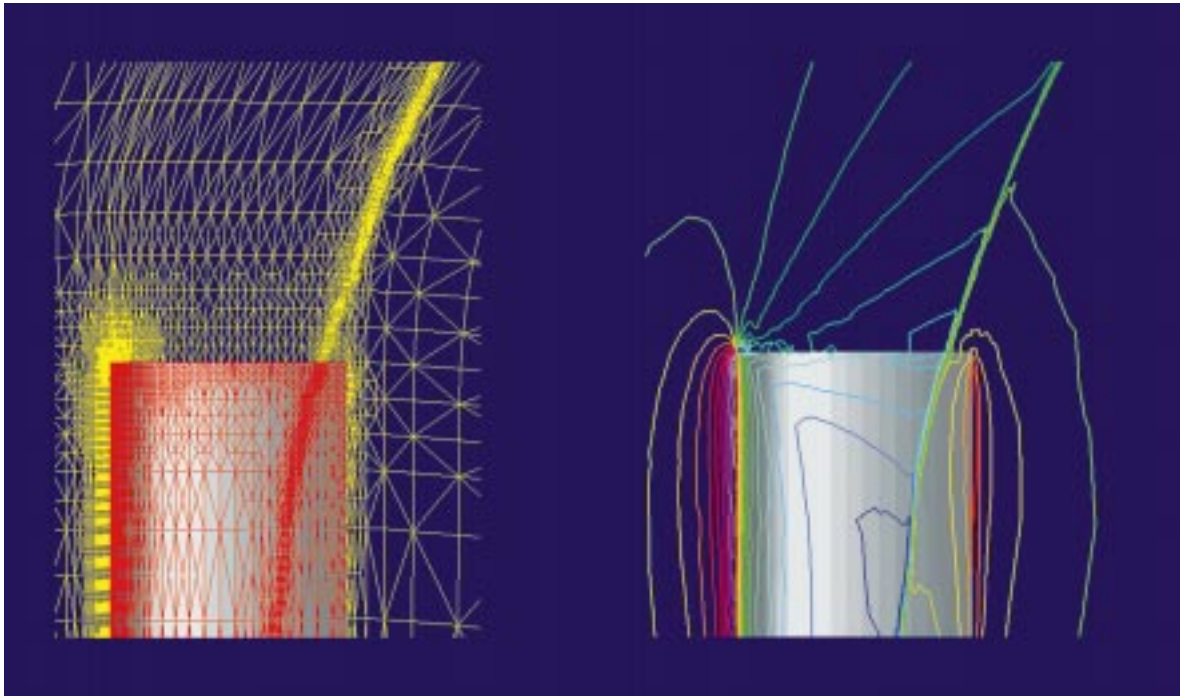
Color Plate 9. The exVis ImageViewer window (left) shows pressure-sensitive paint data for the OAW-3 oblique all-wing model. The white line segments are slice tools that have been interactively placed on the image. The GraphViewer (right) shows x-y plots of the coefficient of pressure versus length along the tool for each selection. The highlighted peak (the red marker on the green graph) was selected in the GraphViewer, resulting in showing the black spot along the gray tool where this value occurs. The third window (top right) is the simple user interface used to access datafiles and create ImageViewers and GraphViewers. (Usselton, p. 48)



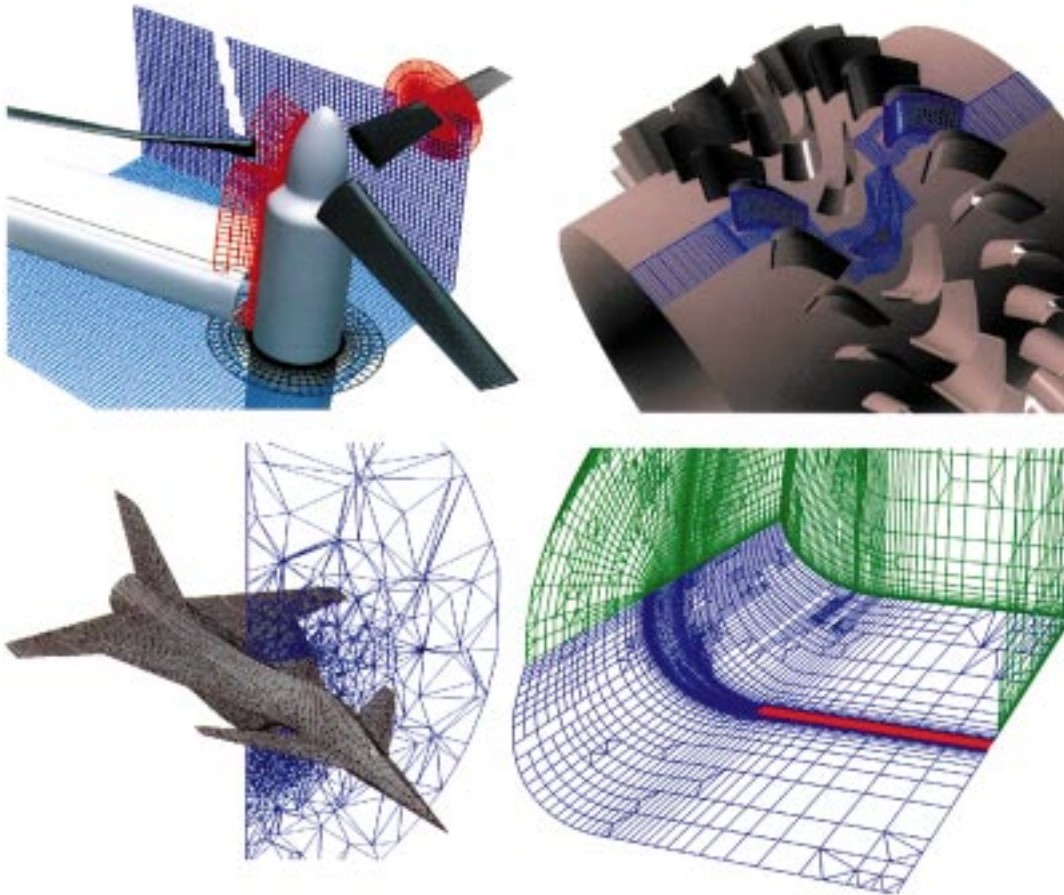
Color Plate 10. Noise-level contours measured on 4.7%-scale DC-10 semi-span model in the Ames 12-Foot Pressure Wind Tunnel with 52-element Boeing phased microphone array. (Horne, p. 56)



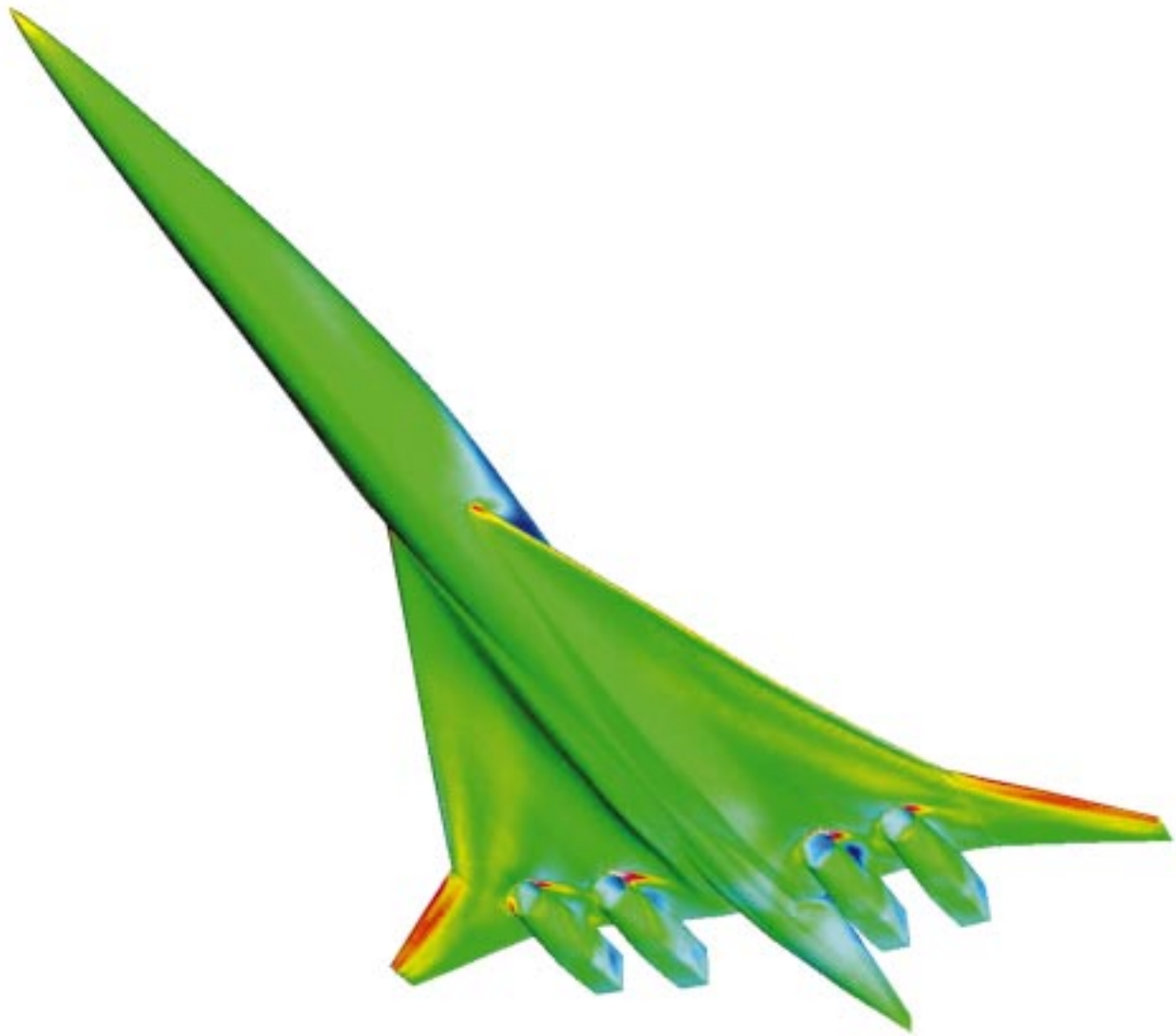
Color Plate 11. Surface pressure contours for multiple design variable study: (a) original wing; (b) modified wing with four design variables; (c) modified wing with five design variables. (Greenman, p. 58)



Color Plate 12. Final mesh and computed pressure contours in the rotor plane. (Biswas, p. 59)



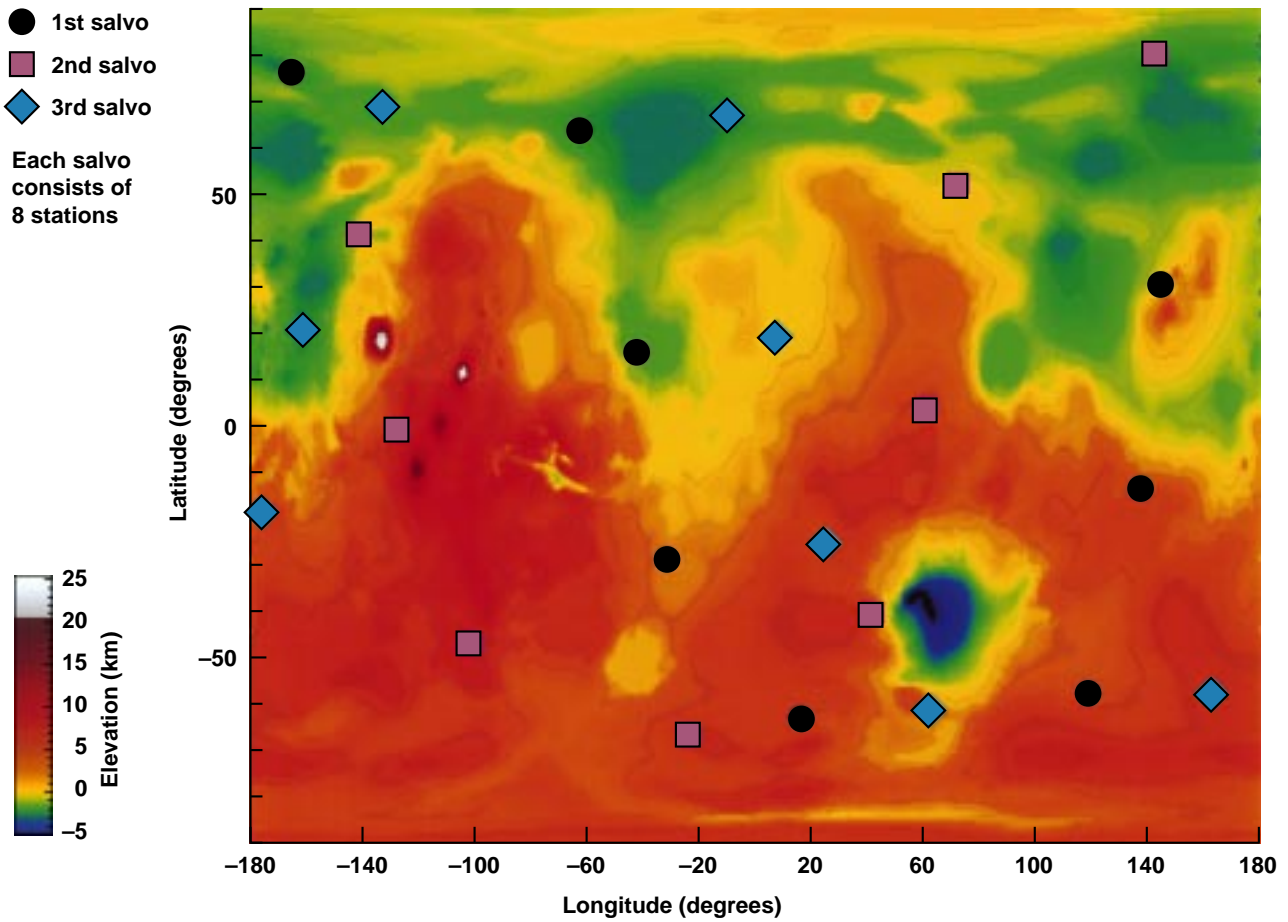
Color Plate 13. Four different types of grids used in computational fluid dynamics. Clockwise from upper left: multiple overlapping zone structured grid for the V-22 tiltrotor aircraft; periodic multizone structured grid for turbomachinery; hybrid structured and unstructured grid for a helicopter rotor; unstructured tetrahedral grid for the Langley fighter. (Bryson, p. 61)



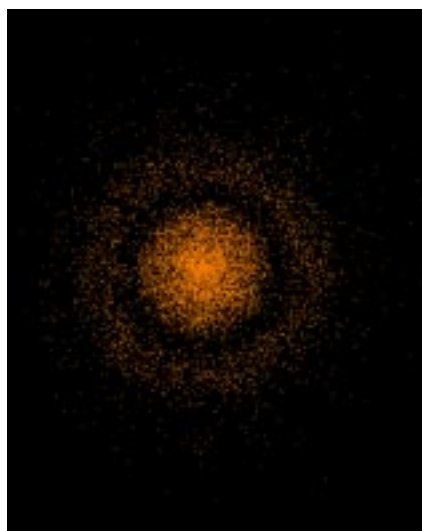
Color Plate 14. Optimized HSR configuration. (Cliff, p. 67)



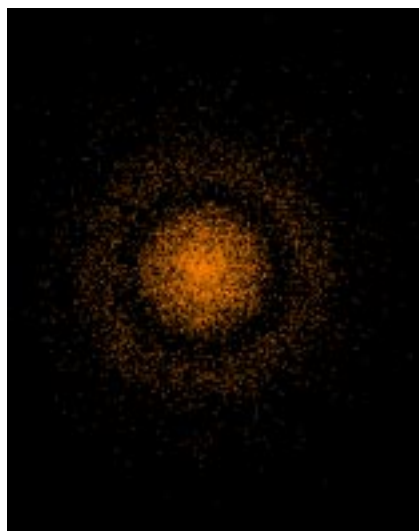
Color Plate 15. Thin cirrus clouds scattered the light of the stars in this rare color photograph of the trail of an alpha-Monocerotid passing the star Sirius, captured by the Dutch Meteor Society observer Robert Haas at the Alcudia-de-Guadix location in Spain during the meteor outburst of November 22, 1995. (Jenniskens, p. 81)



Color Plate 16. An illustration of possible network of 24 PASCAL stations on Mars. This network is achievable using centrifugal release from a spin-stabilized carrier spacecraft and two propulsive time-of-arrival adjustments. Three groups of eight stations each follow three sinusoidal loci and are marked by black circles (1st salvo), red squares (2nd salvo), and blue diamonds (3rd salvo). Topography is shown in color contours. (Haberle, p. 88)

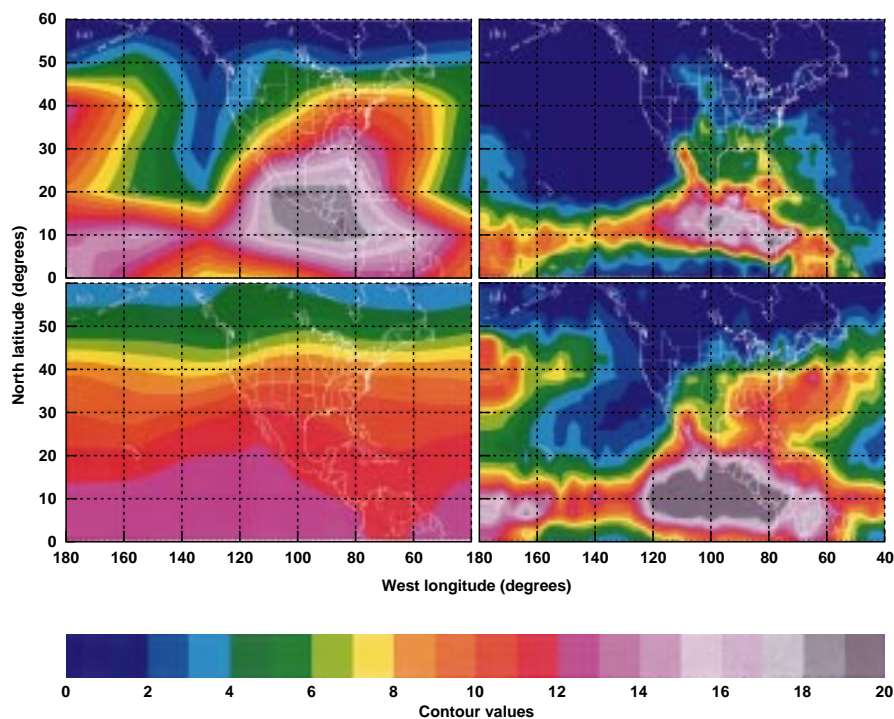


Color Plate 17. The disk, showing a pronounced annular gap at the halo/epicycle frequency resonance. This pattern persists for the entire length of the experiment, which is on the order of a Hubble time. (Smith, p. 91)



Color Plate 18. Strong, non-axisymmetric structure is evident in the disk at late times in the experiment. This bar is absent when the halo remains static. Such offset bars are often seen at the centers of disk galaxies. (Smith, p. 91)

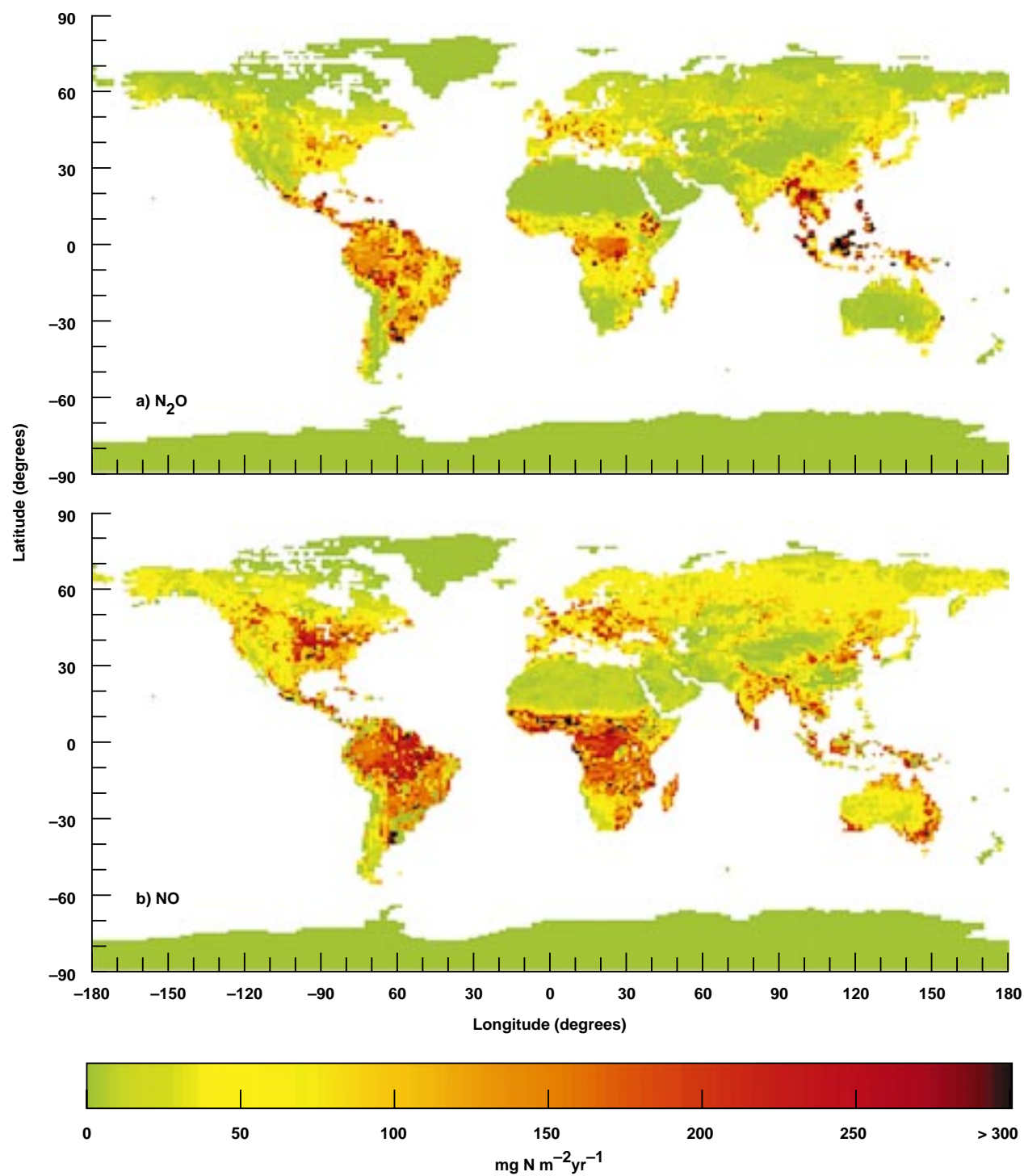
Meteorological Data for the Summer (JJA) Season



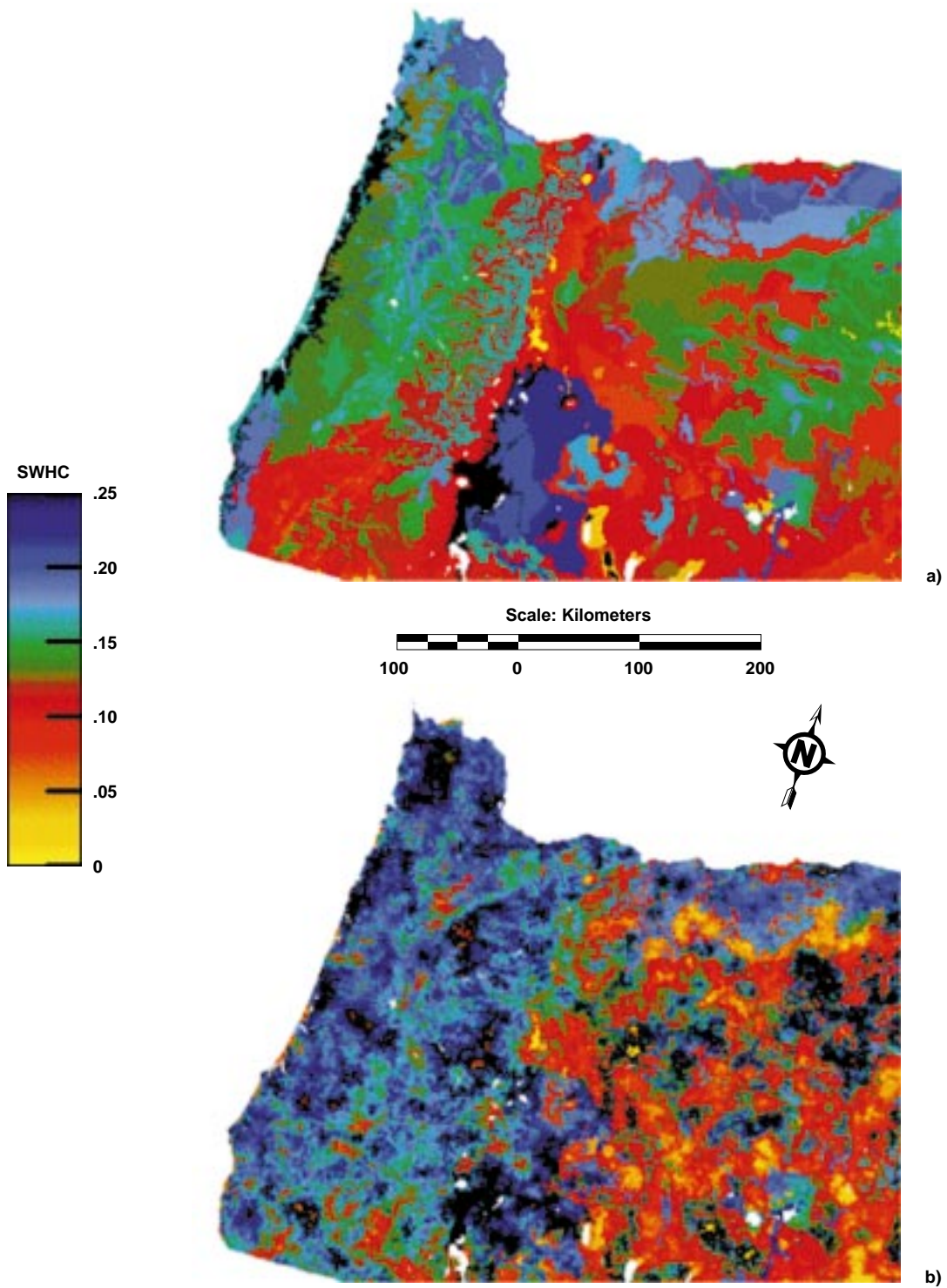
Color Plate 19. (a) The SAGE II frequency of cloud occurrence from 0 to 100% in 5% increments. (b) The HIRS frequency of cloud occurrence from 0 to 30% in 1.5% increments. (c) The average tropopause height from 27,000 to 67,000 feet in increments of 2,000 feet. (d) The MLS-derived water vapor overburden from 4 to 24 precipitable microns in increments of 1 micron. (Haas, p. 95)



Color Plate 20. The image of the skull of the female from the Visible Human dataset is visualized on the screen of the Immersive WorkBench. Rei Cheng (left) and Muriel Ross are studying the 3-D reconstruction with the aid of special glasses. Rei Cheng is demonstrating special gloves that will be used to manipulate instruments and pieces of bone or other tissue in the immersive environment. (Ross, p. 119)



Color Plate 21. Global patterns of annual (a) N_2O and (b) NO emissions from soils. (Potter, p. 149)



Color Plate 22. Top map: Conventional map of soil water holding capacity (SWHC) using homogeneous polygons. Bottom map: Map of SWHC developed in this research. (Coughlan, p. 152)

REPORT DOCUMENTATION PAGE

Form Approved
OMB No. 0704-0188

Public reporting burden for this collection of information is estimated to average 1 hour per response, including the time for reviewing instructions, searching existing data sources, gathering and maintaining the data needed, and completing and reviewing the collection of information. Send comments regarding this burden estimate or any other aspect of this collection of information, including suggestions for reducing this burden, to Washington Headquarters Services, Directorate for Information Operations and Reports, 1215 Jefferson Davis Highway, Suite 1204, Arlington, VA 22202-4302, and to the Office of Management and Budget, Paperwork Reduction Project (0704-0188), Washington, DC 20503.

1. AGENCY USE ONLY (Leave blank)	2. REPORT DATE September 1997	3. REPORT TYPE AND DATES COVERED Technical Memorandum	
4. TITLE AND SUBTITLE Research and Technology 1996		5. FUNDING NUMBERS	
6. AUTHOR(S) Ames Investigators			
7. PERFORMING ORGANIZATION NAME(S) AND ADDRESS(ES) Ames Research Center Moffett Field, CA 94035-1000		8. PERFORMING ORGANIZATION REPORT NUMBER A-976441	
9. SPONSORING/MONITORING AGENCY NAME(S) AND ADDRESS(ES) National Aeronautics and Space Administration Washington, DC 20546-0001		10. SPONSORING/MONITORING AGENCY REPORT NUMBER NASA TM-112195	
11. SUPPLEMENTARY NOTES Point of Contact: John T. Howe, Chief Scientist, Ames Research Center, MS 200-16, Moffett Field, CA 94035-1000 (650) 604-5500 or contact person(s) at the end of each article			
12a. DISTRIBUTION/AVAILABILITY STATEMENT Unclassified — Unlimited Subject Category 99		12b. DISTRIBUTION CODE	
13. ABSTRACT (Maximum 200 words) This report highlights the challenging work accomplished during fiscal year 1996 by Ames research scientists, engineers, and technologists. It discusses research and technologies that enable the Information Age, that expand the frontiers of knowledge for aeronautics and space, and that help to maintain U. S. leadership in aeronautics and space research and technology development. The accomplishments span the range of goals of NASA's four Strategic Enterprises: Aeronautics and Space Transportation Technology, Space Science, Human Exploration and Development of Space, and Mission to Planet Earth. The primary purpose of this report is to communicate knowledge—to inform our stakeholders, customers, and partners, and the people of the United States about the scope and diversity of Ames' mission, the nature of Ames' research and technology activities, and the stimulating challenges ahead. The accomplishments cited illustrate the contributions that Ames is making to improve the quality of life for our citizens and the economic position of the United States in the world marketplace.			
14. SUBJECT TERMS Aeronautics, Space transportation, Space sciences, Earth sciences, Life sciences, Information technology, Research and technology		15. NUMBER OF PAGES 201	16. PRICE CODE A09
17. SECURITY CLASSIFICATION OF REPORT Unclassified	18. SECURITY CLASSIFICATION OF THIS PAGE Unclassified	19. SECURITY CLASSIFICATION OF ABSTRACT	20. LIMITATION OF ABSTRACT